THE EFFECT OF MOMENT-ROTATION JOINT BEHAVIOUR ON THE DISPLACEMENTS OF PORTAL FRAMES

by
Heindrich Louw Albertyn

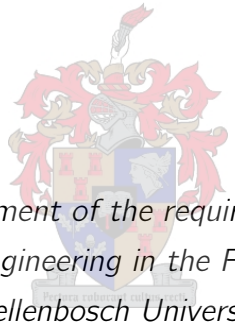

Thesis presented in fulfilment of the requirements for the degree of Master of Science in Engineering in the Faculty of Engineering at Stellenbosch University

Supervisors:
Professor PE Dunaiski
Doctor TN Haas

December 2011

DECLARATION

By submitting this thesis electronically, I declare that the entirety of the work contained therein is my own, original work, that I am the Sole author thereof (save to the extent explicitly otherwise stated), that reproduction and publication thereof by Stellenbosch University will not infringe any third party rights and that I have not previously in its entirety or in part submitted it for obtaining any qualification.

Date: .....

Signature: .....

SYNOPSIS

Higher grade steels are being rolled in South Africa by suppliers and results in structural members having an increased axial and bending moment capacity due to an increased yield stress. Structural elements used in designs are stronger and therefore lighter sections with sufficient axial and bending moment capacity are used. Displacements of structural elements are calculated using the stiffness and Young's modulus of a profile. These values are not affected by the increased yield stress in higher steel grades and therefore have a negative effect on the displacements of the structure. The potential of these higher grade structural elements are not utilized through serviceability limit state criteria, since the displacement determination does not account for the increased capacities of higher grade steels, but only stiffness and elasticity of the members.

Structural analysis of portal frames does not account for the real behaviour of steel connections and column bases. It is assumed that connections and bases are either fully rigid or perfectly pinned. This assumption is used in the analysis and design of the structure. Although it is assumed that connections and bases are either rigid or pinned, the real behaviour is in between these two extremes. Rigid connections exhibit a certain flexibility under loading whereas pinned bases provide a certain restraint under loading. The real behaviour of connections and bases are referred to as the moment-rotation behaviour of the connection. For a certain applied moment to the connection or base, the connection exhibits a certain rotation.

The focus of this study is placed on the accuracy and feasibility of modelling the real behaviour of connections and bases in a structural analysis of a portal frame. A connection stiffness is determined from the connection's moment-rotation behaviour, and is assigned to a rotational spring of zero length in a structural analysis. An experimental investigation was conducted to obtain the real displacement data of a portal frame subject to loads for two different support conditions, i.e. a perfect hinge and grouted-support. A perfect hinge support was used to isolate the moment-rotation response of the ridge and eaves connection. The experimental results were used to compared to the results obtained from a structural analysis to determine the accuracy of the numerical results.

A real design case was investigated with load combinations imposed on the frame in accordance with SANS 10160:2011. Three methods of modelling connections and bases in an analysis were considered. Firstly modelling connections as rigid and bases as pinned, secondly modelling connections as linear rotational springs and bases as pinned. Lastly was to model connections as linear rotational springs and bases as non-linear rotational springs. The outcome of the research was that more accurate displacements of a portal frame could be obtained by modelling the real behaviour of rigid connections as rotational springs, but this is not the case with grouted column bases. It is thus not feasible to model the real behaviour of connections and bases in a structural analysis as the current method of modelling connections as rigid and bases as pinned provides reliable and accurate displacement results.

SAMEVATTING

Hoë graad staal word tans in Suid Afrika gerol deur verskaffers en lei daartoe dat strukturele elemente oor 'n groter aksiale- en buigmomentkapasiteit het as gevolg van 'n groter vloeispanning. Strukturele elemente in ontwerpe is sterker en gevolglik het ligter elemente die benodigde aksiale- en buigmoment-kapasiteit. Verplasings van strukturele elemente word bepaal vanaf die styfheid en Young modulus van die element. Hierdie waardes word nie beïnvloed deur die groter vloeispanning van hoë graad staal nie, en het dus 'n negatiewe uitwerking op die verplasings van die struktuur. Die potensiaal van die gebruik van hoë graad staal word nie benut in die geval van voldoening aan diensbaarheids kriterium nie, aangesien verplasings bepaal word vanaf die styfheid en elastisiteit van die elemente, en nie vloeispanning nie.

Strukturele analise van portaalrame neem nie die ware gedrag van konneksies en kolomvoetstukke in ag nie. Die aanname word gemaak in analises en ontwerpe dat konneksies en voetstukke óf rigied óf geskarnierd is. Hierdie is slegs 'n aanname en in die werklikheid lê die ware gedrag van konneksies en voetstukke tussen hierdie grense. Rigiede konneksies toon 'n sekere buigbaarheid tydens belasting en geskarnierde voetstukke toon 'n sekere beperking teen rotasies. Die ware gedrag van konneksies en voetstukke word gedefinieer as moment-rotasie gedrag. Vir 'n spesifieke aangewende moment, ondergaan die konneksie of voetstuk 'n sekere rotasie.

Hierdie studie fokus op die akkuraatheid en uitvoerbaarheid van die modellering van die ware gedrag van konneksies en voetstukke in 'n strukturele analise van portaalrame. Die styfheid van 'n konneksie word bepaal vanaf sy unieke moment-rotasie gedrag, en word ingevoer as 'n styfheid van 'n rotasieveer in 'n strukturele analise. 'n Eksperimentele ondersoek was gedoen om verplasingswaardes van 'n portaalraam onder belastings te bepaal. Twee ondersteunings is ondersoek in die eksperimentele program, naamlik 'n geskarnierde ondersteuning asook 'n breivul ondersteuning. Die gebruik van die geskarnierde ondersteuning isoleer die moment-rotasie gedrag van die nok en dakrand konneksies. Die eksperimentele resultate was gebruik om die akkuraatheid van die resultate vanaf die strukturele analise te ondersoek.

Laastens was 'n ontwerpsprobleem ondersoek deur laskombinasies, soos bepaal volgens die riglyne van SANS 10160:2011, op 'n portaalraam aan te wend. Drie gevalle van modellering van konneksies in 'n strukturele analise is ondersoek. Eerstens om konneksies as rigied en voetstukke as geskarnierd te beskou. Tweedens was die konneksies as linieêre rotasievere gemodelleer en voetstukke as geskarnierd te beskou. Laastens was om konneksies as linieêre rotasievere te modeleer en voetstukke as nie-linieêre rotasievere. Die navorsing het getoon dat meer akkurate verplasings van portaalrame bepaal kan word deur rigiede konneksies te modelleer as rotasievere, maar dit is nie die geval met breivul ondersteunings nie. Die gevolg is dat die uitvoerbaarheid van die modellering van konneksies en voetstukke as rotasievere nie effektief is nie, aangesien die huidige metode van die modellering van konneksies as rigied en voetstukke as geskarnierd akkurate en betroubare resultate lewer.

ACKNOWLEDGEMENTS

I would like to express my gratitude to the following:

Professor PE Dunaiski for creating the opportunity, leading and funding the study. Thank you for the valuable lessons you have passed on to me and making time no matter what the circumstances were. You will remain in our thoughts.

Doctor TN Haas for his assistance, guidance and encouragement.

Professor JA Wium for his valuable insights.

Charlton Ramat and **Rheeza Ras** for their assistance with the experimental setup.

Johan van der Merwe for manufacturing the test specimens.

Helmutt Bowls and **Greg Mitchell** of FEAS (Pty) Ltd for their technical support on the finite element models.

Peter Smulders for proof reading this thesis.

My **Parents** for their encouragement and unending support.

And most importantly my **Heavenly Father** who makes all things in life possible and blessing me with the ability and intelligence to complete this project.

This thesis is dedicated to all in the fight against cancer, those who have won and those who have lost.

TABLE OF CONTENTS

LIST OF FIGURES

LIST OF TABLES

LIST OF ABBREVIATIONS

AISC	American Institute of Steel Construction
CFS	Cold-formed Lipped Channel
DOF	Degree of Freedom
HSFG	High Strength Friction Grip
IPE	I-profile Européennes (French: European I-beam profile)
LC	Load Combination
LRFD	Load and Resistance Factor Design
LVDT	Linear Variable Displacement Transducer
PR	Partially-restrained
SABS	South African Bureau of Standards
SAISC	Southern African Institute of Steel Construction
SANS	South African National Standard

LIST OF SYMBOLS

LATIN LETTERS

A = Area

A_b = Cross-sectional area of a bolt, based on its nominal diameter

A_{eff} = Effective cross-sectional area

A_m = Area of the fusion face of a weld

A_n = Area of openings where external pressure is zero or negative

A_{req} = Required area of contact

A_t = Area of openings

A_v = Shear area

A_w = Effective throat area of a weld

a = Transverse distance from outer fastener centre to flange tip

B_r = Factored bearing resistance of a member or component

b = Breadth or width

C_{pe} = External pressure coefficient

C_{pi} = Internal pressure coefficient

c_{prob} = Probability factor

$C_r(z)$ = Roughness factor

C_r = Factored compressive resistance of a member or component

C_{rx} = Factored compressive resistance of a member or component about its strong axis

C_{ry} = Factored compressive resistance of a member or component about its weak axis

C_u = Ultimate compressive force in member or component

C_w = Warping torsional constant

C_y = Axial compressive force in member at yield stress

C_0 = Topography (orography) factor

d = Along-wind dimension of builidng

d_h = Bolt hole diameter

E = Young's modulus

e = Eccentricity (In the case of wind calculations is e = b or 2h whichever is smaller)

F = Force

F_H = Horizontal force

F_v = Vertical force

F_x = Force in x-direction

F_y = Force in y-direction

f = Unit Stress or strength

f_{cu} = Specified compressive cube strength of concrete at 28 days

f_s = Ultimate shear stress

f_u = Specified minimum tensile strength

f_y = Yield stress

f_{yc} = Yield stress of the column

G = Shear modulus of steel

g = Transverse spacing between fastener gauge lines (gauge distance)

h = Height

h_w = Clear depth of web between flanges or between web fillets of a rolled section

h_{wc} = Clear depth of the column web

I = Moment of inertia

I_y = Moment of inertia about the weak axis of a member or component

J = St. Venant torsion constant of a cross-section

K = Effective length factor

K_{ii} = Element node stiffness

k_c = Distance from outer face of flange to web-toe of fillet of an I-section or channel

k_v = Shear buckling coefficient

L = Gross Length

L_x = Effective length of member about its strong axis

L_y = Effective length of member about its weak axis

ΔL = Total elongation

l_1 = Equivalent length along which yielding takes place

M = Moment

M_b = Beam applied moment

M_c = Column applied moment

M_{cr} = Critical elastic moment of a laterally unbraced beam

M_p = Plastic moment

M_u = Ultimate bending moment in a member or component

M_{ux} = Ultimate bending moment in a member or component about its strong axis

M_{rx} = Factored moment resistance of a member or component about its strong axis

ΔM = Incremental nodal moment

m = Number of faying surfaces or shear planes in a bolted joint

n = Number of shear connecters or bolts

P_u = Applied load per bolt

p_b = Vertical distance between to fasteners measured centre-to-centre

Q = Prying force

Q_n = Characteristic value of an imposed load

q = Transverse distance from the web fillet toe to the centre of the first fastener

q_k = Characteristic value of a uniformly distributed load

q_p = Peak wind pressure

r = Radius of gyration

r_x = Radius of gyration of a member about its strong axis

r_y = Radius of gyration of a member about its weak axis

S_c = Connection stiffness

s = Centre-to-centre longitudinal spacing (pitch) of any two successive fastener holes

T_r = Factored tensile resistance of a member or component

T_u = Ultimate tensile force in a member or component

t_f = Flange thickness

t_{fc} = Thickness of the column flange

t_p = Endplate or baseplate thickness

t_w = Web thickness

t_{wc} = Thickness of the column web

U_{1x} = Factor to account for moment gradient and for second order effects of axial force acting on the deformed member in the x-direction

u_1 = First nodal direction

u_2 = Second nodal direction

u_3 = Third nodal direction

V_r = Factored shear resistance of a member or component

v = Poisson's ratio

v_b = Basic wind speed defined at 10 m above ground in terrain category B

$v_{b,peak}$ = Peak basic wind speed ($v_{b,peak} = 1{,}4v_b$)

$v_{b,0}$ = Fundamental value of the basic wind speed corresponding to the specific geographical location

$v_p(z)$ = Peak wind speed at height z

W = Width-to-thickness ratio

W_e = External wind pressure

W_{lim} = Limiting width-to-thickness ratio

x_u = Tensile strength of weld metal

Z_e = Elastic section modulus of a steel section

Z_{pl} = Plastic section modulus of a steel section

z = Height above ground level

z_e = Reference height relevant to external pressure

z_g = Gradient height

z_0 = Height of the reference plane

GREEK LETTERS

α = Pitch angle of roof

Δ = Displacement

θ = Rotation

$\varepsilon_{plastic}$ = Plastic strain

ε = Normal strain

θ_b = Beam rotational deformation

θ_c = Column rotational deformation

$\Delta\theta$ = Incremental nodal rotation

λ = Non-dimensional slenderness ratio

μ = Opening ratio

ρ = Air density

σ = Stress

ϕ = Resistance factor for structural steel

ϕ_b = Resistance factor for bolts

ϕ_c = Resulting rotation in connection

ϕ_w = Resistance factor for weld metal

ω_2 = Coefficient to account for increased moment resistance of a laterally unsupported beam segment when subject to a moment gradient

Chapter 1

INTRODUCTION

The use of pitched roof structural steel portal frames has spread throughout the industrial, commercial and agricultural sectors of the economy. As few portal frames are required to construct a structure having a large plan area. These structures are easy to design, are easily erected and results in a very effective structure in terms of space utilisation and cost.

Higher grade steel profiles are being rolled in South Africa by steel suppliers. These higher grade steels possess a greater yield stress, which results in an increased axial and bending capacity. Modern designs utilize these higher steel grades through the use of more slender structural elements in portal frames and other structural applications. Displacements of structural elements are determined from the stiffness and elasticity of the member. Higher grade steels have a higher yield stress but the stiffness and elasticity of the profile is not affected. The result is that displacements are negatively affected with the use of higher grade steels as slender structural elements. The use of more slender structural elements thus result in the criteria set by serviceability limit state becoming the determining criteria for design parameters, rather than the criteria set by ultimate limit state. Holický supports this statement with the following words: "Serviceability is becoming a fundamental concept of advanced engineering design in construction" (Holický, 2010). Serviceability limit state for building structures sets an informative guideline to the maximum permissible displacements a structure may undergo due to normal occupancy, typical use and external factors imposed on the structure.

The question is asked if it would be possible to determine displacements of portal frames more accurately through the modelling of the real behaviour of joints and column bases in structural analyses. This is so that more slender structural elements could be utilized to their full potential by their conforming to serviceability limit state, and thus leading to more effective and reliable designs. The current method of displacement determination is to perform a structural analysis on a portal frame where it is assumed that connections and bases are either infinitely rigid or perfectly pinned. In an ideal world connections can be regarded as being infinitely rigid or pinned, but in practice all connections possess certain flexibility and restraint characteristics. Rigid connections possesses a certain flexibility which will increase the displacements of the structure under loading. This phenomenon is in contrast with that of pinned column bases, where a pinned column base possesses a certain restraint which decreases the displacements of the structure.

This study investigates the modelling of real connection and column base behaviour in pitched roof portal frame structures to determine displacements more accurately. It involves determining the stiffness of a connection or a column base through it's unique moment-rotation response under loading. The moment-rotation behaviour of a connection or a base is defined as the in-plane rotational deformation exhibited by the connection or base due

to in-plane loads imposed thereon. The principle of the moment-rotation behaviour of connections is defined and explained fully in section 2.5. The determined stiffness will be used in the structural analysis of a portal frame by modelling joints and column bases as rotational springs of zero length in structural analysis. The displacements determined from the analysis will be compared to the experimental results, in order to assess the accuracy and feasibility of the proposed modelling technique of portal frame structures.

The objectives for this study are:

1. Determination of the moment-rotation behaviour of joints and column bases in portal frames through non-linear, three-dimensional finite element analysis.
2. Conducting of experimental investigation to obtain real displacement data for a portal frame.
3. Determination of the optimum rotational spring stiffness of joints and column bases for a structural analysis.
4. Comparison of an analysis assuming rigid connections and pinned bases to an analysis using rotational springs and to experimental displacement data.
5. Assessing the accuracy of modelling real connection and column base behaviour in an analysis for determining displacements.
6. Assessing the feasibility of taking into account the real behaviour of connections and bases in the structural analysis of portal frames.
7. Using the methods of structural analysis on a reference portal frame involving design load cases for serviceability limit state comparison purposes.

The effect of moment-rotation joint and base behaviour on the displacements of portal frames is determined by achieving the listed objectives of the study. This will arrive at the necessary results to formulate conclusions as to the accuracy and feasibility of the proposed method of more accurate displacement determination of portal frames. The study is limited to the analysis of pitched roof portal frames with haunched beam-column connections, extended endplate ridge connection and pinned bases. The reader is referred to sections 3.4 and 3.5 for the detailed scope and limitations of the study. The feasibility of the method of using rotational springs to model joint and base behaviour in a structural analysis, also assesses the significance of determining displacements of the structure more accurately. This research answers the question of whether, the full potential of more slender structural elements are utilized in modern designs, or whether further research is required in modelling the real behaviour of joints in structural analyses for design purposes.

A literature study is presented extending from portal frame connections and bases through to the analyses of these structures and rotational springs. The principle, functioning and mathematical background of rotational springs is introduced and explained fully. Furthermore the analysis involving rotational springs and the determination of a spring stiffness from the connection's moment-rotation response is explained. The literature study is concluded with a brief background to Eurocode's semi-rigid design procedure. The aim of the literature study is to provide the reader with the necessary technical background to clarify the procedure of investigation, as well as all the technical aspects and principles referred to in the study.

The literature study is followed by a methodology chapter explaining the detailed procedure that was followed in order to conduct the research in terms of data required. The procedures which were followed, and the analyses performed to meet the set objectives to finally arrive at conclusions are discussed in chapter three. Scope and limitations sections are also found in chapter three as has already been stated above.

The body of the research is presented in chapters four to seven. Chapter four starts with the three dimensional non-linear analysis of portal frame connections and column bases. A finite element analysis is performed to determine each connection's unique moment-rotation response under loading. All technical aspects such as analysis type, element type, contact and interaction properties regarding the finite element models, are presented in chapter four. The results from each finite element model in terms of the moment-rotation behaviour, the ultimate moment capacity and the mode of failure are also presented.

Chapter five discusses the experimental investigation conducted for the study. The main objective of the experimental investigation is to obtain real displacement data of a portal frame structure. Aspects covered are the analysis and design of the test specimen, the prediction of response and the measurement of data. This is followed by test results and a brief summary.

Chapters four and five are brought together in chapter six where a structural analysis is performed on the test specimen. Structural analyses of portal frames are presented in terms of the displacement determination as well as the design forces and the bending moments. Aspects such as software choice, rotational spring stiffness determination, analysis type and load cases investigated, are presented prior to the results from the structural analysis. Analyses using rigid connections and pinned bases are compared to analyses using rotational springs as connections. Experimental results from chapter five are used for comparison and accuracy assessment in order to arrive at the desired conclusions for the study. Inaccuracies presented by the comparison of results are researched and discussed in terms of sensitivity analysis performed on certain components of the structure, with specific reference to grout stiffness and bolt preload. Chapter six is summarized with a conclusion.

Chapter seven involves the structural analysis of a reference portal frame to compare and summarize all analysis techniques used in the research, in terms of a real design problem. Load combinations for the design according to the South African loading code (SANS10160:2011), are presented together with informative guideline of the maximum allowable displacements of steel structures, according to the South African hot-rolled steel design code (SANS10162-1:2005). Two load combinations have been identified for the determination of the maximum vertical and horizontal displacement of the structure. Both these load combinations are presented for three variations of modelling connections in the structural analysis of a portal frame. The results are tabulated and presented in the force-displacement curves to provide a comparative illustration of the displacement results. The chapter is summarized with a conclusion on the displacement results for each load combination, as well as a recommendation for obtaining the maximum displacements of the structure for design purposes.

Finally conclusions are made in terms of the outcomes of the research. The feasibility of the proposed methods of structural analysis are discussed as well as recommendations for future research regarding the matters addressed and questions raised during this research.

Chapter 2

LITERATURE REVIEW

2.1 BACKGROUND TO PORTAL FRAMES

Single-storey portal frame structures are used in industrial, commercial and agricultural applications. The main portal structure consists of columns and roof girders manufactured from I- or H-sections. The connections between the structural elements are in most cases bolted connections, where the beam-column and ridge connections are moment-fixed haunch-type or endplate connections and the column bases are endplate connections. These connections are discussed in detail in the sub-sections.

2.2 BEAM-COLUMN CONNECTIONS

Beam-column connections transfer forces from the beam to the column and vice-versa. To simplify the construction of steel structures, beam-column connections are commonly designed as bolted connections. The most common bolted beam-column connections are flush endplate, extended endplate, stiffened endplate and haunch connections.

A haunch connection refers to a beam-column connection that transfers forces between the column and the roof girder of a portal frame as shown in figure 2.1. Forces transferred include axial compression or tension forces, bending moments as well as vertical shear forces (Kruger et al., 1995). Due to the fact that the connection transfers a moment between the structural components, the connection is classified as moment fixed (SAISC, 1992). This attribute of the connection is due to the layout of the components in the connection, i.e. bolts and the distance from the bolt centres to adjacent webs and flanges of the structural components. Torsional forces are not taken into account in the studies of the behaviour of this type of connection (Lui and Chen, 1987).

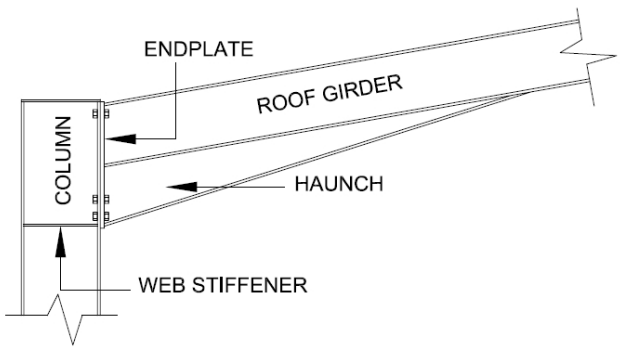

Figure 2.1: A typical haunch connection using I-sections.

Haunch connections are designed to economize the size of the girder (Moore and Wald, 2003). This statement is supported by the fact that the maximum moment occurs near the column joint with the roof girder. The roof girder has an increased bending capacity at the haunch since it is welded to the girder along the full length of the haunch. The conclusion can therefore be made that in haunch connections the roof girder can be made of a lighter section as the haunch provides sufficient moment capacity at the end of the member, where the maximum bending moment occurs. The haunch therefore increases the bending moment capacity of the beam-column connection.

As already mentioned, haunch connections are designed as moment-fixed connections (SAISC, 1992). As all forces and moments are transferred between the structural members joined by the connection, a haunch must be designed for sufficient shear strength and moment resistance. The behaviour of connections under loading is discussed in section 2.5.

An extended endplate connection is also commonly used in portal frame beam-column connections due to the layout of the components (SAISC, 1992). The greater of the moments caused by wind uplift, self-weight or imposed loads, is transferred to the adjacent member through the bolts at the top or bottom of the connection depending on the direction of the applied moment. The extension of the endplates provides an increased stiffness and resistance in the tension zone of the connections as they can accommodate more bolt rows on those parts of the endplate that are outside the profiles of the structural elements. This results that the adjacent columns will need web stiffeners in these tension zones.

2.3 RIDGE CONNECTIONS

Ridge or apex connections as they are sometimes referred to, are moment-fixed beam connections at the top of portal frames. The layout of ridge connections is similar to that of moment-fixed beam-column connections, i.e. flush endplate, extended endplate and apex connections similar to a portal haunch. Figure 2.2 illustrates an extended endplate ridge connection and a haunched apex connection respectively.

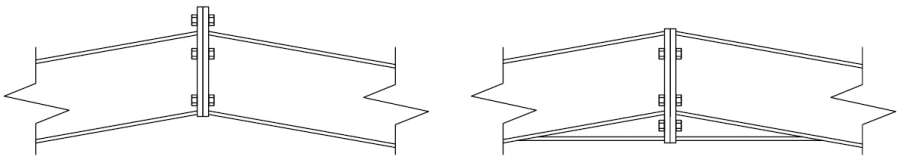

Figure 2.2: Elevation layouts of extended endplates and haunches used on apex or ridge connections respectively.

2.4 COLUMN BASES

Column bases provide support to the columns of steel structures and can be classified according to their layout into two different types. The first type is pinned column bases which are considered as pinned connections, i.e. not providing any restraint against rotation of the column at the base. A typical characteristic of a pinned column base is the two or more holding-down bolts that are situated within the flanges of the column, symmetrical to the centroid of the column section.

The second type of column bases is fixed bases which are identified by the positions of the holding-down bolts, of which there are typically four or more situated outside the column flanges on the endplate. Gusset plates are added in certain cases to increase the stiffness of the base plate. In most cases thicker base plates are also used compared to the base plates of pinned bases, as more stiffness and moment capacity is provided to the

connection by thicker base plates. Figure 2.3 illustrates an elevation layout of a pinned and a fixed column base respectively. Column bases are designed according to the response under loading required from them or as per the

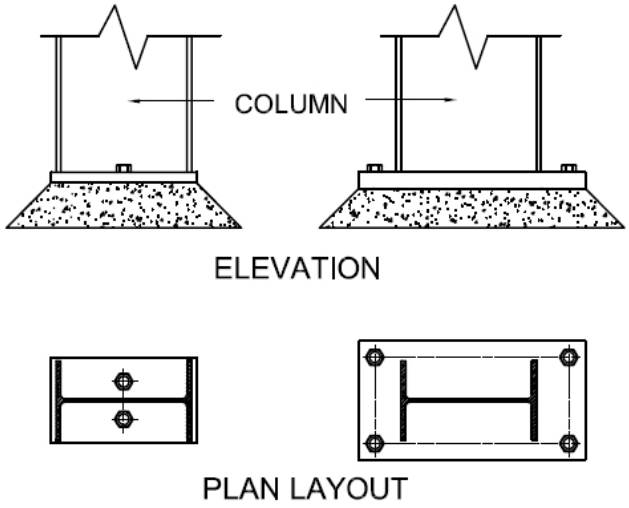

Figure 2.3: Elevation layout of typical pinned and fixed column bases.

analysis performed on the structure.

2.5 BACKGROUND TO MOMENT-ROTATIONAL JOINT RESPONSE

In section 2.2 it was stated that a connection transfers forces between the structural members connected by it. Forces transferred include, axial forces, shear forces and bending moments. Connections subject to loading and therefore transferring forces between members, exhibit deformation. The most prominent deformation is rotational deformation due to bending moments applied to the connection. Rotational deformation is denoted by the symbol theta (θ). Deformations caused by axial and shear forces are negligibly small in comparison to rotational deformation and thus will not be considered in this study of connection response due to loading (Kruger et al., 1995). It is therefore concluded that connection rotation is a function of the moment applied to the connection.

The rotation (θ) of a connection is defined as the change in angle between the structural components connected to it. This is illustrated in figure 2.4 by means of a deformed beam-column connection.

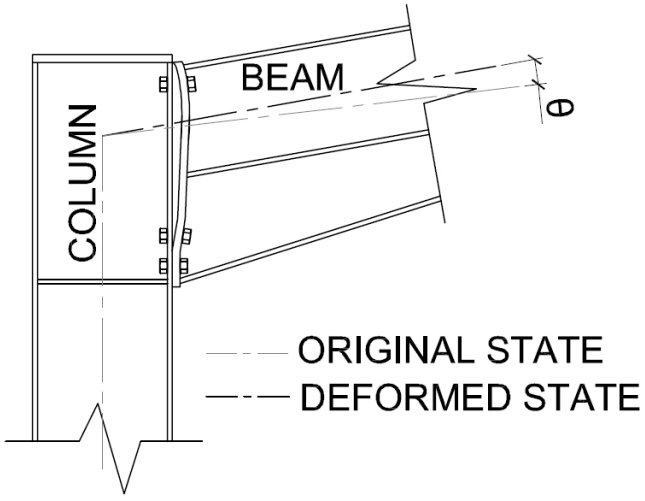

Figure 2.4: Rotational deformation of a connection subject to a moment. (Shi et al., 2007)

Traditional structural steel design methods and codes assume steel connections to be classified into two categories. The first category is pinned connections which assumes that only axial and shear forces are transferred between structural members. It is also assumes that pinned connections in analysis procedures acts as a hinge and is free to rotate under load. The second category of which it is assumed that all forces including bending moments are transferred between structural members, is termed moment-fixed connections. The analysis procedures assume this connection to be infinitely stiff and does not allow rotational deformation under loading.

Research involving experimental investigations indicate that a unique moment-rotation relationship is exhibited by every steel connection under loading. The analysis assumptions described above therefore do not correlate with the real behaviour of connections under loading. Figure 2.5 illustrates the real behaviour of connections in terms of moment-rotation behaviour. The horizontal axis (θ) in figure 2.5 represents a pinned connection referred

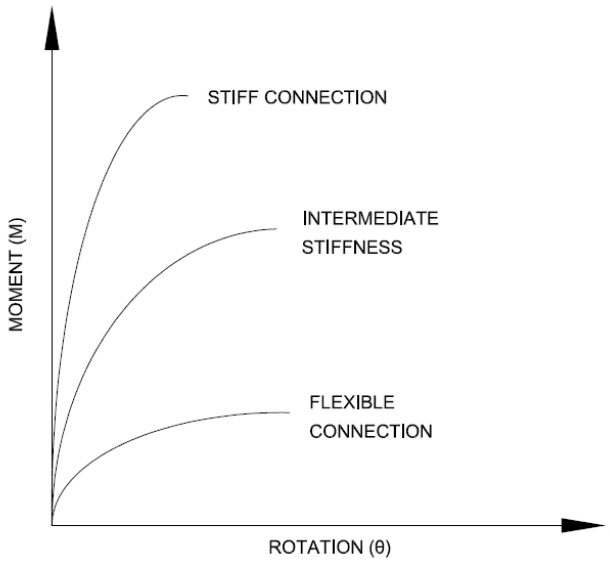

Figure 2.5: Moment-rotation behaviour of connections. (Kruger et al., 1995)

to above as the first category, where the vertical axis (M) represents the behaviour of a fully rigid connection (Kruger et al., 1995). It is clearly indicated that the real behaviour of a connection under loading is somewhere in between these two extreme forms of behaviour. The plotted moment-rotation curves are non-linear throughout the entire curve. However, Lui and Chen indicated that although the nature of the curve does not exhibit any linear zones, it can be assumed that the initial portion is linear for serviceability limit state investigations and analysis, but not for ultimate limit state considerations (Lui and Chen, 1987).

The moment-rotation curve indicates accurately the connection response under loading. During unloading, the connection exhibits a linear moment-rotation curve in the form of a line parallel to the slope of the initial part of the moment-rotation curve exhibited by the connections under loading (Lui and Chen, 1987). The unloading behaviour of the connection is also exhibited when the applied load directions are changed. This is discussed further in section 2.6.3.

The characteristics of a connection are illustrated by the moment-rotation curve of the connection. Characteristics include stiffness, moment capacity and ductility of the connection (Abolmaali et al., 2005). The stiffness is determined by the slope of the curve, whereas the ultimate moment capacity is given by the peak of the curve (Kruger et al., 1995). It is also noted that with greater flexibility of the connection, greater rotational deformation is exhibited by the connection and causes less moment being transferred between the structural members (ECCS, 1992).

2.6 EFFECT OF MOMENT-ROTATION BEHAVIOUR OF JOINTS AND BASES ON PORTAL FRAMES

The real behaviour of joints and bases in a frame analysis will influence the displacements, axial force distribution and bending moments, as well as failure modes. Gerstle supports this statement in his article stating that, by neglecting to take into account the real joint behaviour, the response predictions will be unrealistic and will lead to less optimal designs (Gerstle, 1988).

2.6.1 JOINT BEHAVIOUR

When considering a typical moment-fixed beam-column joint, the assumption is made that all forces and moments are transferred through the connecting members with no deformation of the connection. Due to the flexible response of the joint, a rotational deformation is exhibited by the connection under loading. The deformation delays the moment transfer between the structural members, as a certain rotational deformation needs to take place in the connection before the ultimate moment is transferred between the members (Lui and Chen, 1987). This behaviour leads to larger displacements before the ultimate capacity of the connection is recorded. Note that the ultimate load-carrying capacity of the frame is not affected by the more flexible joint behaviour if the ultimate capacity of the connection is sufficient or greater than the capacity of a joining structural member. The force and moment distribution in the structural members are also affected an a similar manner. The moment distribution is affected as the connection deforms under loading and which will therefore not perfectly transfer moments between the structural members as would be the case with fully-rigid joints. Furthermore, due to the increased flexibility of the connection, the effective length of the column increases in comparison with a fully-rigid connection (Gerstle, 1988).

2.6.2 COLUMN BASE BEHAVIOUR

Column bases have opposing effects on the frame compared to the described joint behaviour, depending on the layout of the base plate. If the column base is considered as pinned in the ideal case, lower displacements will be exhibited by the real frame, as a rotational restraint is provided by the plate-concrete interaction. Rotational restraint also causes a non-zero moment at the column base, opposing the result obtained from the analysis using a pinned column base (Jaspart et al., 2008). The effective length of the column also decreases due to the rotational restraint at the base (Howlett et al., 1981).

Fully-rigid bases exhibit rotational deformation under loading. Increased displacement is exhibited by the frame due to the real behaviour of a rigid base not being infinitely rigid. The moment at the base of the column will be slightly lower than the predicted moment obtained from the structural analysis due to rotational deformation taking place (Jaspart et al., 2008). The rotational deformation will also increase the effective length of the column.

Taking the real behaviour of column bases into consideration is necessary for the following reasons (Melchers, 1992):

1. Steel structure designs can be optimized by implementing efficient boundary conditions for structural members depending on their functionality and layout.
2. Accurate displacement prediction in structural analysis.

2.6.3 NECESSITY OF TAKING INTO ACCOUNT THE MOMENT-ROTATION BEHAVIOUR OF JOINTS AND BASES

From the above it is clear that taking into account the real behaviour of joints and bases in a structural analysis leads to the following accurate results:

1. Ultimate frame load capacity.
2. Economical steel structures.
3. Predicted displacements.

These results can be optimized even further in design procedures by taking material and geometric non-linearities into account (Kruger et al., 1995).

Various studies and experimental investigations have been performed on steel connections in determining their moment-rotation response and ultimate moment capacity. It is however noted that although the connection conforms to ultimate limit state criteria, the displacements recorded at ultimate limit state are even greater than the displacements recorded at serviceability limit state (Christopher and Bjorhovde, 1999). The unique moment-rotation joint behaviour exhibited by connections leads to the conclusion that each connection's real behaviour must not be considered in isolation, but must rather be used in the analysis of the full structure in order to consider the effects of the surrounding members joined by the connections (ECCS, 1992).

2.7 MODELLING JOINTS AS ROTATIONAL SPRINGS

Research has found that joints and bases can be modelled accurately in a structural analysis as rotational springs (Simitses et al., 1984; Chan et al., 2005). This section focuses on the theory of springs in finite element analyses and the determination of the rotational spring stiffness to be used in frame analyses.

SPRINGS IN FINITE ELEMENT ANALYSIS

As stated, joints and bases can be modelled as rotational springs as shown in figure 2.6. In section 2.5 it was stated that the deformations caused by axial and shear forces are negligibly small compared to rotational deformations caused by a moment applied to the connections. A rotational spring has the ability to simulate joint behaviour accurately for all practical purposes as it exhibits rotational deformation under loading, but not transverse displacements. A rotational spring is considered to be dimensionless in size as it simplifies calculations and does not act as a beam element.

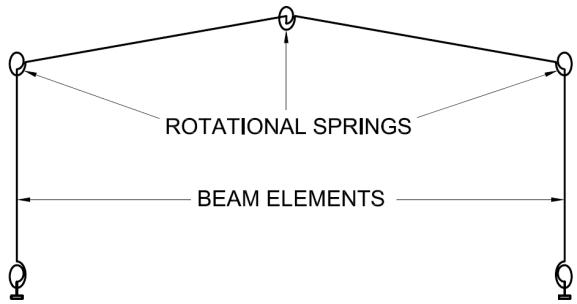

Figure 2.6: Portal frame analysis modelling connections as rotational springs.

Chan and Chui explains the implementation of rotational springs at the ends of a beam element in terms of the stiffness matrix as follows (Chan and Chui, 2000):

Figure 2.7 shows a rotational spring subject to a moment and exhibiting rotational deformation θ_b of the beam and θ_c, representing the rotational deformation of the column. Note that the two rotational deformations are not necessarily equal due to the properties of the structural elements. The applied moments, M_b and M_c are equal and opposite due to equilibrium requirements as given in equation 2.1.

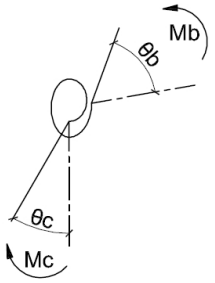

Figure 2.7: Rotational spring under deformation. (Chan and Chui, 2000)

$$M_c + M_b = 0 \tag{2.1}$$

and

$$M_c = S_c(\theta_c - \theta_b) \tag{2.2}$$

$$M_b = -M_c = S_c(\theta_b - \theta_c) \tag{2.3}$$

where

$M_b = Beam\ moment\ at\ the\ connection$

$M_c = Column\ moment\ at\ the\ connection$

$S_c = Connection\ stiffness$

Equation 2.2 can now be rewritten in the incremental stiffness matrix form given in equation 2.4 as:

$$\begin{pmatrix} \triangle M_c \\ \triangle M_b \end{pmatrix} = \begin{bmatrix} S_c & -S_c \\ -S_c & S_c \end{bmatrix} \begin{pmatrix} \triangle \theta_c \\ \triangle \theta_c \end{pmatrix} \tag{2.4}$$

where

$\triangle M_c, \triangle M_b = incremental\ nodal\ moments$

$\triangle \theta_c, \triangle \theta_b = incremental\ nodal\ rotations$

The instantaneous connection stiffness is now given by equation 2.5.

$$S_c = \frac{dM}{d\phi_c} \tag{2.5}$$

and

$$\phi_c = \theta_c - \theta_b \tag{2.6}$$

where

$M = moment\ at\ the\ joint$

$\phi_c = resulting\ rotation\ in\ connection$

The connection stiffness matrix is now incorporated into the conventional stiffness matrix for beam elements to account for the joint flexibility. Similar to equation 2.4, the stiffness equation for a beam element is given in equation 2.7 below.

$$\begin{pmatrix} \triangle M_{bi} \\ \triangle M_{bj} \end{pmatrix} = \begin{bmatrix} K_{ii} & K_{ij} \\ K_{ji} & K_{jj} \end{bmatrix} \begin{pmatrix} \triangle \theta_{bi} \\ \triangle \theta_{bj} \end{pmatrix} \tag{2.7}$$

Subscripts i and j refer to the end nodes of the beam element and K_{ii} to the element stiffness. Combining equation 2.4 with equation 2.7 by adding a rotational spring to each beam end, results in the following:

$$\begin{pmatrix} \triangle M_{ci} \\ \triangle M_{bi} \\ \triangle M_{bj} \\ \triangle M_{cj} \end{pmatrix} = \begin{bmatrix} S_{ci} & -S_{ci} & 0 & 0 \\ -S_{ci} & S_{ci} + K_{ii} & K_{ij} & 0 \\ 0 & K_{ji} & S_{cj} + K_{jj} & -S_{cj} \\ 0 & 0 & -S_{cj} & S_{cj} \end{bmatrix} \begin{pmatrix} \triangle \theta_{ci} \\ \triangle \theta_{bi} \\ \triangle \theta_{bj} \\ \triangle \theta_{cj} \end{pmatrix} \tag{2.8}$$

Equation 2.8 can be further refined by eliminating internal degrees of freedom and transforming to the global coordinate system of the model.

DETERMINATION OF ROTATIONAL SPRING STIFFNESS FROM MOMENT-ROTATION CURVE

Modern structural analysis software has the capability of incorporating rotational springs in frame analyses. It is therefore necessary to determine the rotational stiffness of the spring used in a frame analysis. Certain software do allow the use of a non-linear spring stiffness in analyses. The non-linear approach to an analysis involves a piece-wise linear approach through performing in the analysis in time increments. Loads are applied in increments after which the deformation and load effects need to be carried forward in each increment. This method of analysis is highly specialized and time-consuming with the results produced being quite complex to interpret. It can be concluded that implementing these software packages in practice is inefficient as they are not always available in most engineering design offices. Simitses *et al.* supports this statement in a study performed using non-linear rotational spring stiffness in frame analyses. The study led to the conclusion that the difference in global structural response was negligibly small compared to performing the same analysis with linear rotational spring stiffness (Simitses et al., 1984).

As discussed in section 2.5, the stiffness of a connection is determined by the first derivative of the moment-rotation curve, or the slope of the curve as it is more commonly referred to. Studies conducted incorporating connection flexibility in frame analyses resulted in to two possible stiffness formulations that are used in frame analyses. These are referred to as the initial stiffness and the secant stiffness to the working moment capacity of the connection (Gerstle, 1988). In figure 2.8 it can be seen that the unloading stiffness of the connection is a linear line parallel to the initial stiffness of the connection (Christopher and Bjorhovde, 1999).

2.8 SECOND ORDER ANALYSIS

A common frame analysis technique used in practice is a first order linear elastic analysis. This analysis technique, which has been used throughout the industry for many years, has several drawbacks. The basic principle of a first order analysis is that displacements of the structure are assumed to be small and therefore calculates member

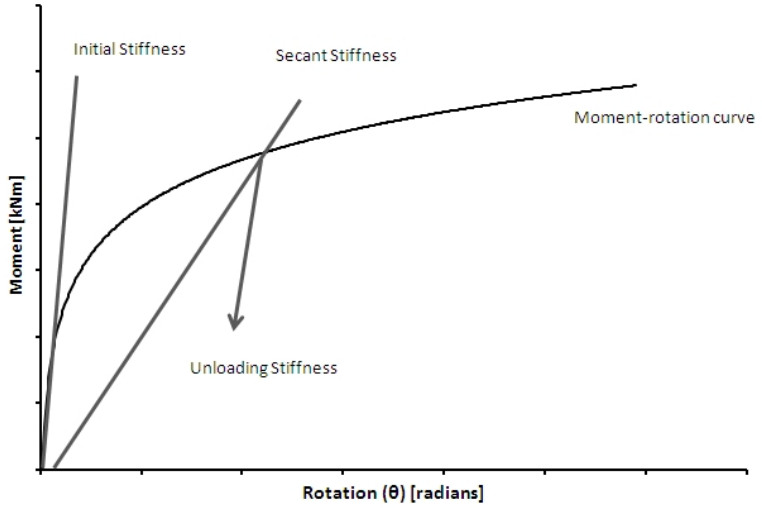

Figure 2.8: Determination of rotational spring stiffness from M-θ curve. (Christopher and Bjorhovde, 1999)

forces based on the undeformed shape of the structure (Chen et al., 1996). The linear nature of the analysis therefore produces linear load-displacement behaviour. It furthermore fails to account for the plasticity of the material and the geometrical non-linear behaviour of the structure (Chen et al., 1996).

Modern design practice utilizes a second order analysis technique in order to produce more accurate results for calculated displacements, forces and moments. A second order analysis takes into account the deformed shape of the structure in the calculation of displacements and forces (Chen et al., 1996). The distribution of bending moments is significantly affected when compared to the results produced by a first order analysis. Literature refers to second order analysis as structural analysis that include P-Delta effects.

The P-Delta effect refers to the member curvature ($P - \delta$) and the member instability ($P - \Delta$) of a frame subjected to applied loads (Chen et al., 1996). These P-delta effects are produced as the frame is gradually loaded. The axial force in a member causes a curved deformation of the member when compared to the undeformed shape of the member (CTICM and SCI, 2008). Curvature of a member under load is referred to as the $P - \delta$ effect. The second order analysis determines the curvature of the members under each load increment and carries it forward to the next load increment for analysis of the structure in the deformed state (Chen et al., 1996).

$P - \Delta$ effects refer to the sway of the structural members in a frame due to axial loading (CTICM and SCI, 2008). Sway is the displacement of the member ends in the deformed structural state (Chen et al., 1996). As described above, the deformed state of the member is determined for each load increment and is carried forward to the next load increment of the analysis.

Second order analyses account for the effects on the structure as it deforms in the analyses, but it does not provide any inelastic structural response information (Chen et al., 1996). It is common to find that the ultimate loads calculated to be resisted by the frame are lower than those calculated from a first order elastic analysis, but greater accuracy is achieved through a second order analysis.

2.9 SEMI-RIGID DESIGN

Research has indicated that 50% of the total cost of steel structures can be related to the type of the connections used (Mativo et al., 2005). Modern analyses and design techniques have been researched and developed in order to optimize the design of steel structures by considering the real behaviour of joints and their effect on frame response in terms of displacements, force and moment distribution. The Load and Resistance Factor Design (LRFD) specifications of the American Institute of Steel Construction (AISC) have adopted the use of the real behaviour of joints in frame design (Mativo et al., 2005). Joints are classified according to the restraint provided by the connection. Semi-rigid design according to AISC specifications, involves regarding a connection as a partially-restrained (PR) connection, therefore the restraint provided by the connection lies between that of simple- and fully-restrained connections. Designs implementing PR connections must provide proof of the connection resistance in the form of a technical investigation or of the analytical method used.

Eurocode 3 adopted semi-rigid design in their design specifications known as the component method. The component method is used to calculate the strength and stiffness of joints to be used in analysis and design (Jaspart, 2002). Although this study does not involve semi-rigid design, a short overview of the basic principle of semi-rigid design according to the Eurocode 3 component method is discussed in section 2.9.1.

The South African National Standard for Limit-state design of hot rolled steelwork provides no guidelines for semi-rigid design as the Eurocode does, but rather follows a similar approach to that of the AISC. The moment-rotation behaviour of the joints being used in an analysis, has to be obtained from a research test or from a technical report. Furthermore the joint must be analyzed by linear analysis using the secant stiffness from the moment-rotation curve of the joint or by a full non-linear analysis using the obtained moment-rotation curve of the joint (SANS10162-1:2005).

2.9.1 EUROCODE 3 COMPONENT METHOD FOR JOINT REPRESENTATION

The Eurocode component method determines the strength and stiffness of joints in an analysis which takes into account each individual component in the joint (Jaspart, 2002) by implementing the following steps:

1. Identification of the active components in the connection depending on the loading.
2. Evaluating the mechanical characteristics and properties of the identified components..
3. Regarding the joint now as an assembly of all the identified active components and determining the mechanical characteristics and properties of the assembly.

The Eurocode calls the way a joint is modelled in an analysis as joint representation (Jaspart, 2002). Joint representation is divided into the following four sections:

- Characterization, which refers to the stiffness, strength and ductility of the joint.
- Classification, which refers to the boundary conditions provided by the joint to the frame.
- Modelling, which refers to the way the joint is modelled in the frame analysis.
- Idealization, which refers to the moment-rotation curve of the joint used in the analysis.

Joints are classified according to their stiffness in comparison with the stiffness boundaries set out in the code. An initial design stiffness is calculated according to formulas as set out in the code. The initial stiffness is compared to the stiffness boundaries after which the joint is designed according to the stiffness, i.e. rigid, semi-rigid or pinned.

Connection strength is determined by comparing the design moment of the joint to the strength boundaries set out in the code. Once again these boundaries are used to classify the joint as full strength, partial strength or pinned. Limited research has been done on the ductility of joints. Eurocode 3 provides guidelines to classify a joint according to ductility considerations (EN1993-1-8, 2005). However, only guidelines for common beam-column joints have been set out in the code.

The joint has to be modelled in a frame analysis to provide sufficient resistance and rotational stiffness as determined by the criteria set out according to joint representation in the code. The code provides a guideline to the type of analysis that needs to be conducted according to the results of the joint classification set out in table 2.1 below (EN1993-1-8, 2005).

Table 2.1: Joint modelling according to Eurocode 3. (EN1993-1-8, 2005)

Method of Global Analysis	**Classification of Joint**		
Elastic	Nominally pinned	Rigid	Semi-rigid
Rigid-Plastic	Nominally pinned	Full-strength	Partial-strength
Elastic-Plastic	Nominally pinned	Rigid and full-strength	Semi-rigid and partial-strength Semi-rigid and full-strength Rigid and partial strength
Type of joint model	Simple	Continuous	Semi-continuous

Column bases follow a similar approach as do joints in the component method. The steps of identification, characterization, assembly, classification and modelling need to be performed on the bases similar to that of joints. The difference with bases is with the components considered. Base classification takes into account the following components (Wald et al., 2008):

- Base plate and concrete block in compression.
- Bending of the base plate.
- Anchor bolts in tension and shear.

Chapter 3

RESEARCH METHODOLOGY

3.1 INTRODUCTION

This chapter describes the research methodology followed for investigating the structural analysis for modelling real connection behaviour in the displacement determination of portal frames. The data required for the investigation as well as for its implementation is discussed, as well as the method followed in order to arrive at the required results. Scope and limitation sections are provided in order to present the extent of the research, after which the chapter ends with a conclusion.

The methodology described in this chapter will focus on the determination of displacements of portal frame structures taking into account the moment-rotation behaviour of connections and column bases in the structural analysis of portal frames.

3.2 PORTAL FRAMES

Portal frame structures consist of columns and girders forming a portal frame. These members are placed along the length of the structure at fixed intervals, and so provide the outside dimensions of the structure. The portals are laterally connected by purlins which in turn support the cladding for the roof and walls. Bracing systems provide stability and lateral support to the structure.

Portal frames are designed in order to support the following loads in accordance with South African National Standard: Basis of Structural Design and Actions for Buildings and Industrial Structures part one clause 7.3 (SANS10160:2011):

1. Structure own-weight together with an imposed load applied uniformly across the full roof.
2. Structure own-weight together with an imposed load applied uniformly over half the roof.
3. Wind imposed along the structure.
4. Wind imposed across the structure.

As stated above, loads are determined according to the SANS 10160:2011 parts one to three. The South African National Standard: Part 1 The structural use of steel (SANS10162-1:2005) is then used to design the structure according to limit state design methods.

3.2.1 REFERENCE PORTAL FRAME FOR RESEARCH

A reference portal frame, spanning 12 m and 4,5 m in total height, was designed for the purpose of this investigation. The frame originated during previous studies conducted at Stellenbosch University regarding the determination of the moment-rotation behaviour of beam-column haunch connections (Truter, 1997) and column bases (Mostert, 1998). Since these studies were completed and published, the SABS 0160 and SANS 10162 were revised, updated and reprinted. It was therefore decided to re-design the reference portal frame having similar dimensions and sections in accordance with the latest SANS 10160 and SANS 10162, as well as to use the latest steel grade rolled in South Africa since 2008, i.e. S355JR steel. Appendix A contains all the design calculations of the reference portal frame and appendix B the detailed drawings.

3.3 METHODOLOGY

The research methodology consists of various phases of data collection and the analysis of different load cases to be applied in order to asses the accuracy and feasibility of the proposed method of displacement determination of portal frames. Figure 3.1 at the end of this section illustrates a flow chart of the research methodology.

3.3.1 DATA REQUIRED

EXPERIMENTALLY-RECORDED PORTAL FRAME DISPLACEMENTS

An experimental investigation was conducted to accurately determine the displacements of a portal frame structure subjected to certain loads. Due to the nature of the reference portal frame structure used in previous studies, it would be uneconomical and unfeasible to construct a 12 m span portal frame for an experimental investigation in the laboratory. It was therefore decided to design a 5 m span portal frame and subject it to similar load cases having similar layout of the structural elements as well as similar connections and their components. The 5 m span experimental frame (or test specimen) serves as a scaled-down model of the reference portal frame, which will be used for obtaining accurate and real displacement data of a portal frame structure. The test specimen will be tested under vertical and horizontal loads, as well as for two types of support conditions. Different load cases ensure accurate displacement data of the test specimen in different response systems and displacement directions. Furthermore, two different support conditions will be used in the experimental investigation, creating true modelling support conditions and real construction support conditions. Different supports create the opportunity to isolate the real effect of the moment-rotation behaviour of column bases and therefore assesses the deformation effects of the rigid connections separately. All necessary testing apparatus as well as measuring equipment used in the Structural Engineering Laboratory at Stellenbosch University is frequently inspected and serviced in order to ensure that reliable and accurate data is generated during testing.

MOMENT-ROTATION BEHAVIOUR OF CONNECTIONS AND BASES

The moment-rotation behaviour of steel connections is mostly determined experimentally for accuracy purposes and is unique to each structural steel connection. Mathematical models of moment-rotation determination has been researched in the past, but tends to be not sufficiently accurate unless determined from previous experimental data. It is therefore necessary to develop finite element models of each connection in order to determine the moment-rotation behaviour of the connections used this investigation. Truter's work provides experimental results for a haunched beam-column connection of the reference portal frame (Truter, 1997). An accurate finite element model containing contact and interaction definitions of the structural components and the material models is to be developed of Truter's experimentally-investigated beam-column haunch connection. The results of the finite element model will be assessed against against Truter's experimental results. If the finite element model yields acceptable results, the modelling standards of this model will be used for all the finite element models throughout

the study.

Finite element models were developed to the standards of the model accurately simulating the experimental results of Truter. A model of each connection used in this study will provide a moment-rotation behaviour unique to that connection that will then be used for the structural analysis of the portal frame. Finite element models were developed for the following connections in this study:

1. Haunch connection investigated by Truter to set the modelling standards.
2. Test specimen haunch connection.
3. Test specimen ridge connection.
4. Test specimen column base and grouted support.
5. Reference portal frame haunch connection.
6. Reference portal frame ridge connection.
7. Reference portal frame column base and support.

3.3.2 STRUCTURAL ANALYSIS

A second order analysis is usually conducted to analyze a portal frame. As stated, it is necessary to take into account for the real behaviour of joints, as the elastic deformation of joints and bases contribute to the overall maximum displacements of the structure. It is thus proposed by this study to investigate the feasibility of taking into consideration the real behaviour of joints in the structural analysis of portal frames. This is achieved by modelling a joint as a rotational spring with a linear stiffness. The rotational spring will therefore transfer the rotational stiffness of the joint to the beam elements connected to it, i.e. the beam elements representing the structural components can rotate in-plane about each other, and are not connected infinitely rigid as assumed in typical structural analyses of portal frames.

The moment-rotation behaviour of connections indicate the stiffness of a connection through the slope of the curve. A linear stiffness of the connection modelled can thus be determined from the slope of the curve at various points, for example the initial linear elastic stiffness or the secant stiffness of the working moment of the connection. This is explained in detail in section 2.7. Applying the determined stiffness to a linear value for a rotational spring will thus simulate the real connection stiffness in the structural analysis of the structure. The moment-rotation curves obtained from the finite element models described above, provide the necessary data in order to determine a spring stiffness for each connection.

A structural analysis of the test specimen was performed by using rotational springs. Comparing the displacements obtained from the analysis to the experimental results will assess the accuracy of the proposed method of analysis, i.e. modelling real connection behaviour through linear rotational springs. Furthermore, it will be required to obtain the optimum spring stiffness value from the moment-rotation curves of the connections.

The successful determination of the optimum rotational spring stiffness for modelling connections will lead to the use of rotational springs in the analysis of the reference portal frame. The reference portal frame analysis will involve applying loads according to SANS 10160:2011 parts one to three. Loads are spread across the structure simulating self-weight, imposed loads and wind loads. Column bases will also be modelled as rotational springs taking into account the rotation of the column base on the concrete. Accurate displacements of the structure can thus be obtained from this analysis by using the real behaviour of joints and bases.

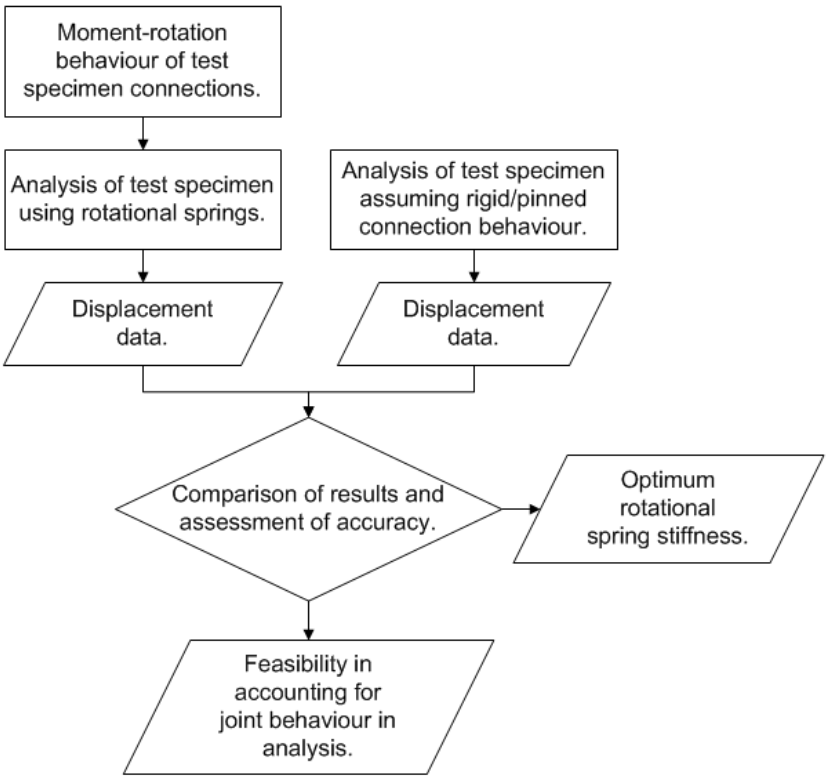

Figure 3.1: Basic process of assessing the accuracy of structural analysis using rotational springs.

3.4 SCOPE OF RESEARCH

This research deals with the modelling of real connection behaviour in the structural analysis of pitched roof portal frames, to determine displacements of the structure under loading. Connections include grouted pinned column bases, haunched beam-column connections and an extended endplate ridge connection. Displacements of the structure are assessed by the set criteria of serviceability limit state for design purposes. Serviceability limit state requirements refer to the elastic response of the structure to normal occupancy and external factors. The analyses performed on the portal frames ensure that all components of the structure remain within their elastic range and no plastic deformation occurs. A two dimensional (in-plane) second order elastic analysis is performed in all cases, as this is sufficient to model the portal frame response under loading for the determination of displacements, design forces and bending moments. The scope of the research involves only the determination of more accurate displacements of portal frames for serviceability limit state requirements. It does not apply to semi-rigid design and redistribution of moments in the structural members for ultimate limit state design requirements, as in the case of semi-rigid design principles.

Three-dimensional, finite-element connection models do involve non-linear elastic perfect plastic analyses, however no strain-hardening is defined in these analyses. Connection stiffness values are obtained from the elastic region of the connection's moment-rotation behaviour, except in the case of modelling of column bases where the connection is modelled with a non-linear stiffness.

3.5 LIMITATIONS

This investigation proposes a method which takes into account the real behaviour of joints in analysis. There is however certain limitations to the practicality and implementation of the method. Moment-rotation data for joints are not widely available for connections. This is mainly due to the fact that each connection is unique due to the components the connection consists of, and due to their layout and dimensions. Databases containing

moment-rotation data for certain connections have been created through research and studies conducted throughout the world. However, unless the designer uses the exact layout and dimensions of a connection from a database, the data is of no value to the designer. Therefore in most cases it is left to the designer to create finite element models of the designed connections or perform experimental tests, both of which are too time consuming and ineffective for design offices. Software for creating complex finite element models of connections including contact and interaction modelling, are expensive and out of scope for everyday design-office use.

A method for displacement determination is also just as good as the feasibility of the method. It is of no use implementing a method that has not been found feasible to determine accurate displacements of structures. It is therefore part of the scope of this research to investigate the method of taking into account real joint behaviour in structural analyses, as well as investigating the feasibility of the method for implementation in design offices.

3.6 CONCLUSION

This chapter described the data required as well as the methodology to be followed to arrive at a conclusion of the research. This chapter is followed by a chapter discussing the finite element models used to obtain all moment-rotation curves and a chapter on the experimental investigation conducted. Finally there are chapters on the structural analyses that have been conducted to arrive at the required results and the conclusions of the research that have been arrived at.

Chapter 4

FINITE ELEMENT ANALYSIS

Experimental studies were conducted as part of many research programmes in the field of engineering so as to provide knowledge of and solutions to problems facing designers. Conducting experimental programmes for each engineering problem would be the ideal, but extremely inefficient with regards to time and cost. Modern computer technology provides engineers with the opportunity to obtain analytical solutions to engineering problems through the application of finite elements. The finite element method is a numerical simulation of engineering problems through finite elements described by differential equations and integral expressions. (Cook et al., 2002) It is thus unnecessary to conduct expensive and time-consuming experiments if an accurate finite element model of the problem can be created to provide a solution to the problem.

Modern finite element software is utilized throughout the engineering industry and these softwares vary in complexity and even to a certain extend in accuracy. For the purpose of modelling the connections used in this study, ABAQUS Standard version 6.10-2 software will be used as it has the ability to accurately model the connections, the components they consist of and the interaction between these components. It is however necessary to calibrate and validate these finite element models to ensure the accuracy of the simulation. Previous studies conducted at Stellenbosch University ((Truter, 1997), (Mostert, 1998)) provide experimental results of portal haunch connections and column bases respectively. The experimental results from these studies are used together with the modelling standards and procedures, as described in Prabha *et al.* to verify the accuracy of the finite element models developed in this study (Prabha et al. (s.a.)).

This chapter starts with the explanation of the modelling standards implemented in the development of the finite element models of the connections and column bases. Each connection is considered independently in terms of response, mode of failure and moment-rotation curves. Note that due to the unsymmetrical layout of the connections, a different moment-rotation curve is exhibited by each connection for upward and downward, in-plane rotational deformation and therefore two moment-rotation curves are presented for each connection providing two stiffness values depending on the deformation.

4.1 MODEL DESIGN

4.1.1 ELEMENT TYPE AND MESH DENSITY

Rectangular solid elements are used for the analysis of the connections. Solid elements are also referred to as brick elements. The motivation behind the use of solid elements is that they would accurately model all the components of the connection in three dimensions. Each component is created as a part, meshed with solid elements across

their geometry. Meshed parts are then used to create an assembly for each connection model. Solid elements can be of linear or quadratic nature. Linear solid elements possess eight nodes, whereas quadratic solid elements have 20 nodes as shown in figure 4.1. Each node has three translation degrees of freedom (DOF's), one in each nodal direction. This results in a total of 24 DOF's for linear solid elements and 60 DOF's for quadratic solid elements. Solid elements exhibit bending accurately if meshed sufficiently dense over the height of the component in bending. Accurate simulation of bending is a vital attribute required of the connection models developed for the purpose of obtaining the response under loading of the connection (Cook et al., 2002). An element exhibiting accurate bending will result in accurate displacements being recorded throughout the analysis, resulting in accurate moment-rotation curves being available for the purpose of the study.

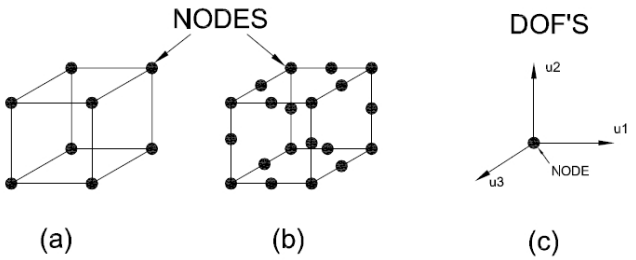

Figure 4.1: Linear (a) and quadratic (b) solid elements with their nodal degrees of freedom (c). (Cook et al., 2002)

FOUR POINT BEAM TEST

A simple four point beam test was conducted analytically and theoretically to determine the mesh density, solid element type as well as the element integration complexity. The four point beam test involves a simply supported beam with equal loads spaced equally from the beam ends. This layout of loads and supports results in a constant bending moment generated between the two loads in the beam. See figure 4.2 for illustration.

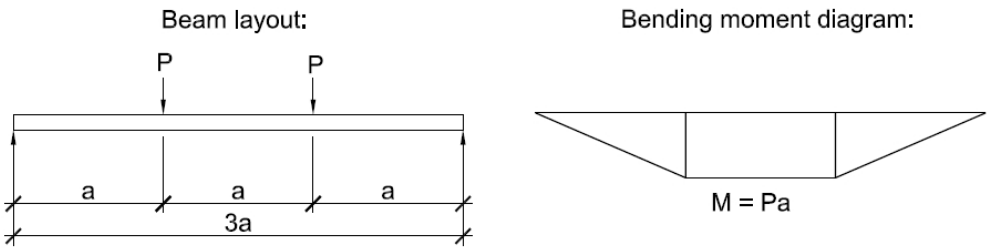

Figure 4.2: Four point beam test layout and bending moment diagram.

For the purpose of the exercise, a simple rectangular beam of 600 mm in length, 10 mm in height and 20 mm in width of Grade 300W steel was chosen to compare the displacements and stresses from the analysis with the theoretically calculated displacements and stresses. The material properties as well as the calculation of the necessary section properties are shown below (SAISC, 2008).

$$E = 200\ GPa$$
$$v = 0,3$$
$$f_y = 300\ MPa$$

$$I = \frac{1}{12}bh^3 = 1666,67\ mm^4$$

Assigning a load P of 500 N to the beam layout as shown in figure 4.2, the maximum displacement and stress in the extreme fibres at midspan are calculated as follows (SAISC, 2008; Craig, 2000):

$$\Delta = \frac{Pl^2a}{24EI}\left(3 - 4\left(\frac{a}{l}\right)^2\right) = 11,49\ mm$$

$$M = Pa = 100\ N.m$$
$$\sigma = \frac{My}{I} = 299,99MPa$$

A similar beam was modelled using ABAQUS, varying the total number of elements through the height of the beam in elevation, as well as varying the solid element type and integration complexity.

Integration complexity refers to the type of integration used on the elements during analysis. Full integration uses eight integration points for a linear solid element and provides sufficient accuracy for the analysis as all stiffness coefficients are integrated in the analysis process. (Cook et al., 2002) Reduced integration uses only one integration point for a linear solid element. The reduction in number of integration points is computationally efficient, but the accuracy is affected. Full integration of linear solid elements were used for all finite element analyses performed in this study.

Figure 4.3 illustrates the von Mises stresses in the beam analysis performed for the four point beam test implementing two elements through the height of the beam. Von Mises stresses are used for illustrations of finite element models throughout this study. Von Mises equivalent stress uses the maximum-distortion-energy theory to form an equivalent stress quantity at a certain point (Craig, 2000). The use of von Mises stresses are thus motivated as it provides the maximum equivalent stress at each point,illustrate maximum stresses and yielding of the material through contour plots. Some of the results from the various element configurations investigated are tabulated below in table 4.1.

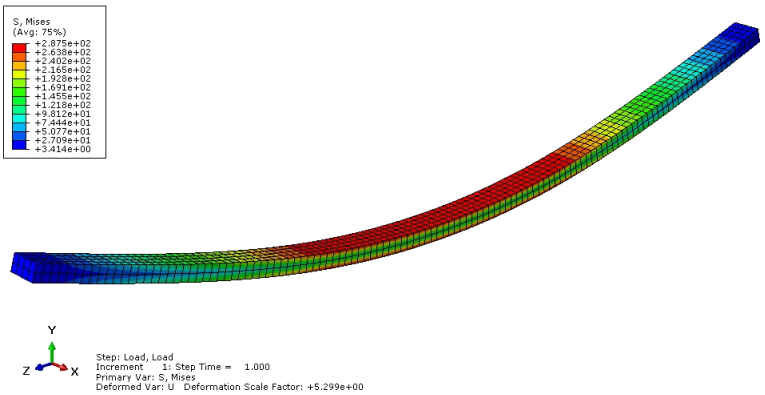

Figure 4.3: Finite element analysis of the described four point beam test showing von Mises stresses.

The results in table 4.1 leads to the conclusion that two linear solid elements (C3D8) through the height of the beam provides accurate results in terms of displacement and also exhibits accurate bending which forms a vital component in the analysis results from the models developed in the study. Using four linear, solid elements through

Table 4.1: Displacements (Δ) and stresses (σ) from four point beam test analysis varying element types and mesh density.

Number of elements		**1**		**2**		**4**		**2**
Description, integration	**Element**	**Δ [mm]**	**σ [MPa]**	**Δ [mm]**	**σ [MPa]**	**Δ [mm]**	**σ [MPa]**	**Analysis time**
Linear, reduced	C3D8R	-1056.910	0.076	-15.279	199.190	-12.265	239.801	1 sec
Linear, full	C3D8	-13.956	354.965	**-11.318**	**284.958**	-11.427	291.701	1.3 sec
Quadratic, reduced	C3D20R	-11.506	300.000	-11.508	300.000	-11.508	300.000	3.4 sec
Quadratic, full	C3D20	-11.506	299.999	-11.507	299.999	-11.508	299.999	5.9 sec
Theoretical				-11.49	299.99			

the height of the beam will increase the accuracy of the model in terms of displacements but also increases the computation time substantially. This makes the exercise time-consuming and inefficient as some models already take approximately 12 hours to analyze during the initial simulations. It was thus decided to model two solid elements through the thickness of each flange of the structural members in the connection models presented in this chapter. Similar geometry of the elements in the flange are used to mesh the web, resulting in a fine mesh across the height of the meshed structural member, ensuring that accurate bending is modelled. The last column of the table provides the analysis time for the beam with two elements in height, but different element types. It is clear from the results that using quadratic elements significantly increases analysis time and the increased accuracy is not worth the extra time of analysis. Note that geometrical non-linearity is modelled to increase accuracy as deformation takes place.

4.1.2 MATERIAL MODEL

The displacement of a structure, according to the criteria set by serviceability limit state, is determined by the elastic response of the structure under loading. It would thus be accurate to model the connections according to the elastic perfectly plastic material model. The elastic perfect plastic material model assumes a component to be elastic until yield stress is reached. After yielding of the member, increased displacements are recorded for a small increase in force, and plastic hinges are allowed to be formed in the model. No strain-hardening effects of the material are assumed in the elastic perfectly plastic material model, but rather a plastic strain limit. This plastic strain refers to the strain in the element at yield stress and is determined by equation 4.1 below. See figure 4.4 for a graphical representation of the material model.

$$\varepsilon_{plastic} = \frac{f_y}{E} \tag{4.1}$$

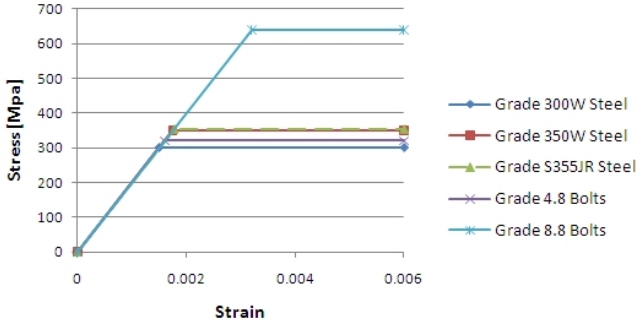

Figure 4.4: Bi-linear elastic perfect plastic material model.

Sections are defined on the three-dimensional parts of the components in the connection. The definition of sections enables parts to posses different material properties according to their nature in practice. This enables accurate material simulation during the finite element analysis.

4.1.3 CONTACT AND INTERACTION MODELLING

Accurate simulation of real connection behaviour is dependent on the interaction between the components of the connection. Interaction of components refer to the way components in the connections, i.e. bolts, column flanges and endplates, make contact and react towards one another in terms of slipping or sliding and protrusion. This is achieved by creating a contact definition between adjacent components and defining their interaction in a normal and tangential direction. Areas of contact in the models include steel-to-steel to simulate bolt and endplate or column flange contact, as well as steel-to-concrete in the case of holding-down bolts cast into concrete or grout.

Sliding between components is also defined. Sliding refers to the mathematical formulation and limits to sliding between adjacent surfaces in the model. Small surface-to-surface sliding between adjacent surfaces is thus defined in order for slipping to occur between components. Note that the slipping only occurs if the shear force causing slipping is greater than the frictional resistance of the surfaces defined in the interaction definition. Prabha *et al.* investigated the finite element modelling of steel connections in ABAQUS in order to determine their moment-rotation behaviour (Prabha et al., s.a.). Their results correlated well with experimental results and therefore it was decided to adopt their interaction definition for the modelling of the connection used in this study.

Normal contact was defined as "hard" contact with the allowance of components to separate. Hard contact refers to a mathematical formulation of adjacent surface contact that does not allow a master- and slave-surface to intersect each other due to compressive forces. The allowance of separation allows components to separate in the case of tensile forces between the adjacent surfaces. In terms its tangential behaviour, the friction formulation was given as penalty friction using a coefficient of 0,3 for steel-to-steel interactions. Penalty friction refers to the principle in mathematical formulation of friction by a penalty function (Cook et al., 2002). This means that frictional resistance between adjacent surfaces is implemented in the model to a simulate roughness between the surfaces to a given coefficient of friction. Concrete-to-steel interactions were modelled by implementing penalty friction with a friction coefficient of 0,4. In each case of contact, the beam endplate or column flange are defined as the master surface and the bolt surface in contact with a master surface, is defined as the slave surface. Figure 4.5 illustrates the contact definition of a beam endplate and column flange, with the column flange set as the master surface and the endplate as the slave surface.

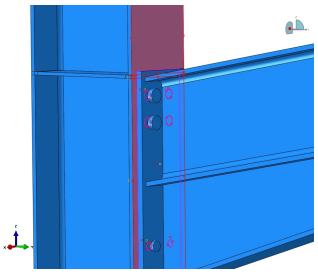

Figure 4.5: Contact definition and interaction of master (red) and slave (pink) surfaces.

At the start of the analysis, adjacent surfaces in a 1 mm boundary were constrained in order for a non-singular stiffness matrix to formulate. Once contact has been established, these constraints were released. Initiating the contact step in the analysis, bolt pretension is applied in order to ensure continuity between the components in the connection after which the initial constraints were released. Bolt pretension was determined according to the "turn

of the nut" method, implemented according to the procedure stipulated in the Southern African Steel Construction Handbook (SAISC, 2008) for bolted connections not using High Strength Friction Grip (HSFG) bolts. This method is explained in detail by Kulak *et al.* and states that bolt pretension according to the method referred to is 70% of the bolt proof stress (Kulak et al., 2001). A load step follows the contact step in the analysis where bolt lengths are restricted to the pretensioned length when the loading is applied to the model.

4.2 COMPARISON OF FINITE ELEMENT ANALYSIS RESULTS WITH EXPERIMENTAL RESULTS

An experimental study was conducted by Truter at Stellenbosch University to determine the moment-rotation behaviour of a portal haunch connection (Truter, 1997). Comparing finite element results with experimental results will assess the accuracy of the finite element model in terms of material properties, interaction definition and boundary conditions. With acceptable correlation of the two moment-rotation curves considered, finite element models can be developed to similar standards. This is in order to determine the moment-rotation relationship of numerous steel connections without an experimental investigation having to be conducted on each connection required for the study.

Figure 4.6 illustrates the finite element model of the haunch connection which was originally tested by Truter. The boundary conditions were similar to the experimental conditions implemented by Truter, i.e. the column base fully restrained against all displacement and rotation. The load was applied as a single point load on the beam end at an angle of 60° with the horizontal axis, similar to the experimental load application used by Truter. A reference point was defined at the beam end in the finite element model and was used for defining load application. This reference point was then constrained to the beam end face with a kinematic couple constraint definition. A special kinematic master-slave constraint links the translational and rotational degrees of freedom between a single node and the degrees of freedom of a given set of nodes. The applied force on the reference node is thus applied to all the nodes on the face of the beam.

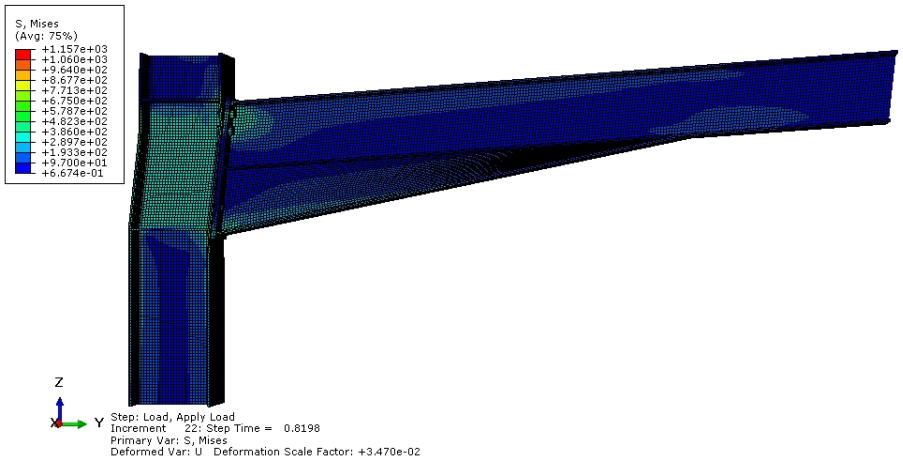

Figure 4.6: Finite element model of the haunch connection which was experimentally investigated by Truter, showing von Mises stresses.

The experimental and analytical moment-rotation curves, as well as a fourth order polynomial regression line are presented in figure 4.7 below. The experimental curve exhibits interference initially. The interference could be a result of measuring equipment slipping over a surface or due to the load application of the hydraulic actuator not being uniform. The experimental regression curve was compared to the analytical curve and it was accepted that the analytical curve is sufficiently accurate. The initial linear region of the experimental regression correlates perfectly with the initial linear region of the analytical curve. The effect of strain hardening will not be exhibited

by the analytical curve due to the material model defined in the finite element model.

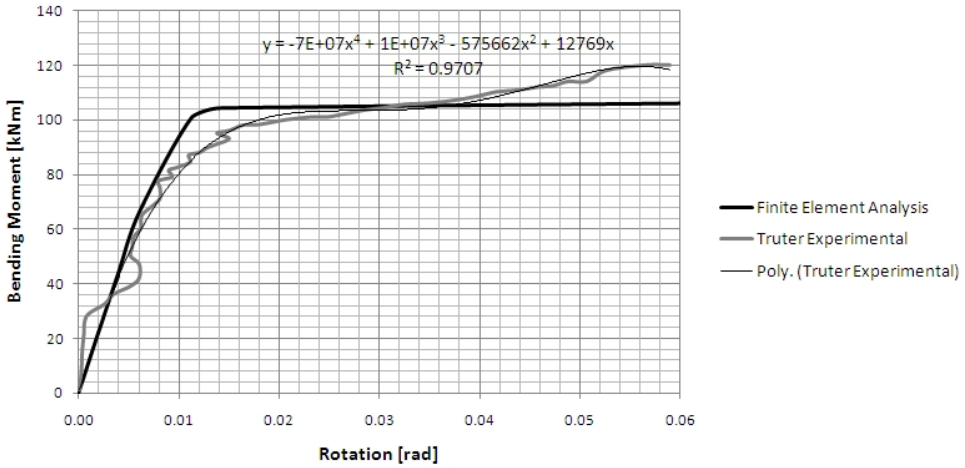

Figure 4.7: Comparison of experimental and analytical moment-rotation curves for the haunch connection investigated by Truter.

It is concluded that the finite element model is sufficiently accurate for the determination of the moment-rotation behaviour of the connections. Similar standards were used to develop finite element models for the determination of moment-rotation behaviour of the connections used in this study. Moment-rotation behaviour curve-determination implemented in this model will be used throughout all the connections presented in this chapter, i.e. fully constrain the one end of the structural component (column in this case) and applying a point load to the free end of the other structural component (beam in this case). This causes a moment in the centre of the connection, determined by multiplying the applied force by the length of the lever arm.

4.3 TEST SPECIMEN PORTAL FRAME HAUNCH CONNECTION

It was stated that each connection exhibits a different stiffness value for each direction of in-plane rotational deformation. This is due to the layout of the connection's components. The haunch connection modelled is designed to withstand greater upward in-plane rotational deformation than downward in-plane rotational deformation. Portal frame design, in most cases, uses the wind-uplift force as the dominant load case on the structure when compared to own-weight and imposed loads. Therefore, the haunch connection exhibits greater ultimate moment capacity for in-plane upward deformation and rotation. Figure 4.8 illustrates the von Mises stresses which developed for in-plane rotational deformation of the experimental portal frame haunch connection for downward and upward deformation respectively.

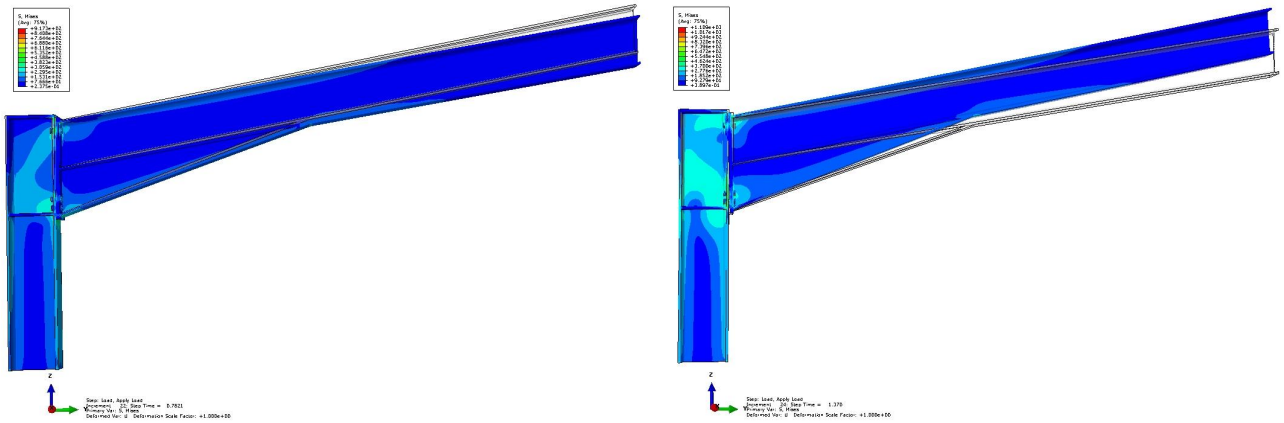

Figure 4.8: Finite element analysis results showing von Mises stresses of the experimental haunch exhibiting downward and upward in-plane rotational deformation respectively.

Dimensions and properties of the model are similar to the haunch connection of the experimental frame investigated and explained in chapter 5. Bolts are M6 of grade 8.8, beam and column consist of $IPE_{AA}100$ steel profiles of grade 350W while plates are of grade 300W steel. A detail drawing of the connection can be found in appendix C.

4.3.1 MOMENT-ROTATION BEHAVIOUR FOR IN-PLANE DOWNWARD ROTATION

When applying a downward force to the beam-end of the connection, the beam endplate undergoes single curvature bending, separating from the column flange at the top and compressing the column flange at the bottom of the endplate. Bolts in the top row of the connection transfer the forces to the column flange, causing greater stress values than in the endplate because the flange is thinner than the endplate. Material yielding followed by plastic deformation is first exhibited by the bolt in the centre of the shank. The mode of failure of this connection can therefore be described as yielding and plastic deformation of the bolts in the top row of the connection. Figure 4.9 illustrates the deformation of the endplates as well as the plastic strain developed in the top row of bolts.

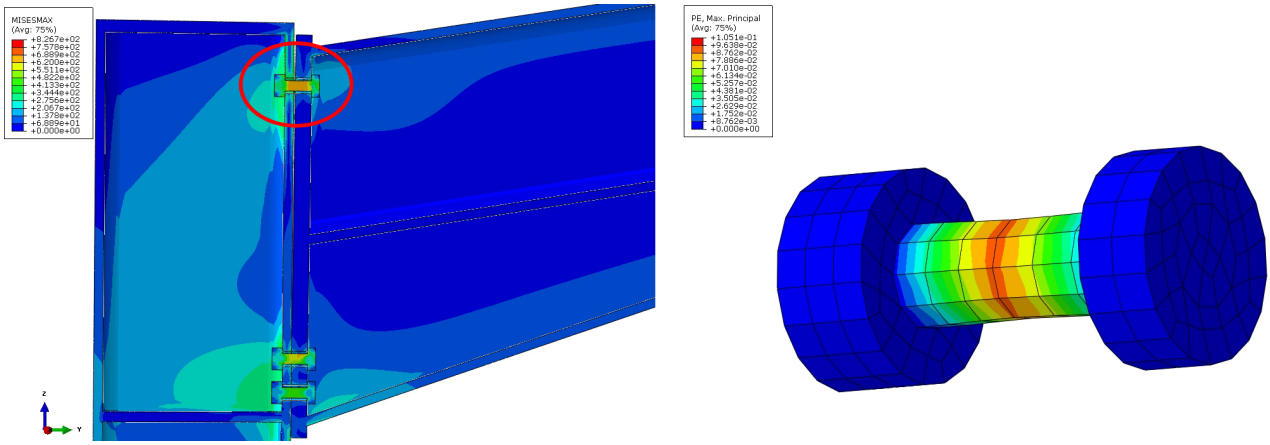

Figure 4.9: Sectional view of the von Mises stresses in the test specimen haunch connection for in-plane downward rotational deformation and plastic strain developed in the bolts respectively.

The moment-rotation behaviour of the connection for in-plane downward deformation is illustrated by figure 4.10. Note that an ultimate moment capacity of 10,805 kNm is reached after plastic deformation has taken place.

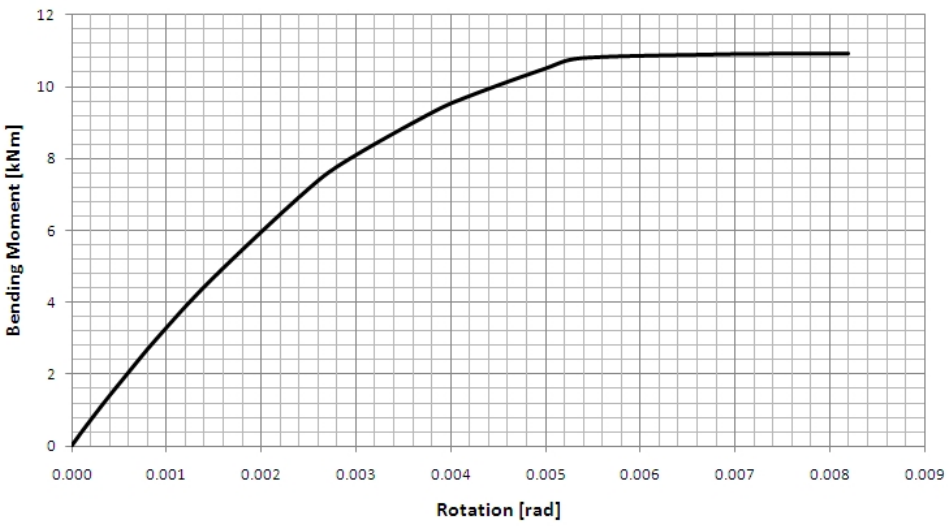

Figure 4.10: Moment-rotation curve for in-plane downward rotational deformation of the test specimen haunch connection.

4.3.2 MOMENT-ROTATION BEHAVIOUR FOR IN-PLANE UPWARD ROTATION

An upward force applied to the connection exhibits a somewhat different response when compared to the downward force described earlier. The endplate is substantially stiffer than the column flange, but both exhibit double curvature bending under deformation. Double curvature bending is due to the two rows of bolts in the lower part of the connection forcing the column flange and endplate to create an inflection point in bending between the two rows of bolts. Failure occurs with the yielding and failure of the bottom row of bolts in the connection and is illustrated in figure 4.11. The deformation of the endplates and column flange as well as the plastic strain developed in the bottom row of bolts are similar to those referred to in section 4.3.1. Note how the plastic strain initially develops to the side of the bolt shank which means that the bolt undergoes bending deformation due to the endplate and column flange deformation, and not due to pure tension as assumed in design calculations. The bending deformation of the bolts due to excessive endplate and column flange deformation is termed prying action.

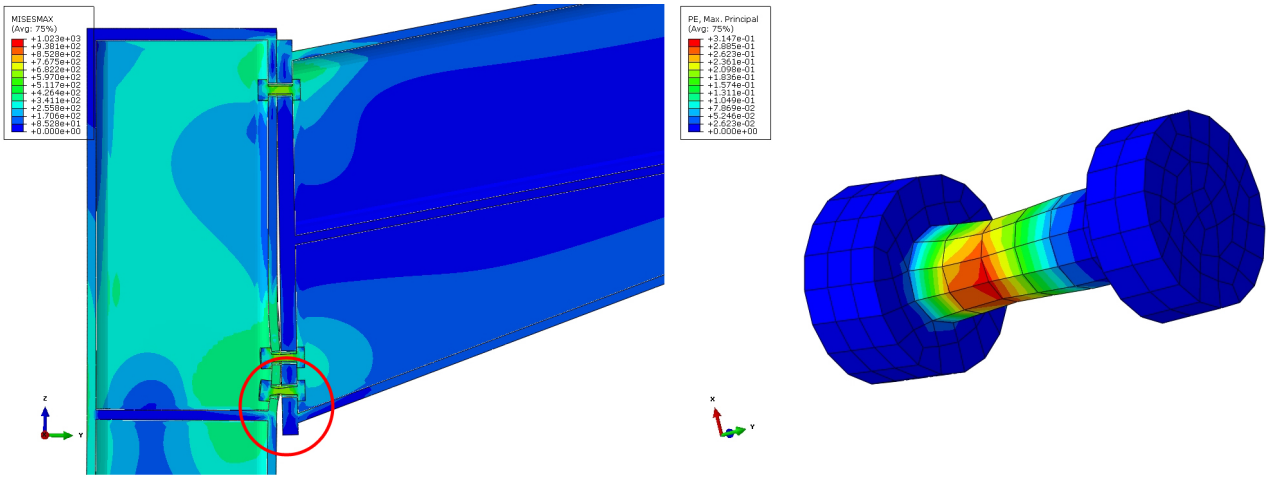

Figure 4.11: Sectional view of the von Mises stresses in the test specimen haunch connection for in-plane upward rotational deformation and plastic strain developed in the bolts respectively.

Figure 4.12 illustrates the moment-rotation behaviour of the connection for in-plane upward deformations. An ultimate moment capacity of 17,062 kNm is reached. This is substantially greater than the 10,805 kNm for in-plane downward deformation discussed above and supports the statement regarding the greater design strength for in-plane upward rotational deformation of the connection.

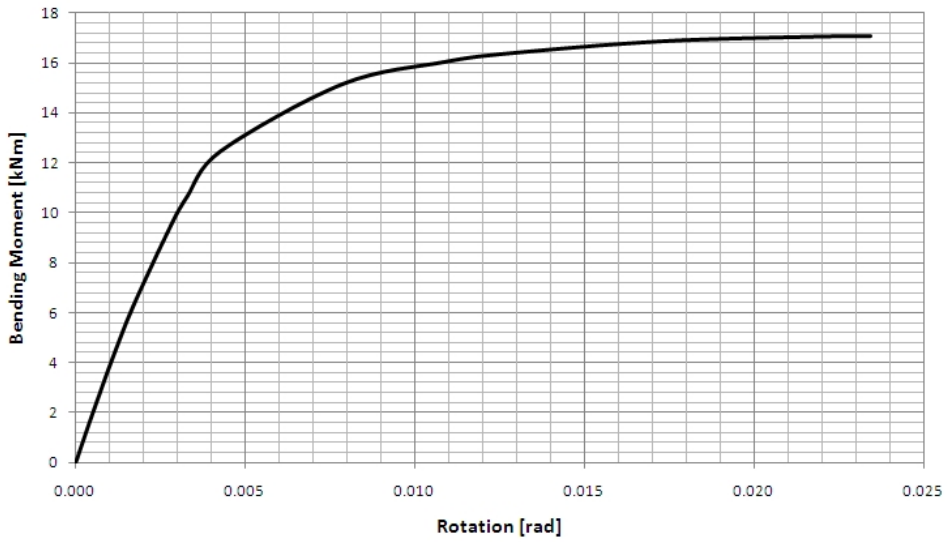

Figure 4.12: Moment-rotation curve for upward in-plane rotational deformation of the test specimen haunch connection.

4.4 TEST SPECIMEN RIDGE CONNECTION

Portal frame ridge connections deform in the opposite direction to the in-plane rotation of the haunch connection due to the layout and response of the frame for vertically applied loads. The ridge connection therefore extends above the connection to form an extended endplate, providing an increased stiffness and moment capacity against uplift forces applied to the portal frame. A load application interface was developed in order to apply loads to the test specimen in the experimental investigation, and therefore the endplates extend substantially below the connection creating an interface for load application by means of a fork design. Layouts of the test setup and load application interfaces are attached as appendix D. The experimental ridge connection now has a symmetrical layout in terms of the endplate extensions and bolts. It was decided to model the connection exactly as on the test specimen in order to ensure that an accurate moment-rotation curve was obtained for analysis. Bolts are M10 of grade 8.8, beams consist of $IPE_{AA}100$ steel profiles of grade 350W and plates are of grade 300W steel. A detailed drawing of the connection can be found in appendix C.

Figure 4.13 illustrates the in-plane rotational deformation of the experimental portal frame ridge connection for in-plane downward and upward deformation respectively.

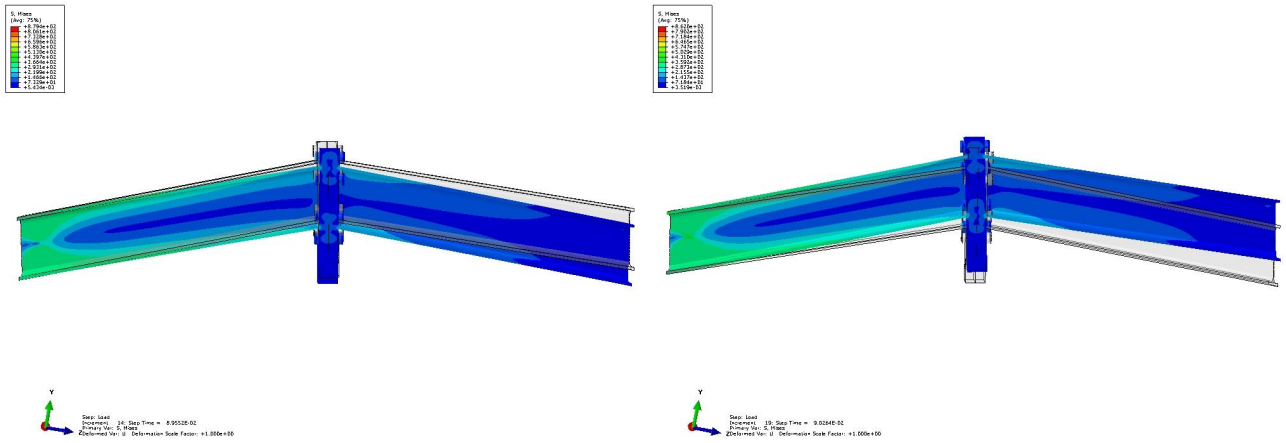

Figure 4.13: Finite element analysis results showing von Mises stresses of the test specimen ridge exhibiting in-plane downward and upward rotational deformation respectively.

It is clear from figure 4.13 that the von Mises stresses develop at the fixed support end of the model. As stated, the connection is designed to support the load application interface of the experimental investigation, which therefore led to a substantially greater endplate thickness and bolt size as would have been required under normal conditions to join the two girders. Failure takes the form of yielding and plastic deformation of the girder flange, after first plastic strain has developed in the girder flange at the support according to figure 4.14. The accuracy of the moment-rotation curve is not questioned, as the moment for the curve is at the centre of the connection and the corresponding rotation results from the rotation of the girders at the point where the endplates initially make contact and later deform and separate.

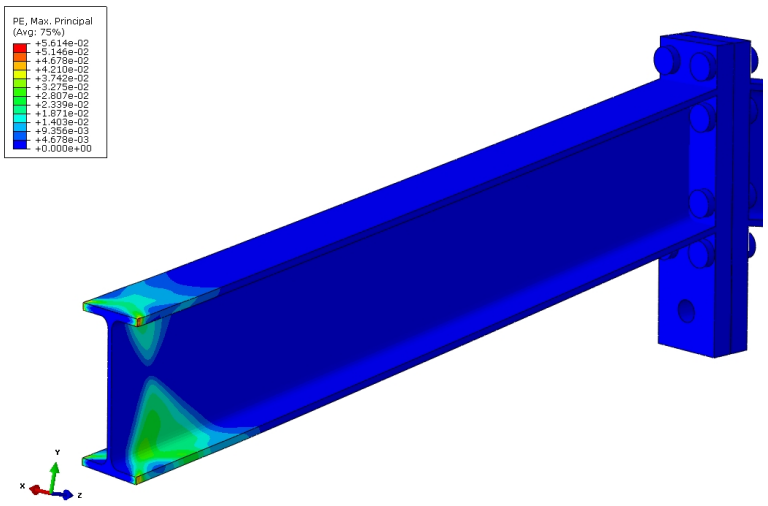

Figure 4.14: Plastic strain developed in the test specimen ridge connection.

4.4.1 MOMENT-ROTATION BEHAVIOUR FOR IN-PLANE DOWNWARD ROTATION

Figure 4.15 illustrates the moment-rotation behaviour of the test specimen ridge connection for downward deformations. An ultimate moment capacity of 5,97 kNm is reached by the connection, after which the girder profile flange undergoes yielding and plastic deformation. The moment-rotation curve in figure 4.15 does not illustrate perfect plastic deformation due to plastic deformation first being formed in the flange profile as illustrated in figure 4.14. Yielding of components is however noticed due to the non-linear nature of the curve.

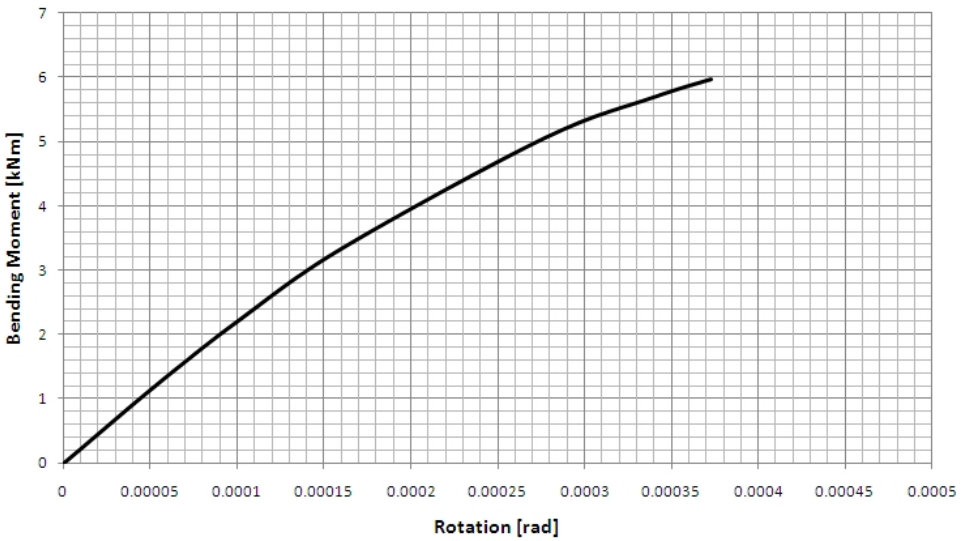

Figure 4.15: Moment-rotation curve for downward in-plane rotational deformation of the test specimen haunch connection.

4.4.2 MOMENT-ROTATION BEHAVIOUR FOR IN-PLANE UPWARD ROTATION

The moment-rotation behaviour of the test specimen ridge connection for upward deformations is presented in figure 4.16. The initial slope is similar to the initial slope of the curve presented in figure 4.15, leading to the conclusion that there is a similar initial stiffness of the test specimen ridge connection for both directions of in-plane rotational deformation. This behaviour is explained by the symmetrical layout of the connection in terms of

bolt layout, size and the distances they are from profile flanges. An ultimate moment of 6,017 kNm is reached, followed by the yielding and plastic deformation of the girder flanges.

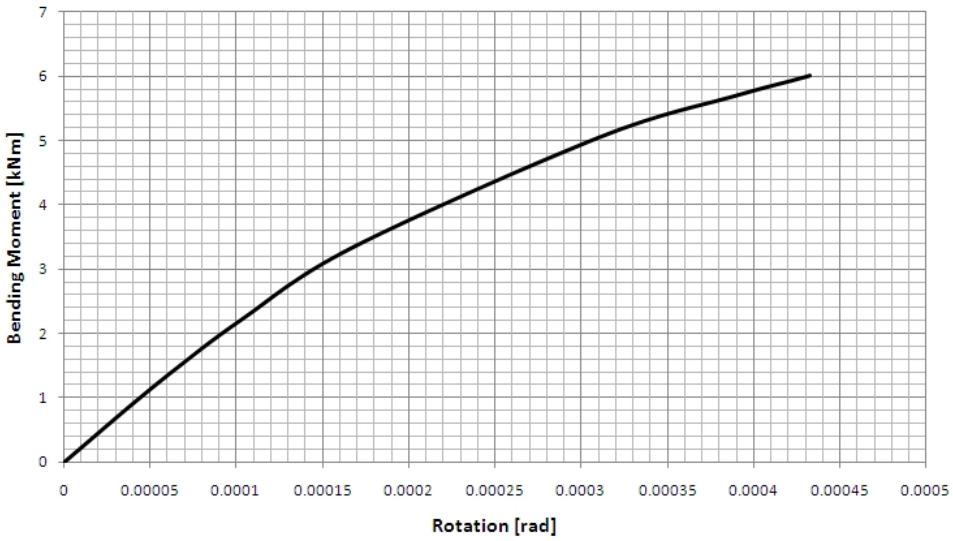

Figure 4.16: Moment-rotation curve for upward in-plane rotational deformation of the test specimen haunch connection.

4.5 TEST SPECIMEN GROUT SUPPORT

A grout support for the test specimen in the experimental investigation, was manufactured in order to create a support interface similar to true construction conditions of portal frame bases and is discussed in section 5.1.3 of chapter 5. A non-shrink cementitious grout was cast onto a 12 mm steel plate fixed to the beam/column testing apparatus referred to in section 5.2 of chapter 5. It was decided to model the full support interface in order to ensure accuracy of the moment-rotation behaviour of the support. This was motivated by the fact that the 12 mm thick steel plate, fixed with M24 grade 4.8 bolts, could also undergo finite rotational deformation during loading of the test specimen and this deformation must therefore be determined for the accuracy of the connection response. A model was created with the 12 mm baseplate on a rigid surface with a contact definition and interaction defined between them of similar standards as steel-to-steel contact. The rigid surface represents the support beam of the testing apparatus in the laboratory, described in section 5.2 and is assumed to be rigid due to the substantially greater stiffness in comparison with the testing components. Bolts are fully clamped at the plane of the rigid surface and are pretensioned similar to all other bolts modelled.

Non-shrink cementitious grout was modelled with the following properties:

$$E = 23,3\ GPa$$
$$v = 0,2$$
$$f_y = 66\ MPa$$
$$Ultimate\ plastic\ strain = 0,00283$$

Holding-down bolts are M6 grade 8.8, column consist of a $IPE_{AA}100$ steel profile of grade 350W and the base plate is of grade 300W steel. Figure 4.17 below illustrates the deformation of the connection due to loading as well as the plastic strain developing in the holding down bolts of the baseplate. Failure is thus in the form of yielding and plastic deformation of the holding-down bolts.

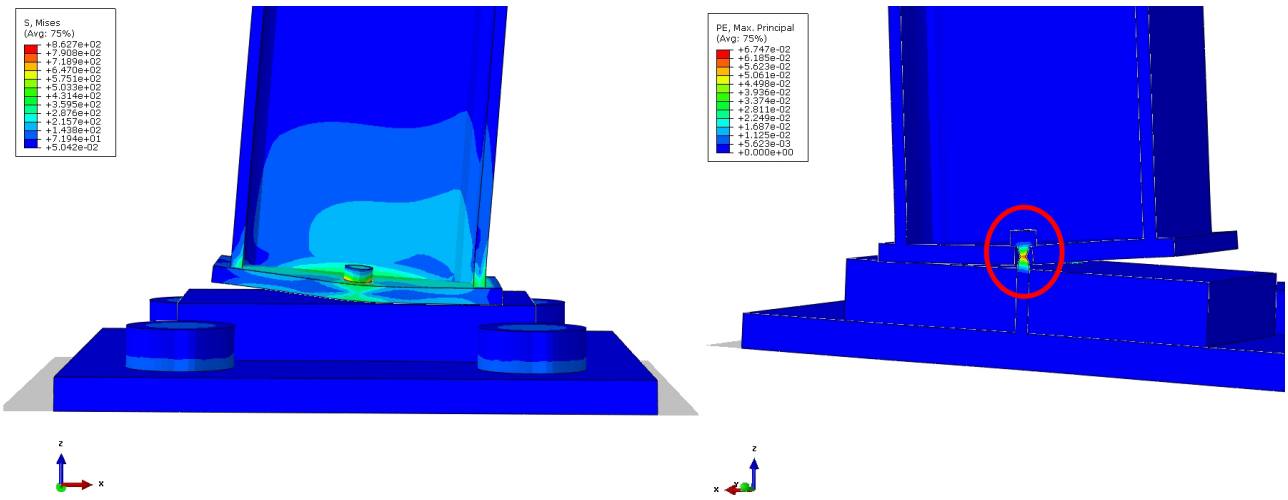

Figure 4.17: Finite element analysis results showing von Mises stresses of the grouted support exhibiting in-plane rotational deformation and plastic strain exhibited by the holding-down bolts respectively.

The perfect symmetrical layout of the connection ensures a similar moment-rotation relationship for both directions of in-plane rotational deformation, and therefore only one moment-rotation curve is presented for this connection. Figure 4.18 shows the moment-rotation behaviour of the connection. An ultimate moment capacity of 1,542 kNm is reached by the connection. Initially this value seemed very low but as the connection is designed as a pinned connection, it means that the connection is not subject to any moment loads in the ideal situation of structural analysis. A perfectly pinned connection's moment-rotational behaviour is given by the horizontal axis of the moment-rotation curve, as explained in section 2.5. It is therefore obvious from the moment-rotation curve illustrated below that the real response of pinned joints do exhibit rotational restraint and will reduce the displacements of the column of the test specimen.

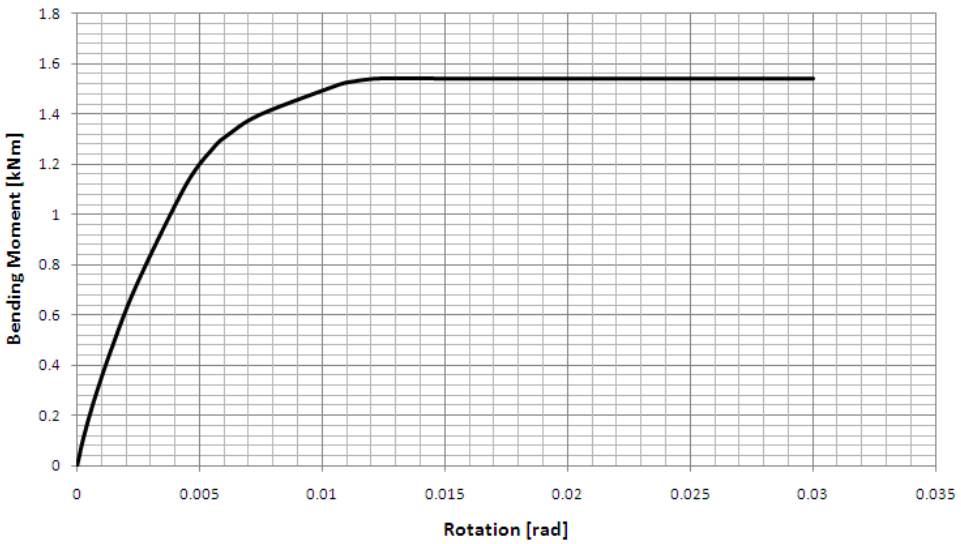

Figure 4.18: Moment-rotation curve for grout support condition of the test specimen.

4.6 REFERENCE PORTAL FRAME HAUNCH CONNECTION

The test specimen haunch connection presented in section 4.3 was intentionally designed according to the same principles as the reference portal frame haunch connection. This means that the connection is designed for the worst-load case which is the uplift action of wind on the structure rather than self-weight and imposed loads acting downward. Layout of the connection must create greater stiffness for in-plane upward rotational deformation

than for in-plane downward deformation. Bolts are M16 of grade 8.8, the column is a 254x146x31 I-section and the beam an IPE 200 steel profile. Both steel sections and the endplate are of grade S355JR steel. Detailed design calculations of the connection are shown in Appendix A section A.10.2 and a detail drawing in Appendix B. Figure 4.19 below illustrates the von Mises stresses in the connection for in-plane downward and in-plane upward deformations respectively.

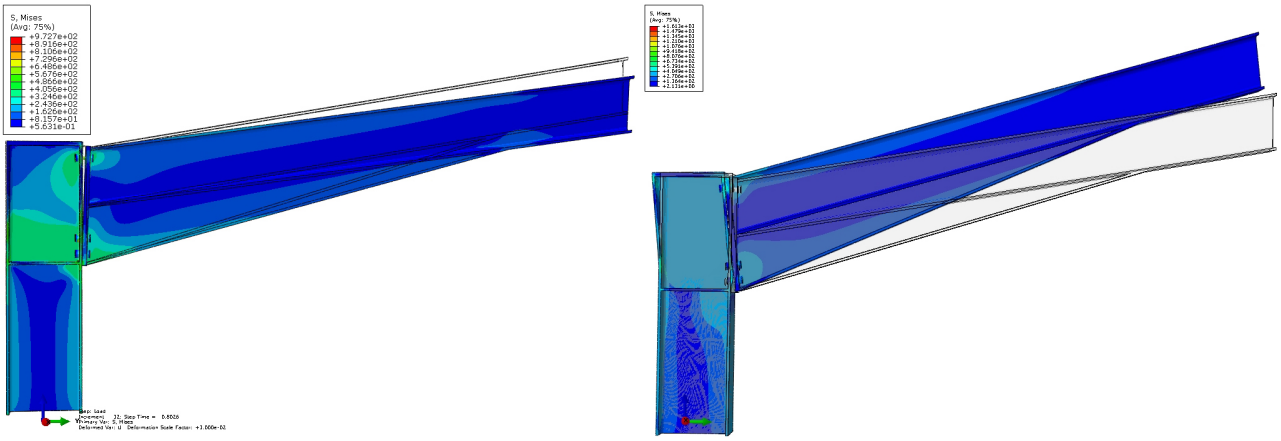

Figure 4.19: Finite element analysis results showing von Mises stresses of the reference portal frame haunch exhibiting downward and upward in-plane rotational deformation respectively.

4.6.1 MOMENT-ROTATION BEHAVIOUR FOR IN-PLANE DOWNWARD ROTATION

In-plane downward rotation deforms the haunch connections in such a way that the beam endplate undergoes single curvature bending deformation with a single row of bolts being subjected to tensile forces and stresses due to this deformation. Tensile stresses develop in the middle bolt row, but are not as severe as those in the top row of bolts. Failure is in the form of yielding and plastic deformation of the top bolt row. This is illustrated in figure 4.20.

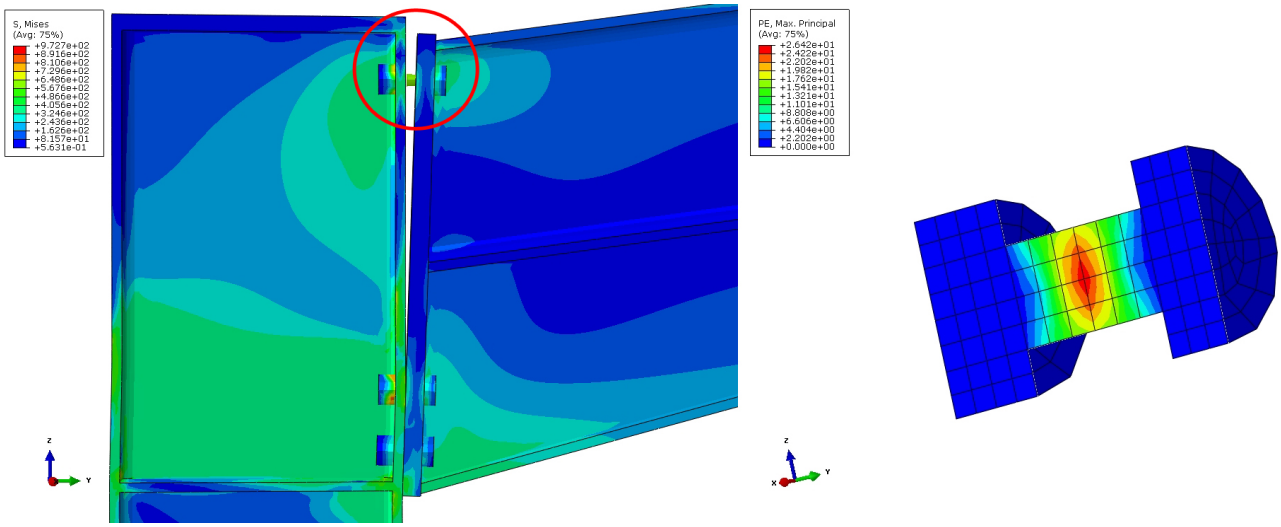

Figure 4.20: Sectional view of the von Mises stresses in the reference portal frame haunch connection for in-plane downward rotational deformation and plastic strain developed in the bolts respectively.

Figure 4.21 presents the moment-rotation behaviour of the connection for in-plane downward deformation. An ultimate moment capacity of 88,43 kNm is reached.

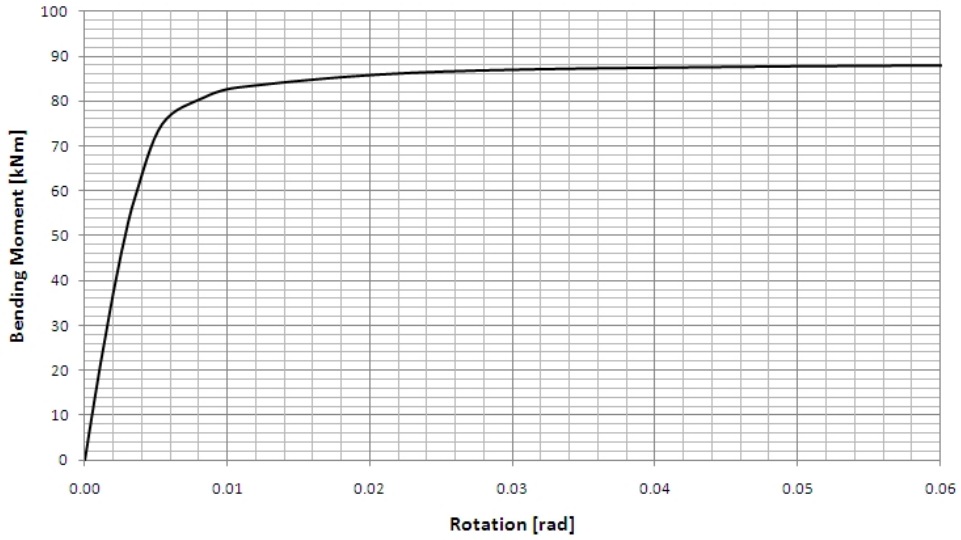

Figure 4.21: Moment-rotation curve for in-plane downward rotational deformation of the reference portal frame haunch connection.

4.6.2 MOMENT-ROTATION BEHAVIOUR FOR IN-PLANE UPWARD ROTATION

Figure 4.22 illustrates the connection behaviour due to in-plane upward rotation. The column web exhibits shear deformation but it is the endplate and column flange deformation that are more prominent. Both exhibit deformation in the form of double curvature with an inflection point between the two bottom bolts of the connection. The endplate does not exhibit deformations as severe as the column flange due to the increased stiffness of the component provided by the thickness of the plate. All four bottom bolts exhibit bending deformation due to prying action instead of expected pure tension as assumed in the design. First yielding and plastic deformation takes place in the bottom row of bolts as illustrated with the plastic strain formation in the figure referred to.

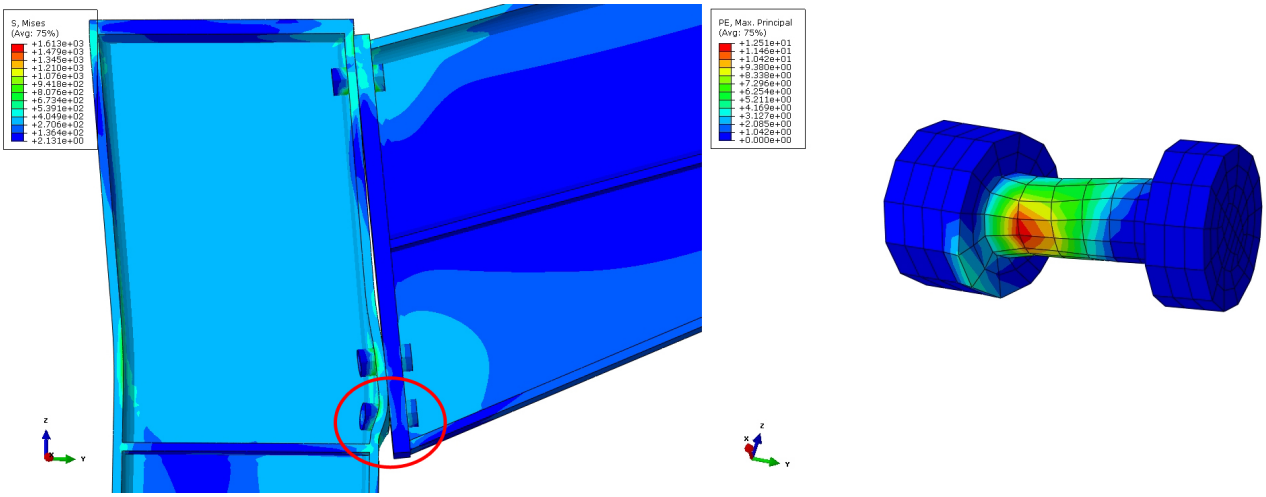

Figure 4.22: Sectional view of the von Mises stresses in the reference portal frame haunch connection for in-plane upward rotational deformation and plastic strain developed in the bolts respectively.

The moment-rotation behaviour is presented in figure 4.23 with an ultimate moment of 108,68 kNm.

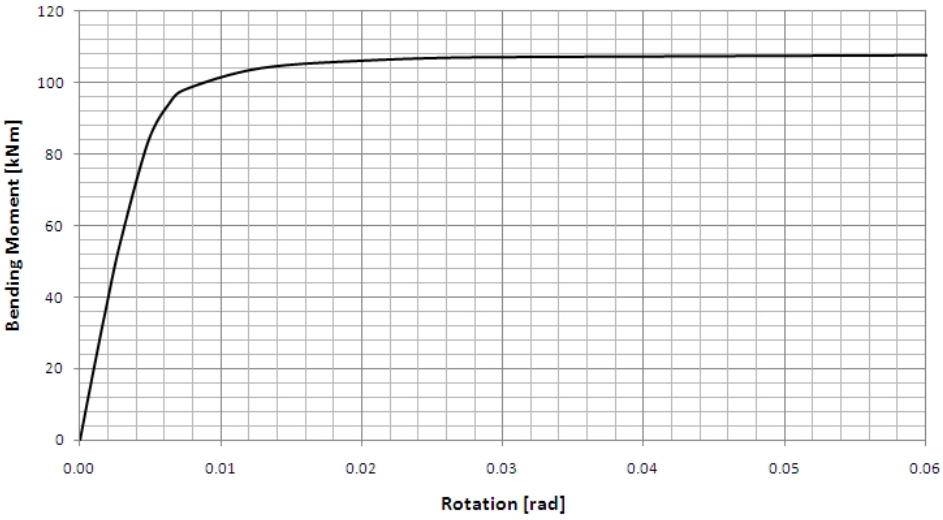

Figure 4.23: Moment-rotation curve for in-plane upward rotational deformation of the reference portal frame haunch connection.

4.7 REFERENCE PORTAL FRAME RIDGE CONNECTION

The reference portal frame has an extended endplate connection joining the two girders. Extending the endplate upwards allows the accommodation of another row of bolts to increase the stiffness for in-plane downward deformation. The structural response of the portal frame under the worst load case, i.e. wind uplift forces, causes the ridge connection to undergo in-plane downward deformation. Design calculations of the ridge connection is presented in section A.10.3 of appendix A together with a detail drawing in appendix B. Determination of the moment-rotation behaviour of this connection was done in a manner similar to that of the test specimen ridge connection as explained in section 4.4, but the connection was optimized to ensure sufficient strength against the load cases applied to it. Therefore plastic strain first occurred within the connection as expected. Figure 4.24 illustrates the von Mises stresses for the in-plane downward and in-plane upward rotational deformations respectively.

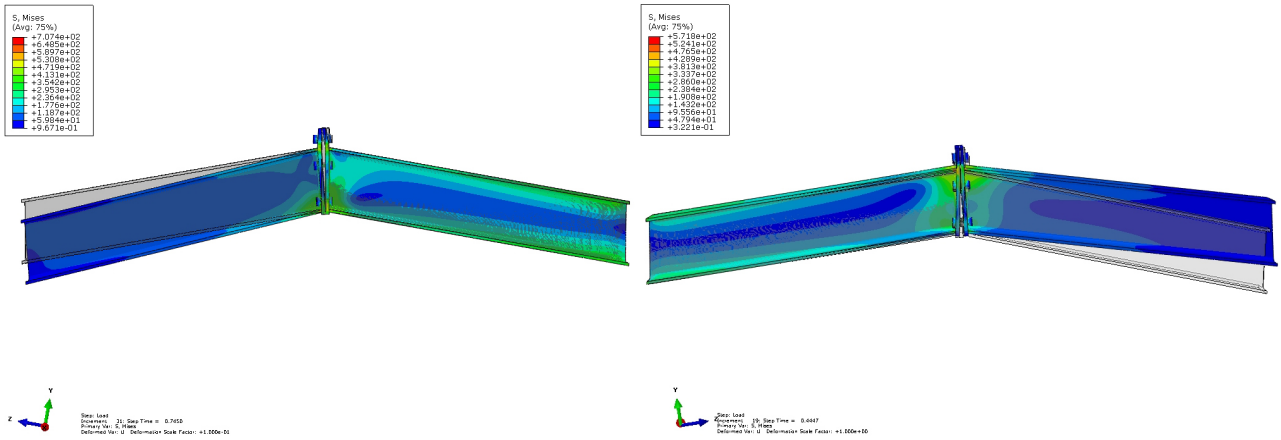

Figure 4.24: Finite element analysis results showing von Mises stresses of the reference portal frame ridge exhibiting downward and upward in-plane rotational deformation respectively.

4.7.1 MOMENT-ROTATION BEHAVIOUR FOR IN-PLANE DOWNWARD ROTATION

Downward in-plane deformation causes both endplates to exhibit double curvature deformation, resulting in the two top bolt rows undergoing bending deformation besides the tensile forces developing in these components. An inflection point on the endplates forms at the girder top flanges due to the support provided by these flanges. The top row of bolts first exhibits material yielding and plastic deformation to the side of the bolt shank. The bending deformation of the bolts explains the uneven formation of plastic strain in the bolts due to prying action. Figure 4.25 illustrates the deformation of the connection for in-plane downward deformation and plastic strain forming in the bolts respectively.

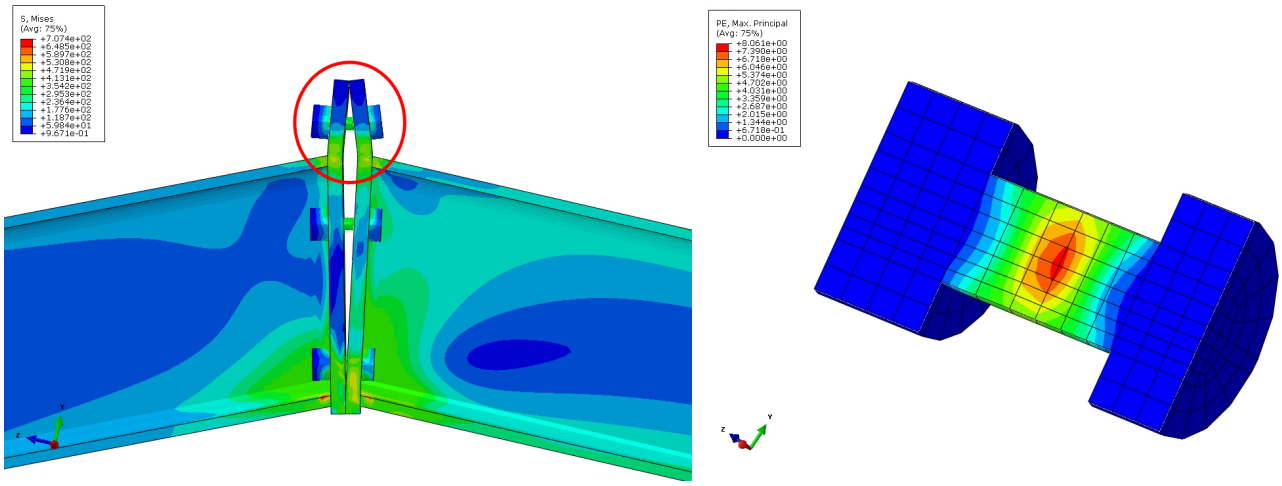

Figure 4.25: Von Mises stresses in the reference portal frame ridge connection due to in-plane downward rotational deformation and plastic strain developing in the bolts respectively.

Figure 4.26 illustrates the moment-rotation behaviour of the connection. A ultimate moment of 38.81 kNm is reached.

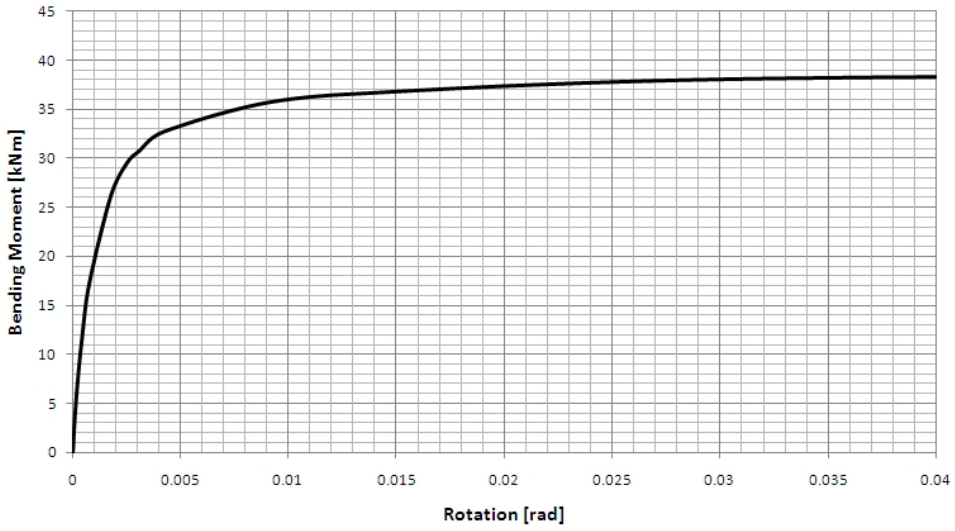

Figure 4.26: Moment-rotation curve for in-plane downward rotational deformation of the reference portal frame ridge connection.

4.7.2 MOMENT-ROTATION BEHAVIOUR FOR IN-PLANE UPWARD ROTATION

In-plane upward deformation of the connection causes the endplates in the connection to undergo single curvature bending deformation. Single curvature bending of the endplates appears to be a less stiff form of deformation than double curvature bending and will result in greater deformations of the connection under loading. The response is also explained by the single row of bolts that develop tension forces in this direction of in-plane deformation. Figure 4.27 below illustrates the deformation of the connection as well as plastic strain developing in the bottom row of bolts. The mode of failure can therefore be described as the material yielding and plastic deformation of the bolts in the bottom row.

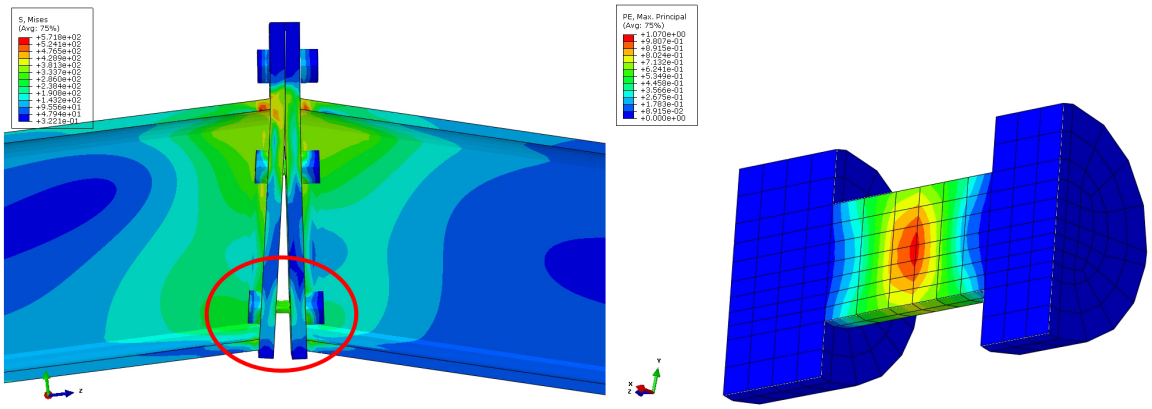

Figure 4.27: Von Mises stresses in the reference portal frame ridge connection due to in-plane upward rotational deformation and plastic strain developing in the bolts respectively.

Figure 4.28 below illustrates the moment-rotation behaviour of the ridge connection for in-plane upward deformation, an ultimate moment of 22,11 kNm is reached.

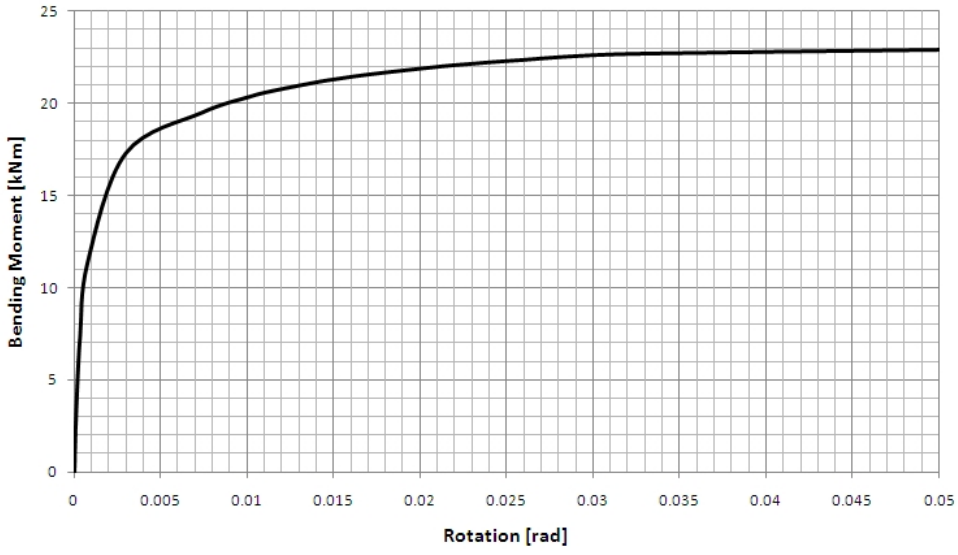

Figure 4.28: Moment-rotation curve for in-plane upward rotational deformation of the reference portal frame ridge connection.

4.8 REFERENCE PORTAL FRAME COLUMN BASE

A column base provides a connection interface between the columns of the reference portal frame and the concrete foundation. The base was regarded as a pinned base during the structural analysis and therefore was similarly

designed. As presented in section 2.4, pinned column bases have a symmetrical layout with two anchor bolts on the strong axis of the column profile. Full design calculations for the reference portal frame column base can be found in section A.10.1 and a detail drawing in appendix B.

The column is a 254x146x31 I-profile with an 18 mm endplate welded to the end of the column along the perimeter of the profile. Two commercial-quality anchor bolts are designed for casting into the concrete foundation together with anchor plates to withstand pullout forces on the bolts. A grout interface similar to the grout presented in section 4.5, is provided between the base plate and the conrete foundation. This is normal construction practice as the frame is leveled with the anchor bolts after which the void between the baseplate and the concrete is filled with cementitious grout. No specific design calculations have been performed on the concrete foundation and the size was obtained from a previous study on the moment-rotation behaviour of column bases. Mostert determined a concrete foundation of 2 m x 2 m x 800 mm to be of sufficient size to withstand the design forces imposed by the column on the foundation (Mostert, 1998). Figure 4.29 below illustrates the von Mises stresses developed in the column base during in-plane rotational deformation.

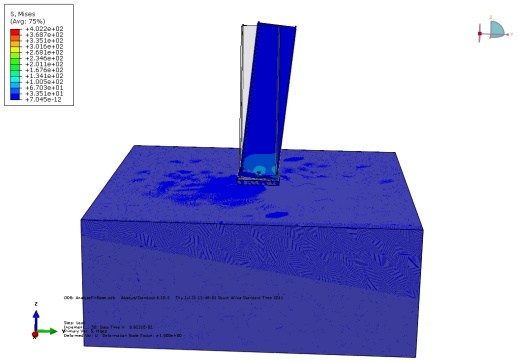

Figure 4.29: Finite element analysis results showing von Mises stresses in the reference portal frame column base due to in-plane rotational deformation.

Figure 4.30 illustrates the deformation of the column base and the plastic strain developing in the anchor bolt respectively. The off-centre development of plastic strain in the anchor bolt shank is due to the bending deformation exhibited by the anchor bolt during loading.

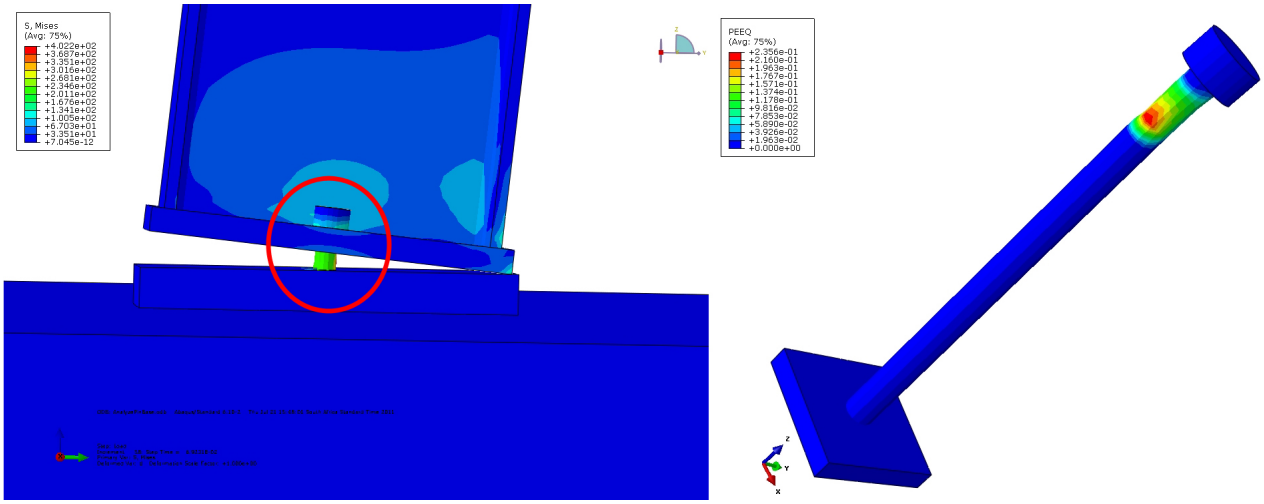

Figure 4.30: Von Mises stresses in the reference portal frame column base due to in-plane rotational deformation and plastic strain developing in the anchor bolts respectively.

The moment-rotation behaviour of the column base is presented in figure 4.31 below. An ultimate moment capacity of 7.048 kNm is reached when yielding of the anchor bolts and plastic deformation takes place.

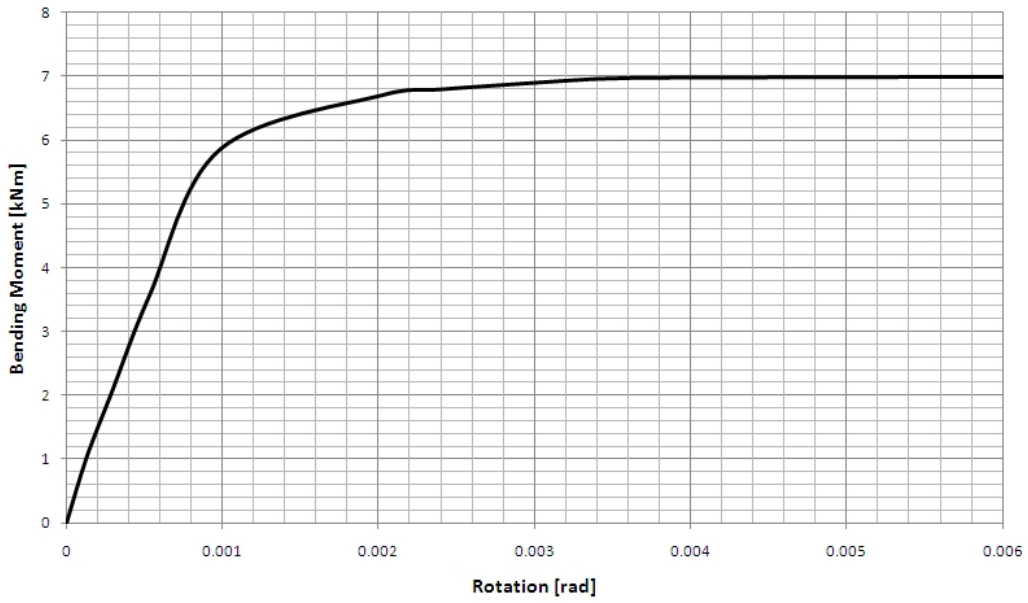

Figure 4.31: Moment-rotation curve for in-plane rotational deformation of the reference portal frame column base.

4.9 CONCLUSION

This chapter discussed the three-dimensional non-linear finite element models that were developed of the steel connections and used in the study. The chapter initiated with some accuracy tests to the element type and mesh density. Modelling standards in terms of contact and interaction modelling, integration complexity, element type and mesh densities were discussed. Although the modelling standards were mostly adopted from Prabha *et al.*, they were verified by performing an analysis on a haunch taken from a previous study and comparing the analytical results with the experimental results presented in the study (Prabha et al., s.a.; Truter, 1997). Comparison of the results led to the conclusion that the modelling standards used provided sufficiently accurate results and that all finite element models of connections and bases would be done to similar standards referred to above. Finite element models were developed for all the connections investigated in the study, namely:

1. Test specimen haunch connection.
2. Test specimen ridge connection.
3. Test specimen grout support.
4. Reference portal frame haunch connection.
5. Reference portal frame ridge connection.
6. Reference portal frame pinned column base.

Results from each analysis were presented in terms of von Mises stresses, illustrated to provide a visual image of the deformation of the connection under loading. Furthermore the mode of failure, the ultimate moment capacity and moment-rotation response for each direction of in-plane rotational deformation were presented. The moment-rotation behaviour of each connection is used in chapters six and seven for determining a rotational spring stiffness to model the connection's behaviour in the structural analysis of a portal frame.

Chapter 5

EXPERIMENTAL INVESTIGATION

An experimental investigation of the in-plane behaviour of a portal frame was conducted to determine the displacements of a portal frame subjected to loads. The importance of the in-plane behaviour of the portal frame is emphasized as this is similar to the ideal conditions assumed in a two-dimensional analytical structural analysis of portal frames. The results of the investigation are required for the accurate comparison of displacement determination of the structure using second order analysis with the implementation of rotational springs in second order analysis as described in section 2.7. The results from the experimental investigation will be used to assess the feasibility of determining the optimum rotational spring stiffness for modelling connections in second order analysis.

5.1 EXPERIMENTAL TEST SPECIMEN

A 5m span experimental portal frame was designed and constructed for the purpose of the experimental investigation. Figure 5.1 illustrates its basic layout and dimensions.

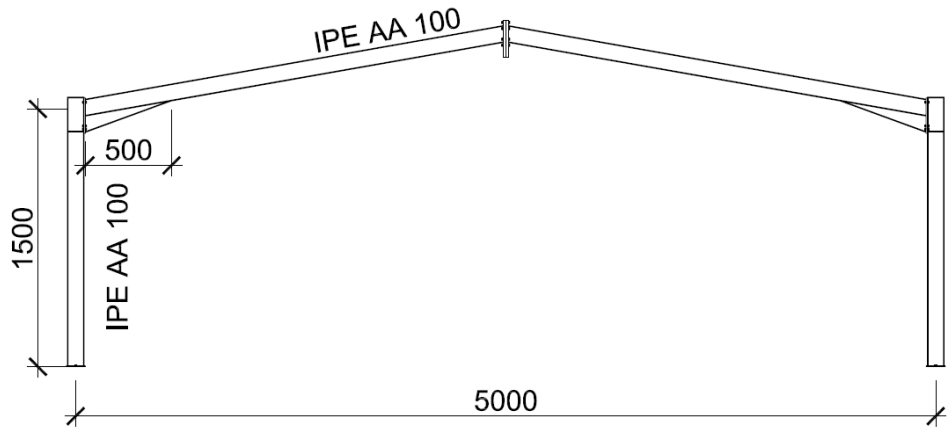

Figure 5.1: 5m Span experimental portal frame.

5.1.1 LOADS

The test specimen was regarded as being a typical portal frame in a structure 12,5 m x 5 m in plan and having a ridge height of 1,941 m. Spacing between portals of 2,5 m was used for all load calculations. Adopting the

above, the loads to be used in the analysis and the design of the test specimen were calculated according to the procedures set out in the South African National Standard: Basis of Structural Design and Actions for Buildings and Industrial Structures parts one to three (SANS10160:2011).

The roof was considered to be inaccessible in the calculation of imposed loads. Wind loads were determined using a characteristic wind speed of 28 $m.s^{-1}$ and it was assumed that the structure was constructed on a terrain having a B classification as described in the SANS 10160:2011.

5.1.2 STRUCTURAL ANALYSIS AND DESIGN

Prokon Structural Analysis software was used to analyze the portal frame in order to obtain the required design forces and moments. Column bases were modelled as "pinned" joints, beam-column connections as rigid haunch connections and the apex as a rigid extended endplate connection. These assumptions were made for the purpose of the analysis, as it conforms to the methods and assumptions commonly used for analysis in design offices.

The steel sections were calculated according to the procedures set out in the South African National Standard: The structural use of steel (SANS10162-1:2005). The smallest sections capable of supporting the loads applied to the frame in the analysis were chosen and the connections between them were designed according to the procedures set out in the Southern African Institute of Steel Construction Limit State Design of Connections (SAISC, 1992) and the Steel Construction Handbook (SAISC, 2008).

Columns and girders were constructed using $IPE_{AA}100$ I-sections, grade S350W steel, whereas all plates were made of steel grade 300W. These sections were available from the local steel supplier at the time of the design and construction of the test specimen. It is common in portal frame design to select similar steel sections for columns and girders.

5.1.3 SUPPORTS

Two types of column supports where designed for the test specimen, firstly a hinge-type pin support and secondly a support with a grout interface to simulate construction practice conditions.

HINGE SUPPORT

It was decided to design a hinge support as a support interface for the column base of the portal frame in order to provide similar boundary conditions as used in the frame analysis. This created the opportunity to isolate the effect of the restraint provided by the interface between the column base endplate and the concrete/grout as found in normal construction practice. By isolating this effect, the real effect of the moment-rotation of the beam-column connection and the apex connection can be recorded. The hinge support is similar to the support simulated in the structural analysis.

GROUTED SUPPORT

The grouted support provides a cementitious grout interface between the column base endplate and the plane frame structure of the laboratory, simulating normal construction practice. Note that the column base is designed as a pin support by means of the layout of the bolts on the baseplate. The cementitious grout provides some restraint against rotation, conflicting with the boundary conditions of the frame analysis of the structure and therefore it is necessary to record the effect of the real support conditions in the behaviour of the structure under loading. Figure 5.2 illustrates the hinge type and grouted supports to be used in the experimental investigation respectively.


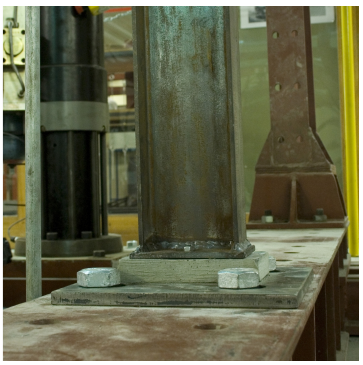

Figure 5.2: Hinge column base support and grouted column base support respectively.

5.2 TEST SPECIMEN SUPPORT STRUCTURE

The Stellenbosch University Structural Engineering laboratory's multipurpose beam/column testing apparatus was used to support the test specimen when conducting experiments (Koen, 2003). This testing facility provides a support interface for the simulation of ideal in-plane conditions as lateral support can be provided by means of steel cables. Steel cables of 4 mm in diameter are used and fixed to the flanges at the following positions on the test specimen:

- Midspan of the column.
- Midspan of the girder.
- Top end of the column.
- Both ends of the girder.

Figure 5.3 below illustrates the multipurpose beam/column testing apparatus in the structural laboratory. Note the beam running laterally in the support portals for supporting of the cables. The testing apparatus is also bolted to the laboratory's concrete floor along its length and the two end support portals are fixed with beams to the laboratory's concrete structure.

Figure 5.3: Experimental setup in the plane frame system.

5.3 LOAD APPLICATION & MEASUREMENTS

5.3.1 LOAD APPLICATION

Loads applied to the test specimen are illustrated in Figure 5.4. P_h and P_v represent the action induced by wind, whereas P_g represents the imposed load on the roof. Vertical and horizontal loads were applied separately. Although it is preferred that the loads be applied simultaneously, such simultaneous load application is made unnecessary by the available facilities for applying normal loading under deformed conditions, and therefore the separate application of loads will be used during the investigation.

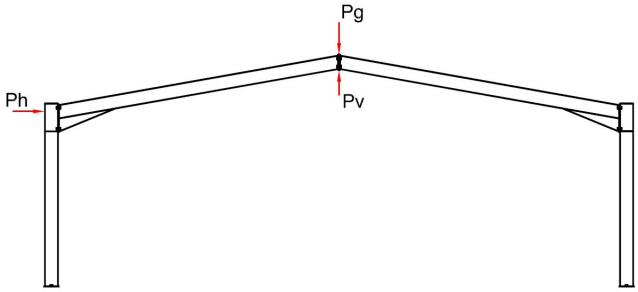

Figure 5.4: Loads applied to test specimen.

Vertical loads were applied by a hydraulic actuator with a capacity of 60 tons and a range of 75 mm. The horizontal load was applied by a hydraulic actuator with a capacity of 25 tons and a range of 150 mm. Both hydraulic actuators are illustrated in figure 5.5

Figure 5.5: Load application with an hydraulic actuator and inline load cell for upward and sideward load application shown respectively.

Settling loads were applied to the test specimen to enable the structural components in the connection to settle before the maximum of the planned load case was applied. Two settling loads, equal to 30% and 50% of the total load, were applied to the test specimen. The loads were applied separately and were released to allow the test specimen's structural components to "seat" properly in position and return to their original state. Testing of each type of load case was performed three consecutive times in order to develop accurate linear regressions of the recorded displacements of the test specimen.

5.3.2 MEASUREMENTS

For the purpose of the investigation it was required to measure applied loads and displacements. Loads applied by the actuators were measured by a 20 ton and a 5 ton load cell respectively for vertically and horizontally applied loads. The load cells are placed in-line with the actuators, i.e. measuring the load on the actuator as it was being applied to the load application interface.

Positions of maximum displacement on the test specimen was determined by means of a second order frame analysis. The identified positions of maximum displacements on the frame were measured by linear variable displacement transducers (LVDT's) during tests and recorded for later processing. The LVDT's were fixed to stand supports independent of the test specimen. Measuring displacement of the girder for a horizontal load case (P_h in figure 5.4) is not possible by using a LVDT because the bi-directional displacement of the structure at the point of maximum displacement on the girder can not be measured with a normal LVDT.

It was therefore decided to use the ARAMIS optical measuring system as it can measure bi-directional displacement on the girder of the portal frame. The ARAMIS system uses a stereo optical system to record displacements and deformations of a certain point on the test specimen. This point is identified by creating a white square on the test specimen and painting a sprinkle pattern on the square. The ARAMIS system measures and records the displacements and deformations of the point matrix (created by the sprinkle pattern) in order to calculate displacements and strains of the test specimen. Both LVDT's and the ARAMIS system is illustrated in figure 5.6 respectively.

Figure 5.6: LVDT's measuring the test specimen ridge displacement and the ARAMIS optical measuring system shown respectively.

The positions of the LVDT's are illustrated in figure 5.7 below.

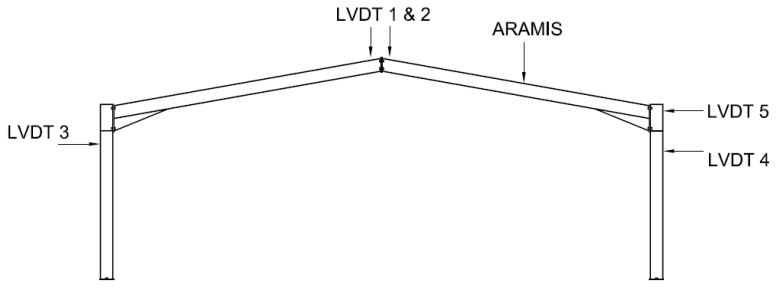

Figure 5.7: Positions of displacement measurements on the test specimen.

Table 5.1 below provides the characteristics of the LVDT's implemented for load measurements as illustrated in figure 5.6.

Table 5.1: Characteristics of the LVDT's implemented for displacement measurements.

LVDT	Range	Type
1	100 mm	Plunger
2	100 mm	Plunger
3	50 mm	Plunger
4	50 mm	Plunger
5	50 mm	Plunger

5.3.3 LOAD COMBINATIONS

The test specimen was designed to support the following load cases:

- Load case 1: Vertical load applied downward at the apex.
- Load case 2: Vertical load applied upward at the apex.
- Load case 3: Horizontal load applied at the haunch.

Due to the nature of permanent, imposed and wind loads, which are spread across the structural member, it is necessary to apply the point loads to the test specimen in the laboratory to simulate similar conditions to real load application conditions.

The following loads were applied to the structure:

1. Vertical downward force of 4,96 kN, causing a bending moment of 2,6 kNm at the haunch (Load case 1).
2. Vertical upward force of 12,8 kN, causing a bending moment of 6,67 kNm at the haunch (Load case 2).
3. Horizontal lateral force of 7,85 kN, causing a bending moment of 6,67 kNm at the haunch (Load case 3).

Note that 6,67 kNm is the design moment of the haunch connection.

5.4 PREDICTION OF BEHAVIOUR

5.4.1 MAXIMUM LOADS & FAILURE

The maximum horizontal and vertical loads were calculated according to the resisting capacity of the frame by using second order analysis in Prokon software. In all cases, failure will be in the form of column deformation and yielding. Table 5.2 presents the failure load of the test specimen for each load described in section 5.3.1 together with the correlating displacement. Note that the test specimen will not be tested to failure in this study.

Table 5.2: Maximum loads resisted by test specimen obtained from second order analysis.

Load	Second Order Analysis	Vertical Displacement	Horizontal Displacement
Vertical Downward	16,40 kN	42,51 mm	9,51 mm
Vertical Upward	16,65 kN	42,34 mm	9,46 mm
Horizontal Lateral	10,30 kN	13,16 mm	51,11 mm

5.4.2 DISPLACEMENTS

Second order, structural analysis was used to obtain the expected maximum displacements of the test specimen for each load case. The results are presented below.

LOAD CASE ONE: VERTICAL DOWNWARD FORCE OF 4,96 kN

A vertical downward force applied at the ridge of the test specimen yielded a maximum vertical displacement of 12,68 mm at the ridge . The maximum corresponding horizontal column displacement was 2,84 mm. Figure 5.8 illustrates the test specimen in its original and deformed state.

Figure 5.8: Predicted deformation of the test specimen for load case one.

LOAD CASE TWO: VERTICAL UPWARD FORCE OF 12,80 kN

A vertical upward force applied at the ridge of the test specimen yielded a maximum vertical displacement of 32,55 mm at the ridge. The maximum horizontal column displacement was 7,27 mm. Figure 5.9 illustrates the test specimen in the original and deformed state.

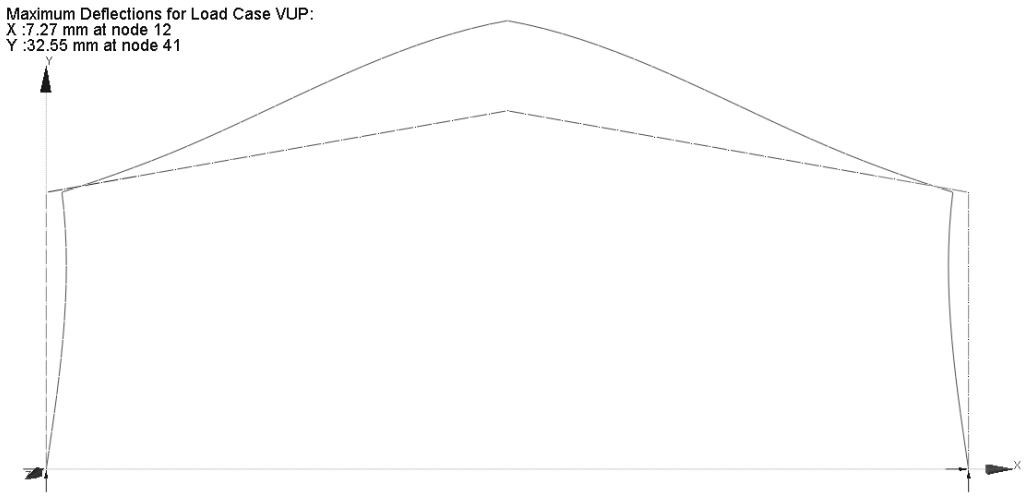

Figure 5.9: Predicted deformation of the test specimen for load case two.

LOAD CASE THREE: HORIZONTAL LATERAL FORCE OF 7,85 kN

A horizontal force applied at the top of the column of the test specimen resulted in a maximum horizontal displacement of 38,82 mm at the top of the column. The maximum corresponding vertical displacement was 9.99 mm on the girder. Figure 5.10 below illustrates the test specimen in its original and deformed state.

Figure 5.10: Predicted deformation of the test specimen for load case three.

5.5 EXPERIMENTAL RESULTS

The results from the experimental tests are presented in figure 5.11 through to figure 5.22. Each load case has been applied to the test specimen for the hinge- and grouted-support condition. Table 5.2 below summarizes the tests performed, support condition and figure in the text presenting the results. The test results are compared and summarized in section 5.6 of this chapter and discussed in section 5.7.

Table 5.3: Summary of the tests performed and the accompanying figures presenting the results.

Tests	Load Case	Support Condition	Result Figures	
			Vertical Displacement	Horizontal Displacement
1 to 3	1	Hinge	Figure 5.11	Figure 5.12
4 to 6	2	Hinge	Figure 5.13	Figure 5.14
7 to 9	3	Hinge	Figure 5.16	Figure 5.15 & 5.16
10 to 12	1	Grouted	Figure 5.17	Figure 5.18
13 to 15	2	Grouted	Figure 5.19	Figure 5.20
16 to 18	3	Grouted	Figure 5.22	Figure 5.21 & 5.22

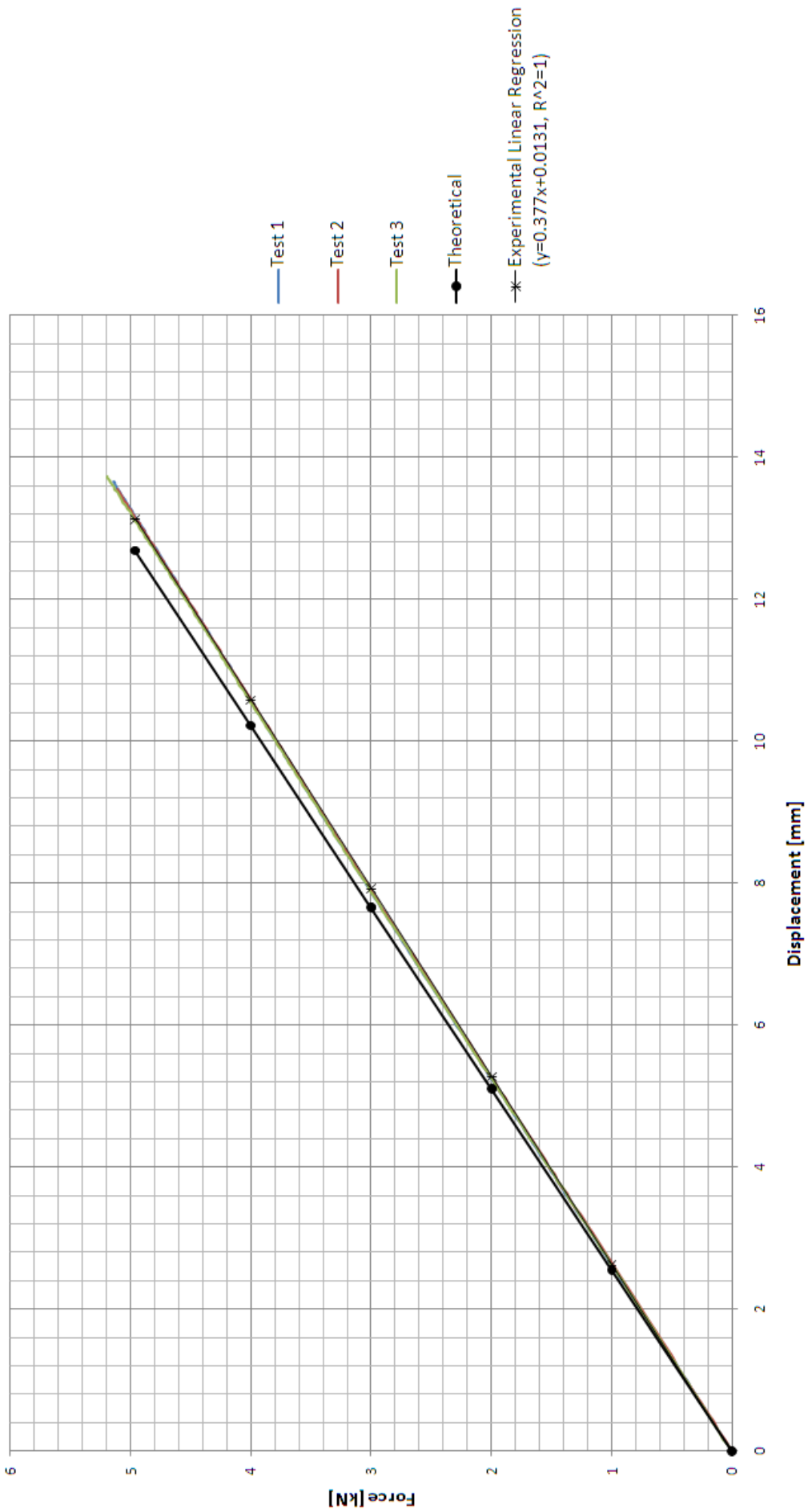

Figure 5.11: Vertical ridge displacement due to a vertical downward force of 4,96 kN applied at ridge. (Tests 1 to 3, hinge supports)

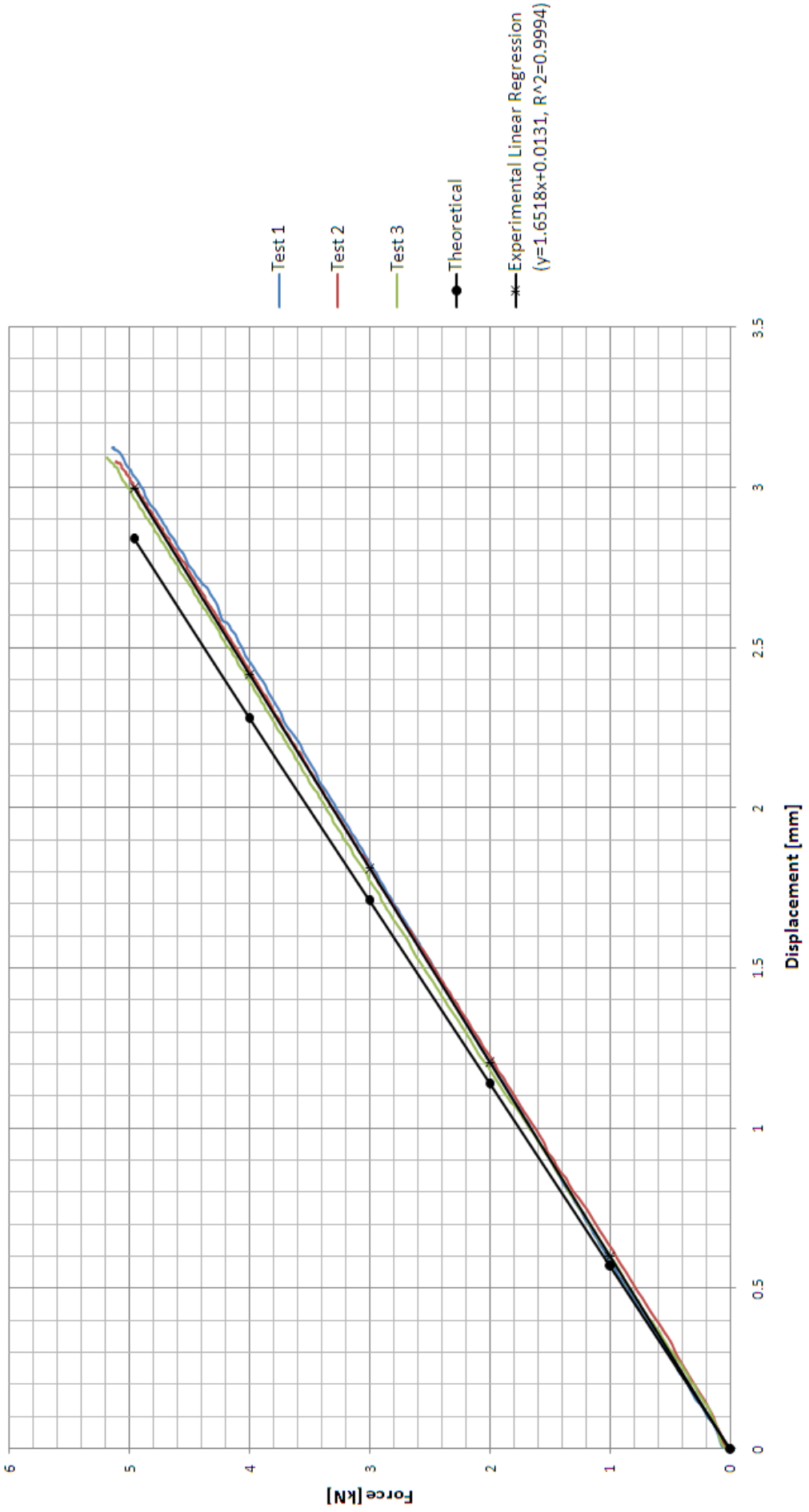

Figure 5.12: Horizontal column displacement due to a vertical downward force of 4,96 kN applied at ridge. (Tests 1 to 3, hinge supports)

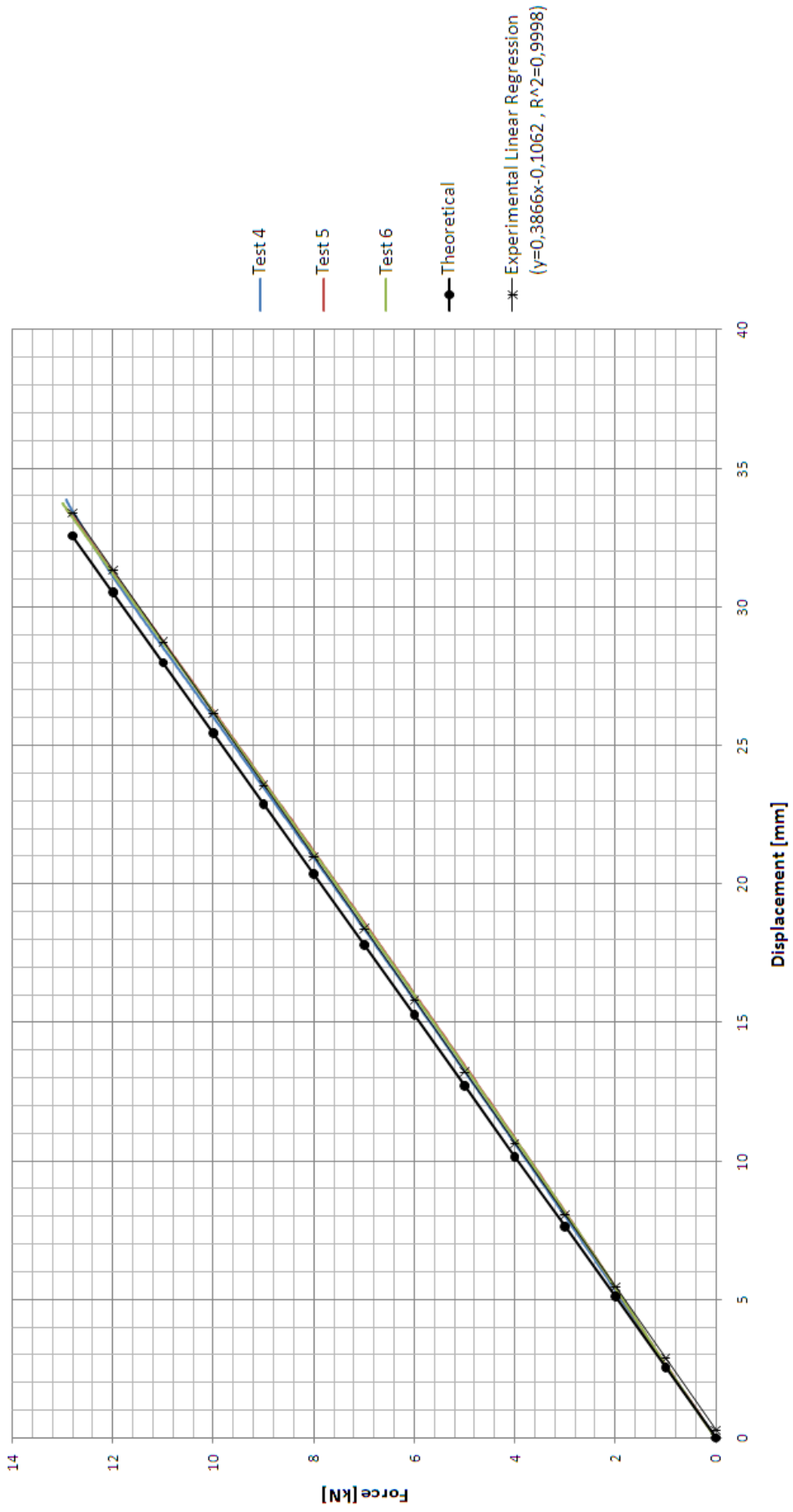

Figure 5.13: Vertical ridge displacement due to a vertical upward force of 12,8 kN applied at ridge. (Tests 4 to 6, hinge supports)

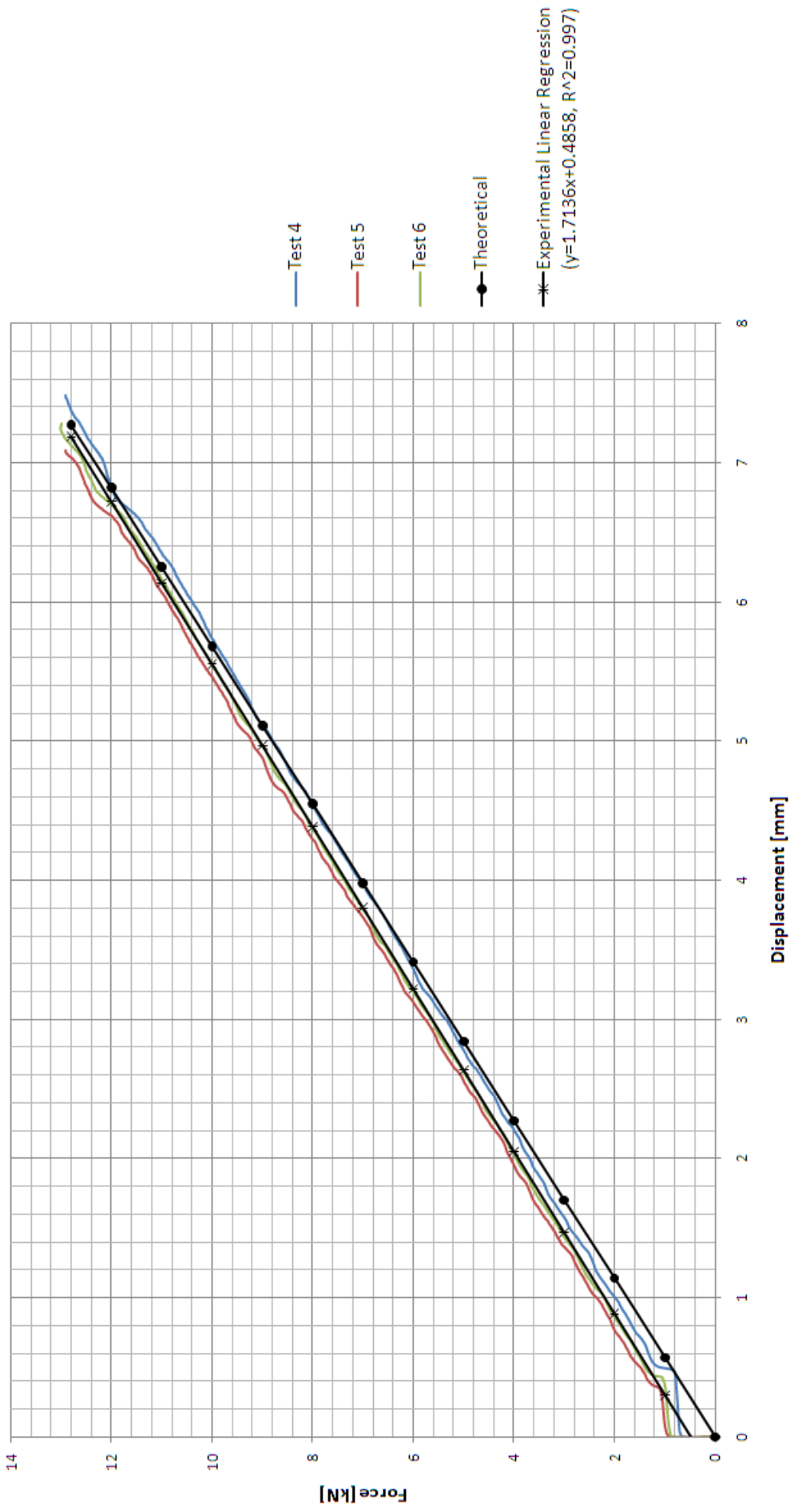

Figure 5.14: Horizontal column displacement due to a vertical upward force of 12,8 kN applied at ridge. (Tests 4 to 6, hinge supports)

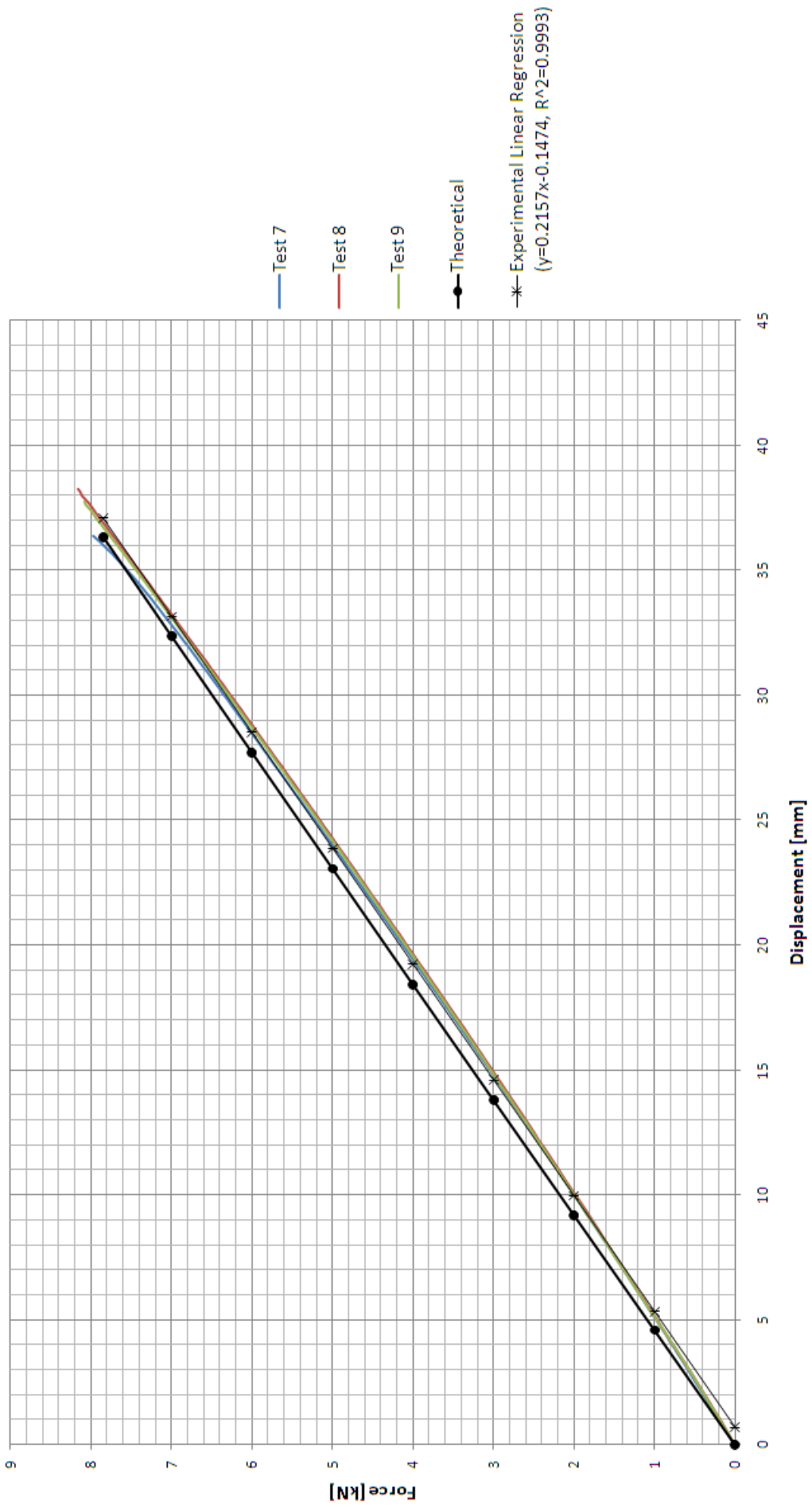

Figure 5.15: Horizontal column displacement due to a horizontal force of 7,85 kN applied at top of column. (Tests 7 to 9, hinge supports)

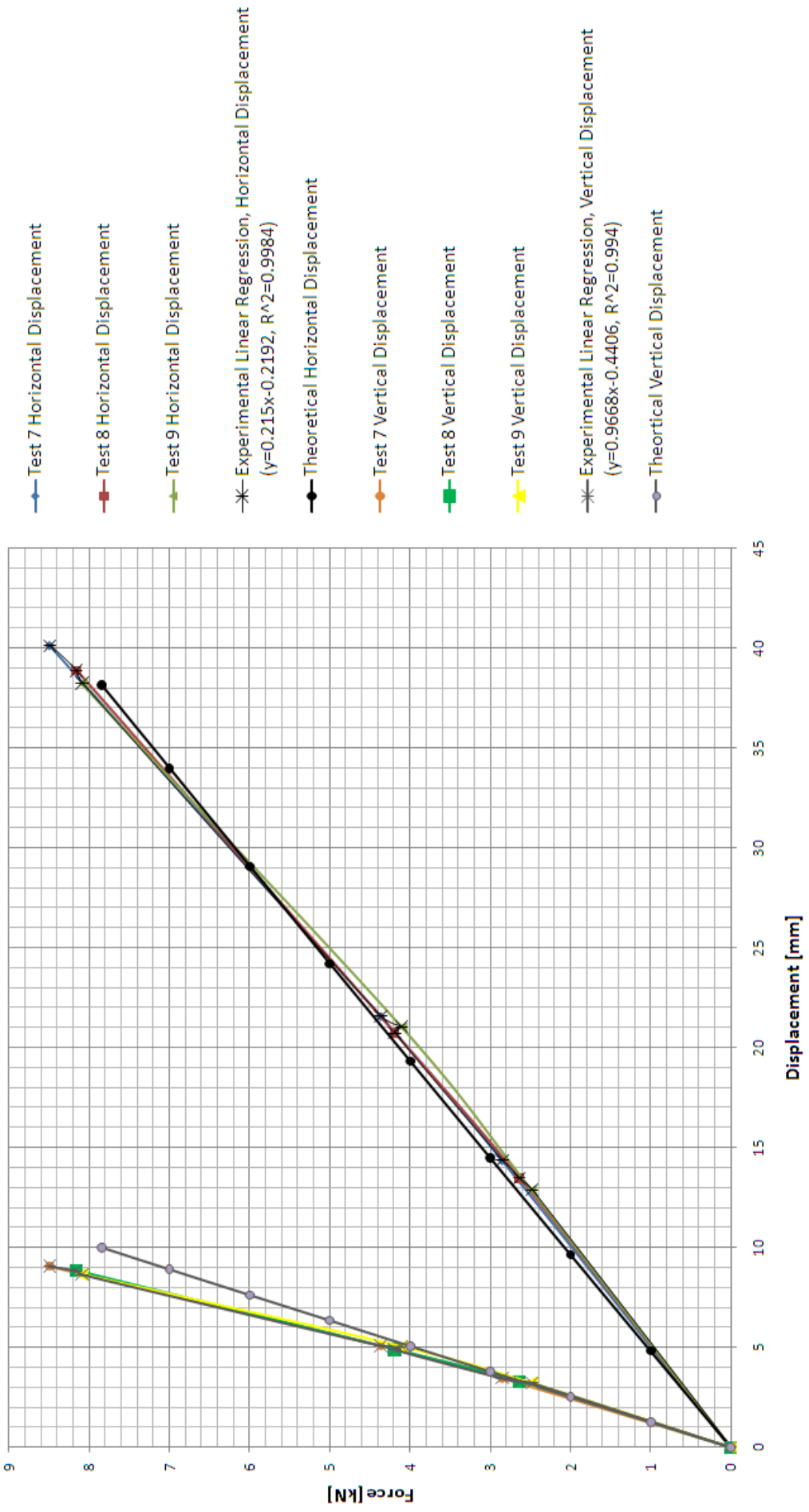

Figure 5.16: Horizontal and vertical girder displacement due to a horizontal force of 7,85 kN applied at top of column. (Tests 7 to 9, hinge supports)

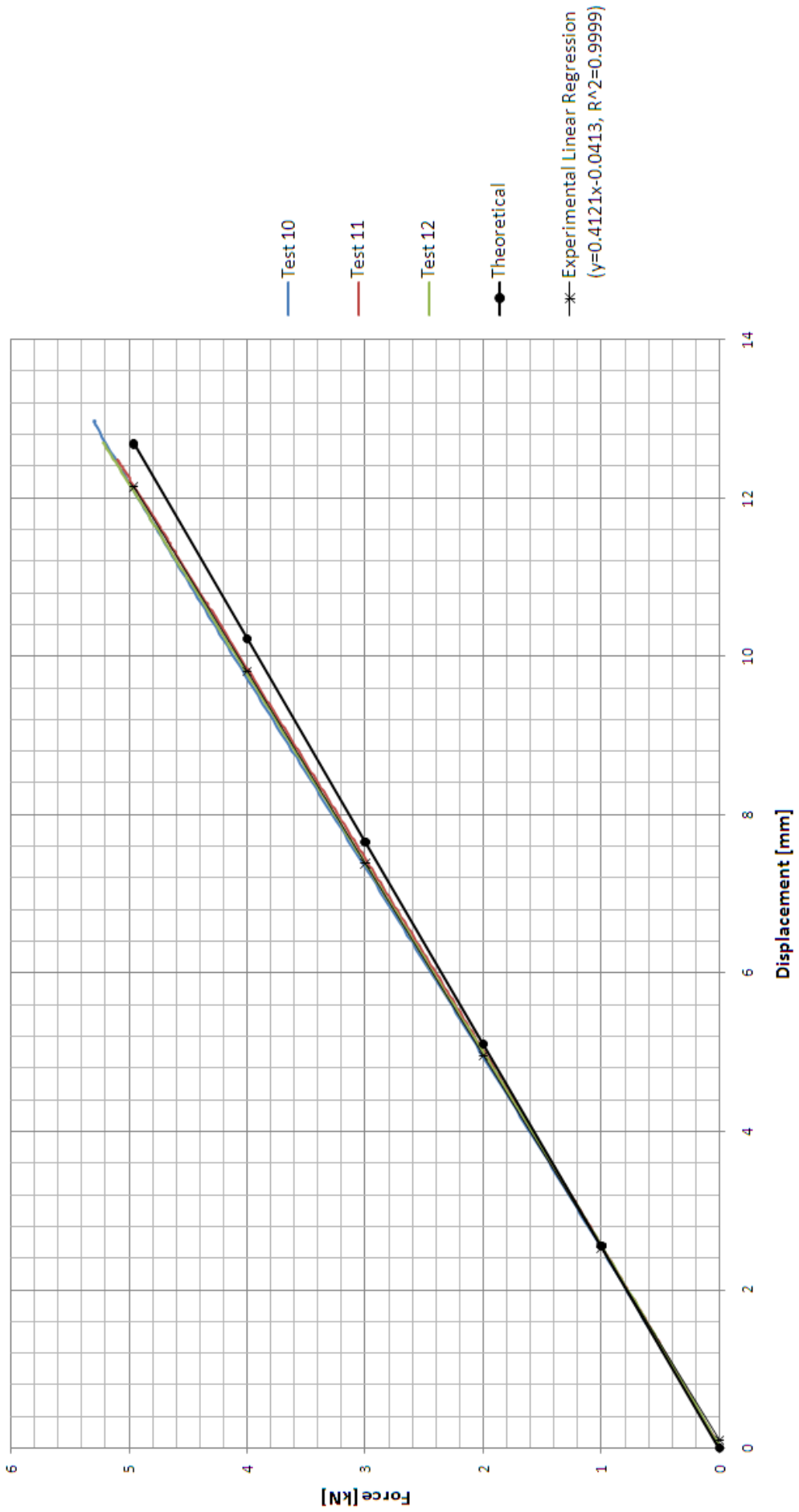

Figure 5.17: Vertical ridge displacement due to a vertical downward force of 4,96 kN applied at ridge. (Tests 10 to 12, grouted supports)

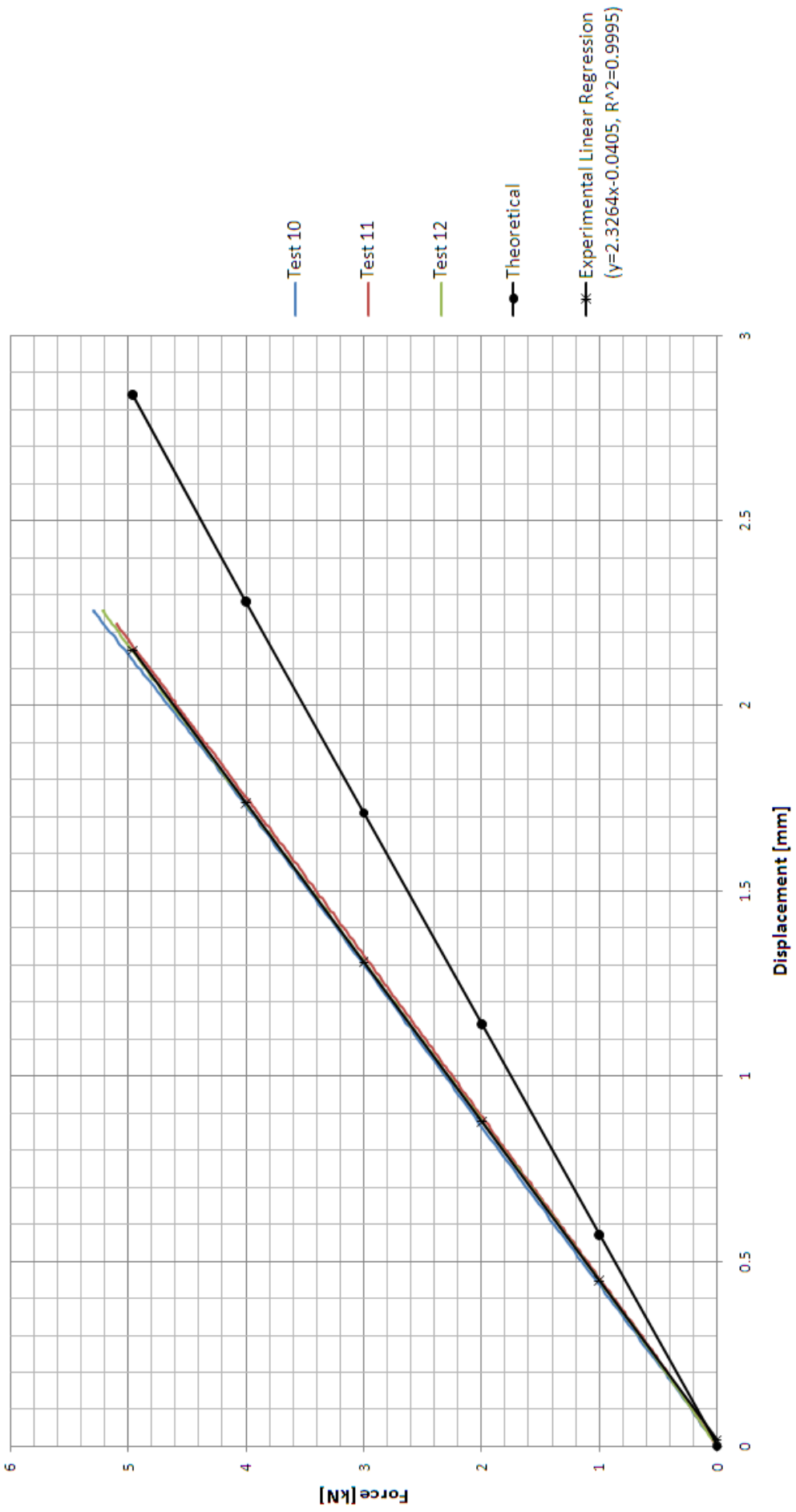

Figure 5.18: Horizontal column displacement due to a vertical downward force of 4,96 kN applied at ridge. (Tests 10 to 12, grouted supports)

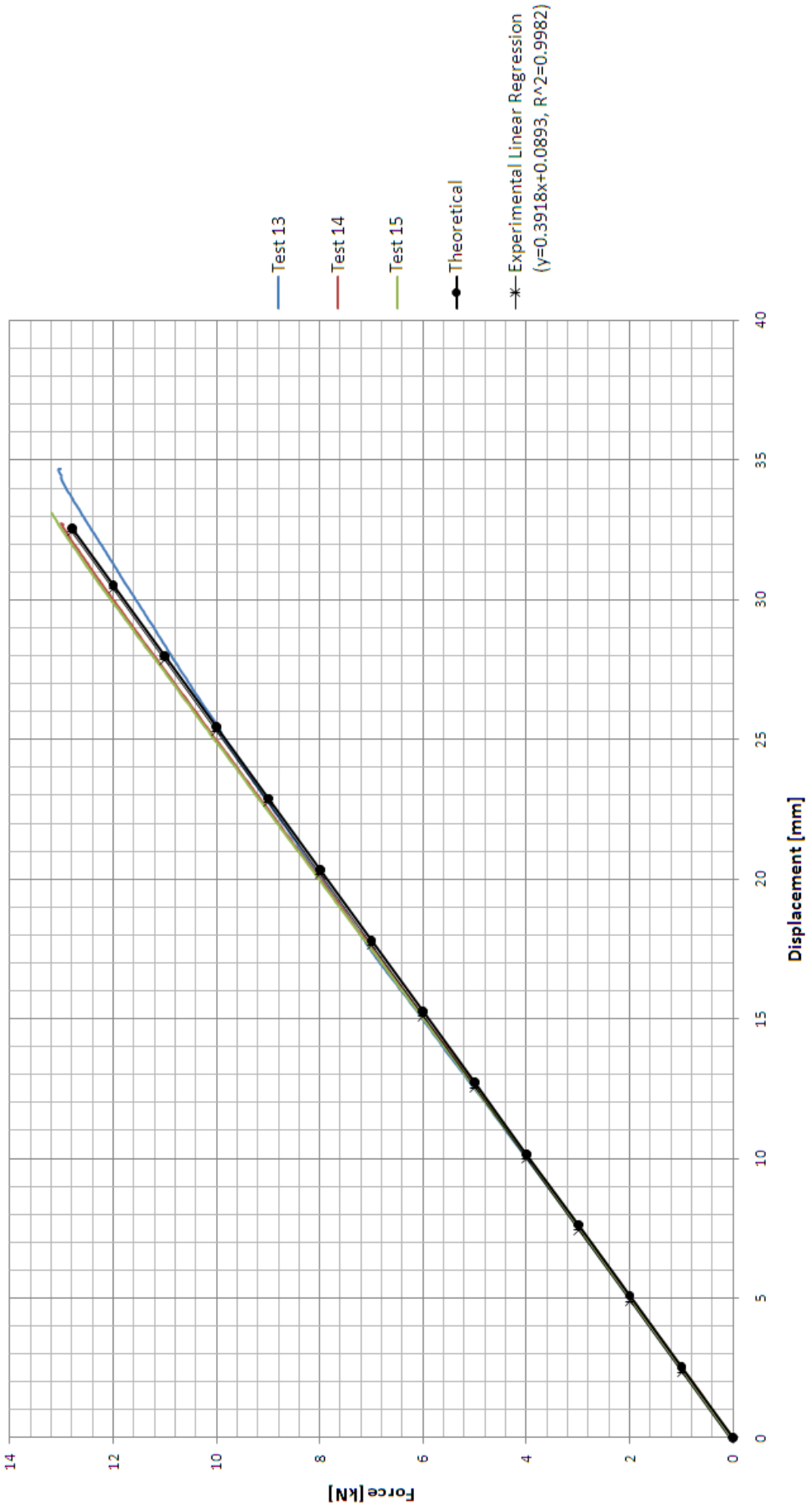

Figure 5.19: Vertical ridge displacement due to a vertical upward force of 12,8 kN applied at ridge. (Tests 13 to 15, grouted supports)

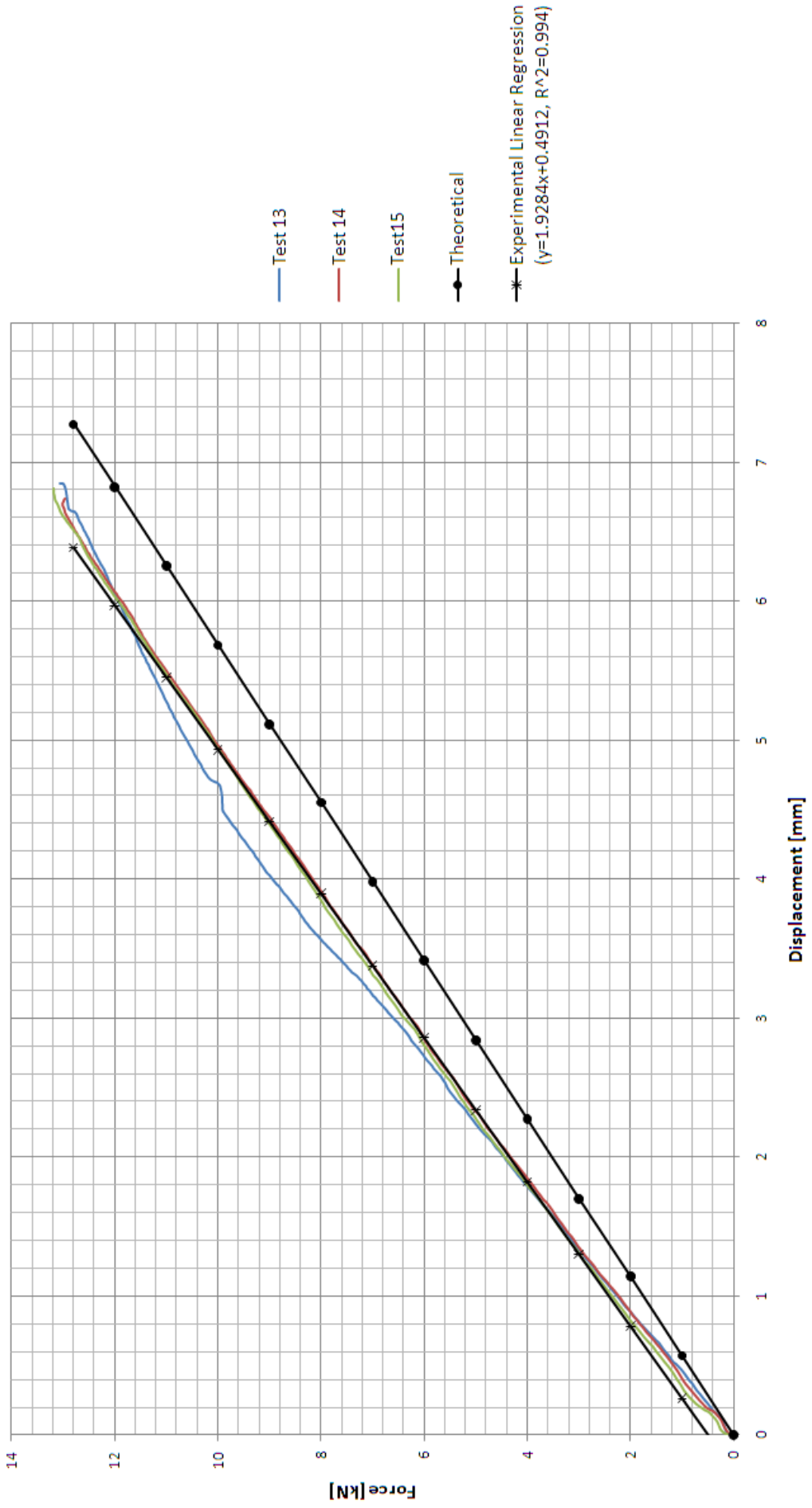

Figure 5.20: Horizontal column displacement due to a vertical upward force of 12,8 kN applied at ridge. (Tests 13 to 15, grouted supports)

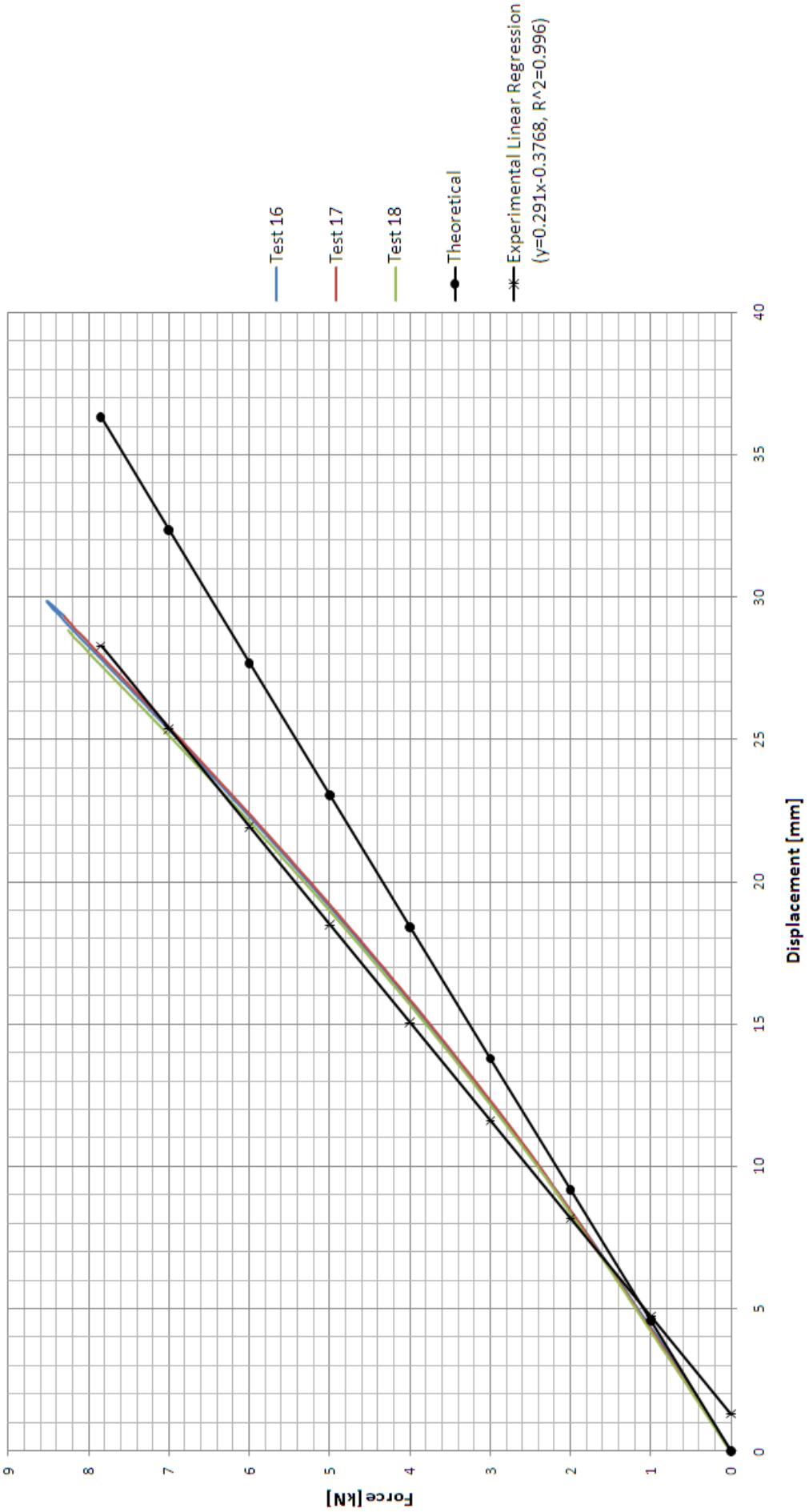

Figure 5.21: Horizontal column displacement due to a horizontal force of 7,85 kN applied at top of column. (Tests 16 to 18, grouted supports)

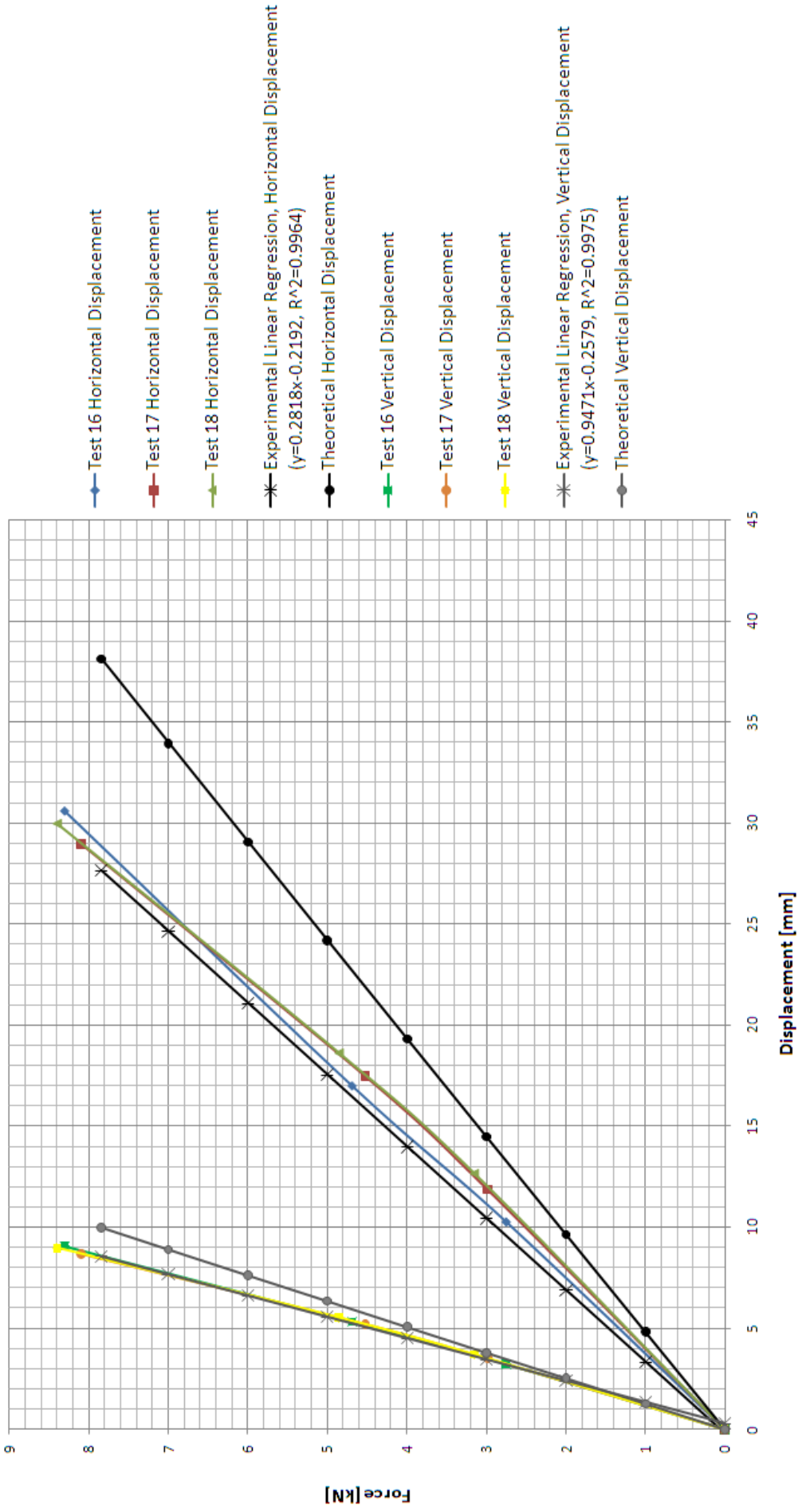

Figure 5.22: Horizontal and vertical girder displacement due to a horizontal force of 7,85 kN applied at top of column. (Tests 16 to 18,grouted supports)

5.6 COMPARISON OF RESULTS

Results from this experimental investigation are explained in this section and summarized in table 5.4 below.

Table 5.4: Difference in real displacements and theoretical predicted displacements for each load case and support condition.

Load Case	Support Condition	Load [kN]	Theoretical Displacement				Experimental Regression				Displacement Difference				% Error			
			Vertical [mm]	Horizontal [mm]			Vertical [mm]	Horizontal [mm]			Vertical [mm]	Horizontal [mm]			Vertical		Horizontal	
			Ridge	Column		Girder	Ridge	Column		Girder	Ridge	Column		Girder	Ridge	Girder	Column	Girder
					Column				Column				Column					
1	Hinge	4,96	12.68	2.84		9.98	13.12	2.99		8.58	-0.44	-0.16		1.41	-3.37	16.38	-2.04	3.23
1	Grouted	4,96	12.68	2.84		9.98	12.14	2.15		8.56	0.54	0.69		1.42	4.48	16.58	28.47	31.81
2	Hinge	12,80	32.55	7.27		32.55	33.38	7.19		32.44	-0.83	0.08		0.89	-2.50	2.75	13.90	
2	Grouted	12,80	32.55	7.27		32.55	32.44	6.38		37.53	0.89	0.89		1.41	2.75	16.38	-2.04	3.23
3	Hinge	7,85	9.98	36.32	38.11		8.58	37.08	37.53		1.41	-0.76	1.21		16.38	-2.04	3.23	
3	Grouted	7,85	9.98	36.32	38.11		8.56	28.27	27.64		1.42	8.05	8.79		16.58	28.47	31.81	

5.6.1 LOAD CASE ONE

Load case one simulates the own-weight of purlins and sheeting and the imposed loads on the structure. This load case is represented by an applied load of 4,96 kN to the ridge of the test specimen in a downward direction, as explained in section 5.3.3. From the curves in figures 5.11 and 5.12, it is clear that the deformations of the frame was linear elastic and therefore no permanent deformations took place in the structural members or connections. The predicted displacements from the second order analysis were less than the linear regression of the actual results of the experimentally-recorded displacements. Comparing the experimental results of the hinge support with the results of the grout support, it is emphasized that the displacements recorded using the hinge support are significantly greater.

5.6.2 LOAD CASE TWO

Load case two simulates the wind uplift forces on the structure and is represented by an applied load of 12,80 kN to the ridge of the test specimen in an upward direction, as per section 5.3.3. A much larger force was applied to the test specimen in load case two if compared to load cases one and three. Load case two causes the haunch connection to experience a much greater moment causing upward deformation of the connection in which the haunch provides the most resistance due to the layout of it's structural components. The experimental curves show that the frame has never undergone any plastic deformations because a linear elastic region is noted throughout the load application curve. The grout support condition caused smaller displacements to be recorded.

5.6.3 LOAD CASE THREE

Load case three represents the final load case where a horizontal force of 4,96 kN is applied to the top of the column simulating a wind force to the side of the structure. This load case exhibits a different deformation pattern compared to the previous two load cases as the haunch connection is subject to opposite direction deformations. The haunch on its the load-application side, deforms against its weaker rotational resistance direction, whereas the haunch on the remaining side deforms against it's stronger rotational resistance direction, as explained in section 4.3. This is due to the layout of the components in the haunch connections. Comparison of the results of load case three for the different support conditions leads to the conclusion that the grouted support condition substantially reduces the recorded displacements of the structure.

5.7 DISCUSSION

Considering the results of the hinge support condition of the test specimen, it is noted that the predicted displacements of the test specimen through second order analysis are accurate when compared to the experimental results shown in table 5.4. The mean of the percentage error in the displacement prediction is 4,579 with a standard deviation of 4,404. It was expected that the difference would be small as the support condition of the test specimen is similar to the ideal support condition as defined in the second order frame analysis of the test specimen. In all cases the real displacement of the test specimen was more than the predicted value from the second order analysis. It is thus clear that the rotational deformation of the connections does affect the frame's overall response in terms of displacements.

The grouted support condition of the test specimen slightly changed this perspective. Each load case exhibited smaller displacements of the test specimen when compared to the predicted results from second order analysis. This is because the restraint provided by the grout interface to the column base plate does not provide idealistic hinged conditions as in the case of the hinge support. This is explained in greater detail in sections 2.4 and 2.6.2. For grouted support conditions the mean of the percentage error in the displacement prediction is 14,714 with a

standard deviation of 8,908.

This chapter is concluded with the statement that the predicted displacements from second order analysis of the frame are accurate compared to the recorded displacements of the test specimen for load cases one, two and three. The only significant inaccurate result is recorded for load case three if the grouted support conditions are considered. This is due to the fact that for a horizontal force applied to the column top, the displacements are substantially more significant in the horizontal directions. The support condition of the column base thus plays a major role in the response of the test specimen in terms of displacements and more specifically of horizontal displacements. The restraint caused by the grouted support thus significantly lowers the recorded displacement for the considered load case and support. It is emphasized that this greatly affects the mean and standard deviation values referred to above for grouted support conditions and is presented in table 5.5.

Table 5.5: Mean and standard deviation of percentage in error of displacement predictions for each support condition.

	% Error in Displacement Prediction	
Support Condition	**Mean**	**Standard Deviation**
Hinge	4,579	4,404
Grouted	14,714	8,908

Chapter 6

STRUCTURAL ANALYSIS OF THE TEST SPECIMEN

The structural analysis performed on a portal frame similar to the test specimen is discussed in this chapter. The structural analysis is performed to provide comparative results to the experimental results for the purpose accuracy assessment. Moment-rotation results from chapter four are implemented as a spring stiffness in a structural analysis, using rotational springs as connections. The results obtained are compared to the experimental results from chapter five in order to assess the accuracy and feasibility of the analysis method when using rotational springs to model real connection behaviour.

The chapter begins with a discussion on the analysis of portal frames in terms of displacement determination as well as obtaining design forces and bending moments for design purposes. The use of a specific software package for the analysis is motivated and followed by a discussion on the determination of a rotational spring stiffness to model each individual connection in the analysis. Load cases imposed on the frame in the analysis are similar to those in chapter five but is discussed briefly, as these are applied in the analysis and provide comparative results. An analysis of the test specimen for each load case and support condition as explained in section 5.1.3, is performed and the results are presented. The results from the analysis of each support condition are summarized at the end of each section.

A sensitivity analysis is presented to investigate certain inaccuracies exhibited by the analysis of the test specimen. The chapter is concluded with a brief discussion of the findings and results of the structural analysis and the sensitivity analysis performed on the test specimen.

6.1 ANALYSIS OF PORTAL FRAMES

It is common design office practice to perform a linear static analysis or second order analysis on portal frames. The columns and girders are modelled as beam elements and all connections are assumed to be rigid in the case of moment-fixed connections or hinged in the case of pinned connections. As a portal frame commonly contains a haunch at the beam-column connections and in some cases at the ridge, it is modelled as a tapered section. Tapered sections assign the moment of inertia value of the beam section to the ridge side of the beam-column haunch. The moment of inertia is then increased linearly along the length of the haunch to the moment of inertia of the desired haunch depth on the endplate side of the connection to form the haunched section. It is assumed that the flange of the girder lies on the neutral axis of the haunched beam and therefore does not contribute a significantly to the bending resistance of the connection to warrant the development of the complex model for it.

Figure 6.1 illustrates a typical design office analysis layout of the test specimen described in chapter five. Note the tapered section is illustrational to the increasing stiffness of the haunches modelled in the frame. From the figure it is also clear that a fine mesh of beam elements are used for the analysis as this will result in accurate displacement data of the frame. Displacements are calculated at each node and beam element ends, and therefore a denser mesh of beam elements will result in more accurate results.

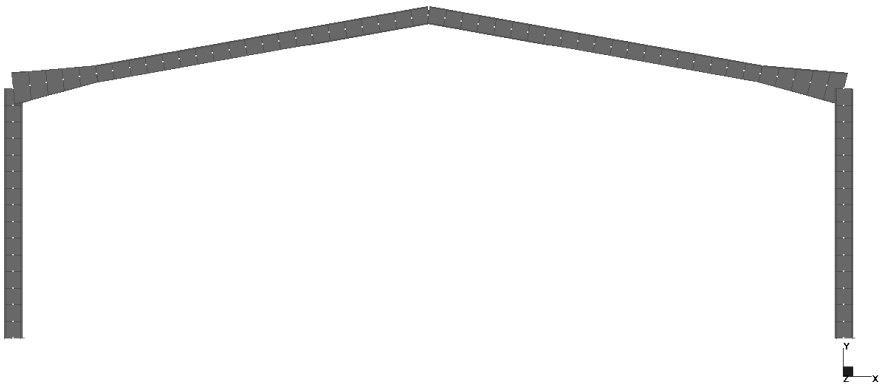

Figure 6.1: Structural analysis layout of the experimental portal frame.

A linear static analysis or second order analysis is then performed on the frame in order to obtain the displacements, design moments and forces to be used for designing the structure to the criteria set by ultimate and serviceability limit states. Second order analysis accounts for the P-delta effects in the members and therefore provides more accurate results compared to linear static analysis. This is discussed in detail in section 2.8 of chapter 2.

6.2 CHOICE OF SOFTWARE

Strand7 Finite Element Analysis software was used for all the structural analyses performed on the test specimen. The choice of software was motivated by the accurate results it produces in second order analysis as well as the modelling of rotational springs between beam elements as connections. A further motivation was to develop a method of displacement determination that could be implemented in design offices and therefore a software package used widely in modern design offices had to be used for the analysis. Two packages are widely used in South African design offices, i.e. Prokon Structural Analysis and Design, as well as Strand7. Prokon was assessed by modelling simple structures with rotational springs but the results produced were inaccurate and the response of the structure did not correlate with the real structural response. The results produced by Strand7 however proved to be accurate in terms of displacements and overall structural response.

6.3 ANALYSIS OF PORTAL FRAMES IMPLEMENTING ROTATIONAL SPRINGS

Section 2.7 of chapter 2 focussed on the use of rotational springs in frame analysis in order to account for the real behaviour of joints and bases in the analysis. Figure 2.6 from chapter two is presented in figure 6.2 for illustrational purposes as well as indicating the haunch and ridge connections referred to in this chapter.

The moment-rotation behaviour of each connection is used to calculate the connection stiffness, which is then implemented as a linear rotational spring stiffness in the analysis. The "initial stiffness" as described in section 2.7

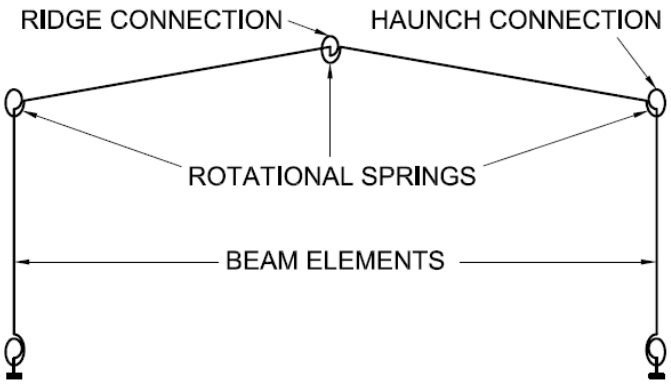

Figure 6.2: Portal frame analysis modelling connections as rotational springs.

is calculated for each connection of the test specimen and is then used in the analysis. The results are presented in this section.

6.3.1 DETERMINATION OF ROTATIONAL SPRING STIFFNESS

Figure 6.3 below illustrates the determination of the initial stiffness of the connection by using a data point in the elastic region of the moment-rotation curve. The curve illustrated is the moment-rotation behaviour of the test specimen haunch connection for in-plane upward deformation.

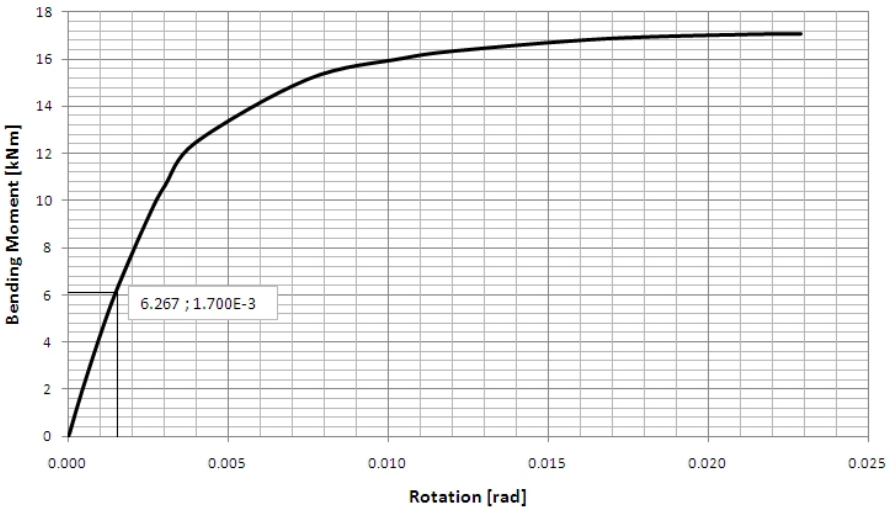

Figure 6.3: Determination of the rotational spring stiffness according to the "initial stiffness" definition.

The spring stiffness is given by equation 6.1:

$$Linear\ spring\ stiffness = \frac{Bending\ moment}{Rotation} \qquad \left[\frac{kNm}{rad}\right] \tag{6.1}$$

The moment-rotation curves presented in sections 4.3 to 4.5 of chapter 4 are used to calculate the linear spring stiffness used in the analysis with rotational springs for the rigid connections of the test specimen. Table 6.1 presents the data points used as well as their representative linear spring stiffness value for each direction of in-plane rotational deformation. Small bending moments values have been chosen to determine the spring stiffness to ensure that the "initial" stiffness as defined in section 2.7 has been determined. The values in bold are used for illustrational purposes in figure 6.3.

Table 6.1: Test specimen rotational spring stiffnesses.

Connection	Direction of In-plane Rotational Deformation	Bending Moment [kNm]	Rotation [rad]	Spring Stiffness [kNm/rad]
Test Specimen Haunch	Downward	0.804	1.855×10^{-4}	4.333×10^{3}
	Upward	**6.267**	**1.700** $\times 10^{-3}$	4.102×10^{3}
Test Specimen Ridge	Downward	0.946	4.129×10^{-5}	22.904×10^{3}
	Upward	0.945	4.138×10^{-5}	22.859×10^{3}

The test specimen haunch connection exhibits a slight difference in stiffness for the two directions of in-plane rotation due to the unsymmetrical layout of the components in the connection. Note that the ridge connection has a similar stiffness for in-plane rotation due to the symmetrical layout of the connection.

6.3.2 ANALYSIS OF THE TEST SPECIMEN

Structural analysis using the rotational spring stiffness determined in section 6.3.1, was used to analyze the test specimen in order to determine the feasibility and accuracy of the frame analysis taking into accounting the real behaviour of joints. Spring stiffness values are assigned as a linear value to the rotational spring.

From a practical point of view, the tapered layout of the beam-column haunch connection provides support to the top of the column over the depth of the haunch. Bolts ensure support to the column by the haunch at the top and the bottom thereby creating a significant increase in the stiffness of the column in the top region. A frame analysis using beam elements does not account for this almost rigid stiffness of the top part of the column and is therefore modelled as a rigid link in frame analysis implementing rotational springs as illustrated in figure 6.4. The tapered section in the frame analysis only provides an increased stiffness to the beam elements used to model the girder at the haunched length and not the column.

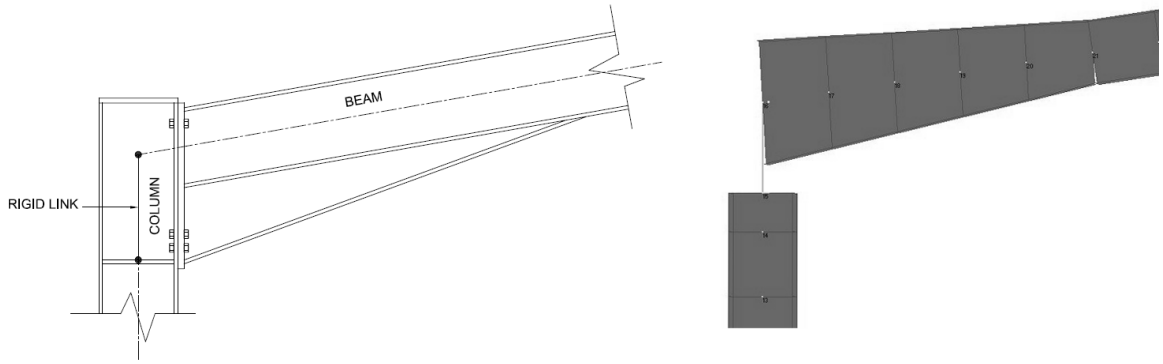

Figure 6.4: Rigid link used to simulate haunch support in the column.

6.3.3 LOAD CASES IMPOSED IN ANALYSIS

Three load cases have been considered for use in the frame analysis. These load cases are similar to the load cases imposed on the test specimen during the experimental investigation. Loads are applied as point loads according to the constraints of the experimental setup and the availability of equipment in the laboratory. The magnitude of the point loads were determined by obtaining loads that generate the same bending moments in the beam-column

connections as the real design load cases determined in accordance with SANS 10160:2011 parts one to three. In each load case all components of the test specimen remain within their elastic region and no plastic deformation takes place. This is similar to the criteria set by serviceability limit state requirements.

Load case one simulates the own-weight of purlins, sheeting and cladding on the structure and a vertical downward load of 4.96 kN was applied at the ridge of the test specimen. In the opposite direction load case two is applied vertically upward at the ridge of the test specimen. Load case two simulates the uplift forces caused by wind on the structure and is the worst load case for design purposes of the portal frame. Wind is also simulated by load case three, which is a horizontal load applied to the top of the column of the structure. Figure 6.5 illustrates the three load cases considered in the frame analysis of the test specimen to asses the accuracy of implementing rotational springs. The latter two load cases cause the design moment of the beam-column connection to be generated at the beam-column connection of the test specimen.

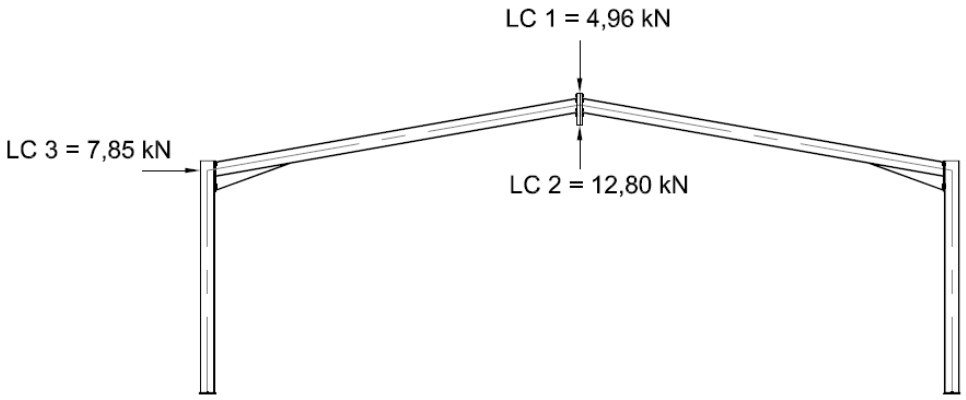

Figure 6.5: Load cases considered during frame analysis.

Figure 6.6 below illustrates the deformation pattern of the structure under each of the load cases described.

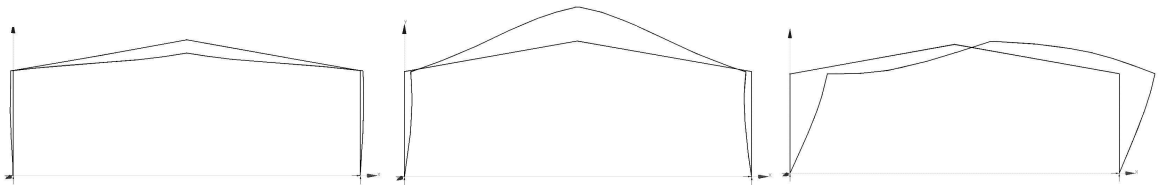

Figure 6.6: Predicted deformation of the structure for each of the three load cases described.

6.4 PORTAL FRAME ANALYSIS WITH HINGE SUPPORTS

Loads have been applied to the experimental test specimen (discussed in chapter five) to obtain real and accurate displacement data. Three different load cases, as well as two different support conditions were considered for the test specimen. A total of six different tests were therefore performed on the test specimen. Using a hinge support in the experimental tests created an opportunity to isolate the effect of column base behaviour in the portal frame analysis. The hinge support is similar to the true modelling conditions used in the frame analysis for pinned column supports. All three load cases and their results for the frame supported by perfect hinges are discussed in this section. Note that all analyses referred to are second order analyses performed on the structure.

6.4.1 LOAD CASE ONE

The load is applied to the frame as a vertically downward point load at the ridge node of the frame. Displacements were recorded at nodes similar to the positions where displacements were measured on the test specimen (figure 5.7). The results are presented in table 6.2.

Table 6.2: Displacement data from analysis of load case one, hinge supports.

Analysis	Displacement	Value [mm]	Experimental Regression [mm]	Difference [mm]	% Error
Rigid Connections & Pinned Bases	Vertical Ridge	13.498	13.123	0.375	2.86
	Horizontal Column	2.740	2.997	-0.257	-8.58
Rotational Springs & Pinned Bases	Vertical Ridge	**13.129**	13.123	0.006	0.046
	Horizontal Column	**2.47**	2.997	-0.527	-17.58

From table 6.2 it is clear that the analysis using rotational springs, results in significantly more accurate vertical displacement being recorded than the analysis which assumes the connections to be rigid. For horizontal displacement however, the results were less accurate and the difference in displacement was 0.527 mm. Various tolerances are applicable during the recording of experimental data and affects the measurements. These tolerances are discussed in the summary at the end of this section. A 0.527 mm difference could thus be regarded as insignificantly small. Table 6.2 is illustrated graphically in figure 6.7.

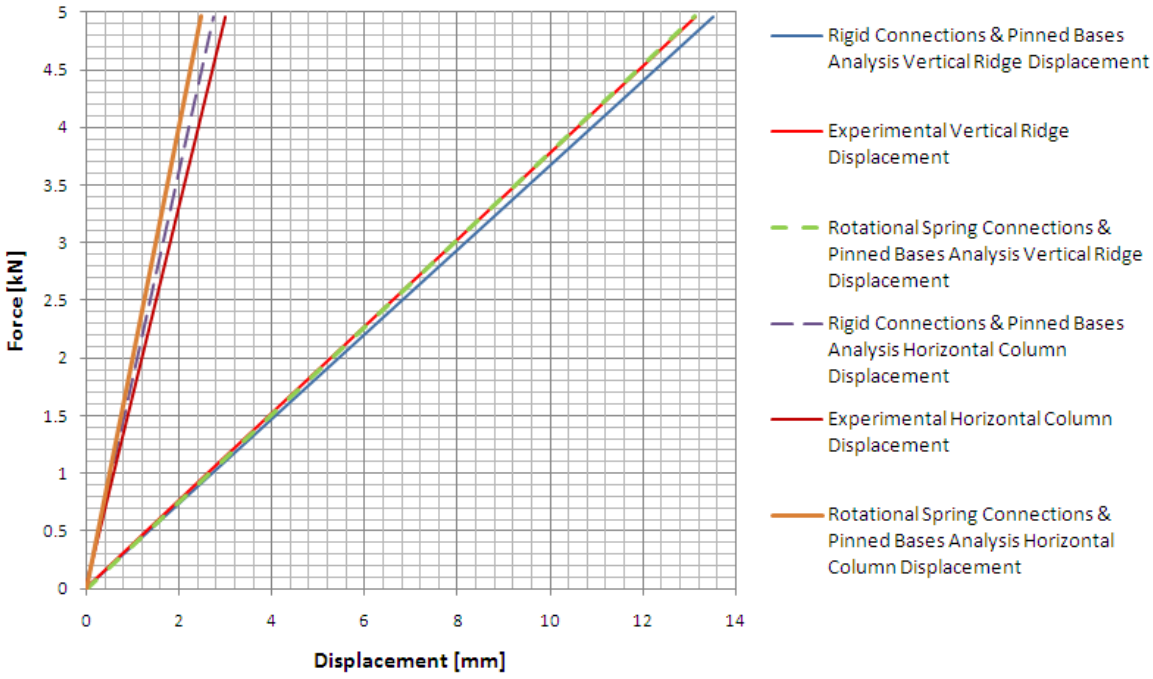

Figure 6.7: Displacement results of the analysis of load case one, hinge supports.

6.4.2 LOAD CASE TWO

A vertical upward point load is applied to the ridge node of the frame. Displacements are recorded at nodes similar to those of load case one. Displacement results are presented in table 6.3 below.

Table 6.3: Displacement data from analysis of load case two, hinge supports.

Analysis	Displacement	Value [mm]	Experimental Regression [mm]	Difference [mm]	% Error
Rigid Connections & Pinned Bases	Vertical Ridge	33.786	33.384	0.402	1.20
	Horizontal Column	7.161	7.098	0.063	0.89
Rotational Springs & Pinned Bases	Vertical Ridge	**32.845**	33.384	-0.539	-1.61
	Horizontal Column	**6.493**	7.098	-0.605	-8.52

From table 6.3 it can be concluded that both methods of analysis prove to be sufficiently accurate. The results produced by the analysis using rigid connections are more accurate than the analysis using rotational springs. Once again the horizontal displacement of the rotational spring analysis seems inaccurate by 8,52%. However it must be borne in mind that the difference of 0.605 mm does not take into account the measurement and manufacturing tolerances of the test specimen used in the experimental investigation. This is discussed in the summary at the end of this section. Table 6.3 is illustrated graphically in figure 6.8.

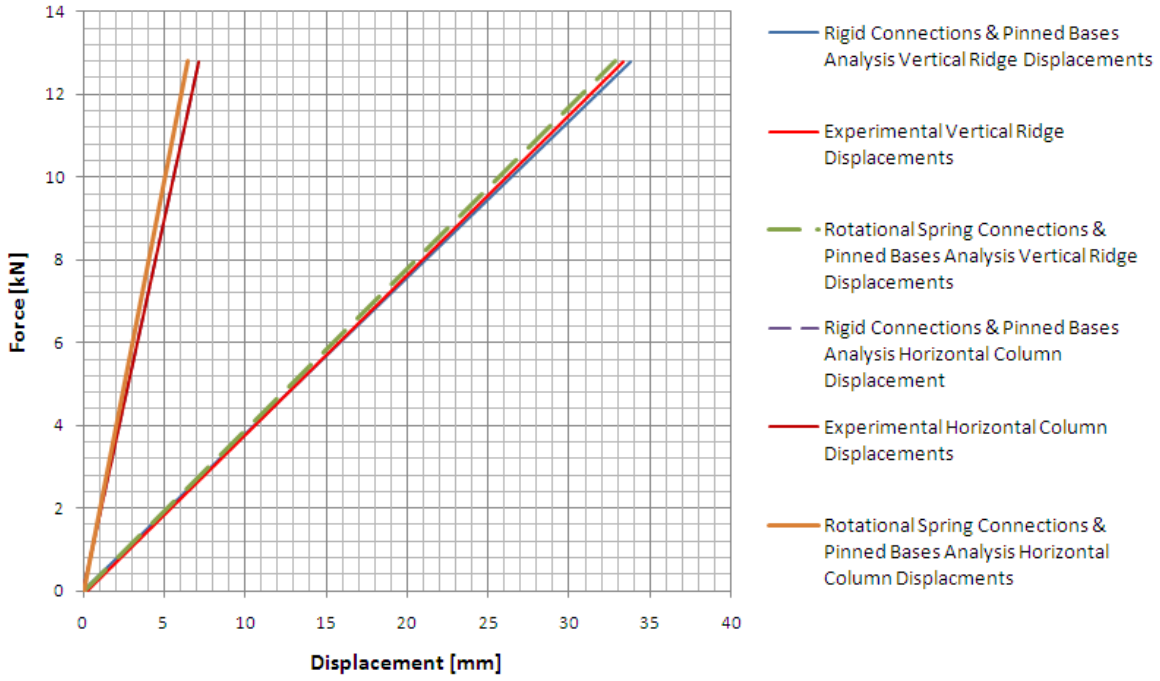

Figure 6.8: Displacement results of the analysis of load case two, hinge supports.

6.4.3 LOAD CASE THREE

A horizontal point load is applied to the top of the column. Displacements are recorded at a node in the midpoint of the girder and on the opposite column top to which the force has been applied (figure 5.7). Table 6.4 presents the results.

It is clear from table 6.4 that the horizontal displacements from the rotational spring analysis are significantly more accurate that the results from the analysis using rigid connections. Vertical girder displacement deviates in a similar way from the experimental regression value. It is noted that the exact position of the optical measuring system used to record experimental displacements, is not always at the exact position of the node used to record analytical

Table 6.4: Displacement data from analysis of load case 3, hinge supports.

Analysis	Displacement	Value [mm]	Experimental Regression [mm]	Difference [mm]	% Error
Rigid Connections & Pinned Bases	Horizontal Column	38.813	37.328	1.485	3.98
	Horizontal Girder	40.426	37.831	2.595	6.86
	Vertical Girder	9.524	8.716	0.808	9.27
Rotational Springs & Pinned Bases	Horizontal Column	**36.594**	37.328	-0.734	1.97
	Horizontal Girder	**38.194**	37.831	0.363	0.96
	Vertical Girder	**9.530**	8.716	0.814	9.34

displacements. Tolerances are present during the measurement of displacements and is discussed in the summary at the end of this section. Table 6.4 is illustrated graphically in figures 6.9 and 6.10.

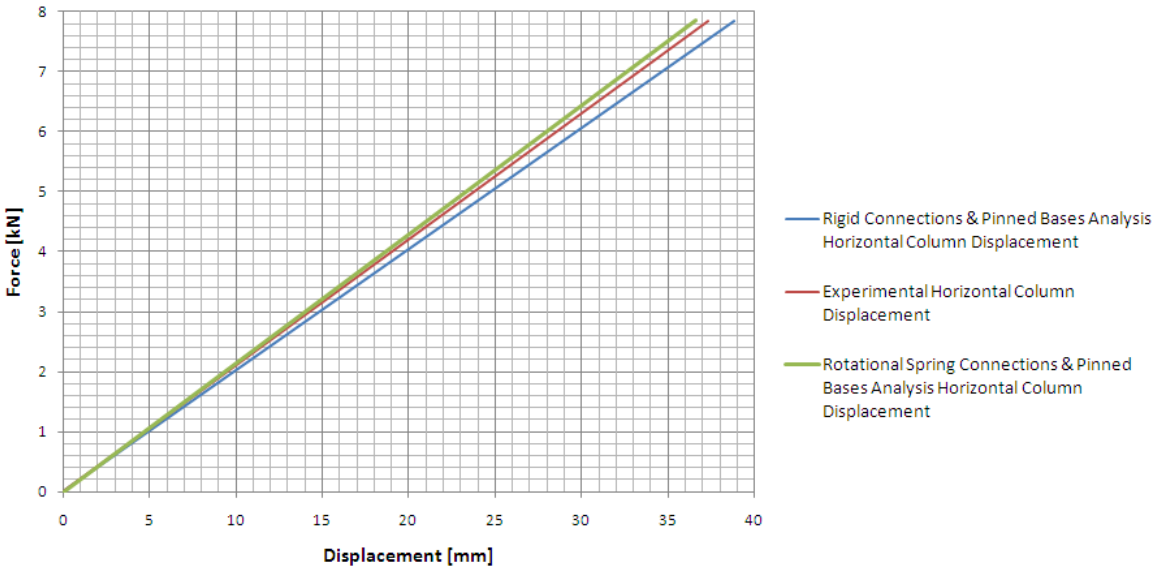

Figure 6.9: Column displacement results of the analysis of load case three, hinge supports.

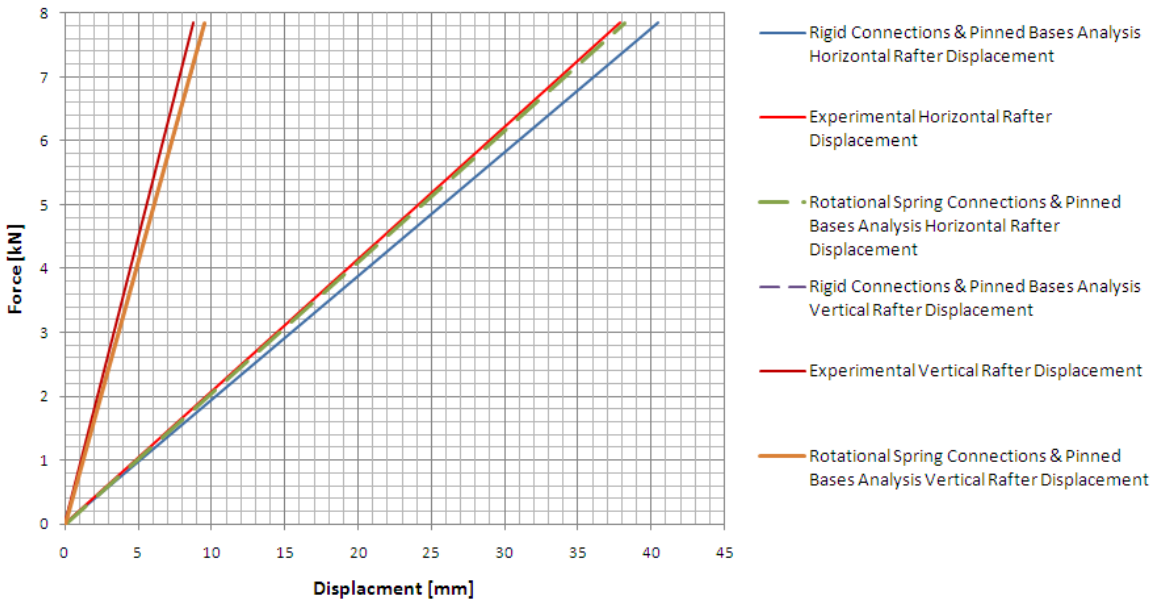

Figure 6.10: Girder displacement results of the analysis of load case three, hinge supports.

6.4.4 SUMMARY OF RESULTS

Three load cases were considered with results varying in accuracy if the analysis using rotational springs were considered. In each case the displacements in a direction similar to that of the applied force, was within an accuracy of 2%. The displacement in a direction perpendicular to the applied force proved to be less accurate, however the difference in each case was less than 1 mm. It must be considered that various tolerances are present when recording data during an experimental test.

Although measuring equipment is calibrated to a certain extent, measurement differences of 0.5 mm are regarded as insignificantly small. The measurement direction of the LVDT's are not always perfectly perpendicular to the displacement direction. This causes inaccuracies as rotations are present in the structural members and not measured by the LVDT. Furthermore are manufacturing tolerances are also present and the steel profiles supplied may deviate from the exact values given in the Southern African Steel Construction Handbook (SAISC, 2008), which were used for the input to the structural analysis. Young's modulus and Poisson's ratio were also taken from literature and deviations could be present in the test specimen. The analytical model was set up as accurately as possible, but certain deviations could not be eliminated.

The conclusion is made that a structural analysis which uses rotational springs to model rigid connection response does result in more accurate displacements being recorded if the frame is supported by a perfect hinge. The perfect hinge is similar to that modelled in an analytical frame analysis. A structural analysis using rigid connections is also regarded as being sufficiently accurate, however the overall frame response is affected if the real behaviour of connections are considered.

6.5 PORTAL FRAME ANALYSIS WITH GROUTED SUPPORTS

In the previous section it was stated that a structural analysis of portal frames using rotational springs does result in more accurate displacement predictions when compared to an analysis which assumes connections to be rigid. Real column base behaviour significantly affects the response of the structure to certain loads, with the most prominent affects being noted with horizontal loads. A structural analysis assuming the perfect hinge supports described in the previous section, does not take into account for the real behaviour of column bases. The results from the analysis were compared to the experimental results of the test specimen supported by hinges, as being the ideal condition simulated in analysis of pinned column bases. In practice a pinned base is not perfectly pinned. Structural analyses in this section will include the moment-rotation of the column base by modelling the column base as a non-linear rotational spring. The results from the analysis are then compared to the experimental results of a test specimen supported by grouted supports.

Column bases are modelled as non-linear rotational springs. A non-linear input of stiffness is required as the connections are designed to be pinned. Grouted infill below the baseplate provides restraint against rotation, causing a moment to be generated at the column base. Furthermore the rotation of the column base is restricted but not to the extent of rigid-designed connections. It is therefore a motivation to model column bases non-linearly in second order analysis. With each iteration in a second order structural analysis, the column base stiffness is then revised for a certain rotation and carried forward to the next iteration of the analysis. In all load cases, rotation of the base causes yielding to take place in the connection, but not plastic deformation. The latter statement is supported by comparing the reaction rotation to the moment-rotation curve of the column base. Rigid connections do not undergo severe deformations during serviceability load cases and stay within the elastic region of the connection's moment-rotation curve. It is therefore not necessary to model a rigid-designed connection as a

non-linear rotational spring.

Displacement results from the three load cases are presented and discussed below.

6.5.1 LOAD CASE ONE

This analytical model is exactly similar to the model described in section 6.4.1 of this chapter. The effective length of the column is reduced as the grouted support does not cause a 40 mm increase in column length as does the hinged support. Furthermore it is the moment-rotation behaviour of the grouted supports that is simulated as non-linear as described above. Table 6.5 presents the displacement results.

Table 6.5: Displacement data from analysis of load case one, grouted supports.

Analysis	Displacement	Value [mm]	Experimental Regression [mm]	Difference [mm]	% Error
Rigid Connections & Pinned Bases	Vertical Ridge	13.291	12.136	1.155	9.52
	Horizontal Column	2.657	2.149	0.508	23.64
Rotational Springs	Vertical Ridge	**11.942**	12.136	-0.194	-1.60
	Horizontal Column	**2.146**	2.149	-0.003	-0.14

It is clear from the results that the analysis using rotational springs is significantly more accurate for a vertical downward load applied at the ridge of the portal frame. Both vertical and horizontal displacements have a percentage error of less than 2%. Figure 6.11 illustrates the results from the two types of analyses of load case one.

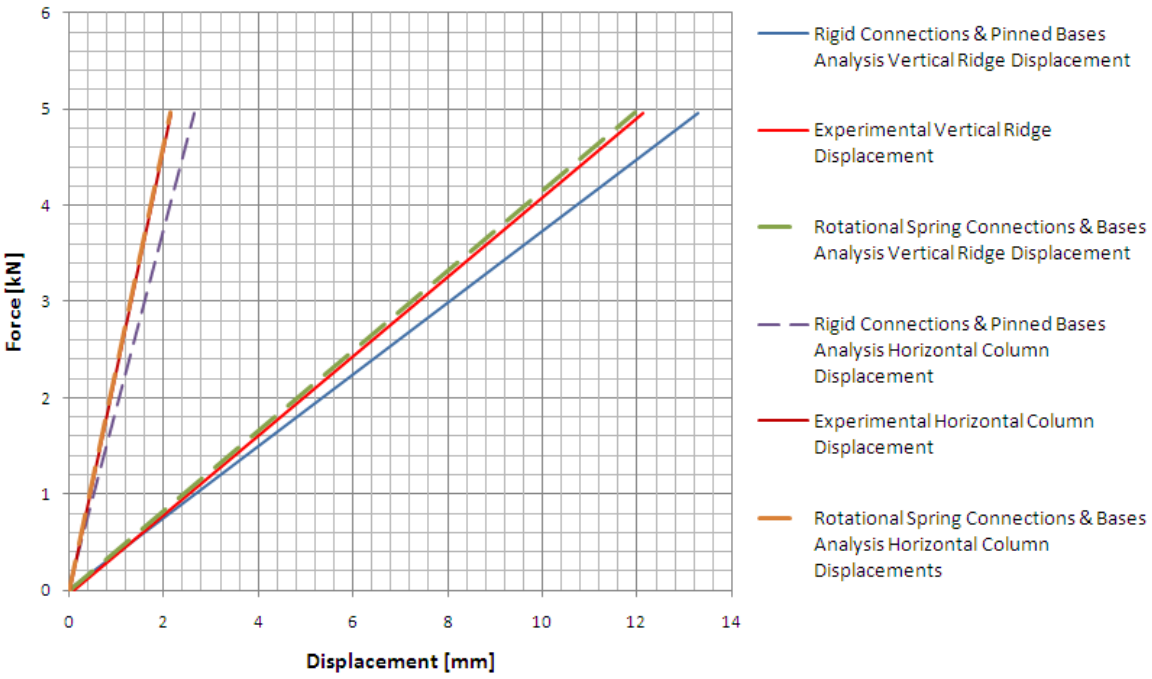

Figure 6.11: Displacement results of the analysis of load case one, grouted supports.

6.5.2 LOAD CASE TWO

Load case two is similar to load case one, except for a greater force being applied in an opposite direction at the ridge. Displacements are recorded at the same nodal positions but the results are quite different to the results of load case one. Table 6.6 presents the results for the non-linear column base modelling of load case two.

Table 6.6: Displacement data from analysis of load case two, grouted supports.

Analysis	Displacement	Value [mm]	Experimental Regression [mm]	Difference [mm]	% Error
Rigid Connections & Pinned Bases	Vertical Ridge	33.266	32.442	0.824	2.54
	Horizontal Column	6.940	6.302	0.638	10.12
Rotational Springs	Vertical Ridge	**30.379**	32.442	-2.063	-6.36
	Horizontal Column	**5.683**	6.302	-0.619	-9.82

In both cases the displacements are under-predicted. Vertical displacements are the most important in this load case, as the force is applied vertically. It is noted that the accuracy of the analysis which uses rigid connection behaviour, produces significantly more accurate results compared to the analysis which uses rotational springs to model real connection response. Rigid connection analysis results in a percentage error of less than 3% for vertical displacements. In both methods of analysis the horizontal displacements exhibit a significant percentage error. Once again it is noted that the difference in displacements, compared to the experimental regression results, is less than 1 mm. This difference can be explained by the tolerances in the measurement of data during experimental testing. Figure 6.12 presents the displacement results of load case two graphically.

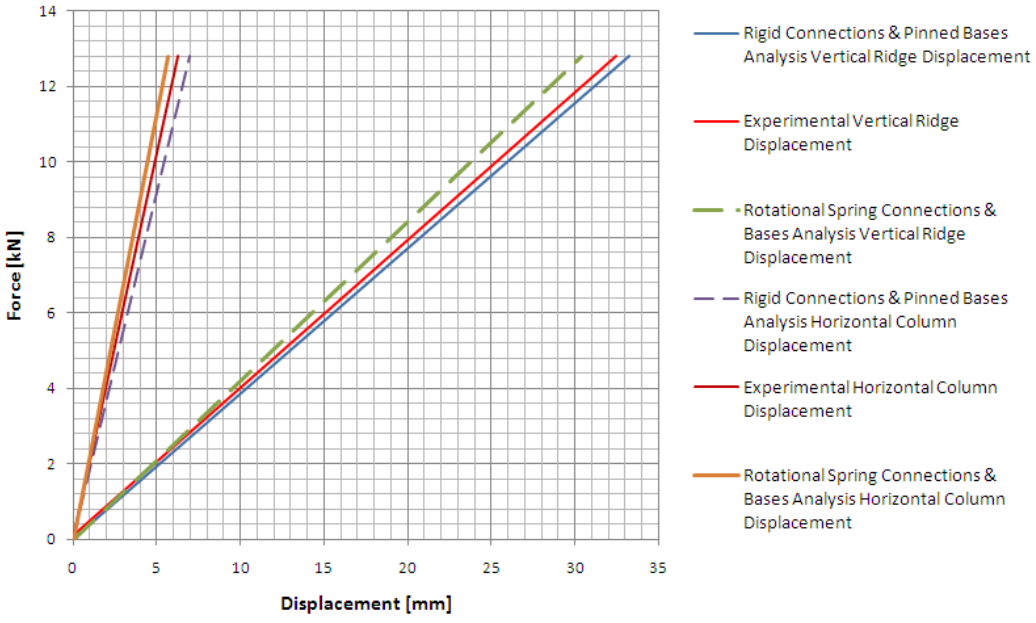

Figure 6.12: Displacement results of the analysis of load case two, grouted supports.

6.5.3 LOAD CASE THREE

Load case three provides valuable data for the accurate assessment of modelling real column base response. Horizontal forces applied to the top of the column cause the column deformation to contribute substantially to the

displacements of the structure. The stiffness of the column base plays a vital role in the stiffness of the column itself in bending moment distribution (as the base is not perfectly pinned) and therefore in the effective length and deformation pattern. Displacements are measured at points of maximum displacement of the column and the girder, i.e. at the top of the column and midpoint of the girder respectively. Table 6.7 presents the results for load case three of the structure using non-linear column base behaviour.

Table 6.7: Displacement data from analysis of load case three, grouted supports.

Analysis	Displacement	Value [mm]	Experimental Regression [mm]	Difference [mm]	% Error
Rigid Connections & Pinned Bases	Horizontal Column	36.378	28.639	7.739	27.02
	Horizontal Girder	37.950	28.850	9.100	31.54
	Vertical Girder	9.325	8.636	0.689	7.09
Rotational Springs	Horizontal Column	**23.498**	28.639	-5.141	-17.95
	Horizontal Girder	**24.680**	28.850	-4.17	-14.45
	Vertical Girder	**7.186**	8.636	-1.45	-16.79

Results show that both methods of displacement prediction result in estimates not significantly accurate if compared to the experimental regression results. Rigid connection analysis overpredicts displacements to such an extend that data is in excess of 27% in error for horizontal displacements. This is explained by the fact that the column base is modelled as being perfectly pinned, which however is not the case because the grout support provides rotational restraint as described earlier. Non-linear column base behaviour is modelled in the rotational spring analysis, and although displacements are underpredicted in this analysis it does result in more accurate displacements if compared to the rigid connection analysis. A percentage error of less than 18% is noted for all directions of displacement. This section is followed by a section describing a sensitivity analysis on the grouted column base support in order to identify the error in displacement prediction of modelling non-linear column bases. Figures 6.13 and 6.14 illustrate the displacement results for all the analyses of load case three.

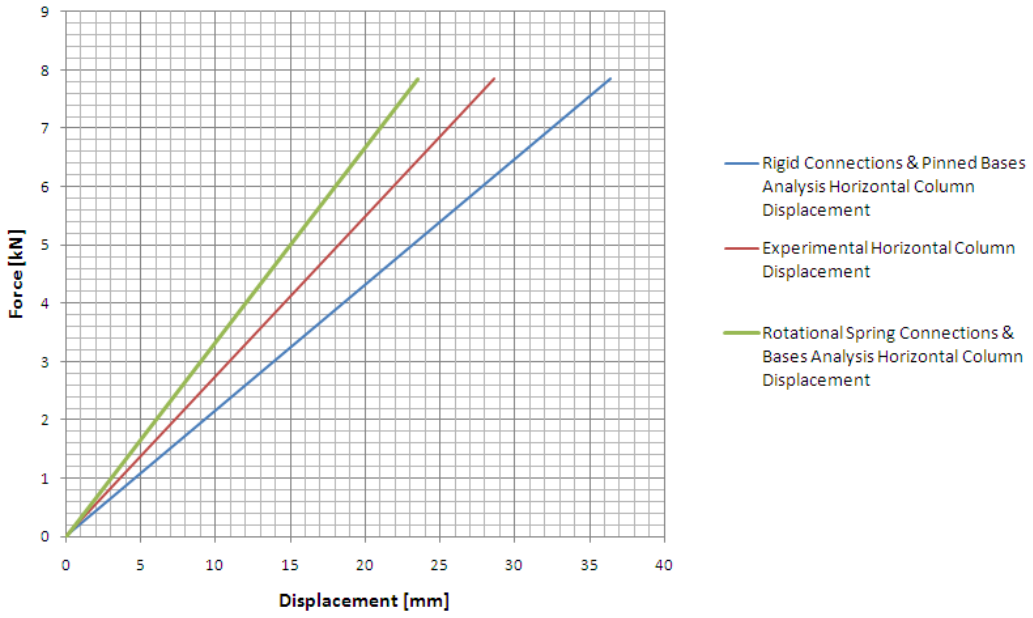

Figure 6.13: Column displacement results of the analysis of load case three, grouted supports.

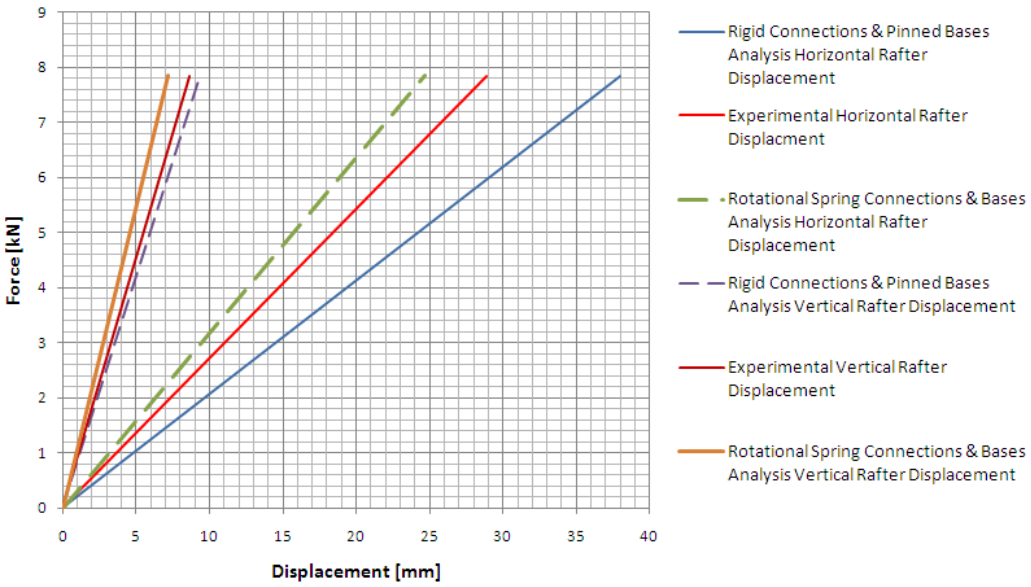

Figure 6.14: Girder displacement results of the analysis of load case three, grouted supports.

6.5.4 SUMMARY OF RESULTS

The previous section regarding the analysis of the portal frame supported by perfect hinges concluded that modelling real connection behaviour with rotational springs does result in more accurate displacement results. This perspective changed with the modelling of real column base behaviour. Load case one presented more accurate results with the analysis using rotational springs whereas the remaining two load cases did not. The results of load case three show the most severe influence of the column base response as explained, and did result in more accurate displacements than the rigid connection analysis. The results are not sufficiently accurate as the percentage error in each case is greater than 5%. This section is followed by a sensitivity analysis of column base behaviour to identify the possible causes for inaccuracy in the displacement results.

6.6 SENSITIVITY ANALYSIS OF COLUMN BASE RESPONSE

The results of the previous section created a necessity to perform a sensitivity analysis on the column base response in order to identify the possible cause of inaccurate displacement results. The following aspects were identified as parameters in the stiffness of the column base and which therefore affect the accuracy in displacement prediction due to the non-linear response of the column base in the analysis using rotational springs:

- Preload on holding-down bolts.
- Stiffness of the grouted interface.
- Stiffening of cementitious grout under loading.

The listed aspects were researched and are presented in sections 6.6.1 through to 6.6.3.

6.6.1 EFFECT OF PRELOAD ON HOLDING-DOWN BOLTS

Ordinary bolts in bolted steel connections are tightened according to the "turn of the nut" method (Kulak et al., 2001). Various studies indicate that the method referred to results in a bolt preload of approximately 70% of the proof stress of the bolt. Throughout this study a 70% bolt preload has been applied to all bolts in the finite element analysis. It is however noted that the bolt preload has not been measured in the experimental investigation and could be thought to affect the overall frame response in terms of displacements. It was therefore decided to perform a sensitivity analysis on bolt preload of the holding-down bolts of the grouted supports in order to shed some light onto the matter.

Figure 6.15 presents the moment-rotation behaviour of the test specimen grouted supports, at bolt preloads of 0%, 5%, 35% and 70% respectively.

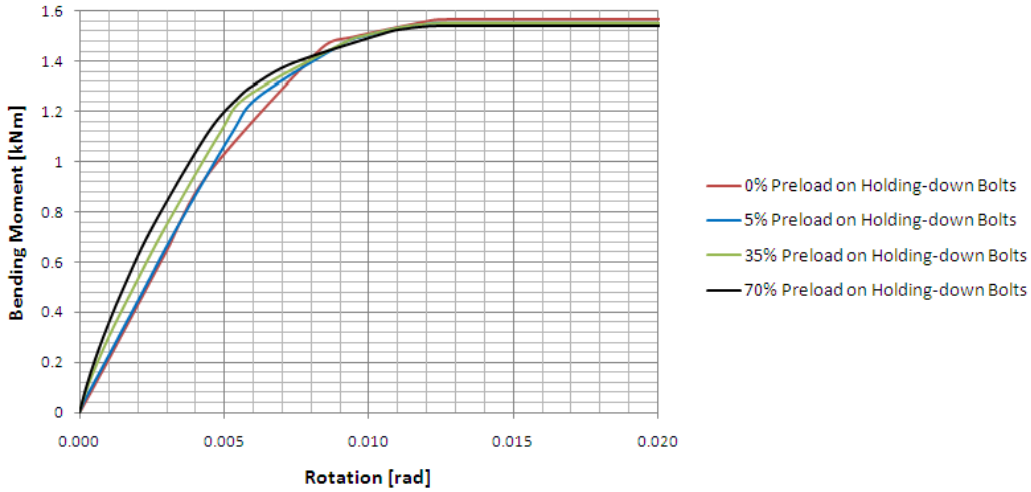

Figure 6.15: Moment-rotation behaviour of test specimen grouted support at different bolt preloads.

It is clear from the figure that the initial stiffness of the connection is significantly affected by the percentage preload on the holding-down bolts. The ultimate moment capacity of the connection is not affected by bolt preload and is almost similar for each bolt preload percentage.

The various stiffnesses for column base response have been implemented in the analysis of load case three and the results are presented in table 6.8.

Table 6.8: Effect of preload on column base holding-down bolts for frame response.

Bolt Preload	Base Rotation [rad]	Moment-Rotation Stiffness at Base [kNm/rad]	Column Displacement [mm]
0%	0.02957	52.989	34.768
5%	0.01775	87.541	23.413
10%	0.01776	87.445	23.420
35%	0.01778	87.117	23.450
70%	0.01783	86.499	23.500

The table presents the rotation of the column base of the analysis of load case three. This was obtained from the analysis at maximum loading on the frame for load case three. Each percentage of bolt preload resulted in a similar reaction-rotation at the base. Figure 6.15 was used to obtain the corresponding bending moment

of the reaction-rotation presented in table 6.8. The base stiffnesses were then determined and is presented in table 6.8. It is clear from the table that similar connection stiffness is also exhibited for each case of bolt preload.

The case of no bolt preload resulted in a base-rotation of almost double the rotation resulting from a case of bolt preload. This is explained by the fact that due to the absence of load on the bolt, minor slip of the baseplate over the holding-down bolts occurs, resulting in a substantially larger rotation of the connection. Finally this effect is carried through to the resulting stiffness of the connection at the reaction-rotation, which is substantially smaller and results in a significantly larger maximum column displacement of the frame. The overall response of the frame is illustrated in figure 6.16 by the horizontal column displacement of load case three. Column displacements for pre-loaded bolts are similar and therefore only a force displacement curve for 70% bolt preload is presented in the figure.

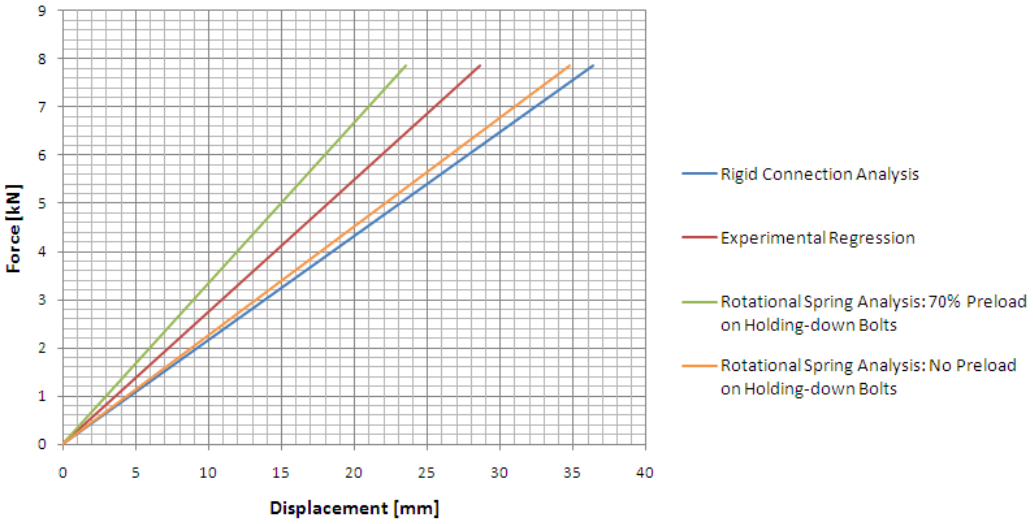

Figure 6.16: Horizontal column displacement for load case three at different bolt preloads.

It is clear that the variations in the preload of the holding down bolts do not affect the overall frame response in terms of displacements. An un-tightened or "loose" bolt does however significantly affect the overall response of the frame in terms of displacements. Both cases predict the displacement of the frame more accurately than an analysis which assumes rigid connections and pinned bases, but the inaccuracy of modelling real non-linear column base response is not explained by the effect of preload on the holding-down bolts.

6.6.2 STIFFNESS OF THE GROUTED INTERFACE

A sensitivity analysis was performed on the moment-rotation behaviour of the test specimen grout support by varying Young's modulus of the grout in the analysis. The sensitivity analysis has been motivated by the fact that the supplier of the grout was not able to supply information regarding Young's Modulus of their product, but only the 7 day and 28 day compressive strengths. Three values of E = 15 GPa, E = 20 GPa and E = 23,3 GPa was chosen for the sensitivity analysis. The results of the moment-rotation behaviour of the test specimen grout support is presented in figure 6.17.

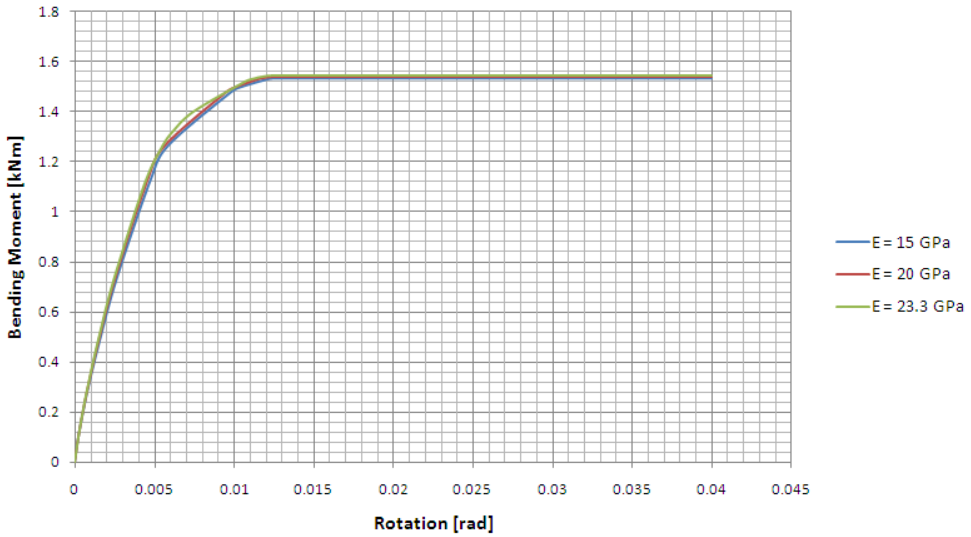

Figure 6.17: Moment-rotation behaviour of test specimen grout support at different grout stiffnesses.

It is clear from the figure that the stiffness of the connection is not affected by varying Young's modulus for the grout interface in the analysis of the connections. The overall effect in frame displacements in presented in table 6.9 for different values of Young's modulus.

Table 6.9: Effect of grout stiffness on frame response.

Young's Modulus [GPa]	Horizontal Column Displacement [mm]
10	23.567
20	23.520
23.3	23.498

The tabulated results indicate that the stiffness of the grouted interface does not affect the overall frame response in terms of horizontal column displacement for load case three.

6.6.3 STIFFENING OF THE CEMENTITIOUS GROUT UNDER LOADING

The response of the column base significantly influences the displacements recorded for load case three, as previously stated. The load is applied perpendicular to the column centreline, and the stiffness of the support condition controls the displacement of the member, due to the effect the stiffness of the support has on the stiffness of the member. A structural element with fixed supports possesses a greater stiffness than a structural member with simple supports. Figure 6.18 presents experimental force vs displacement results for load case three imposed on the test specimen when supported by hinges and by grouted supports. Note that the loading and unloading curve of each support condition is presented in the figure. It is clear from the figure that the force vs displacement curve of the grouted support condition, exhibits a non-linear behaviour compared to the almost perfect linear nature of the hinge-supported force vs displacement curve of the test specimen. The trend of the non-linear curve is of such a nature that the slope increases as the load increases. This behaviour is opposite to the behaviour of yielding components where the slope of the curve decreases with an increase in load.

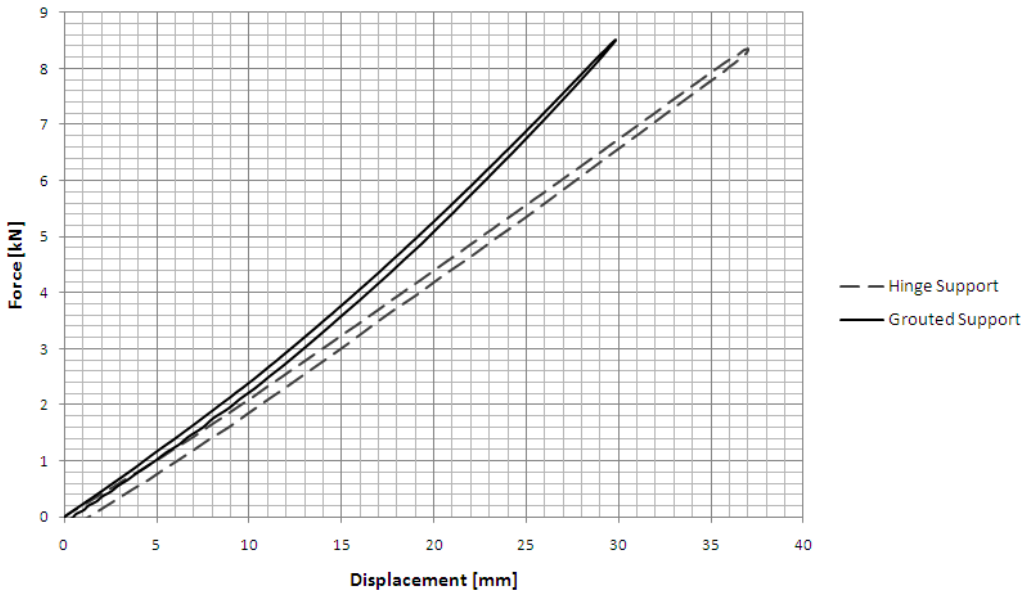

Figure 6.18: Comparison of load case three experimental force-displacement results for hinge and grouted supports respectively.

Cementitious grout is identified as the component in the grouted support which increases in stiffness with loading and causes the structure to stiffen. Five 100 mm cubes were cast to investigate the possible stiffening response of the cementitious grout under loading. Compression tests were performed on the cubes to determine the Young's Modulus of the material from the stress-strain curves. These stress-strain curves of all the cubes are presented in appendix E for reference. The stress-strain data were used to calculate Young's Modulus of the material according to the following procedure (Craig, 2000):

The strain is determined by equation (6.2). The original length in this case was 50 mm as it was the original spacing and measuring distance of the LVDT's used to record displacement during the compression test.

$$\epsilon_{avg} = \frac{\triangle L}{L} \tag{6.2}$$

$$where$$

$$\epsilon = Normal\ strain$$

$$\triangle L = Total\ elongation$$

$$L = Original\ length$$

The average normal stress is given by the following equation:

$$\sigma_{avg} = \frac{F}{A} \tag{6.3}$$

where

$\sigma = Average\ normal\ stress$

$F = Force\ normal\ to\ an\ area$

$A = Area\ on\ which\ the\ force\ acts$

Finally Young's modulus is calculated:

$$E = \frac{\sigma}{\epsilon} \tag{6.4}$$

where

$E = Young's\ modulus\ (elastic\ modulus)$

$\sigma = Average\ normal\ stress$

$\epsilon = Normal\ strain$

Table 6.10 below presents the Young's Modulus for each of the five cementitious grout cubes tested.

Table 6.10: Young's Modulus of the five cementitious grout cubes.

Cube	**Young's Modulus [GPa]**
1	10.40
2	18.71
3	21.29
4	19.91
5	23.56
Mean	**18.77**
Std. Deviation	5.02

Considering the force displacement data of the five cubes tested, the curve of Young's modulus versus the applied force to the cube is presented in figure 6.19 for the initial 100 kN first applied to the cubes.

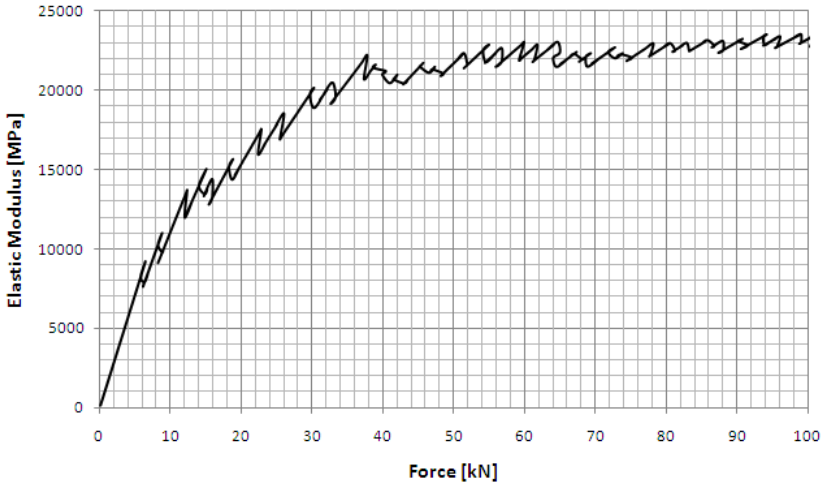

Figure 6.19: Elastic modulus for applied force to a grout cube.

It is clear from the figure that Young's Modulus increases with an increase in the applied force to the cube, i.e. the stiffness of the cube increases as a force is applied to the cube. This behaviour can be applied to the grouted support connections of the test specimen. From figure 6.15 it can be seen that the ultimate moment of the grout support before plastic deformation occurs, is 1.542 kNm at the centre of the connection. This moment can be replaced as an applied force at the tip of the baseplate where the force is transferred to the grout. Dividing the moment by the lever arm obtained from the design drawings in appendix C, the force applied to the grout at the plastic limit of the connection is 29,768 kN. Figure 6.19 clearly illustrates a substantial increase in stiffness of the grout from initial loading to a force of 29,768 kN. The non-linear response of the grout support in figure 6.17 is explained by the stiffening behaviour of the cementitious grout in the grout support connection.

6.7 CONCLUSION

It has been summarized that the analysis using hinged supports leads to significantly more accurate results of displacement determination, if rotational springs are used in the structural analysis to model the real behaviour of joints. The results of the analysis using the response of grouted supports as a non-linear rotational spring, proved more accurate for load case one. The displacements for load case three also proved to be more accurate but an accuracy with less than 5% error could not be obtained.

The sensitivity analysis in the previous section shed some light on the matter and the reason for the inaccuracy could not be explained by the three possible causes investigated. The stiffening of the grout due to loading did present a valuable result, but taking into account the stiffening of grout in design considerations could be neglected as the effect is not of such significance in terms of displacement accuracy. It is however noted that the real displacement of the structure lies somewhere in between the two analysis techniques. The two analysis techniques are the structural analysis which assumes connections to be infinitely rigid and bases perfectly pinned, and the structural analysis which models joints and bases as rotational springs. It is in the hands of the designer to decide on the optimum method of analysis of displacement determination and the degree of conservatism to work with in the design of the structure. The next chapter involves various methods of structural analysis of a 12 m span reference portal frame in order to summarize and compare the different methods followed in the research.

Chapter 7

STRUCTURAL ANALYSIS OF THE REFERENCE PORTAL FRAME

This study focused on the effect of taking into account the moment-rotation joint and column base behaviour for the determination of displacements of portal frames. The modelling of the real behaviour of the joints as rotational springs, was presented in the previous chapter together with the experimental results. Furthermore, an analysis assuming connections to be infinitely rigid and bases perfectly pinned, were also presented for comparative reasons as this is normal practice in design offices.

The previous chapter concluded that modelling the real behaviour of joints in an analysis led to more accurate results in terms of displacement determination. Non-linear column base modelling did not lead to the expected effect of providing more accurate results. The experimental displacements however were somewhere between the results from the analysis of assuming rigid or pinned connections and the analysis implementing rotational springs.

This chapter discusses the following three methods of connection modelling on the reference portal frame:

1. An analysis assuming the connections to be infinitely rigid and column bases perfectly pinned.
2. An analysis modelling the connections as linear rotational springs and column bases perfectly pinned.
3. An analysis modelling the connections as linear rotational springs and column bases as non-linear rotational springs.

The reference portal frame which was used, originated from previous studies conducted at Stellenbosch University. The reader is referred to section 3.2.1 for background information of the reference portal frame. The portal frame spans 12 m and is 4,5 m in height and its detailed design calculations are given in appendix A with detail drawings in appendix B. The motivation behind this chapter is to present the three variations of modelling joints in a structural analysis, to determine displacements on a real design case and to arrive at a conclusion of an effective and accurate method of analysis to obtain the displacements of a structure under loading.

The chapter commences with the determination of load combinations imposed on the portal frame for design purposes according to SANS 10160:2011 parts one to three. Load combinations for designing the reference portal frame according to ultimate limit state, as well as verification of serviceability limit state is presented and discussed. The South African National Standard for steel design, SANS 10162-1:2005, presents an informative guideline to the maximum allowable displacements for steel structures in order to conform to serviceability limit state criteria. These guidelines relevant to the reference portal frame are presented and discussed in section 7.2,

followed by the load combinations imposed on the structure for maximum displacement determinations. Two load combinations are presented, one to determine the maximum vertical displacements and the other to determine maximum horizontal displacements. Detailed displacement results of all three variations of structural analysis are presented for each load combination and discussed. The chapter ends with a brief summary of the results from the analysis of the load combinations imposed on the reference portal frame.

7.1 LOAD COMBINATIONS ACCORDING TO SANS 10160:2011 PART ONE

The analysis of a portal frame for design purposes involves imposing various load combinations on the structure for ultimate limit state design purposes and the verification of serviceability limit state criteria. Ultimate limit state refers to the maximum loads imposed on the structure and are used for designing against failure, whereas serviceability limit state refers to the loads imposed on the structure due to normal occupancy and which are used for displacement determination. Normal occupancy and use of a structure are defined in clause 5.4 of SANS 10160:2011 part one as follows:

- Functioning of the structure.
- Acceptability of the structure in terms of safety en wellbeing.
- Appearance of the structure.

According to clause 7.1.1 of SANS 10160:2011 part one, the following ultimate limit states should be used for designing a building structure:

- STR and STR-P: This refers to the strength of the structural elements needed to provide sufficient resistance against the stresses developed within, due to loading of the structure.
- EQU: Loss of static equilibrium of a structure due to loading.
- GEO: Failure of a structure due to geotechnical foundation failure.
- ACC: Resistance against accidents and seismic activity.
- FAT: Failure of structural members due to fatigue of structural members.

Appendix A contains the detailed design of the reference portal frame according to the STR, STR-P and EQU limit states set above. The listed limit states were verified through determination of various load cases from SANS 10160:2011 part one. Load cases refer to a set of loads applied at identified nodes in the analysis. Identified nodes are nodes in similar positions to purlins supporting cladding and roof sheeting on the structure. The loads are determined through either permanent or imposed loads as well as wind loads on the area contributing to the specific node. These load cases include:

- Load case 1: Permanent loads on the structure.
- Load case 2: Imposed loads on the roof of the structure.
- Load case 3: Imposed loads across half the roof of the structure.
- Load case 4: Wind load along the structure.
- Load case 5: Wind load across the structure.

Refer to table A.1 in appendix A for the nodal loads of each load case.

The listed load cases are multiplied with partial factors to form load combinations for ultimate and serviceability limit states in the analysis. Clauses 7.3 and 8.3 the SANS 10160:2011 part one were used to formulate the following load cases for ultimate and serviceability limit state respectively:

Ultimate limit state:
Load combination 1 (LC1): 1,2 × (Load case 1) + 1,6 × (Load case 2)
Load combination 2 (LC2): 1,2 × (Load case 1) + 1,6 × (Load case 3)
Load combination 3 (LC3): 0,9 × (Load case 1) + 1,3 × (Load case 4)
Load combination 4 (LC4): 0,9 × (Load case 1) + 1,3 × (Load case 5)

Serviceability limit state:
Load combination 5 (LC5): 1,1 × (Load case 1) + 1,0 × (Load case 2)
Load combination 6 (LC6): 1,1 × (Load case 1) + 1,0 × (Load case 3)
Load combination 7 (LC7): 1,1 × (Load case 1) + 0,6 × (Load case 4)
Load combination 8 (LC8): 1,1 × (Load case 1) + 0,6 × (Load case 5)

It is noted that in load combinations seven and eight, the wind load is reduced by a partial factor of 0,6 for serviceability limit state. Building structures are designed for a working life of 50 years according to SANS 10160:2011, clause 4.5. A wind speed for a 50 year return period results in excessive deformations of the structure and leads to an over-conservative approach for displacement determination of the structure. The former South African loading code, SABS 0160:1989, indicated that a wind speed of 10 year return period is to be used for serviceability limit state requirements (SABS0160:1989). With the implementation of SANS 10160:2011, the wind load for serviceability limit state requirements are reduced by a partial factor, instead of determining two wind loads for design purposes.

Steel structures are significantly affected by wind, since the weight and stiffness of the structure does not provide sufficient resistance against the effects of wind as in the case of concrete structures. Analyses results for maximum vertical and horizontal displacements of the structure are presented in table 7.1 for serviceability limit state load combinations.

Table 7.1: Maximum vertical and horizontal displacements for serviceability limit state load combinations.

Load Combination	**Maximum Displacement [mm]**	
	Vertical	**Horizontal**
5	21.56	4.77
6	15.48	7.43
7	**34.74**	6.91
8	5.68	**17.57**

The results indicate that load combinations seven and eight are the worst combinations in terms of structural displacements under loading. Load combinations seven and eight are presented and discussed in the following section.

7.2 RECOMMENDED MAXIMUM STRUCTURAL DISPLACEMENTS ACCORDING TO SANS 10162-1:2005

The South African National Standard for the structural use of steel (SANS10162-1:2005) Annex D, provides an informative guideline to recommended maximum displacements of structures for serviceability limit state. It is stated that certain components of the building structure do contribute to the stiffness of the structure and its displacements. These components include masonry walls, curtain walls and concrete around structural steel members. It is also stated that due to the components listed above, the forces for serviceability limit state may be reduced to a maximum of 15% (SANS10162-1:2005). This approach however would be conservative as the structure could be covered by cladding and roof sheeting, not providing similar stiffness to for example, masonry walls. Table 7.2 provides the informative maximum displacements, at serviceability limit state, related to the reference portal frame.

Table 7.2: Recommended maximum displacements at serviceability limit state (SANS10162-1:2005).

Direction of Displacement	Design Load	Application	Maximum Displacement
Vertical	Variable	Simple span members supporting elastic roof coverings.	1/180 of span
Lateral	Wind	Building sway, due to all effects.	1/400 of building height
Lateral	Wind	Storey drift, with special provisions to accommodate building frame deformation.	1/400 of building height

Section A.8 of appendix A presents the calculation of the maximum allowable displacements of the reference portal frame according to table 7.2. The maximum allowable vertical and horizontal displacement for the reference portal frame are 66,67 mm and 11,40 mm respectively.

7.3 STRUCTURAL ANALYSIS FOR SERVICEABILITY LIMIT STATE REQUIREMENTS

As mentioned, load combinations seven and eight are the worst design load combinations for the reference portal frame in terms of the serviceability limit state. This section presents the determination of spring stiffness values for the connections modelled in the structural analysis followed by both load combinations being presented and discussed.

The chapter commenced with a summary of the three methods of modelling connections in structural analysis performed in the study to obtain the displacements of the structure. Each method of analysis is performed with the two load combinations which are discussed and the results are presented for each load combination.

7.3.1 DETERMINATION OF ROTATIONAL SPRING STIFFNESS

Section 6.3.1 presented the determination of a rotational spring stiffness from a connection's unique moment-rotation curve as well as the spring stiffness values for the connections of the test specimen. Spring stiffness values are required for the connections of the reference portal frame to model the real connection behaviour to determine displacements. The moment-rotation behaviour of the connections of the reference portal frame was presented in sections 4.6 and 4.7. The spring stiffness values are calculated from these curves with equation 6.1 in section 6.3.1, and presented in table 7.3.

Table 7.3: Reference portal frame rotational spring stiffnesses.

Connection	Direction of In-plane Rotational Deformation	Bending Moment [kNm]	Rotation [rad]	Spring Stiffness [kNm/rad]
Reference Portal Frame Haunch	Downward	23.999	1.230×10^{-3}	19.551×10^{3}
	Upward	36.550	1.837×10^{-3}	19.895×10^{3}
Reference Portal Frame Ridge	Downward	11.349	409.000×10^{-6}	27.748×10^{3}
	Upward	11.349	750.000×10^{-6}	15.132×10^{3}

A significant difference in stiffness is noted for the ridge connection in table 7.3. This connection response is explained by the layout of the components of the connections. The connection is designed to withstand greater forces and moments causing in-plane downward deformation rather than in-plane upward deformations. The reader is referred to section 4.7 for a detailed discussion.

7.3.2 LOAD COMBINATION SEVEN

Load combination seven refers to the self weight of the building structure, together with a wind load applied along the length of the building structure. (Section A.4.1) The effect of the wind results in the structure being "lifted" from the foundations. Figure 7.1 illustrates the load vectors obtained from load combination seven, applied at the nodes of the supporting purlins of the structure.

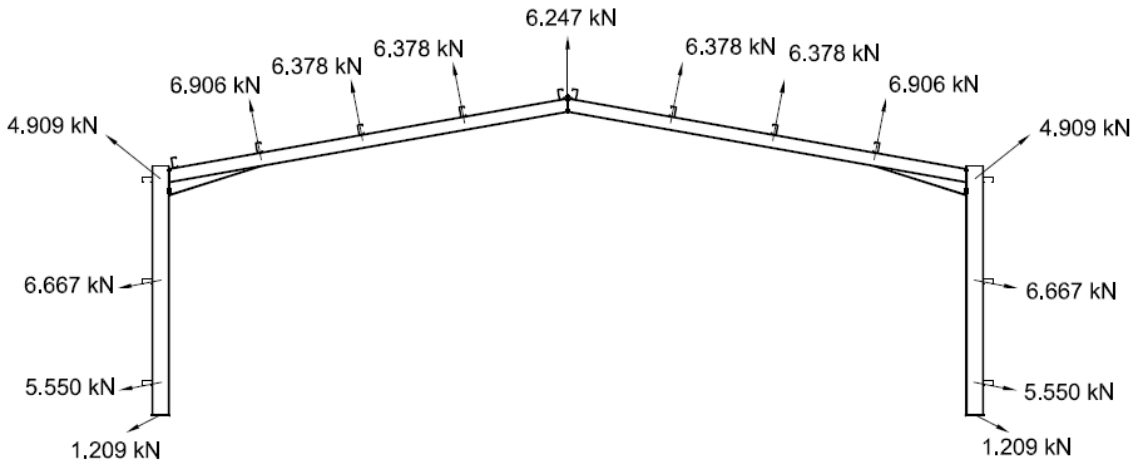

Figure 7.1: Load vectors on the reference portal frame of load combination seven.

The results from the second order analysis of load combination seven is presented in figure 7.2 in terms of vectors indicating displacements of the structure.

The three variations of modelling connections and bases in the structural analysis were performed on the structure and are presented in table 7.4.

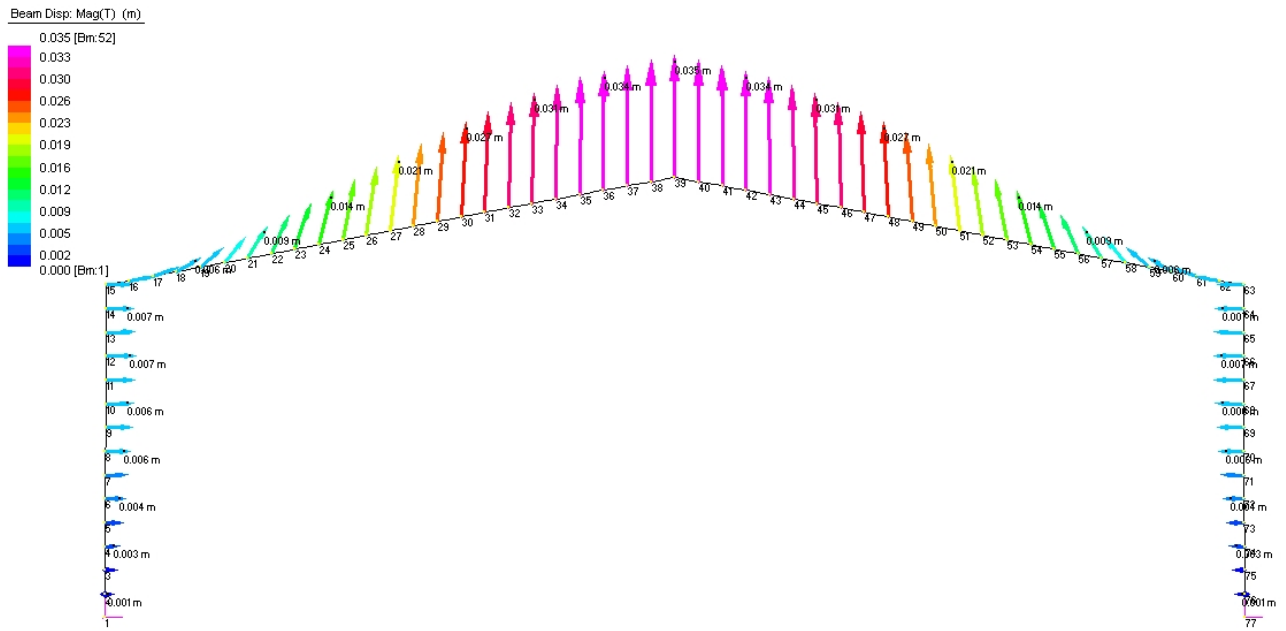

Figure 7.2: Displacement vectors on the reference portal frame of load combination seven.

Table 7.4: Reference portal frame load combination seven, maximum displacement results.

Structural Analysis Variation	Maximum Displacement	
	Horizontal [mm]	Vertical [mm]
Rigid Connections & Pinned Bases	6.905	34.741
Rotational Spring Connections & Pinned Bases	7.294	38.144
Rotational Springs & Bases	6.556	35.656

The tabulated results indicate the maximum displacements of the structure was obtained by modelling connections as rotational springs and bases as being perfectly pinned. This supports the statement made at the beginning of the study, that modelling the real behaviour of rigid connections will increase the displacements being obtained. Furthermore the base is regarded as perfectly pinned which also increases the displacements compared to the real behaviour of grouted pinned bases. Structural analyses assuming infinitely rigid connections and perfectly pinned bases lead to the smallest displacements of the structure. This is explained by the real behaviour of the connections having the most prominent effect on the response of the structure when subjected to load combination seven. The real column base behaviour does not influence the response significantly for this specific load case, as the forces are mostly uplift forces (vertical) and result in an insignificant rotational reaction of the column base. The rotational stiffness of the column base therefore does not have a significant affect on the displacements of the structure for load combination seven.

Figures 7.3 and 7.4 illustrate the force-displacement curves for the maximum vertical and horizontal displacements of the structure respectively. The force is regarded as being the vertical force applied at the ridge of the portal frame. Each figure also indicates the maximum permissable displacement of the structure according to SANS 10162-1:2005.

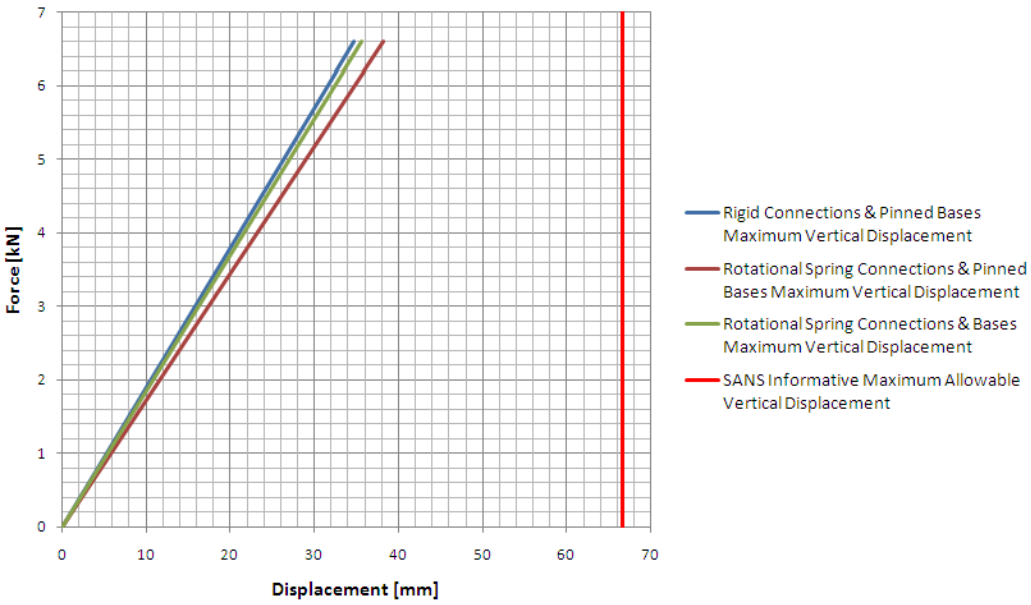

Figure 7.3: Vertical displacement of the reference portal frame for load combination seven.

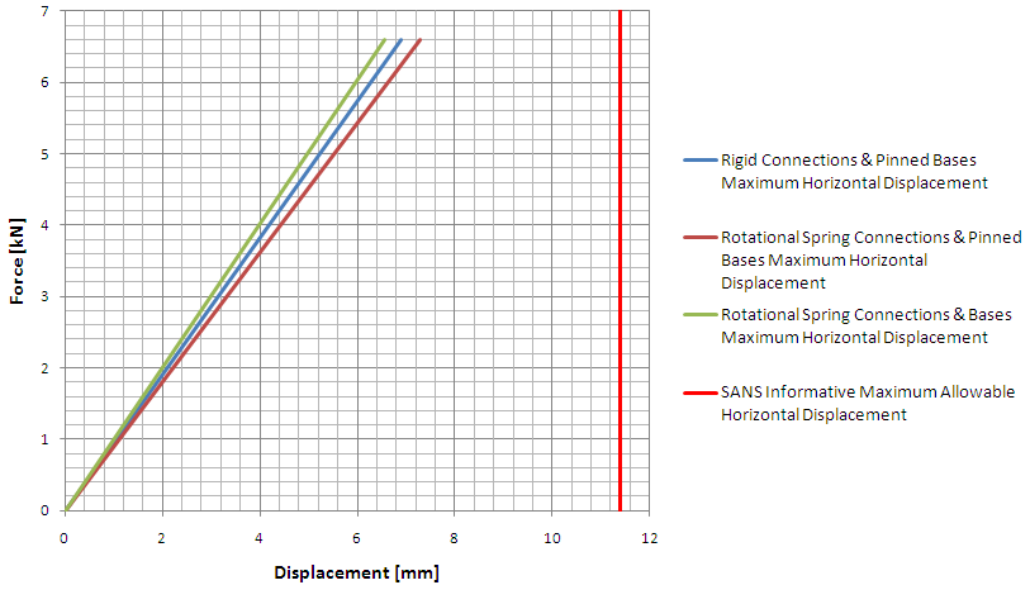

Figure 7.4: Horizontal displacement of the reference portal frame for load combination seven.

In each case the informative maximum allowable displacement was not reached. For load combination seven, it can be reasoned that a structural analysis which uses rotational springs to model connection and column base behaviour, leads to results that are accurate for design purposes. Vertical displacement is the most prominent for load combination seven and therefore the referred-to analysis did lead to greater displacements than the analysis which assumed rigid connections and pinned bases. Furthermore the displacement was less than the displacement recorded from the analysis which used rotational spring connections and pinned bases. The displacement results from analyses using rotational springs for connections and bases are thus regarded as accurate and useable for design purposes.

7.3.3 LOAD COMBINATION EIGHT

Load combination eight involves the selfweight of the structure together with wind pressure across the building. The load combination therefore wants to "push the structure over", with horizontally applied wind forces being the most prominent. Figure 7.5 illustrates the force vectors applied to the reference portal frame model in the

structural analysis.

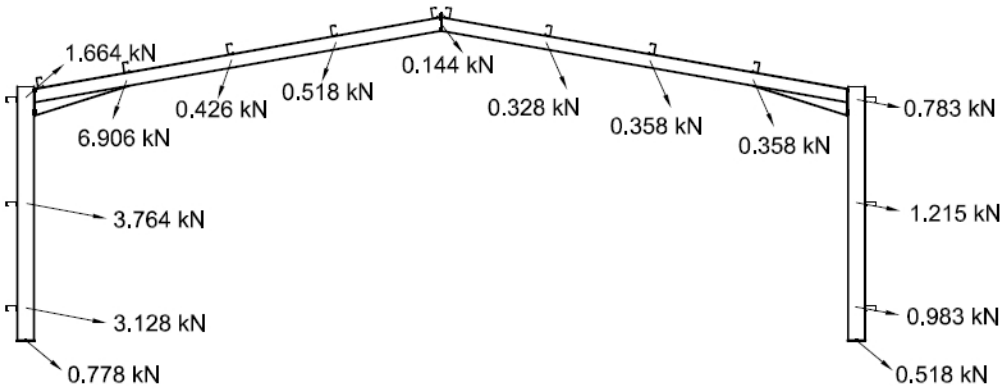

Figure 7.5: Load vectors on the reference portal frame of load combination eight.

The second order analysis on the structure led to the following structural response in terms of the displacement vectors illustrated in figure 7.6.

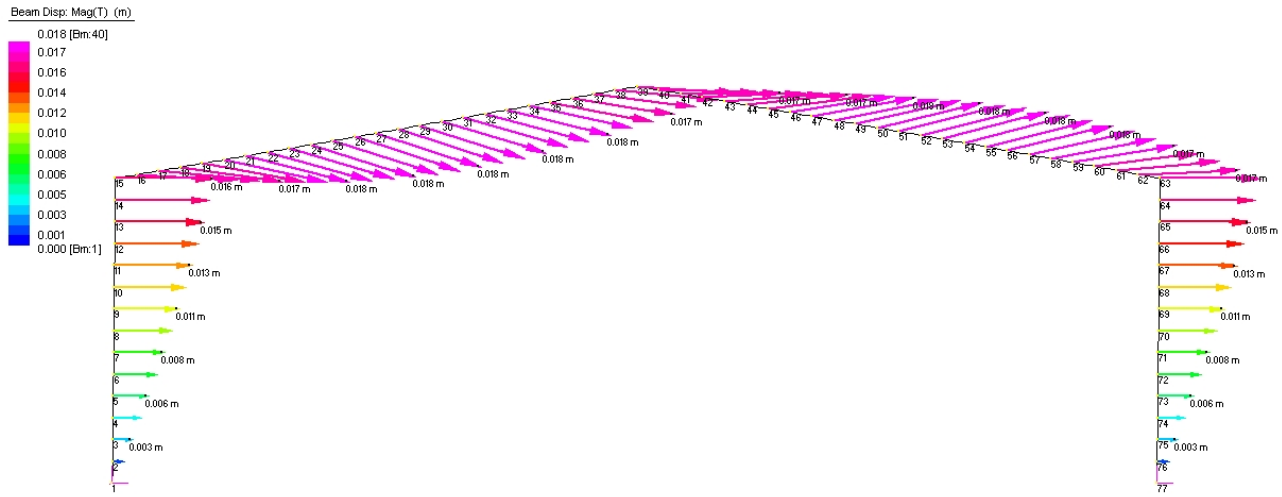

Figure 7.6: Displacement vectors on the reference portal frame of load combination eight.

The three variations of modelling connections and bases in the structural analysis were performed on the structure and are presented in table 7.5.

Table 7.5: Reference portal frame load combination eight, maximum displacement results.

Structural Analysis Variation	**Maximum Displacement**	
	Horizontal [mm]	**Vertical [mm]**
Rigid Connections & Pinned Bases	17.572	5.681
Rotational Spring Connections & Pinned Bases	18.212	5.584
Rotational Springs & Bases	5.486	2.313

Load combination eight presented somewhat different results in terms of displacements when compared to load combination seven. An analysis using rotational springs to model connection behaviour, together with perfectly pinned bases, leads to the expected result of maximum displacement. Modelling the real behaviour of column bases leads to significantly smaller displacement results. Column base behaviour has a significant affect on the horizontal stiffness of the structure as the rotational restraint by the column base increases the stiffness of the structure. The load combination applies mostly horizontal forces to the structure and therefore the displacement

results were significantly reduced when the real behaviour of column bases was modelled in the structural analysis.

Figures 7.7 and 7.8 present the force-displacement results for load combination eight, together with the maximum allowable displacements of the structure referred to in section 7.2. The force in the figures is the maximum horizontal force applied to the structure for load combination eight and is used for illustrational purposes.

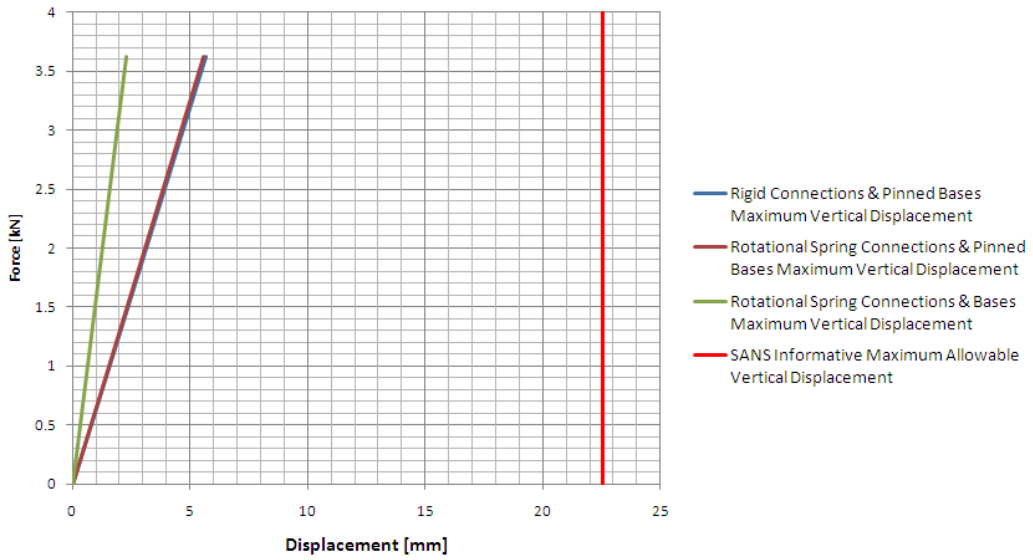

Figure 7.7: Vertical displacement of the reference portal frame for load combination eight.

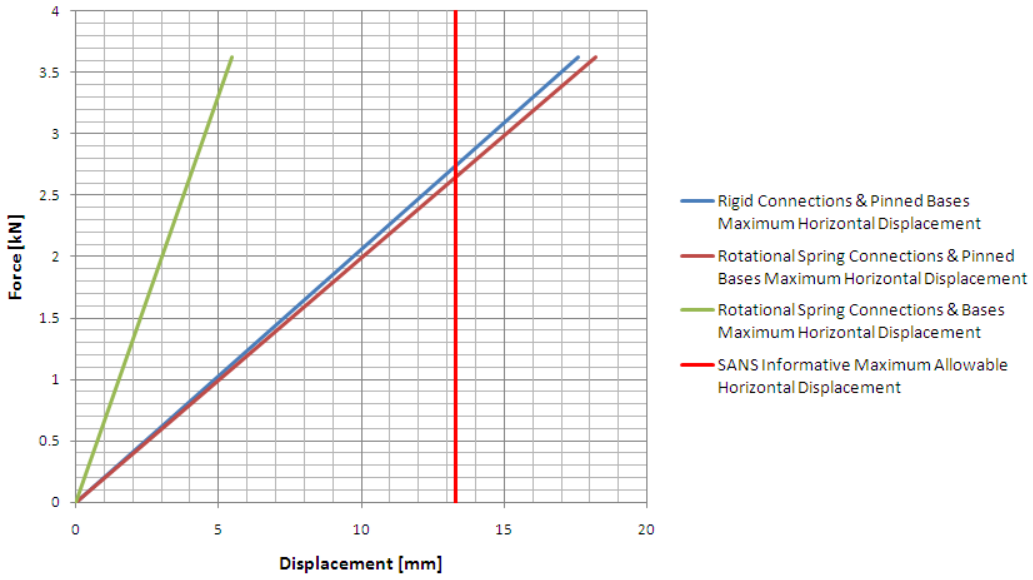

Figure 7.8: Horizontal displacement of the reference portal frame for load combination eight.

Figure 7.8 clearly illustrates the recorded displacements for all analyses that assume that column bases which are perfectly pinned do not conform to the informative guideline of SANS 10162-1:2005. As mentioned, modelling the real behaviour of column bases leads to significantly smaller displacement results due to the increased stiffness of the frame. It would however be rash of the designer to assume the smaller displacement results of the latter variation of the structural analysis. For load combination eight it is recommended for design purposes, to use the displacement results from a structural analysis which assumes connections to be infinitely rigid and bases to be perfectly pinned. The results are accurate and reliable and have not been over-predicted, compared to the results of analyses modelling connections as rotational springs and bases as being perfectly pinned.

7.4 CONCLUSION

The maximum displacement of the structure for the two worst load combinations was presented. Load combination seven had more prominent vertical displacements, whereas load combination eight resulted in greater horizontal displacements. In both load combinations the structural analysis modelling connections as rotational springs together with perfectly pinned bases, resulted in greater displacements than the structural analysis which assumed rigid connections and pinned bases. By reviewing the displacement response of the structure it can be concluded that modelling the real behaviour of rigid connections in a structural analysis will increase the maximum determined displacements. It is however noted that an analysis which assumes rotational spring connections together with perfectly pinned bases, is not recommended for design purposes as displacements are over-predicted due to the real behaviour of column bases not having been taken into account.

An analysis modelling connections and bases as rotational springs leads to accurate results for vertical load combinations but in the case of horizontal load combinations it seems to under-predict displacements. Displacements in the case of horizontal load combinations were significantly smaller due to the stiffness provided by the real response of grouted pinned column bases under loading. It was expected to see reduced displacements when the real behaviour of column bases are modelled, however assuming the real behaviour of column bases in a structural analysis for displacement determination for design purposes is unreliable and is not recommended.

The conclusion is therefore made that structural analyses of portal frames which assume infinitely rigid connections and perfectly pinned bases, lead to accurate and reliable results.

Chapter 8

CONCLUSION AND RECOMMENDATIONS

The chapter presents the conclusions and recommendations based on the findings of the research.

8.1 CONCLUSIONS

The following conclusions can be drawn from each section:

FINITE ELEMENT ANALYSIS

- Accurate bending of a structural member can be modelled using linear solid elements meshed with at least two elements over the height of the member. This was proved by modelling a simple four point beam in bending.
- Elastic perfect plastic material modelling in finite element analyses leads to accurate results in terms of displacements, stresses and strains, as well as the plastic limit of steel connections.
- Modelling definitions in terms of contact and interaction, together with the above material model provided accurate moment-rotation results for a haunch connection in comparison with experimental results. Similar definitions were adopted in the development of all finite element models of steel connections in the study.
- Accurate moment-rotation curves and ultimate moment capacities were obtained through the analysis of finite element models of all the connections investigated in the research.

EXPERIMENTAL INVESTIGATION

- Two support conditions were designed to support the test specimen. This was to isolate the effect of column base behaviour in the overall structural response. A hinge support simulates the perfect condition assumed in structural analysis whereas a grouted support simulated real construction practice.
- Experimental tests were conducted and provided accurate displacement data of the test specimen.
- The real behaviour of rigid connections does result in greater displacements of the test specimen in comparison to the results from second order analysis of the test specimen.
- A second order analysis of a portal frame using perfect hinges as support and modelling connections as infinitely rigid resulted in displacements to an accuracy of less than 5%.

- A second order analysis of a portal frame using grouted interfaces (designed as pinned) as support, modelling connections as infinitely rigid and bases perfectly pinned resulted in displacements in excess of 14% in error.

STRUCTURAL ANALYSIS USING ROTATIONAL SPRINGS TO MODEL CONNECTION BEHAVIOUR

- A stiffness value for a rotational spring was calculated for each connection from its unique moment-rotation behaviour.
- The initial stiffness was found to be the optimum spring stiffness to model the behaviour of rigid connections in a structural analysis.
- The column region supported by a haunch must be modelled as a rigid link in the case of modelling the connections as rotational springs in structural analysis. This is to simulate the increased stiffness of the column due to the haunch in the connection.
- Grouted pinned column bases should be modelled as, non-linear springs. It was found that more accurate displacement results are obtained if the reaction rotation of the pinned base is carried forward to the next iteration in second order analysis.

STRUCTURAL ANALYSIS OF THE TEST SPECIMEN SUPPORTED BY HINGES

- Structural analysis of a portal frame modelling connections as linear rotational springs lead to displacement results within 2% accuracy for vertical and horizontal loads.
- Modelling the real behaviour of connections as springs in structural analysis does lead to more accurate displacement results in comparison to a structural analysis assuming connections as rigid.
- Structural analysis of a portal frame modelling connections as infinitely rigid also leads to accurate results.

STRUCTURAL ANALYSIS OF THE TEST SPECIMEN SUPPORTED BY A GROUTED INTERFACE

- Structural analysis of a portal frame modelling connections as linear rotational springs and bases as non-linear rotational springs lead to accurate results for vertical load cases. This however was not the case for horizontal loads as displacement results was in excess of 5% in error.
- The contribution of real column base behaviour does affect the overall stiffness of the portal frame and is significant for horizontal load cases.

SENSITIVITY ANALYSIS OF COLUMN BASE RESPONSE

- The percentage of preloading on holding-down bolts of the column base does not affect the overall frame response in terms of displacements, except in the case of no preloading, where slipping of the endplate over the bolt occured.
- The elastic modulus of cementitious grout was varied between 15 GPa and 23,3 GPa in finite element analysis. The overall frame response in terms of displacements was not affected by varying the stiffness, and leads to the conclusion that the stiffness of the cementitious grout does not contribute to the stiffness of the column base.
- The non-linear increase in elastic modulus for cementitious grout under loading did affect the overall frame response for horizontal loads, as the force-displacement curve indicated a stiffening nature of the frame's response. The affect however was not as significant to motivate the modelling of the behaviour of cementitious grout under loading in a structural analysis.

STRUCTURAL ANALYSIS OF THE REFERENCE PORTAL FRAME

- Modelling the real behaviour of connections and column bases in a structural analysis as rotational springs does provide the designer with more accurate and useable displacement results for vertical load combinations. This was not the case for horizontal load combinations as the results were in-conservative for design purposes.
- A structural analysis modelling the real behaviour of rigid connections and assuming bases to be perfectly pinned in structural analysis leads to excessive displacements and is regarded as over-conservative for serviceability verification purposes.

8.2 RECOMMENDATIONS

Based on the conclusions of the investigation, the following recommendations are made on structural analysis of portal frames for serviceability limit state verification.

Modelling the real behaviour of connections and column bases in a structural analysis does lead to more accurate displacement results. Unconservative displacement results however were obtained when horizontal load combinations are applied to the frame. Structural analysis assuming connections to be infinitely rigid and bases perfectly pinned leads to consistent and accurate displacement results for vertical and horizontal load combinations. It is recommended to model connections and bases as either infinitely rigid or perfectly pinned in a structural analysis for the determination of displacement for the verification of the design to the criteria set by serviceability limit state.

Structural analysis software must be verified in order to assess the accuracy of rotational springs. Certain software packages have been noted to be inaccurate when modelling rotational springs. This was mainly due to bending moments not being transferred between beam elements connected by a rotational spring. Simple models can be set up to verify analysis results implementing rotational springs.

Obtaining the moment-rotation behaviour of steel connections from a finite element analysis is a time-consuming process and requires complex and expensive software to create models. Various databases are available with numerous connection's moment-rotation data, however each connections possess over a unique moment-rotation response. It is thus the responsibility of the designer to obtain reliable moment-rotation data for each connection being designed. The amount of time the designer needs to spend on obtaining moment-rotational data for each connection in the structure will not be viable in terms of cost as a reduction in the amount of steel used in the design will not be of similar value than the hours spent by the designer.

Although more accurate displacement data is obtained through modelling the moment-rotation response of connections and bases in a structural analysis, it is recommended that the designer model connections and column bases of portal frames as infinitely rigid and perfectly pinned respectively. The results are sufficiently accurate and the procedure is simple, effective and reliable.

8.3 SUGGESTIONS FOR FUTURE RESEARCH

The following suggestions are made as a result of this investigation:

Eurocode 3's component method for semi-rigid design defines an initial stiffness that can be obtained mathematically for a connections prior to the design of the connections. Modelling the initial stiffness as obtained from Eurocode can be compared to the experimental results from the study and could lead to a quicker method

of obtaining a connection stiffness for structural analysis. This however has not been tested and must still be investigated.

An accurate method of modelling real column base behaviour in structural analysis needs to be developed. Assuming connections to be infinitely rigid leads to realistic displacement results, however assuming column bases to be perfectly pinned is over-conservative. Rotational restraint provided by column bases that is designed as pinned bases do contribute significantly to the stiffness of the structure. A structural analysis assuming connections as rigid and modelling the real behaviour of column bases could lead to more accurate displacement results for serviceability limit state verification.

Real connection behaviour as found in practice is non-linear. The study focussed on modelling real connection behaviour as a linear rotational spring. With the development of an accurate material model and accounting for the effects of strain hardening, more accurate moment-rotation curves could be obtained from finite element analyses. Further research could answer the question whether greater accuracy in displacements could be obtained by modelling connections as non-linear rotational springs.

Chapter 9

REFERENCES

Ali Abolmaali, John H. Matthys, Mohammed Farooqi, and Yeol Choi. Development of moment-rotation model equations for flush end-plate connections. *Journal of Constructional Steel Research*, 61(12):1595 – 1612, 2005. ISSN 0143-974X. doi: DOI:10.1016/j.jcsr.2005.05.004. URL http://www.sciencedirect.com/science/article/B6V3T-4GD4SK2-2/2/7938a24a08661310fdf237cddc2600b2. 7

S.L. Chan and P.P.T. Chui. *Non-Linear Static and Cyclic Analysis of Steel Frames with Semi-Rigid Connections*. Elsevier, May 2000. ISBN 978-0-08-042998-4. 10

S.L. Chan, H.Y. Huang, and L.X. Fang. Advanced analysis of imperfect portal frames with semi-rigid base connections. *Journal of Engineering Mechanics*, pages 633 – 640, 2005. doi: DOI:10.1016/(ASCE)0733-9399(2005)131:6(633). URL http://scitation.aip.org. 9

W.F Chen, Y. Goto, and J.Y. Richard Liew. *Stability Design of Semi-Rigid Frames*. John Wiley & Sons, Inc., 1996. ISBN 0-471-07670-8. 12

J.E. Christopher and R. Bjorhovde. Semi-rigid frame design methods for practicing engineers. *Engineering Journal*, pages 12 – 28, First Quarter 1999. 9, 11, 12

R.D. Cook, D.S. Malkus, M.E. Plesha, and R.J. Witt. *Concepts and Applications of Finite Element Analysis*. John Wiley and Sons, Inc., 4th edition, 2002. ISBN 978-0-471-35605-9. 20, 21, 22, 24

Dassaults Systémes Simulia Corp. *ABAQUS/CAE 6.10-2 Documentation*, 2010.

R.R. Jr. Craig. *Mechanics of Materials*. John Wiley and Sons, Inc., 2nd edition, 2000. ISBN 0-471-33176-7. 22, 79

CTICM and SCI. *Facilitating the market development for sections in industrial halls and low rise buildings (SECHALO)*. Research Fund for Coal and Steel RFS2-CT-2008-0030, 2008. The Steel Alliance. 12

ECCS. *Analysis and Design of Steel Frames with Semi-Rigid Joints*. Number 67 in Technical Committee 8 - Structural Stability, Technical Working Group 8.1/8.2 Skeletal Structures. European Convention For Constructional Steelwork, 1992. 7, 9

EN1993-1-8. *Eurocode 3: Design of steel structures - Part 1-8: Design of joints*. European Committee for Standardization, 2005. 14

Kurt H. Gerstle. Effect of connections on frames. *Journal of Constructional Steel Research*, 10:241 – 267, 1988. ISSN 0143-974X. doi: DOI:10.1016/0143-974X(88)90032-6. URL http://www.sciencedirect.com/science/article/B6V3T-47X7CCF-7P/2/e219b13e62b8d3d5fa488305aaa23186. 8, 11

M. Holický. Probability and risk analysis in civil engineering. Stellenbosch University & Czech Technical University, Prague. Lecture Notes., August 2010. 1

J.H. Howlett, W.M. Jenkins, and R. Stainsby. *Joints in Structural Steelwork*. Pentech Press Limited, Estover Road, Plymouth, 1981. ISBN 0-7273-1001-1. 8

J.P. Jaspart. Design of structural joints in building frames. *Prog. Struct. Engng Mater*, 4:18–34, 2002. doi: DOI:10.1002/pse.105. URL http://www3.interscience.wiley.com/cgi-bin/fulltext/93519615/PDFSTART. 13

J.P Jaspart, F. Wald, K Weynand, and N. Gresnigt. Steel column base classification. *HERON*, 53(1/2):69 – 86, 2008. URL http://heron.tudelft.nl/53-12/4.pdf. 8

C.B. Koen. The development of a multi-purpose beam/column testing apparatus. Master's thesis, Stellenbosch University, March 2003. 42

T. S. Kruger, B. W. J. van Rensburg, and G. M. du Plessis. Non-linear analysis of structural steel frames. *Journal of Constructional Steel Research*, 34(2-3):285 – 306, 1995. ISSN 0143-974X. doi: DOI:10.1016/0143-974X(94)00029-H. URL http://www.sciencedirect.com/science/article/B6V3T-3YMWGY0-9/2/2b948a0038fc0def0364d41b94a82566. South Africa. 4, 6, 7, 9

G.L. Kulak, J.W. Fisher, and J.H.A. Struik. *Guide to Design Criteria for Bolted and Riveted Joints*. American Institute of Steel Construction Inc., 2001. ISBN 0-471-83791-1. 25, 76

Strand7 Pty Limited. *Theoretical Manual: Theoretical background to the Strand7 finite element analysis system.* Strand7 Pty Limited, 1st edition, 2005. ISBN 0-957-73452-2.

E.M. Lui and W.F. Chen. Steel frame analysis with flexible joints. *Journal of Constructional Steel Research*, 8:161 – 202, 1987. ISSN 0143-974X. doi: DOI:10.1016/0143-974X(87)90058-7. URL http://www.sciencedirect.com/science/article/B6V3T-47X7CBG-76/2/c287a407a44459b25bc75de79f177ba2. 4, 7, 8

J.M. Mativo, T. Yamasawa, and K. Nogami. Semi-rigid steel connections - an overview. *Tokyo Metropoliton University*, 2005. 13

R.E. Melchers. Column-base response under applied moment. *Journal of Constructional Steel Research*, 23 (1-3):127 – 143, 1992. ISSN 0143-974X. doi: DOI:10.1016/0143-974X(92)90040-L. URL http://www.sciencedirect.com/science/article/B6V3T-47X7CFN-8R/2/9c67396d20dbcac693c49e7033ed436e. Special Issue on Structural Steel Research in Australia. 8

D.B. Moore and F. Wald. *Design of Structural Connections to Eurocode 3 - Frequently Asked Questions*. Building Research Establishment Ltd., Watford, www.fsv.cvut.cz/cestruco, 2003. ISBN 80-01-02838-0. 5

G.M. Mostert. A theoretical and experimental investigation into the moment/rotation relationship of portal frame bases. Master's thesis, Stellenbosch University, 1998. 16, 20, 38

P. Prabha, S. Seetharaman, S. Arul Jayachandran, and V. Marimuthu. Mimicking expensive experiments by abaqus. *Scientists, Structural Engineering Research Centre, CSIR campus, Taramani, Chennai*, 600(113), s.a. 20, 24, 39

SABS0160:1989. *South African Standard: The general procedures and loadings to be adopted in the design of buildings.* The council of the South African Bureau of Standards. 84

SAISC. *Structural Steelwork Connections Limit State Design*. The Southern African Institute of Steel Construction, 1992. ISBN 0 620 15693-7. 4, 5, 41

SAISC. *Southern African Steel Construction Handbook*. The Southern African Institute of Steel Construction, 6th edition, March 2008. ISBN 978-0-620-39810-7. 21, 22, 25, 41, 71

SANS10160:2011. *South African National Standard: Basis of Structural Design and Actions for Buildings and Industrial Structures*. Standards South Africa. 3, 15, 41

SANS10162-1:2005. *South African National Standard: The structural use of steel, Part 1: Limit-state design of hot-rolled steelwork*. Standards South Africa. 3, 13, 15, 41, 85

Yongjiu Shi, Gang Shi, and Yuanqing Wang. Experimental and theoretical analysis of the moment-rotation behaviour of stiffened extended end-plate connections. *Journal of Constructional Steel Research*, 63(9):1279 – 1293, 2007. ISSN 0143-974X. doi: DOI:10.1016/j.jcsr.2006.11.008. URL `http://www.sciencedirect.com/science/article/B6V3T-4MMP2HF-1/2/9145b995baf7e7f2e6d1bd4d091473b6`. 6

George J. Simitses, Jerry D. Swisshelm, and Andreas S. Vlahinos. Flexibly-jointed unbraced portal frames. *Journal of Constructional Steel Research*, 4(1):27 – 44, 1984. ISSN 0143-974X. doi: DOI:10.1016/0143-974X(84)90033-6. URL `http://www.sciencedirect.com/science/article/B6V3T-481DN1T-4/2/bab066a344fcea9d036663df86a7a3d6`. 9, 11

A.N. Truter. An experimental and theoretical investigation into the non-linear moment-rotation response of bolted endplate connections in single storey haunched steel portal frames. Master's thesis, Stellenbosch University, August 1997. 16, 20, 25, 39

F. Wald, Z. Sokol, M. Steenhuis, and J.P. Jaspart. Component method for steel column bases. *HERON*, 51(1/2): 3 to 20, 2008. 14

Appendix A

REFERENCE PORTAL FRAME DESIGN

A.1 LAYOUT

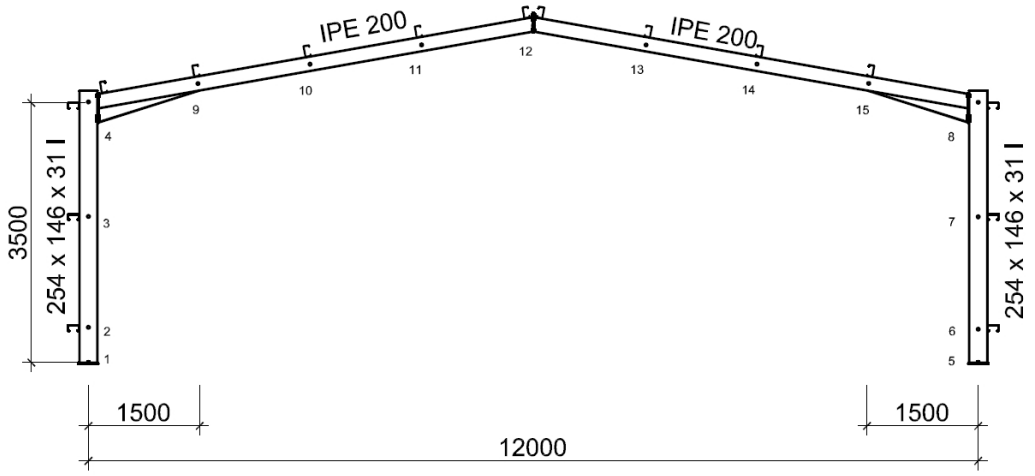

Figure A.1: Portal Frame Layout and Nodes.

Columns: 254x146x31 I
Girders: IPE 200
Purlins: 150x75x20x3,0 CFS
Cladding: 0,58mm Galavanised Steel Sheeting (Cloton)
Spacing: Frames = 5000 mm
Purlins = 1500 mm

A.2 PERMANENT LOADS

Self-weight of the columns and girders are automatically included in the analysis by the software.

SANS 10160-2:2011 (5.2)

Nodes 1 & 5:

$$Purlins: 7,48 \times 5 = 37,4\ kg$$

$$Cladding: 7,62 \times 5 \times 0,25 = 9,5\ kg$$

$$= 46,9\ kg = 0,46\ kN$$

$$F_v = 0,46\ kN$$

Nodes 2 & 6:

$$\begin{aligned} Purlins &: 7,48 \times 5 = 37,4\ kg \\ Cladding &: 7,62 \times 5 \times 1 = 38,1\ kg \\ &= 75,5\ kg = 0,741\ kN \end{aligned}$$

$F_v = 0,741\ kN$

Nodes 3 & 7:

$$\begin{aligned} Purlins &: 7,48 \times 5 = 37,4\ kg \\ Cladding &: 7,62 \times 5 \times 1,5 = 57,15\ kg \\ &= 94,55\ kg = 0,928\ kN \end{aligned}$$

$F_v = 0,928\ kN$

Nodes 4 & 8:

$$\begin{aligned} Purlins &: 7,48 \times 5 = 37,4\ kg \\ Cladding &: 7,62 \times 5 \times 0,75 = 28,58\ kg \\ Roofing &: 7,62 \times 0,762 \times 5 = 29,02\ kg \\ &= 95\ kg = 0,932\ kN \end{aligned}$$

$F_v = 0,932\ kN$

Nodes 9 - 15:

$$\begin{aligned} Purlins &: 7,48 \times 5 = 37,4\ kg \\ Cladding &: 7,62 \times 5 \times 1,523 = 58,03\ kg \\ &= 95,43\ kg = 0,936\ kN \end{aligned}$$

$F_v = 0,936\ kN$

A.3 IMPOSED LOADS

SANS 10160-2:2011

(Table 5)

$$\begin{aligned} A &= 12 \times 5 = 60\ m^2 \\ q_k &= 0,25\ kN/m^2 \\ Nodes\ 4\ \&\ 8: \ Q_n &= 0,762 \times 5 \times 0,25 \\ &= 0,953\ kN \end{aligned}$$

$F_v = 0,953\ kN$

$$Nodes\ 9\ -\ 15:\ Q_n = 1,523 \times 5 \times 0,25$$
$$= 1,904\ kN$$

$F_v = 1,904\ kN$

A.4 WIND LOAD

SANS 10160-3:2011 (6.2.1)

Basic wind speed:

$$v_{b,0} = 28 m.s^{-1}\ \text{(fundamental)}$$

SANS 10160-3:2011 (6.2.3)

Return period 50 years:

$$c_{prob} = \left(\frac{1 - K \times \ln(-(\ln(1-p)))}{1 - K \times \ln(-(\ln(0,98)))}\right)^n$$
$$= 1$$

$c_{prob} = 1$

SANS 10160-3:2011 (6.2.2)

Basic wind speed:

$$v_b = c_{prob} \times v_{b,0} = 1 \times 28 = 28\ m \cdot s^{-1}$$

$v_b = 28\ m \cdot s^{-1}$

SANS 10160-3:2011 (6.3.2)

Terrain Category B.
Column height = 3500 mm
Apex height = 4559 mm
Width of building = 12 000 mm
Length of building = 30 000 mm

SANS 10160-3:2011 (6.3.1)

Columns:

$$\begin{aligned} C_r(z) &= 1,36\left(\frac{z-z_0}{z_g-z_0}\right)^{\alpha} \\ &= 1,36\left(\frac{3,5-0}{300-0}\right)^{0,095} \\ &= 0,891 \end{aligned}$$

$$\begin{aligned} v_p(z) &= C_r(z) \times C_0(z) \times v_{b,peak} \\ &= 1,4 \times 0,891 \times 1 \times 28 \\ &= 34,927\ m \cdot s^{-1} \end{aligned}$$

$$v_p(z) = 34,927\ m \cdot s^{-1}$$

Roof Girders:

$$\begin{aligned} C_r(z) &= 1,36\left(\frac{z-z_0}{z_g-z_0}\right)^{\alpha} \\ &= 1,36\left(\frac{4,6-0}{300-0}\right)^{0,095} \\ &= 0,914 \end{aligned}$$

$$\begin{aligned} v_p(z) &= C_r(z) \times C_0(z) \times v_{b,peak} \\ &= 1,4 \times 0,914 \times 1 \times 28 \\ &= 35,829\ m \cdot s^{-1} \end{aligned}$$

$$v_p(z) = 35,829\ m \cdot s^{-1}$$

SANS 10160-3:2011 (6.4 & Table 4)

PEAK WIND PRESSURE:

Structure at sea level: $\rho = 1,20\ kg/m^3$

Columns:

$$\begin{aligned} q_p(z) &= {}^1/_2 \times \rho \times v_p^2(z) \\ &= {}^1/_2 \times 1,2 \times 34,927^2 \\ &= 731,937\ N/m^2 \end{aligned}$$

$$q_p(z) = 731,937\ N/m^2$$

Roof:

$$\begin{aligned} q_p(z) &= {}^1/_2 \times \rho \times v_p^2(z) \\ &= {}^1/_2 \times 1,2 \times 35,829^2 \\ &= 770,230\ N/m^2 \end{aligned}$$

$$q_p(z) = 770,230\ N/m^2$$

A.4.1 WIND CASE 1:

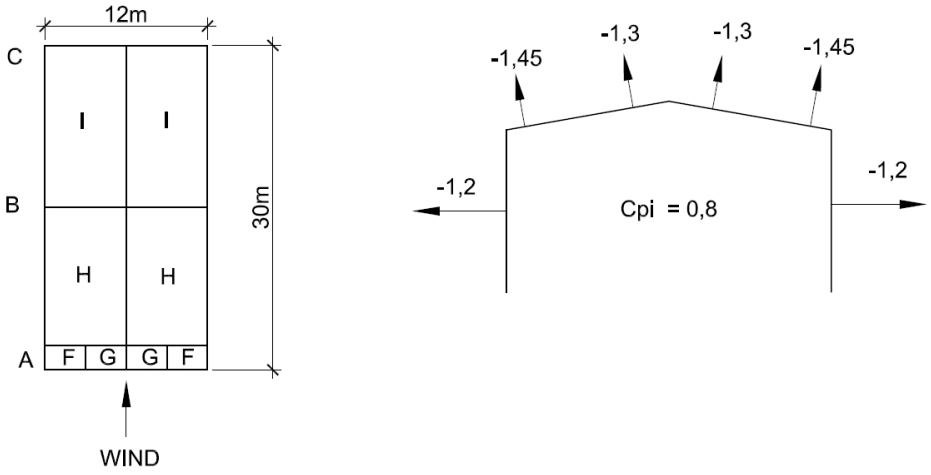

Figure A.2: Wind Case 1 Pressure Coefficients

Wind along structure with doors open.

b = 30 m

h = 4,6 m

e = 9,2 m

SANS 10160-3:2011
(Fig. 8)

Zone	$C_{pe\ 10}$
A	-1,2
B	-0,8
C	-0,5
D	+0,8
E	-0,5

SANS 10160-3:2011
(7.3.9.4)

Openings in D:

$$C_{pi} = \frac{2 \times 0,8}{2} = 0,8$$

SANS 10160-3:2011
(Fig. 11)

Zone	$C_{pe\ 10}$
F	-1,45
G	-1,3
H	-0,65
I	-0,55

SANS 10160-3:2011
(6.5.2.3)

$$W_e = q_p(z_e) \times C_{pe}$$

$$F = W_e \times A$$

$$Node\ 1\ \&\ 5: \ A = 0,25 \times 5 = 1,25m^2$$
$$F_H = 2 \times 1,25 \times 0,732 = 1,830\ kN$$

$$F_H = 1,830\ kN$$

$$Node\ 2\ \&\ 6: A = 1,250 \times 5 = 6,25m^2$$
$$F_H = 2 \times 6,25 \times 0,732 = 9,15\ kN$$

$$F_H = 9,15\ kN$$

$$Node\ 3\ \&\ 7: A = 1,5 \times 5 = 7,5m^2$$
$$F_H = 2 \times 7,5 \times 0,732 = 10,98\ kN$$

$$F_H = 10,98\ kN$$

$$Node\ 4\ \&\ 8: A = 0,75 \times 5 = 3,75m^2$$
$$F_H = 2 \times 3,75 \times 0,732 = 5,49\ kN$$

$$A = 0,762 \times 5 = 3,807\ m^2$$
$$F = 2,25 \times 3,807 \times 0,770 = 6,596\ kN$$
$$F_H = 6,596 \times \cos 80^\circ = 1,145\ kN$$
$$F_V = 6,596 \times \cos 10^\circ = 6,495\ kN$$
$$F_{H\ Total} = 6,635\ kN$$

$$F_{H\ Total} = 6,635\ kN$$
$$F_V = 6,495\ kN$$

$$Node\ 9\ \&\ 15: A = 1,523 \times 5 = 7,616\ m^2$$
$$F = 2,25 \times 7,616 \times 0,77 = 13,195\ kN$$
$$F_H = 13,195 \times \cos 80^\circ = 2,291\ kN$$
$$F_V = 13,195 \times \cos 10^\circ = 12,995\ kN$$

$$F_H = 2,291\ kN$$
$$F_V = 12,995\ kN$$

$$Node\ 10\ -\ 14\ : A = 7,616\ m^2$$
$$F = 2,1 \times 7,616 \times 0,77 = 12,315\ kN$$
$$F_H = 12,315 \times \cos 80^\circ = 2,138\ kN$$
$$F_V = 12,315 \times \cos 10^\circ = 12,128\ kN$$

$$F_H = 2,138\ kN$$
$$F_V = 12,128\ kN$$

A.4.2 WIND CASE 2:

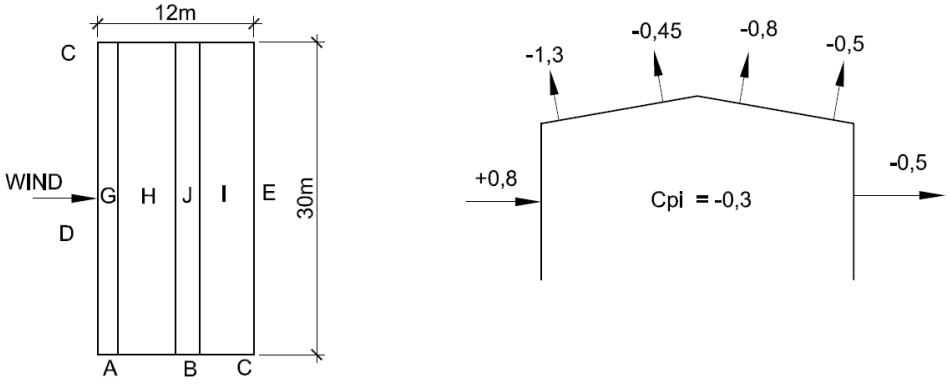

Figure A.3: Wind Case 2 Pressure Coefficients

Wind along structure with doors open.

b = 30 m

h = 4,6 m

e = 9,2 m

SANS 10160-3:2011 (Fig. 8)

Zone	$C_{pe\ 10}$
A	-1,2
B	-0,8
C	-0,5
D	+0,8
E	-0,5

SANS 10160-3:2011 (7.3.9.6 & 7.3.9.2)

Doors closed.

0,10% Openings assumed.

SANS 10160-3:2011 (7.3.9.6)

$$A_t = [2 \times 3,5 \times 30 + 2 \times 3,5 \times 15 + 2 \times {}^1/_2 \times 15 \times 1,1 + 2 \times 30 \times 7,616] \times 0,001$$
$$= 788,46 \times 10^{-3}\ m^2$$

$$A_n = [3,5 \times 30 + 2 \times 3,5 \times 15 + 2 \times {}^1/_2 \times 15 \times 1,1 + 2 \times 30 \times 7,616] \times 0,001$$
$$= 683,46 \times 10^{-3}\ m^2$$

$$\mu = \frac{A_n}{A_t} = \frac{683,46}{788,46} = 0,867$$

SANS 10160-3:2011 (Fig. 16)

$\frac{h}{d} = \frac{4,6}{15} = 0,307$

$C_{pi} = -0,3$

Zone	$C_{pe\ 10}$
F	-1,3
G	-1,0
H	-0,45
I	-0,5
J	-0,8

SANS 10160-3:2011
(6.5.2.3)

$$W_e = q_p(z_e) \times C_{pe}$$
$$F = W_e \times A$$

$Node\ 1 : A = 0,25 \times 5 = 1,25m^2$

$$F_H = 1,1 \times 1,25 \times 0,732 = 1,007\ kN$$

$F_H = 1,007\ kN$

$Node\ 2 : A = 1,250 \times 5 = 6,25m^2$

$$F_H = 1,1 \times 6,25 \times 0,732 = 5,033\ kN$$

$F_H = 5,033\ kN$

$Node\ 3 : A = 1,5 \times 5 = 7,5m^2$

$$F_H = 1,1 \times 7,5 \times 0,732 = 6,039\ kN$$

$F_H = 6,039\ kN$

$Node\ 4 : A = 0,75 \times 5 = 3,75m^2$

$$F_H = 1,1 \times 3,75 \times 0,732 = 3,020\ kN$$

$$A = 0,762 \times 5 = 3,807\ m^2$$
$$F = 1 \times 3,807 \times 0,770 = 2,931\ kN$$
$$F_H = 2,931 \times \cos 80^\circ = 0,509\ kN$$
$$F_V = 2,931 \times \cos 10^\circ = 2,887\ kN$$
$$F_{H\ total} = 2,511\ kN$$

$F_H = 2,511\ kN$
$F_V = 2,887\ kN$

$Node\ 9: A_1 = 0,0508 \times 5 = 0,254\ m^2$

$A_2 = 1,472 \times 5 = 7,362\ m^2$

$F = 1 \times 0,254 \times 0,770 + 0,15 \times 7,362 \times 0,770$

$= 1,046\ kN$

$F_H = 1,046 \times \cos 80^\circ = 0,182\ kN$

$F_V = 1,046 \times \cos 10^\circ = 1,030\ kN$

$F_H = 0,182\ kN$
$F_V = 1,030\ kN$

$Node\ 10\ \&\ 11: A = 1,523 \times 5 = 7,616\ m^2$

$F = 0,15 \times 7,616 \times 0,77 = 0,880\ kN$

$F_H = 0,880 \times \cos 80^\circ = 0,153\ kN$

$F_V = 0,880 \times \cos 10^\circ = 0,886\ kN$

$F_H = 0,153\ kN$
$F_V = 0,886\ kN$

$Node\ 12: A = 0,762 \times 5 = 3,807\ m^2$

$F = 0,15 \times 3,807 \times 0,77 + 0,5 \times 3,807 \times 0,770$

$= 1,905\ kN$

$F_H = 1,905 \times \cos 80^\circ = 0,331\ kN$

$F_V = 1,905 \times \cos 10^\circ = 1,876\ kN$

$F_H = 0,331\ kN$
$F_V = 1,876\ kN$

$Node\ 13: A_1 = 0,254\ m^2$

$A_2 = 7,362\ m^2$

$F = 0,5 \times 0,254 \times 0,77 + 0,2 \times 7,362 \times 0,770$

$= 1,232\ kN$

$F_H = 1,232 \times \cos 80^\circ = 0,214\ kN$

$F_V = 1,232 \times \cos 10^\circ = 1,213\ kN$

$F_H = 0,214\ kN$
$F_V = 1,213\ kN$

$Node\ 14\ \&\ 15: A = 1,523 \times 5 = 7,616\ m^2$

$F = 0,2 \times 7,616 \times 0,77 = 1,173\ kN$

$F_H = 1,173 \times \cos 80^\circ = 0,204\ kN$

$F_V = 1,173 \times \cos 10^\circ = 1,155\ kN$

$F_H = 0,204\ kN$
$F_V = 1,155\ kN$

$$Node\ 8 : A = 0,75 \times 5 = 3,75m^2$$
$$F_H = 0,2 \times 3,75 \times 0,732 = 0,549\ kN$$

$$A = 0,762 \times 5 = 3,807\ m^2$$
$$F = 0,2 \times 3,807 \times 0,770 = 0,586\ kN$$
$$F_H = 0,586 \times \cos 80^\circ = 0,102\ kN$$
$$F_V = 0,586 \times \cos 10^\circ = 0,577\ kN$$
$$F_{H\ Total} = 0,651\ kN$$

$F_{H\ Total} = 0,651\ kN$
$F_V = 0,577\ kN$

$$Node\ 7 : A = 1,5 \times 5 = 7,5m^2$$
$$F_H = 0,2 \times 7,5 \times 0,732 = 1,098\ kN$$

$F_H = 1,098\ kN$

$$Node\ 6 : A = 1,250 \times 5 = 6,25m^2$$
$$F_H = 0,2 \times 6,25 \times 0,732 = 0,915\ kN$$

$F_H = 0,915\ kN$

$$Node\ 5 : A = 0,25 \times 5 = 1,25m^2$$
$$F_H = 0,2 \times 1,25 \times 0,732 = 0,183\ kN$$

$F_H = 0,183\ kN$

A.5 STABILITY

SANS 10162-1:2005
(8.7)

$$Columns : 2 \times 3,5 \times 31,1 = 217,7\ kg$$
$$Girders : 2 \times 6,093 \times 22,4 = 272,966\ kg$$
$$Purlins : 13 \times 5 \times 7,48 = 486,2\ kg$$
$$Cladding : 2 \times 9,593 \times 5 \times 7,62 = 730,987\ kg$$
$$= 1707,853\ kg = 16,754\ kN$$
$$Live\ Load = 15,23\ kN$$

Add to Node 4 a horizontal load of
$(16,754 + 15,23) \times 0,005 = 0,160\ kN$

A.6 LOAD CASES & COMBINATIONS

Load case 1: Permanent loads.
Load case 2: Imposed loads.
Load case 3: Imposed loads across half the roof.
Load case 4: Wind load along the structure.
Load case 5: Wind load across the structure.

Ultimate Limit State:
LC1: 1,2 × (Load case 1) + 1,6 × (Load case 2)
LC2: 1,2 × (Load case 1) + 1,6 × (Load case 3)
LC3: 0,9 × (Load case 1) + 1,3 × (Load case 4)
LC4: 0,9 × (Load case 1) + 1,3 × (Load case 5)

Serviceability Limit State:
LC5: 1,1 × (Load case 1) + 1,0 × (Load case 2)
LC6: 1,1 × (Load case 1) + 1,0 × (Load case 3)
LC7: 1,1 × (Load case 1) + 0,6 × (Load case 4)
LC8: 1,1 × (Load case 1) + 0,6 × (Load case 5)

A.7 SUMMARY OF NODAL LOADS

Table A.1: Summary of Nodal Loads

Node	Load Case 1		Load Case 2		Load Case 3		Load Case 4	
	F_x $[kN]$	F_y $[kN]$	F_x $[kN]$	F_y $[kN]$	F_x $[kN]$	F_y $[kN]$	F_x $[kN]$	F_y $[kN]$
1		-0.46					-1.83	
2		-0.74					-9.15	
3		-0.93					-10.98	
4		-0.93	0.16	-0.95	0.l6	-0.95	-6.64	6.50
5		-0.46					1.83	
6		-0.74					9.15	
7		-0.93					10.98	
8		-0.93		-0.95			6.64	6.50
9		-0.94		-1.90		-1.90	-2.29	13.00
10		-0.94		-1.90		-1.90	-2.14	12.13
11		-0.94		-1.90		-1.90	-2.14	12.13
12		-0.94		-1.90		-0.95		12.13
13		-0.94		-1.90			-2.14	12.13
14		-0.94		-1.90			-2.14	12.13
15		-0.94		-1.90			2.29	13.00

Node	Load Case 5	
	F_x $[kN]$	F_y $[kN]$
1	1.01	
2	5.03	
3	6.04	
4	2.51	2.89
5	0.18	
6	0.92	
7	1.10	
8	0.65	0.58
9	-0.18	1.03
10	-0.15	0.87
11	-0.15	0.87
12	0.18	1.88
13	0.21	1.21
14	0.20	1.16
15	0.20	1.16

A.8 SERVICEABILITY LIMIT STATE

SANS 10162-1:2005

(Annex D)

$$Vertical\ deflection(max) = \frac{1}{180} \times span$$

$$12000 \times \frac{1}{180} = 66,67\ mm$$

$$Horizontal\ deflection(max) = \frac{1}{400} \times height$$

$$4558 \times \frac{1}{400} = 11,40\ mm$$

From analysis:

Load combination 5 vertical deflection = 30,34 mm OK

Load combination 6 horizontal deflection = 16,13 mm not OK

A.9 ULTIMATE LIMIT STATE

A.9.1 COLUMNS

LOAD COMBINATION 1:

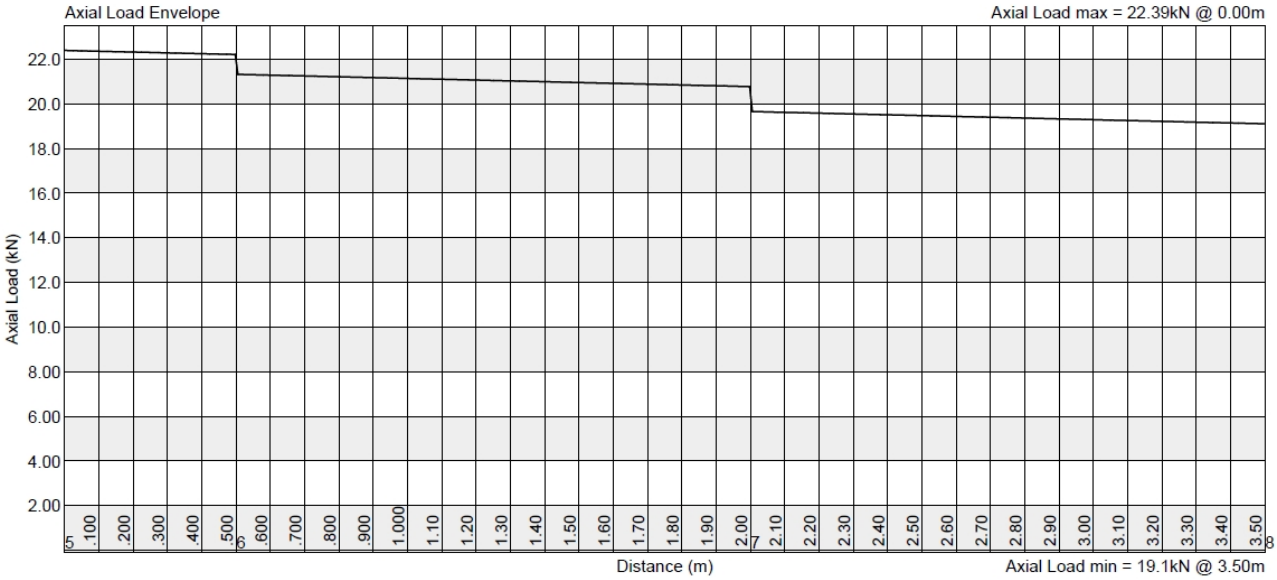

Figure A.4: Column Load Combination 1 Axial Forces

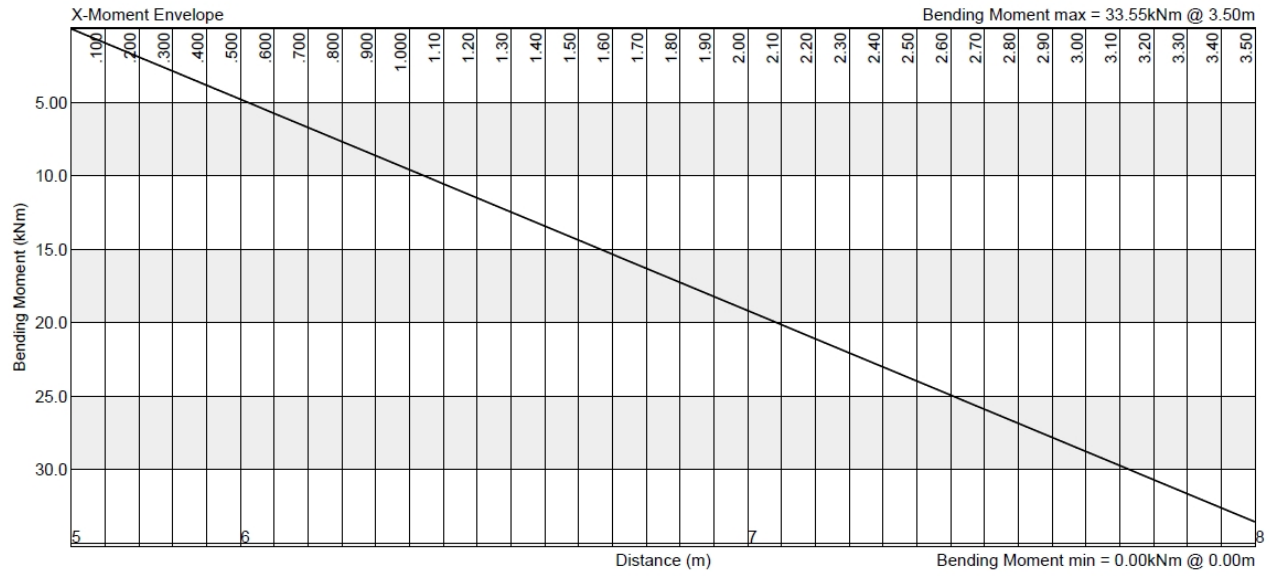

Figure A.5: Column Load Combination 1 Bending Moments

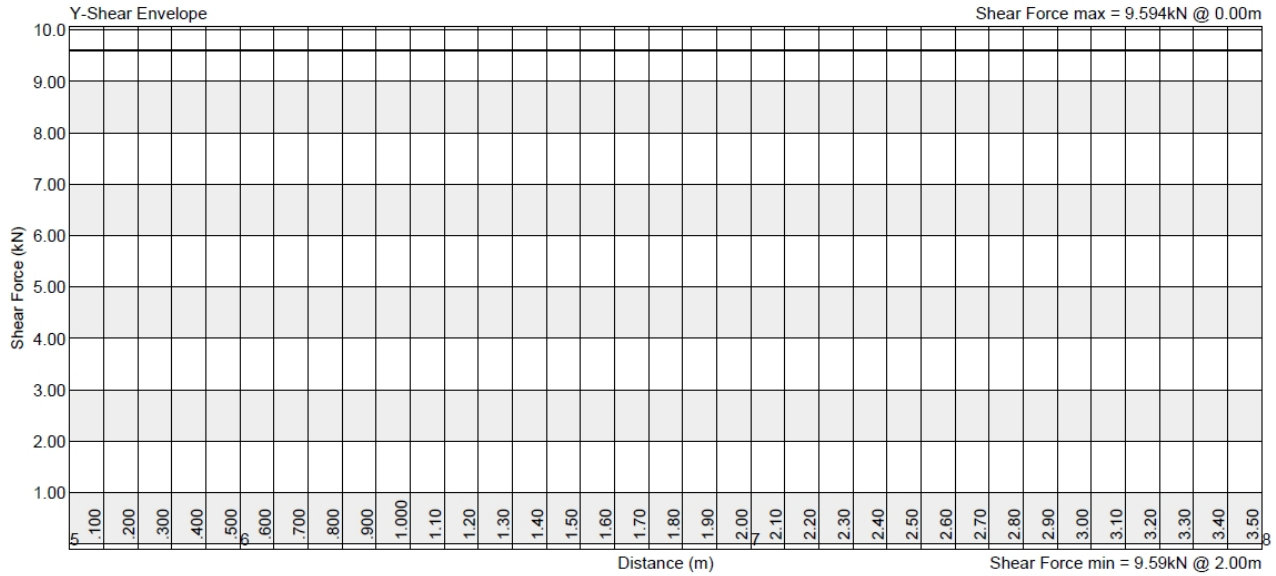

Figure A.6: Column Load Combination 1 Bending Moments

Classification:

SANS 10162-1:2005 (Table 3)

Axial:

$$Flange: \frac{b}{2t_f} = \frac{146,1}{2(8,6)} = 8,49 < \frac{200}{\sqrt{f_y}} = 10,61$$

$Class\ 3$

$$Web: \frac{h-2t_f}{t_W} = \frac{251,4-2(8,6)}{6} = 39,03 > \frac{670}{\sqrt{f_y}} = 35,56$$

$Class\ 4$

Class 4

Flexural:

$$Flange: \frac{b}{2t_f} = \frac{146,1}{2(8,6)} = 8,49 < \frac{170}{\sqrt{f_y}} = 9,023$$

$Class\ 2$

$$Web: \frac{h-2t_f}{t_W} = \frac{251,4-2(8,6)}{6}$$

$$= 39,03 > \frac{1100}{\sqrt{f_y}}\left(1-\frac{0,39C_u}{\phi C_y}\right) = 57,98$$

$$C_u = 22,36\ kN$$

$$C_y = A.f_y = 1416,45\ kN$$

$Class\ 1$

Class 2

Global Element Strength:

SANS 10162-1:2005
(13.8.2b)

$$C_r = C_{rx}$$
$$L_x = 3,5\ mm$$
$$r_x = 105\ mm$$

SANS 10162-1:2005
(13.3.3a)

$$f = \frac{C_u}{A} = \frac{22,39 \times 10^3}{3,99 \times 10^3} = 5,612\ MPa$$
$$W_{lim} = 0,644\sqrt{\frac{k.E}{f}} = 0,644\sqrt{\frac{0,43(200 \times 10^9)}{5,612 \times 10^6}}$$
$$= 79,722$$
$$W = \frac{h - 2t_f}{t_w} = 39,03 < W_{lim}$$
$$A_{eff} = A = 3,99 \times 10^{-3}\ m^2$$

SANS 10162-1:2005
(13.3)

$$\lambda = \frac{KL}{r}\sqrt{\frac{f_y}{\pi^2 E}} = \frac{2(3,5)}{105 \times 10^{-3}}\sqrt{\frac{355 \times 10^6}{\pi^2(200 \times 10^9)}} = 0,894$$
$$C_r = \phi A f_y (1 + \lambda^{2n})^{\frac{-1}{n}}$$
$$= 0,9(3,99 \times 10^{-3}))(355 \times 10^6)(1 + 0,894^{2,68})^{\frac{-1}{1,34}}$$
$$= 842,98\ kN \quad OK$$

$C_r = 842,98\ kN$

SANS 10162-1:2005
(13.5)

$$M_{rx} = \phi Z_{pl} f_y = 0,9(395 \times 10^{-6})(355 \times 10^6)$$
$$= 126,203\ kNm$$

$M_{rx} = 126,203\ kNm$

SANS 10162-1:2005
(13.8.2b)

Interaction:

$$\frac{C_u}{C_r} + \frac{0,85U_{1x}M_{ux}}{M_{rx}} = \frac{22,39}{842,98} + \frac{0,85(33,55)}{126,203} = 0,253 < 1\ OK$$

Lateral Torsional Buckling:

SANS 10162-1:2005
(13.8.2c)

$$C_r = C_{ry}$$
$$L_x = 2(2) = 4\ mm$$
$$r_y = 33,5\ mm$$

SANS 10162-1:2005
(10.4.2.1)

$$\frac{L_y}{r_y} = \frac{4}{33,5 \times 10^{-3}} = 119,403 \ < \ 200$$

SANS 10162-1:2005
(13.3)

$$\lambda = \frac{KL}{r}\sqrt{\frac{f_y}{\pi^2 E}} = \frac{4}{33,5 \times 10^{-3}}\sqrt{\frac{355 \times 10^6}{\pi^2(200 \times 10^9)}} = 1,601$$
$$C_r = \phi A f_y (1 + \lambda^{2n})^{\frac{-1}{n}}$$
$$= 0,9(3,99 \times 10^{-3}))(355 \times 10^6)(1 + 1,601^{2,68})^{\frac{-1}{1,34}}$$
$$= 412,878\ kN \quad OK$$

$C_r = 412,878\ kN$

SANS 10162-1:2005
(13.6a)

$$K = \frac{M_1}{M_2} = 0$$
$$\omega_2 = 1,75$$
$$KL = 2(2) = 4\ m$$
$$M_{cr} = \frac{\omega_2 \pi}{KL}\sqrt{EI_y GJ + \left(\frac{\pi E}{KL}\right)^2 I_y C_w}$$
$$= \frac{1,75\pi}{4}\sqrt{(200 \times 10^9)(4,48 \times 10^{-6})(77 \times 10^9)(88,2 \times 10^{-9})} + \left(\frac{\pi(200 \times 10^9)}{4}\right)^2 (4,48 \times 10^{-6})(66 \times 10^{-9})$$
$$= 117,397\ kNm$$
$$M_p = Z_{pl}.f_y = 395 \times 10^{-6} \times 355 \times 10^6 = 140,225\ kNm$$
$$M_{cr} > 0,67 M_p$$
$$M_r = 1,15\phi M_p\left(1 - \frac{0,28(140,225 \times 10^3)}{117,397 \times 10^3}\right)$$
$$= 96,594\ kNm < \phi M_p$$

$M_r = 96,594\ kN$

SANS 10162-1:2005
(13.8.2c)

Interaction:

$$\frac{C_u}{C_r} + \frac{0,85U_{1x}M_{ux}}{M_{rx}} = \frac{22,39}{412,878} + \frac{0,85(33,55)}{96,594} = 0,349 \ < \ 1 \ OK$$

$$\frac{M_{ux}}{M_{rx}} = \frac{33,55}{96,594} = 0,347 \ < \ 1 \ OK$$

LOAD COMBINATION 3:

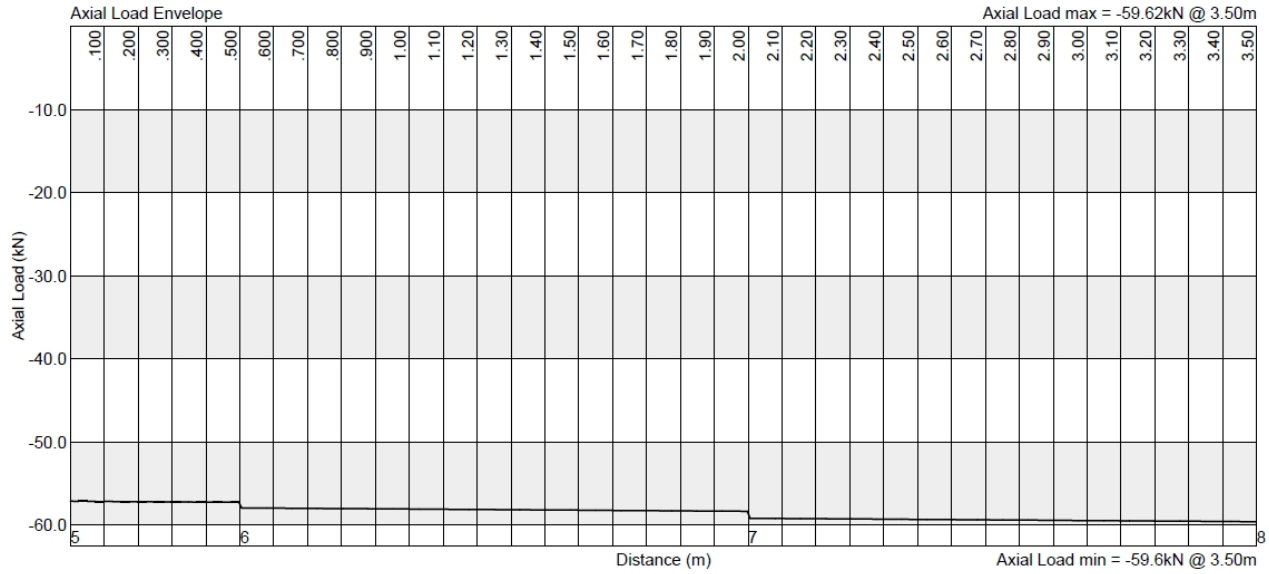

Figure A.7: Column Load Combination 3 Axial Forces

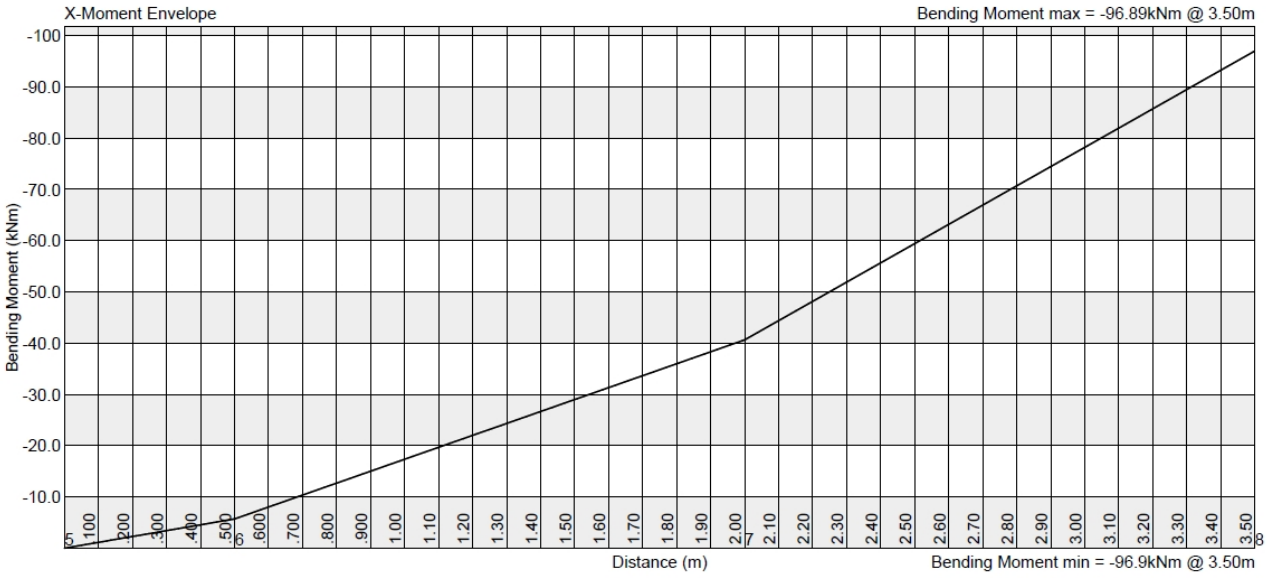

Figure A.8: Column Load Combination 3 Bending Moments

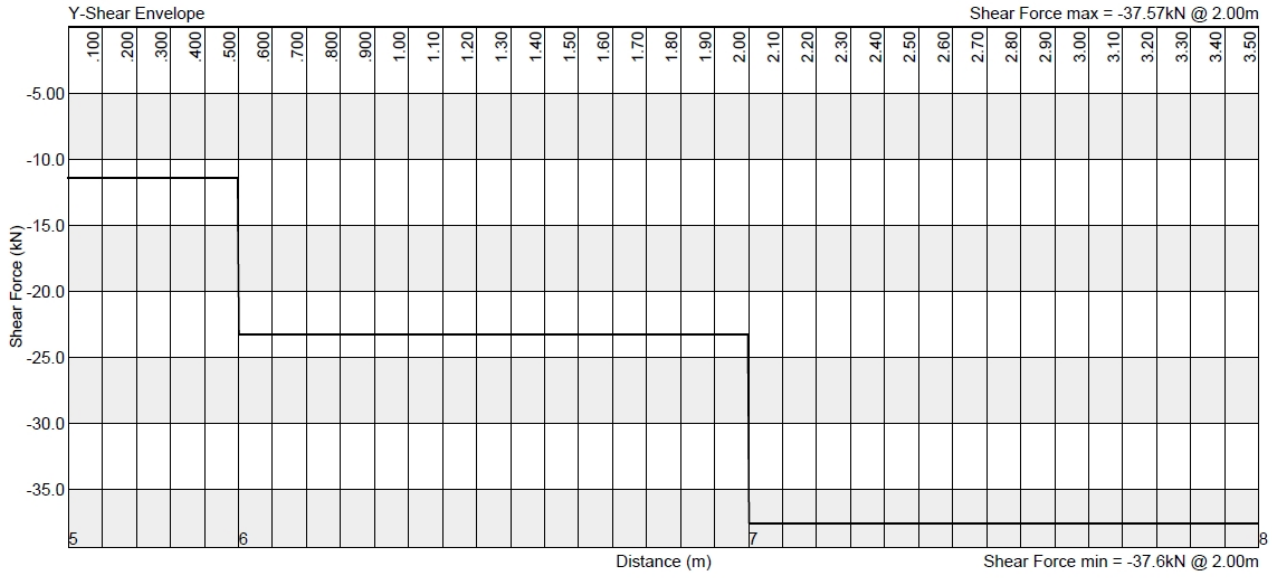

Figure A.9: Column Load Combination 3 Shear Forces

SANS 10162-1:2005

(13.9a)

$$T_r = \phi A f_y = 0,9(3,99 \times 10^{-3})(355 \times 10^6) = 1274,81 \ kN$$

$$T_r = 1274,81 \ kN$$

SANS 10162-1:2005

(13.5)

$$M_r = \phi Z_{pl} f_y = 0,9(395 \times 10^{-6})(355 \times 10^6) = 126,203 \ kNm$$

$$M_r = 126,203 \ kNm$$

SANS 10162-1:2005

(13.9a)

$$\frac{T_u}{T_r} + \frac{M_u}{M_r} = \frac{59,62}{1274,81} + \frac{97,12}{126,203} = 0,816 < 1 \ OK$$

SANS 10162-1:2005

(13.6a)

$$K = 0$$

$$\omega_2 = 1,75$$

$$KL = 2(2) = 4 \ m$$

$$M_{cr} = \frac{\omega_2 \pi}{KL}\sqrt{EI_yGJ + \left(\frac{\pi E}{KL}\right)^2 I_y C_w}$$
$$= \frac{1,75\pi}{4000}\sqrt{(2\times10^5)(4,48\times10^6)(7,7\times10^4)(88,2\times10^3) + \left(\frac{\pi(2\times10^5)}{4000}\right)^2 (4,48\times10^6)(66\times10^9)}$$
$$= 158,99\ kNm$$

$$M_p = Z_{pl}.f_y = 395\times10^{-6}\times355\times10^6 = 140,225\ kNm$$
$$M_{cr} > 0,67M_p$$
$$M_r = 1,15\phi M_p\left(1 - \frac{0,28(140,225\times10^3)}{158,99\times10^3}\right)$$
$$= 109,292\ kNm < \phi M_p$$

$M_r = 109,292\ kN$

SANS 10162-1:2005 (13.9)

$$\frac{M_u}{M_r} - \frac{T_u Z_{pl}}{M_r A} = \frac{97,12\times10^3}{109,292\times10^3} - \frac{59,62\times10^3(395\times10^{-9})}{109,292\times10^3(3,99\times10^{-3})}$$
$$= 0,889 < 1 \quad OK$$

Shear:

SANS 10162-1:2005 (13.4)

No web stiffeners.

SANS 10162-1:2005 (13.4.1.1)

$$k_v = 5,34$$
$$440\sqrt{\frac{k_v}{f_y}} = 440\sqrt{5,34}355 = 53,96 > \frac{h_w}{t_W} = 36,5$$
$$f_s = 0,66f_y = 0,66(355\times10^6) = 234,3\ MPa$$
$$A_v = ht_w = 251,4\times6 = 1,508\times10^3\ mm^2$$
$$= 1,508\times10^{-3}\ m^2$$

$$V_r = \phi A_v f_s = 0,9(1,508\times10^{-3})(234\times10^6)$$
$$= 317,585\ kN > 37,5\ kN \quad OK$$

$V_r = 317,585\ kN$

A.9.2 GIRDERS

LOAD COMBINATION 1:

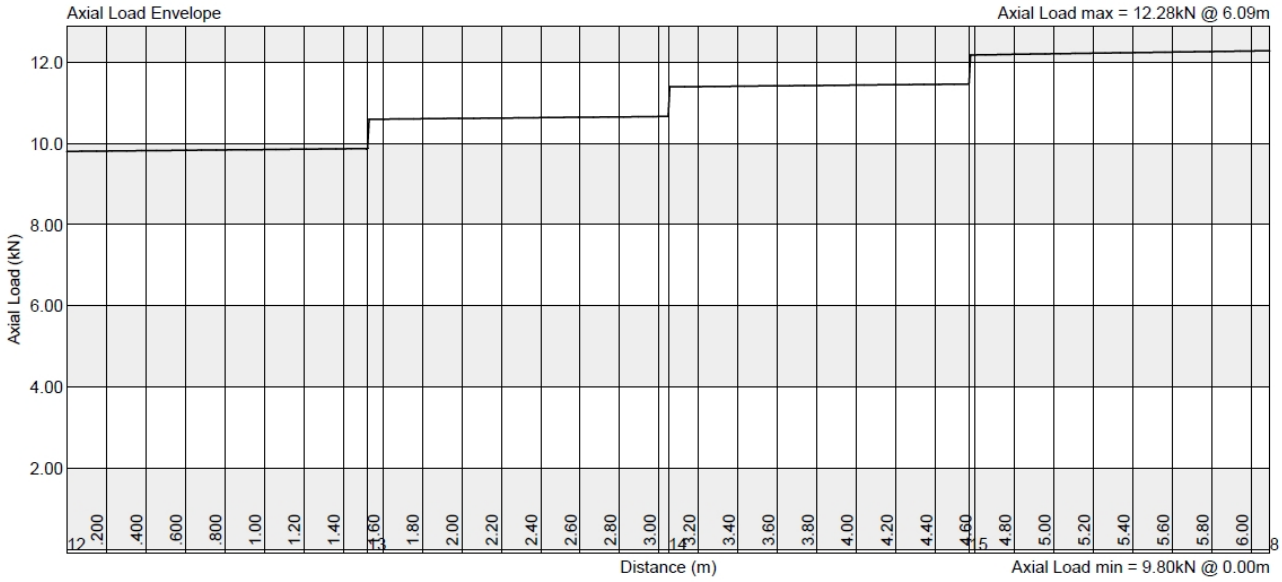

Figure A.10: Girder Load Combination 1 Axial Forces

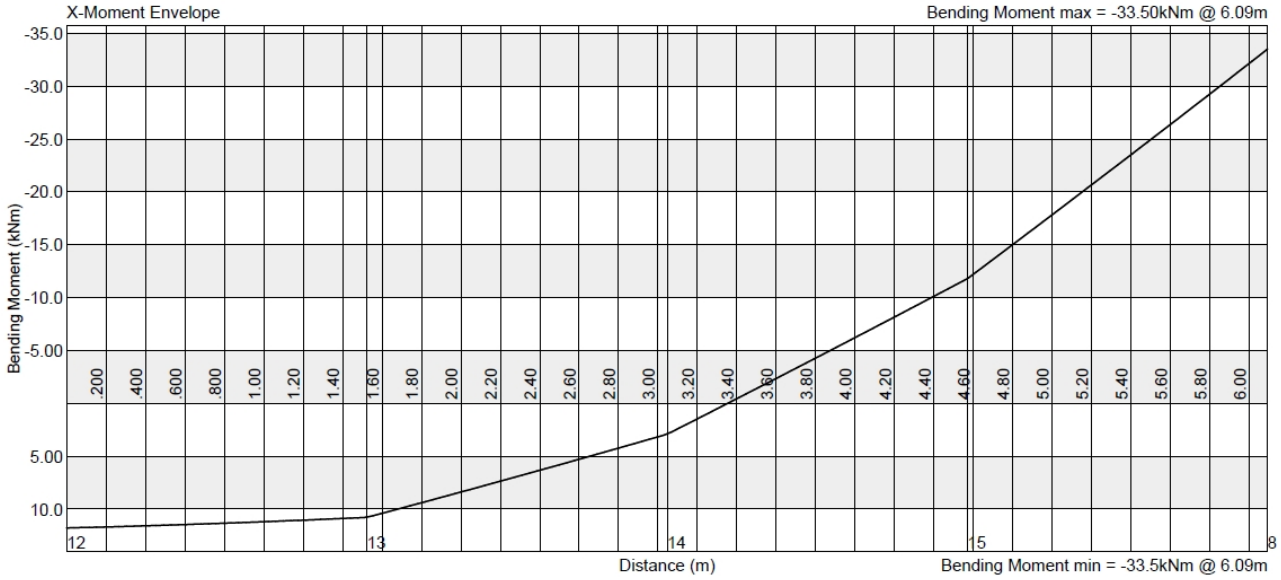

Figure A.11: Girder Load Combination 1 Bending Moments

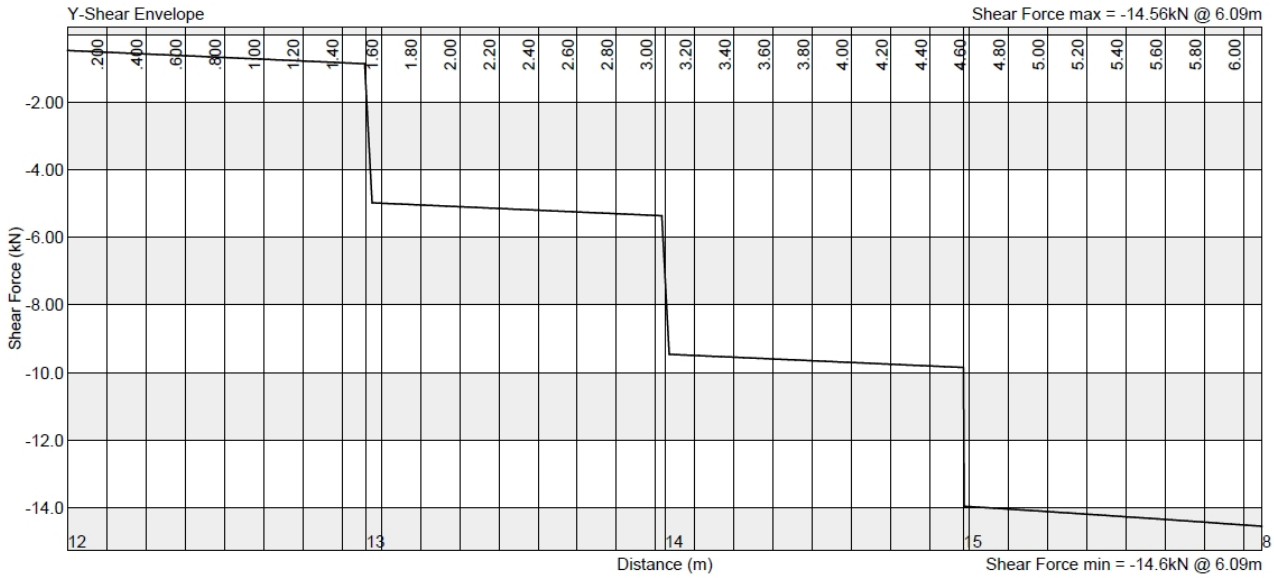

Figure A.12: Girder Load Combination 1 Bending Moments

Classification:

SANS 10162-1:2005 (Table 3)

Axial:

$$Flange: \frac{b}{2t_f} = \frac{100}{2(8,5)} = 5,88 < \frac{200}{\sqrt{f_y}}$$

$$Class\ 3$$

$$Web: \frac{h-2t_f}{t_W} = \frac{200-2(8,5)}{5,6} = 32,68 > \frac{670}{\sqrt{f_y}}$$

$$Class\ 3$$

Class 3

Flexural:

$$Flange: \frac{b}{2t_f} = \frac{100}{2(8,5)} = 5,88 < \frac{145}{\sqrt{f_y}}$$

$$Class\ 1$$

$$Web: \frac{h-2t_f}{t_W} = \frac{200-2(8,5)}{5,6}$$

$$= 32,68 > \frac{1100}{\sqrt{f_y}}\left(1 - \frac{0,39C_u}{\phi C_y}\right) = 58,074$$

$$C_u = 12,30\ kN$$

$$C_y = A.f_y = 1011,75\ kN$$

$$Class\ 1$$

Class 1

Global Element Strength:

SANS 10162-1:2005
(13.8.2b)

$$C_r = C_{rx}$$
$$L_x = 6,093\ mm$$
$$r_x = 82,6\ mm$$

SANS 10162-1:2005
(13.3.1)

$$\lambda = \frac{KL}{r}\sqrt{\frac{f_y}{\pi^2 E}} = \frac{6,093}{82,6\times10^{-3}}\sqrt{\frac{355\times10^6}{\pi^2(200\times10^9)}} = 0,989$$
$$C_r = \phi A f_y(1+\lambda^{2n})^{\frac{-1}{n}}$$
$$= 0,9(2,85\times10^{-3}))(355\times10^6)(1+0,989^{2,68})^{\frac{-1}{1,34}}$$
$$= 548,826\ kN \quad OK$$

$C_r = 548,826\ kN$

SANS 10162-1:2005
(13.5)

$$M_{rx} = \phi Z_{pl} f_y = 0,9(221\times10^{-6})(355\times10^6)$$
$$= 70,610\ kNm$$

$M_{rx} = 70,610\ kN$

SANS 10162-1:2005 Interaction:
(13.8.2b)

$$\frac{C_u}{C_r} + \frac{0,85U_{1x}M_{ux}}{M_{rx}} = \frac{12,30}{548,826} + \frac{0,85(33,58)}{70,610} = 0,427 \ < \ 1\ OK$$

Lateral Torsional Buckling:

SANS 10162-1:2005
(13.8.2c)

$$C_r = C_{ry}$$
$$L_x = 3046\ mm$$
$$r_y = 22,4\ mm$$

SANS 10162-1:2005
(10.4.2.1)

$$\frac{L_y}{r_y} = \frac{3046}{22,4} = 135,982 \ < \ 200$$

SANS 10162-1:2005
(13.3.1)

$$\lambda = \frac{KL}{r}\sqrt{\frac{f_y}{\pi^2 E}} = \frac{3,046}{22,4\times10^{-3}}\sqrt{\frac{355\times10^6}{\pi^2(200\times10^9)}} = 1,824$$

$$C_r = \phi A f_y(1+\lambda^{2n})^{\frac{-1}{n}}$$
$$= 0,9(2,85\times10^{-3}))(355\times10^6)(1+1,824^{2,68})^{\frac{-1}{1,34}}$$
$$= 238,917\ kN \quad OK$$

$C_r = 238,917\ kN$

SANS 10162-1:2005
(13.6a)

$$K = \frac{M_1}{M_2} = \frac{21}{22,64} = 0,928$$

$$\omega_2 = 1,75 + 1,05(0,928) + 0,3(0,928)^2 = 2,983 > 2,5$$

$$KL = 3046\ mm$$

$$M_{cr} = \frac{\omega_2\pi}{KL}\sqrt{EI_yGJ + \left(\frac{\pi E}{KL}\right)^2 I_y C_w}$$
$$= 319,458\ kNm$$

$$M_p = Z_{pl}.f_y = 221\times10^{-6}\times355\times10^6 = 78,46\ kNm$$

$$M_{cr} > 0,67M_p$$

$$M_r = 1,15\phi M_p\left(1 - \frac{0,28(78,46\times10^3)}{319,458\times10^3}\right)$$
$$= 75,622\ kNm > \phi M_p = 70,614\ kNm$$

$M_r = 70,614\ kN$

SANS 10162-1:2005
(13.8.7c)

Interaction:

$$\frac{C_u}{C_r} + \frac{0,85U_{1x}M_{ux}}{M_{rx}} = \frac{12,3}{238,917} + \frac{0,85(33,58)}{70,614} = 0,456 < 1\ OK$$

$$\frac{M_{ux}}{M_{rx}} = \frac{33,58}{70,614} = 0,476 < 1\ OK$$

LOAD COMBINATION 3:

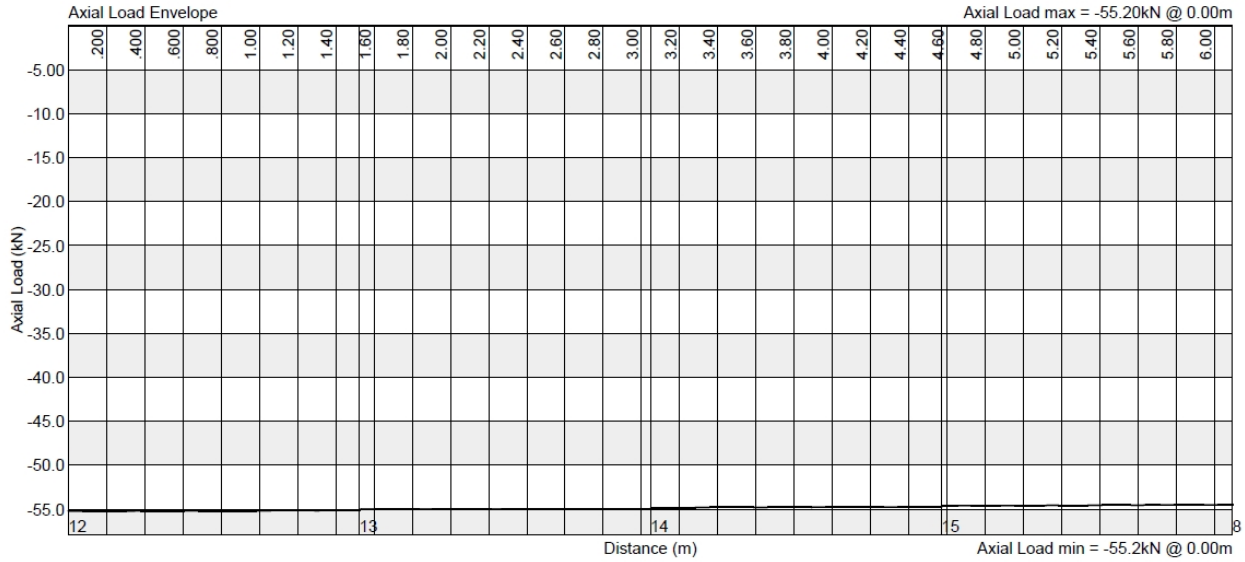

Figure A.13: Girder Load Combination 3 Axial Forces

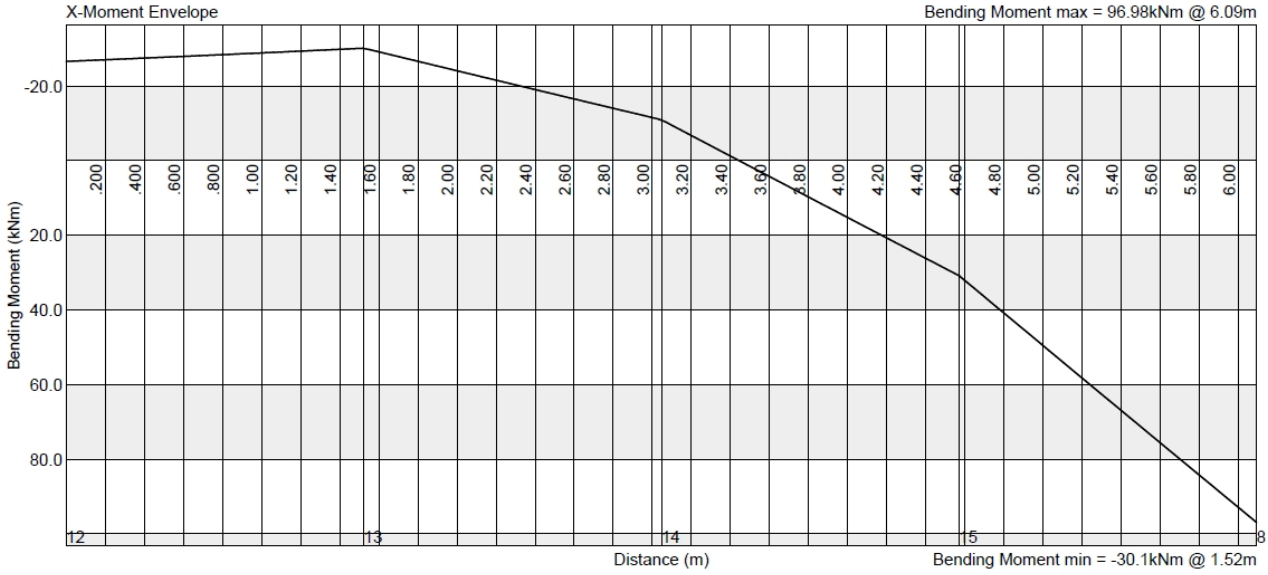

Figure A.14: Girder Load Combination 3 Bending Moments

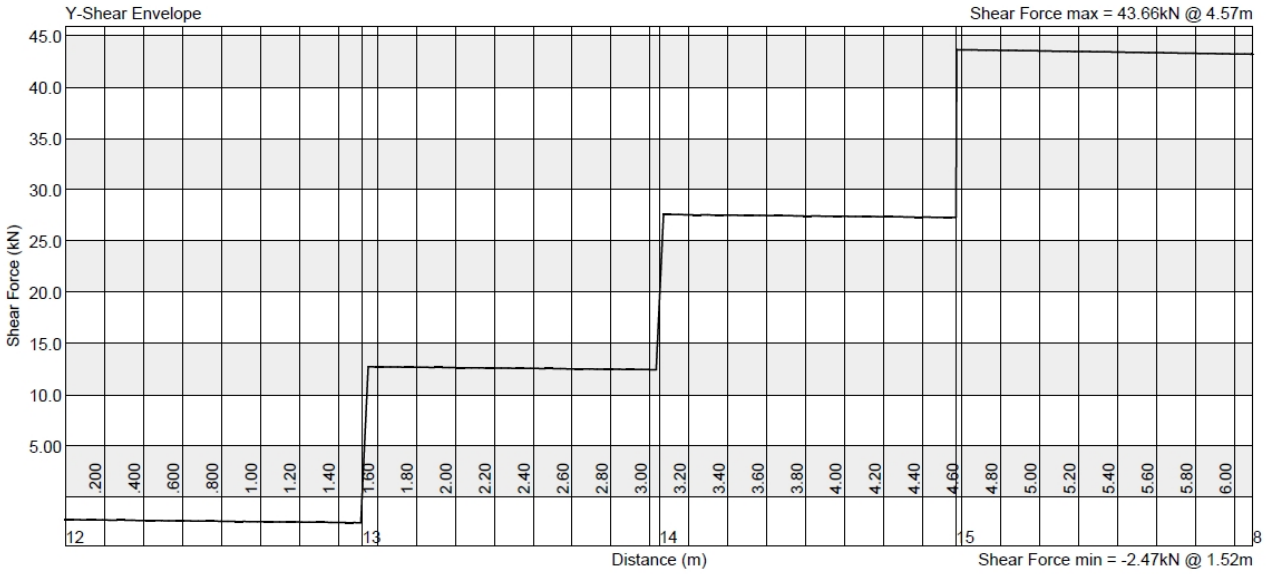

Figure A.15: Girder Load Combination 3 Shear Forces

SANS 10162-1:2005

(13.9a)

$$T_r = \phi A f_y = 0,9(2,85 \times 10^{-3})(355 \times 10^6) = 910,575\ kN$$

$T_r = 910,575\ kN$

SANS 10162-1:2005

(13.5)

$$M_r = \phi Z_{pl} f_y = 0,9(221 \times 10^{-6})(355 \times 10^6) = 70,610\ kNm$$

$M_r = 70,610\ kN$

SANS 10162-1:2005

(13.9a)

$$\frac{T_u}{T_r} + \frac{M_u}{M_r} = \frac{55,27}{910,575} + \frac{31,02}{70,612} = 0,5 < 1\ OK$$

SANS 10162-1:2005

(13.9a)

$$K = \frac{30,14}{30,64} = 0,983$$

$$\omega_2 = 1,75 + 1,05(0,983) + 0,3(0,983)^2 = 3,072 > 2,5$$

$$KL = 3,046\ m$$

$$M_{cr} = \frac{\omega_2 \pi}{KL}\sqrt{EI_yGJ + \left(\frac{\pi E}{KL}\right)^2 I_y C_w}$$
$$= 327,601\ kNm$$
$$M_p = Z_{pl}.f_y = 221 \times 10^{-6} \times 355 \times 10^6 = 78,455\ kNm$$
$$M_{cr} > 0,67M_p$$
$$M_r = 1,15\phi M_p\left(1 - \frac{0,28(78,455 \times 10^3)}{327,601 \times 10^3}\right)$$
$$= 75,756\ kNm > \phi M_p = 70,610\ kNm$$

$M_r = 70,610\ kN$

SANS 10162-1:2005 (13.9)

$$\frac{M_u}{M_r} - \frac{T_u Z_{pl}}{M_r A} = \frac{30,63 \times 10^3}{70,610 \times 10^3} - \frac{55,20 \times 10^3(221 \times 10^{-6})}{70,610 \times 10^3(2,85 \times 10^{-3})}$$
$$= 0,434 < 1 \quad OK$$

Shear:

SANS 10162-1:2005 (13.4)

No web stiffeners.

SANS 10162-1:2005 (13.4.1.1)

$$k_v = 5,34$$
$$440\sqrt{\frac{k_v}{f_y}} = 440\sqrt{\frac{5,34}{355}} = 54,34 > \frac{h_w}{t_W} = 28,393$$
$$f_s = 0,66f_y = 0,66(355 \times 10^6) = 234,3\ MPa$$
$$A_v = ht_w = 200 \times 5,6 = 1,12 \times 10^3\ mm^2 = 1,12 \times 10^{-3}\ m^2$$
$$V_r = \phi A_v f_s = 0,9(1,12 \times 10^{-3})(234 \times 10^6)$$
$$= 236,174\ kN > 43,66\ kN \quad OK$$

$V_r = 236,174\ kN$

A.10 CONNECTIONS

A.10.1 COLUMN BASE

Refer to detail drawing 001-002 in appendix B for layout, dimensions and details.

Load Combination 1:
Axial compression = 22,94 kN
Shear = 9,57 kN

Load Combination 3:
Axial tension = 56,74 kN
Shear = 11,4 kN

Design:

SAISC 2008 (4.12) Contact area required:

$$C_u = 0,6 f_{cu} A_{req}$$
$$A_{req} = \frac{C_u}{0,6 f_{cu}} = \frac{22,36 \times 10^3}{0,6(30 \times 10^6)}$$
$$= 1,242 \times 10^{-3}\ m^2 = 1242,22\ mm^2$$
$$A_{req} < A_g$$
$$Plate: 270 \times 160\ mm$$
$$Tension\ per\ bolt = 28,37\ kN$$

$$Moment\ due\ to\ tension:$$
$$M_u = 28,37 \times 10^3 \times 32 \times 10^{-3} = 907,84\ Nm$$

$$Z_e = \frac{2(55,426 \times 10^{-3}) t_p^2}{6} = 18,475 \times 10^{-3} t_p^2$$

$$\therefore M_r = \phi Z_e f_y$$
$$= 0,9(18,475 \times 10^{-3}) t_p^2 (355 \times 10^6)$$
$$= 5,903 \times 10^6 t_p^2$$
$$\therefore 5,903 \times 10^6 t_p^2 = 1,816 \times 10^3$$

$$\therefore\ t_p = 17,540 \times 10^{-3}\ m = 17,540\ mm$$
$$\therefore 18mm\ Baseplate$$

18mm Baseplate

Bolts

SANS 10162-1:2005 (13.12.1.3)

Use M16 Commercial Quality Bolts.
A concrete bond length of 150 mm is required together with a 10 mm thick 60 mm x 60 mm square anchor plate.

$$\begin{aligned} T_r &= 0,75\phi_b A_b f_u \\ &= 0,75(0,67)\left(\frac{\pi}{4}\right)(16\times10^{-3})^2(365\times10^6) \\ &= 36,877\ kN \end{aligned}$$

$T_r = 36,877\ kN$

SANS 10162-1:2005 (13.12.1.2)

$$\begin{aligned} V_r &= 0,60\phi_b nmA_b f_u \\ &= 0,6(0,67)\left(\frac{\pi}{4}\right)(16\times10^{-3})^2(365\times10^6) \\ &= 29,502\ kN \\ 0,7V_r &= 20,651\ kN \end{aligned}$$

$V_r = 20,651\ kN$

SANS 10162-1:2005 (13.12.1.4)

$$\begin{aligned} \frac{V_u}{V_r}+\frac{T_u}{T_r} &= \frac{11,4}{41,30}+\frac{56,74}{73,75} \\ &= 1,045 < 1,4 \end{aligned}$$

Welds:

SANS 10162-1:2005 (13.13.2.2)

6mm Fillet weld at flanges & web.

$$\begin{aligned} T_r &= 2\times0,67\phi_w A_w x_u(1,5) \\ &= 2\times0,67(0,67)(6\times10^{-3})0,71(146\times10^{-3})(480\times10^6)1,5 \\ &= 402,045\ kN \end{aligned}$$

$$\begin{aligned} T_r &= 0,67\phi_w A_m f_u \\ &= 2\times0,67(0,67)(6\times10^{-3})(0,71)(0,146)(450\times10^6) \\ &= 83,76\ kN \end{aligned}$$

$T_r = 83,76\ kN$

SANS 10162-1:2005

(13.13.2.2)

$$\begin{aligned} V_r &= 0,67\phi_w A_w x_u \\ &= 0,67(0,67)(0,71)(6 \times 10^{-3})(251 \times 10^{-3})(480 \times 10^6) \\ &= 230,396\ kN \end{aligned}$$

$$\begin{aligned} V_r &= 0,67\phi_w A_m f_u \\ &= 0,67(0,67)(4 \times 10^{-3})(251 \times 10^{-3})(450 \times 10^6) \\ &= 202,813\ kN \end{aligned}$$

$V_r = 202,813\ kN$

A.10.2 HAUNCH (BEAM-COLUMN CONNECTION)

Refer to detail drawing 001-003 in appendix B for layout, dimensions and details.

Load Combination 3:

$$T'_u = \frac{M_u}{h_e} + \frac{P_H}{2} = \frac{96,98 \times 10^3}{333 \times 10^{-3}} + \frac{55,2 \times 10^3}{2} = 318,831\ kN$$

Load Combination 1:

$$T'_u = \frac{M_u}{h_e} - \frac{P_H}{2} = \frac{33,50 \times 10^3}{359 \times 10^{-3}} - \frac{12,28 \times 10^3}{2} = 87,175\ kN$$

Bottom Bolts:

SANS 10162-1:2005 (13.12.1.3)

4 M16 Grade 8.8 Bolts

$$\begin{aligned} T_r &= 0,75\phi_b A_b f_u \\ &= 4(0,75)(0,8)\left(\frac{\pi}{4}\right)(16 \times 10^{-3})^2(830 \times 10^6) \\ &= 400,515\ kN \end{aligned}$$

$T_r = 400,515\ kN$

SANS 10162-1:2005 (13.12.1.2)

$$\begin{aligned} V_r &= 0,60\phi_b n m A_b f_u \\ &= 0,6(0,8)(4)(1)\left(\frac{\pi}{4}\right)(16 \times 10^{-3})^2(830 \times 10^6) \\ &= 320,412\ kN \\ 0,7V_r &= 224,288\ kN \end{aligned}$$

$V_r = 224,288\ kN$

SANS 10162-1:2005 (13.12.1.4)

$$\frac{V_u}{V_r} + \frac{T_u}{T_r} = \frac{43,66 \times 10^3}{224,288 \times 10^3} + \frac{318,831 \times 10^3}{400 \times 10^3} = 0,991 < 1,4$$

Top Bolts:

SANS 10162-1:2005 (13.12.1.3)

2 M16 Grade 8.8 Bolts

$$\begin{aligned} T_r &= 0,75\phi_b A_b f_u \\ &= 0,75(0,8)(4)(1)\left(\frac{\pi}{4}\right)(16 \times 10^{-3})^2(830 \times 10^6)(2) \\ &= 200,258\ kN \end{aligned}$$

$T_r = 200,258\ kN$

SANS 10162-1:2005
(13.12.1.2)

$$V_r = 112,144\ kN$$

$V_r = 112,144\ kN$

SANS 10162-1:2005
(13.12.1.4)

$$\frac{V_u}{V_r} + \frac{T_u}{T_r} = \frac{43,66 \times 10^3}{112,144 \times 10^3} + \frac{87,175 \times 10^3}{200,258 \times 10^3} = 0,824 < 1,4$$

Endplate:

SAISC 1992 (7.37)

$$m = \frac{g - t_w - 2e}{2} = \frac{54 \times 10^{-3} - 5,6 \times 10^{-3} - 2(6 \times 10^3)}{2}$$
$$= 18,2 \times 10^{-3}$$

$$l_1 = p_b + 3,5m = 54 \times 10^{-3} + 3,5(18,2 \times 10^{-3})$$
$$= 117,7 \times 10^{-3} < 7m$$

$$t_p = \sqrt{\frac{1,5T'_u m}{\phi l_1 f_y}}$$
$$= \left(\frac{1,5(318,831 \times 10^3)(18,2 \times 10^{-3})}{0,9(117,7 \times 10^{-3})(355 \times 10^6)}\right)^{1/2}$$
$$= 15,214 \times 10^{-3} m$$
$$\therefore 16mm\ Endplate$$

16mm Endplate

SAISC 2008 (p. 7.32) **Prying action:**

$$T_r = 96,5\ kN\ (Table\ 7.2)$$

$$P_u = T_r - \frac{1}{a+b}\left(T_r b - \frac{0,9 f_y I t^2}{4 \times 10^3}\right)$$
$$= 96,5 \times 10^3 - \frac{1}{29 \times 10^{-3} + 23 \times 10^{-3}}\left(96,5 \times 10^3 (23 \times 10^3)\right.$$
$$\left. - \frac{0,9(355 \times 10^6)(66,4 \times 10^{-3})(14 \times 10^{-3})^2}{4 \times 10^3}\right)$$
$$= 101,4 \ kN$$

$$Q = T_r - P_u$$
$$= 96,5 - 101,4 = -4,9 \ kN$$

$$M_r = \frac{0,9 f_y I t^2}{4 \times 10^3}$$
$$= \frac{0,9(355 \times 10^6)(66,4 \times 10^{-3})(14 \times 10^{-3})^2}{4 \times 10^3}$$
$$= 1358 \ kNm$$

$$M_1 = Qa = -4,9 \times 10^3 (29 \times 10^{-3}) = -141 < M_r$$

$$M_2 = T_r b - Q(a+b)$$
$$= 96,5 \times 10^3 (23 \times 10^{-3}) + 141 \times 10^3 (29 \times 10^{-3} + 23 \times 10^{-3})$$
$$= 1358 \ kNm$$

16mm Endplate

Welds:

Full penetration groove weld & 6mm fillet weld at flanges. 6mm Fillet welds at web.

$$T'_u = \frac{M}{h_e} + \frac{P_u}{2}$$
$$= \frac{96,98 \times 10^3}{392 \times 10^{-3}} + \frac{55,2 \times 10^3}{2}$$
$$= 274,998 \ kN$$

SANS 10162-1:2005

(13.13.3.3)

$$T_r = \phi_w \sqrt{(A_n f_u)^2 + (A_w x_u)^2}$$
$$= 0,67 \sqrt{(0,71(6 \times 10^3)(100 \times 10^{-3})(480 \times 10^6))^2}$$
$$\overline{+(8,5 \times 10^{-3}(100 \times 10^{-3})(480 \times 10^3))^2}$$
$$= 305,77 \ kN > A_g f_y = 301,75 \ kN$$

$T_r = 301,75 \ kN$

$$V_r = 0,67\phi_w A_w x_u$$
$$= 0,67(0,67)(0,71)(6 \times 10^{-3})(159 \times 10^{-3})(480 \times 10^{6})$$
$$= 145,948\ kN$$

$$V_r = 0,67\phi_w A_w f_u$$
$$= 0,67(0,67)(0,71)(6 \times 10^{-3})(159 \times 10^{-3})(450 \times 10^{6})$$
$$= 136,826\ kN\ > 43,66\ kN$$

$V_r = 136,826\ kN$

COLUMN:

SAISC 1992 (p.161) Column flange at beam tension flange:

$$s = 54\ mm < 6d = 96\ OK$$
$$g = 54\ mm < 5d = 80\ OK$$
$$r = \frac{b_p - g}{2} = \frac{112 - 54}{2} = 29mm$$
$$n_1 = \frac{b_c - g}{2} = \frac{146,1 - 54}{2} = 46,05mm$$
$$q = \frac{g - t_{wc} - 2r_c}{2} = \frac{54 - 6 - 2(7,6)}{2} = 16,4mm$$

$$T_r = \phi t_{fc}^2 f_{yc}\left(\frac{3,14(q + n_1) + 0,5s}{q + n}\right) + 4\phi P_b\left(\frac{n}{q + n}\right)$$
$$= (0,9)(8,6 \times 10^{-3})^2(355 \times 10^{6})$$
$$\left(\frac{3,14(16,4 \times 10^{-3} + 46,05 \times 10^{-3}) + 0,5(54 \times 10^{-3})}{16,4 \times 10^{-3} + 29 \times 10^{-3}}\right)$$
$$+ 4(0,9)(96,5 \times 10^{-3})\left(\frac{29 \times 10^{-3}}{16,4 \times 10^{-3} + 29 \times 10^{-3}}\right)$$
$$= 116,118 \times 10^{-3} + 221,907 \times 10^{-3} = 338,025\ kN > 274,998\ kN$$

$\therefore$ *Stiffeners required.*

$$T_r = \phi t_{fc}^2 f_{yc} \left(3,14 + \frac{2(2n_1 + s - d_n}{q}\right)$$
$$= (0,9)(8,6 \times 10^{-3})^2(355 \times 10^6) \left(3,14 + \frac{2(46,05 \times 10^{-3}) + 54 \times 10^{-3} - 18 \times 10^{-3}}{16,4 \times 10^{-3}}\right)$$
$$= 258,774\ kN < 274,998\ kN$$

$\therefore$ *Stiffeners required.*

Column web at beam tension flange.

$$T_r = \phi(t_{fb} + 5k_c + 2t_p + 2e)t_{wc}f_{yc}$$
$$= 0,9(8,5 \times 10^{-3} + 5(16,2 \times 10^{-3}) + 2(14 \times 10^{-3}) + 2(6 \times 10^{-3}))(6 \times 10^{-3})(355 \times 10^6)$$
$$= 248,252\ kN < 274,998\ kN$$

$\therefore$ *Stiffeners required.*

Beam compression flange:

$$B_r = \phi(2t_p + 5t_{fc} + 2t_{wc})t_{fb}f_{yb}$$
$$= 0,9(2(14 \times 10^{-3}) + 5(8,6 \times 10^{-3}) + 2(6 \times 10^{-3}))8,5 \times 10^{-3}(355 \times 10^6)$$
$$= 225,408\ kN < 274,998\ kN$$

$\therefore$ *Stiffenersrequired.*

Column web compression yielding:

$$B_r = 248,252\ kN < 274,998\ kN$$

Column web buckling:

$$B_r = \phi 640000 \frac{(t_{fb} + 5k_c + 2t_p)t_{wc}}{(h_{wc}/t_{wc})^2}$$
$$= (0,9)640000 \frac{(8,5 \times 10^{-3} + 5(16,2 \times 10^{-3}) + 2(14 \times 10^{-3}))6 \times 10^{-3}}{(219 \times 10^{-3}/6 \times 10^{-3})^2}$$
$$= 304,807\ kN > 242,486\ kN$$

Column web shear.

$$V_r = 0,66\phi A_v f_y$$
$$= 0,66(0,9)(219 \times 10^{-3})(6 \times 10^{-3})(355 \times 10^6)$$
$$= 277,083\ kN < 43,66\ kN\ OK$$

SAISC 2008 (p. 7.32)

Prying action:

$$T_r = 96,5\ kN\ (Table\ 7.2)$$

$$P_u = T_r - \frac{1}{a+b}\left(T_r b - \frac{0,9 f_y l t^2}{4 \times 10^3}\right)$$
$$= 96,5 \times 10^3 - \frac{1}{46,05 + 24,26}\left(96,5(24,26) - \frac{0,9(355)(173,85)(8,6)^2}{4 \times 10^3}\right)$$
$$= 77,8\ kN$$

$$Q = T_r - P_u$$
$$= 96,5 - 77,6 = 18,7\ kN$$

$$M_r = \frac{0,9 f_y l t^2}{4 \times 10^3}$$
$$= \frac{0,9(355 \times 10^6)(173,85 \times 10^{-3})(8,6 \times 10^{-3})^2}{4 \times 10^3}$$
$$= 1027\ Nm$$

$$M_1 = Qa = 18,7 \times 10^3(46,05 \times 10^{-3}) = 861\ Nm < M_r$$

$$M_2 = T_r b - Q(a+b)$$
$$= 96,5 \times 10^3(24,26 \times 10^{-3}) - 18,7 \times 10^3(46,05 \times 10^{-3} + 24,26 \times 10^3)$$
$$= 1027\ kNm$$

Stiffeners:

SAISC 1992 (p. 143)

Stiffener force = -225,408 + 274,998 = 49,59 kN
Use two 70x8mm stiffeners (234mm high)

$$\begin{aligned} B_r &= 2\phi A_{st} f_{yst} \\ &= 2(0,9)(60 \times 10^{-3})(8 \times 10^{-3})(355 \times 10^{6}) \\ &= 306,72\ kN \end{aligned}$$

$$\frac{b}{t} = \frac{70}{8} = 8,75 < \frac{200}{\sqrt{f_y}}$$

$\therefore$ Stiffeners provide sufficient support for prying of the column flange.
Weld to flange: (5mm Fillet Weld)

$$\begin{aligned} T_r &= 0,67\phi_w A_m f_u \\ &= 0,67(0,67)(0,71)(5 \times 10^{-3})(60 \times 10^{-3})(450 \times 10^{6}) \\ &= 43,027\ kN > 20,253\ kN \end{aligned}$$

Weld to web:

$$\begin{aligned} V_r &= 0,67(0,67)(0,71)(5 \times 10^{-3})(214 \times 10^{-3})(450 \times 10^{-3}) \\ &= 153,463\ kN \end{aligned}$$

Base metal < weld metal.
Endplate: (14mm)

$$\frac{b}{t} = \frac{146,1}{14} = 10,44 < \frac{200}{\sqrt{f_y}}$$

A.10.3 APEX CONNECTION

Refer to detail drawing 001-004 in appendix B for layout, dimensions and details.

Load Combination 3:

$$T'_u = \frac{M_u}{h_e} + \frac{P_H}{2} = \frac{26,61 \times 10^3}{188,45 \times 10^{-3}} + \frac{55,2 \times 10^3}{2} = 168,805\ kN$$

Load Combination 1:

$$T'_u = \frac{M_u}{h_e} - \frac{P_H}{2} = \frac{11,79 \times 10^3}{188,45 \times 10^{-3}} - \frac{9,802 \times 10^3}{2} = 57,662\ kN$$

Top Bolts:

SANS 10162-1:2005 (13.12.1.3)

4 M16 Grade 4.8 Bolts

$$\begin{aligned} T_r &= 0,75\phi_b A_b f_u \\ &= 4 \times 0,75(0,8)(4)(1)\left(\frac{\pi}{4}\right)(16 \times 10^{-3})^2(420 \times 10^6) \\ &= 202,670\ kN \end{aligned}$$

$T_r = 202,670\ kN$

SANS 10162-1:2005 (13.12.1.2)

$$\begin{aligned} V_r &= 0,6\phi_b nmA_b f_U \\ &= 0,6(0,8)(4)(1)\left(\frac{\pi}{4}\right)(16 \times 10^{-3})^2(420 \times 10^6) \\ &= 162,136\ kN \end{aligned}$$

$V_r = 162,136\ kN$

SANS 10162-1:2005 (13.12.1.4)

$$\frac{V_u}{V_r} + \frac{T_u}{T_r} = \frac{2,176}{162,136} + \frac{168,804}{202,670} = 0,846 < 1,4$$

Bottom Bolts:

SANS 10162-1:2005 (13.12.1.3)

2 M16 Grade 4.8 Bolts

$$\begin{aligned} T_r &= 0,75\phi_b A_b f_u \\ &= 2 \times (0,75)(0,8)\left(\frac{\pi}{4}\right)(16 \times 10^{-3})^2(420 \times 10^6) \\ &= 101,335\ kN \end{aligned}$$

$T_r = 101,335\ kN$

SANS 10162-1:2005

(13.12.1.2)

$$\begin{aligned} V_r &= 0,60\phi_b n m A_b f_u \\ &= 0,6(0,8)(2)(1)\left(\frac{\pi}{4}\right)(16\times10^{-3})^2(420\times10^6) \\ &= 81,068\ kN \\ 0,7V_r &= 56,748\ kN \end{aligned}$$

$V_r = 56,748\ kN$

SANS 10162-1:2005

(13.12.1.4)

$$\frac{V_u}{V_r}+\frac{T_u}{T_r}=\frac{2,176}{56,748}+\frac{57,662}{101,3365}=0,596<1,4$$

Endplate:

SAISC 1992 (p. 166)

$$\begin{aligned} p_f &= 47\ mm \\ g &= 62\ mm \\ b_p &= 112mm \end{aligned}$$

$$\begin{aligned} p_e &= \frac{\sqrt{(g^2+p_f^2)}}{127}p_f \\ &= \frac{\sqrt{(62^2+47^2)}}{127}47 \\ &= 28,793mm \end{aligned}$$

$$\begin{aligned} M_e &= T_b p_e \\ &= 28,280\times10^3(28,793\times10^{-3}) \\ &= 814,252\ kN \end{aligned}$$

$$\begin{aligned} t_p &= \sqrt{\frac{6M_e}{\phi b_p f_y}} \\ &= \sqrt{\frac{6(814,252)}{(0,9)(112\times10^{-3})(355\times10^6)}} \\ &= 11,685\times10^{-3}\ m = 11,685\ mm \end{aligned}$$

$\therefore 12mm\ Endplate\ required.$

12mm Endplate

SAISC 2008 (p. 7.32)

Prying action:

$$T_r = 50,70\ kN\ (Table\ 7.2)$$

$$\begin{aligned} P_u &= T_r - \frac{1}{a+b}\left(T_r b - \frac{0,9 f_y l t^2}{4 \times 10^3}\right) \\ &= 50,7 \times 10^3 - \frac{1}{60,9 \times 10^{-3}}((50,7 \times 10^3 (26,75 \times 10^{-3}) \\ &\quad - \frac{0,9(355 \times 10^6)(50 \times 10^{-3})(12 \times 10^{-3})^2}{4 \times 10^3}) \\ &= 37,9\ kN \end{aligned}$$

$$\begin{aligned} Q &= T_r - P_u \\ &= 12,8\ kN \end{aligned}$$

$$\begin{aligned} M_r &= \frac{0,9 f_y l t^2}{4 \times 10^3} \\ &= \frac{0,9(355 \times 10^6)(50 \times 10^{-3})(14 \times 10^{-3})^2}{4 \times 10^3} \\ &= 575\ Nm \end{aligned}$$

$$M_1 = Qa = 12,8 \times 10^3 (34,55 \times 10^{-3}) = 438 < M_r$$

$$\begin{aligned} M_2 &= T_r b - Q(a+b) \\ &= 50,7 \times 10^3 (26,37 \times 10^{-3}) - 11,1 \times 10^3 (60,92 \times 10^{-3}) \\ &= 575\ kNm \end{aligned}$$

$\therefore$ 12mm Endplate OK.

12mm Endplate

Welds:

Full penetration groove weld & 6mm Fillet welds at web.

$$\begin{aligned} T'_u &= \frac{M}{h_e} + \frac{P_u}{2} \\ &= \frac{26,62 \times 10^3}{194,45 \times 10^{-3}} + \frac{55,2 \times 10^3}{2} \\ &= 164,448\ kN \end{aligned}$$

SANS 10162-1:2005

(13.13.3.3)

$$\begin{aligned} T_r &= \phi_w A_n f_u \\ &= 0,67(8,5 \times 10^{-3})(100 \times 10^{-3})(480 \times 10^{6}) \\ &= 273,36\ kN \end{aligned}$$

$T_r = 273,36\ kN$

$$\begin{aligned} V_r &= 0,67\phi_w A_w x_u \\ &= 0,67(0,67)(0,71)(6 \times 10^{3-})(159 \times 10^{-3})(480 \times 10^{6}) \\ &= 145,948\ kN \end{aligned}$$

$V_r = 145,948\ kN$

Appendix B

REFERENCE PORTAL FRAME DRAWINGS

The following drawings are included in this appendix:

- 001-001: Reference Portal Frame Layout
- 001-002: Column Base Detail
- 001-003: Haunch Connection Detail
- 001-004: Apex Connection Detail

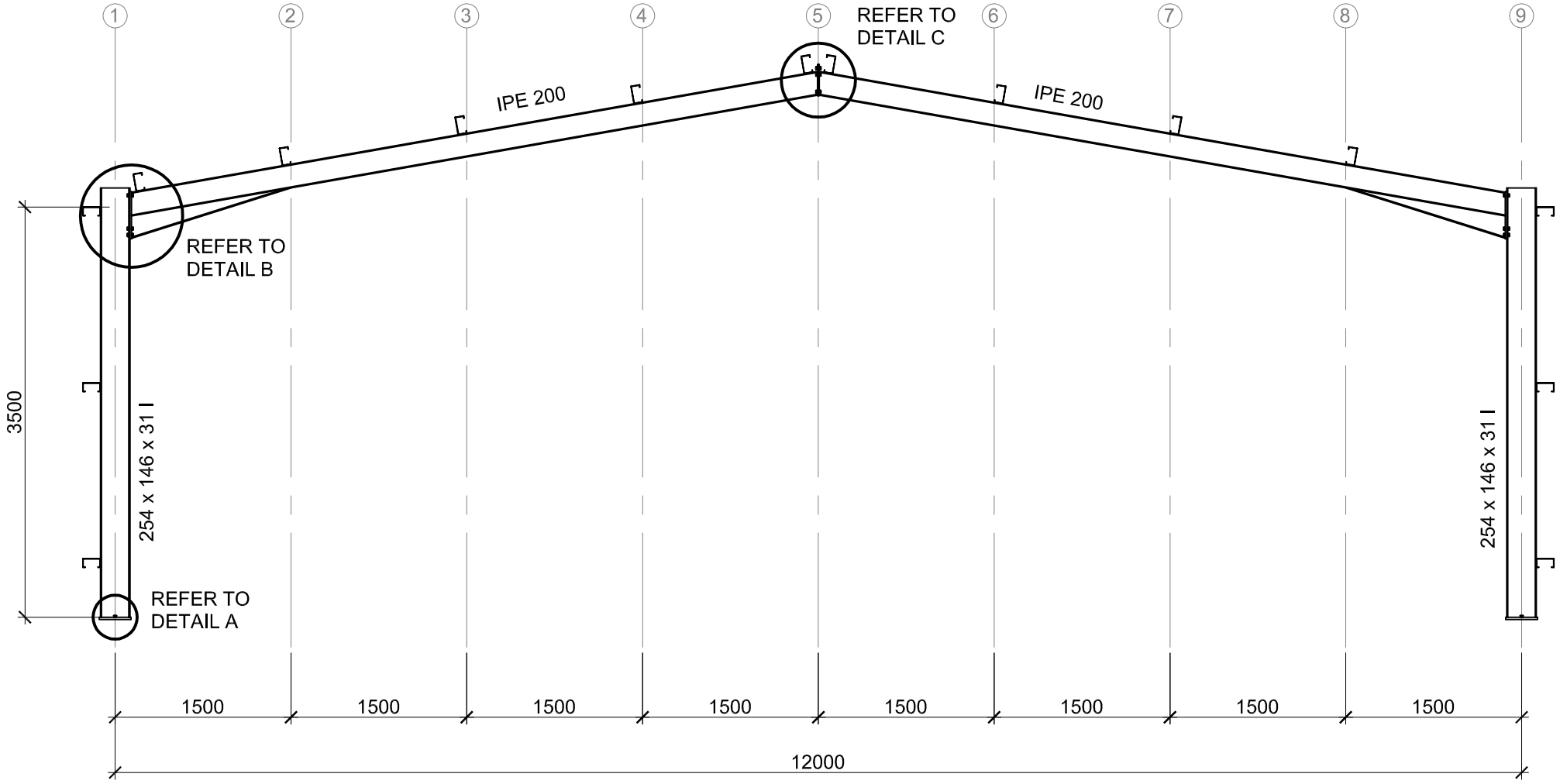

UNIVERSITY OF STELLENBOSCH			SCALE 1:50 MEASURED IN mm	TITLE PORTAL FRAME LAYOUT	
STUDENT No. 14527774	DRAWN BY HL ALBERTYN		DATE 14/01/2011	SHEET 1 OF 1	No. 001-001

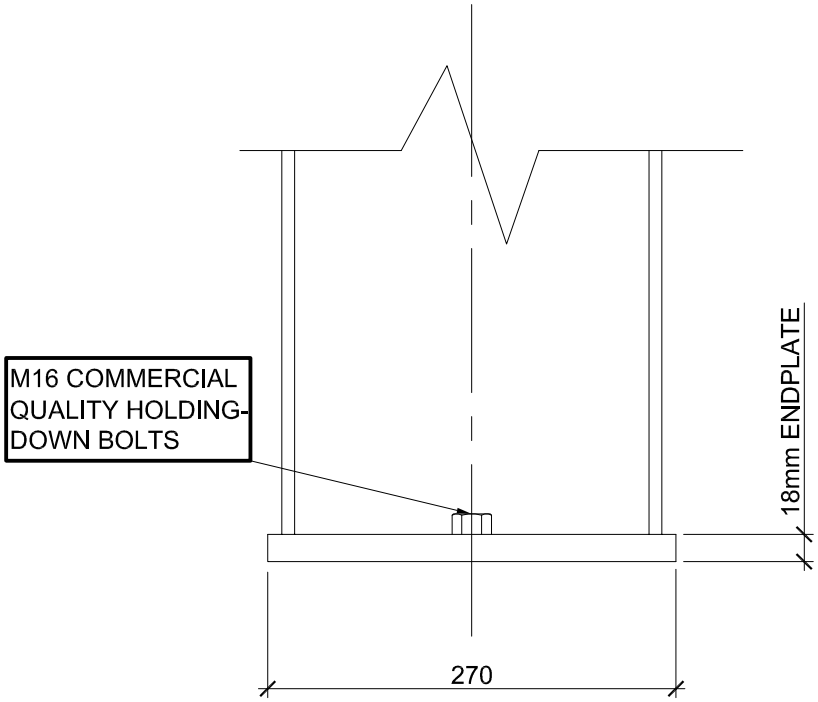

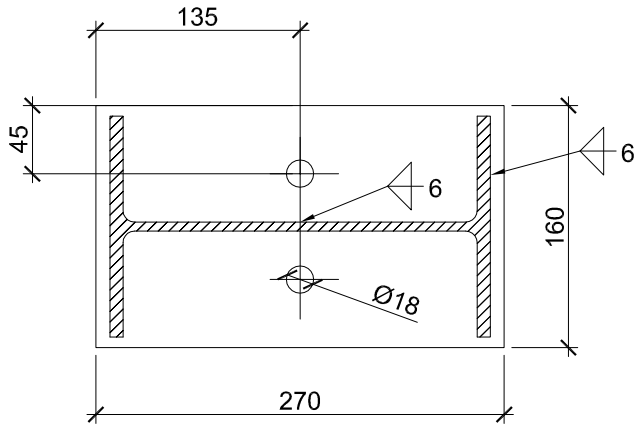

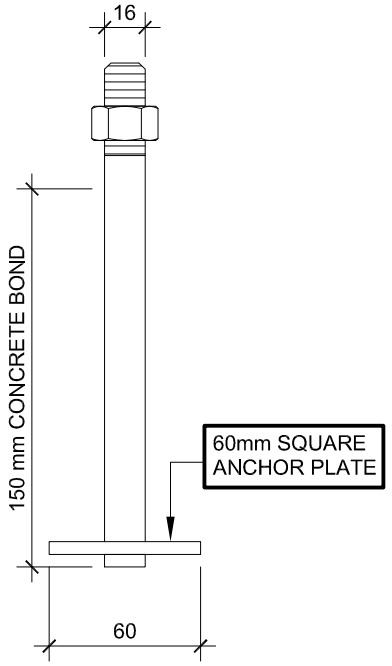

DETAIL A
COLUMN BASE DETAIL

HOLDING DOWN BOLT DETAIL
SCALE 1:2

NOTE:
ALL WELDS E70XX
HOLES TO BE DRILLED
STEEL GRADE 355W

UNIVERSITY OF STELLENBOSCH			SCALE 1:5 MEASURED IN mm	TITLE COLUMN BASE DETAIL	
STUDENT No. 14527774	DRAWN BY HL ALBERTYN		DATE 14/01/2011	SHEET 1 OF 1	No. 001-002

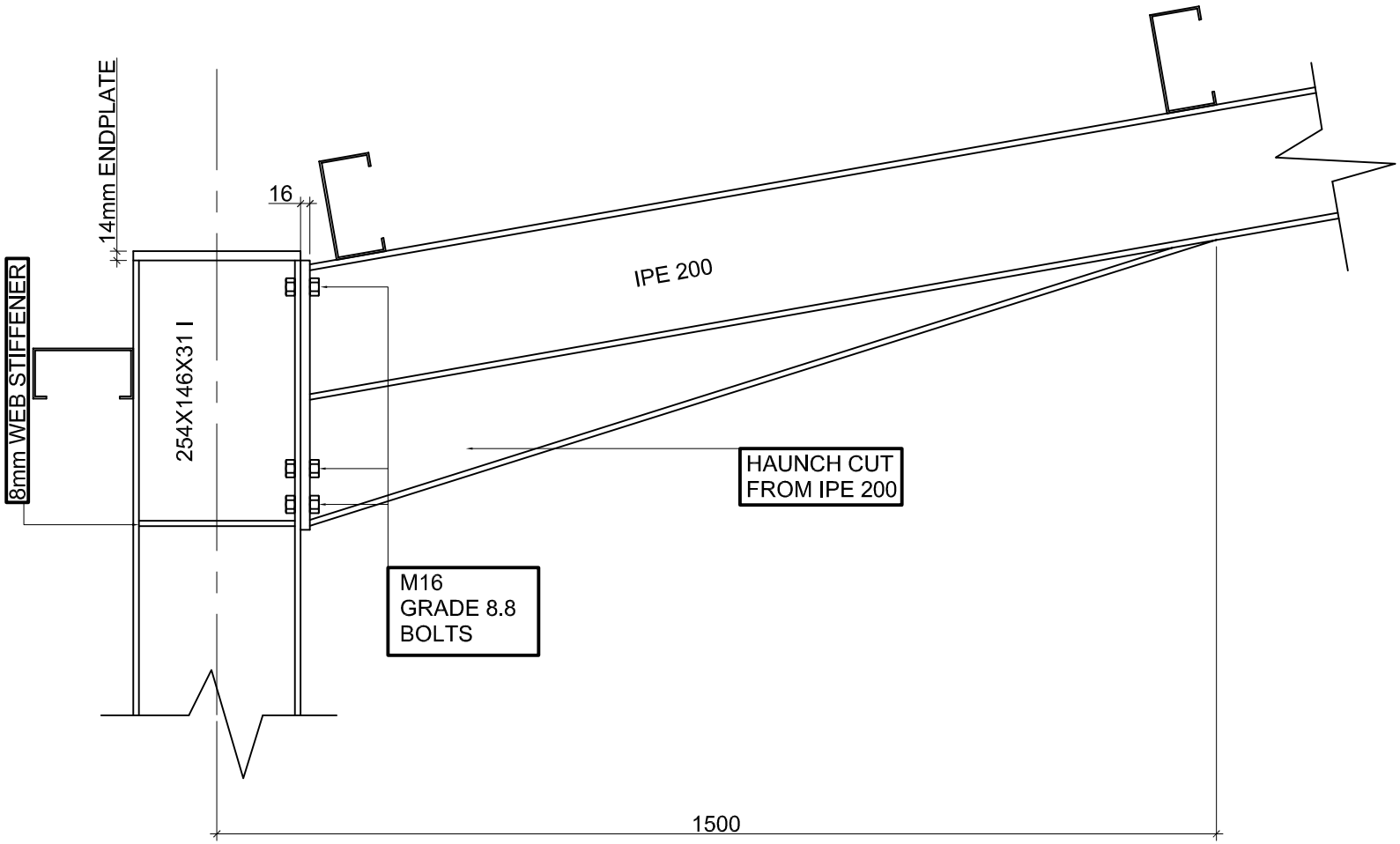

DETAIL B
BEAM TO COLUMN HAUNCH

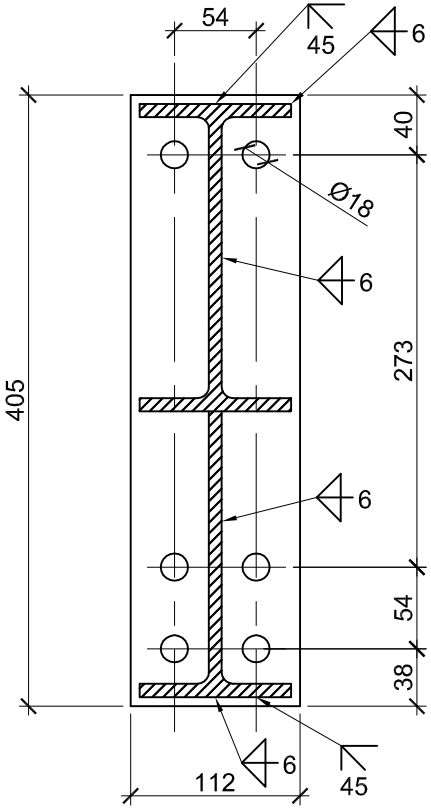

16mm ENDPLATE
SCALE 1:5

NOTE:
ALL WELDS E70XX
HOLES TO BE DRILLED
STEEL GRADE 355W

UNIVERSITY OF STELLENBOSCH		SCALE 1:10 MEASURED IN mm	TITLE HAUNCH CONNECTION DETAIL	
STUDENT No. 14527774	DRAWN BY HL ALBERTYN	DATE 14/01/2011	SHEET 1 OF 1	No. 001-003

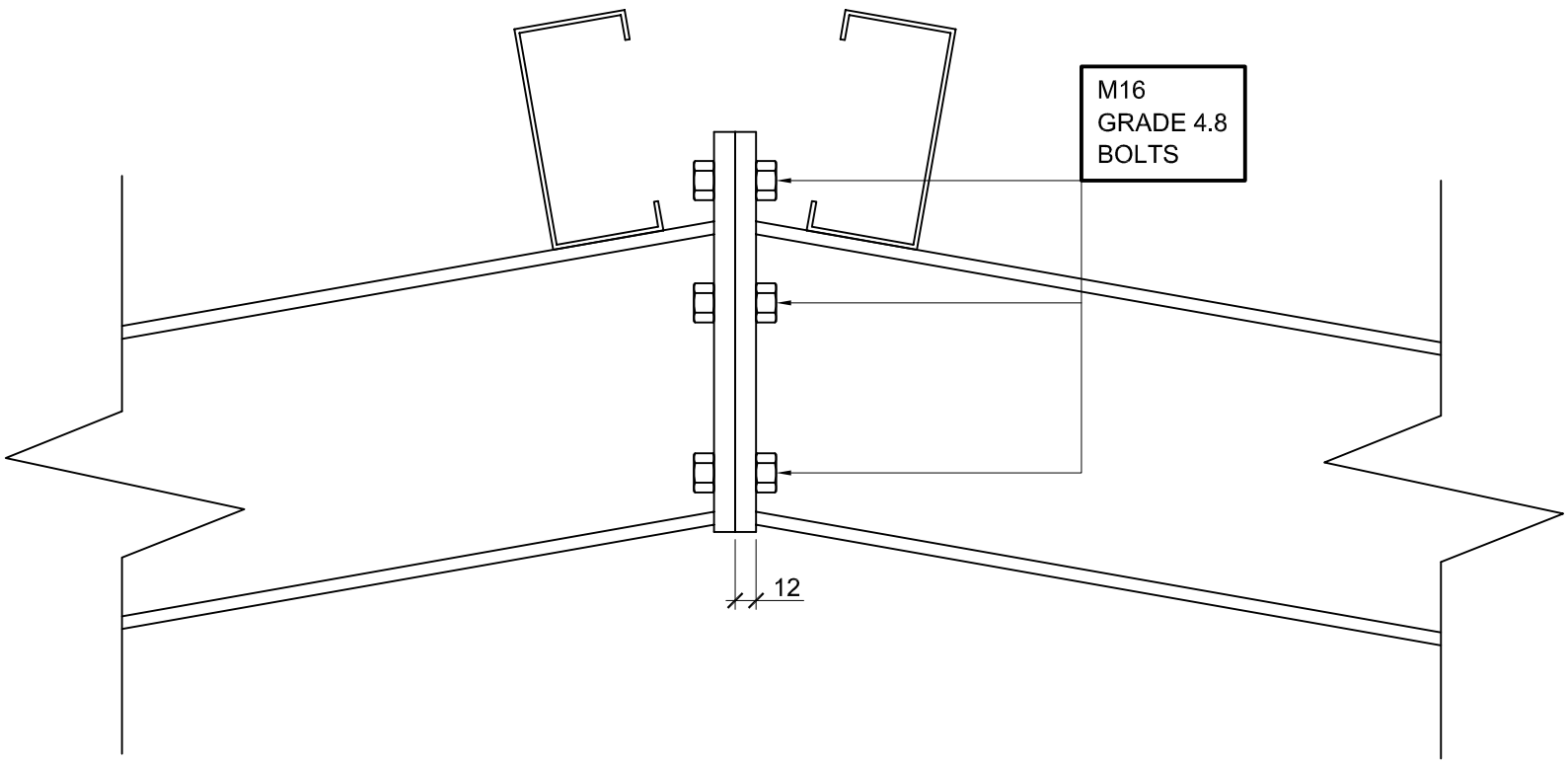

DETAIL C
APEX CONNECTION

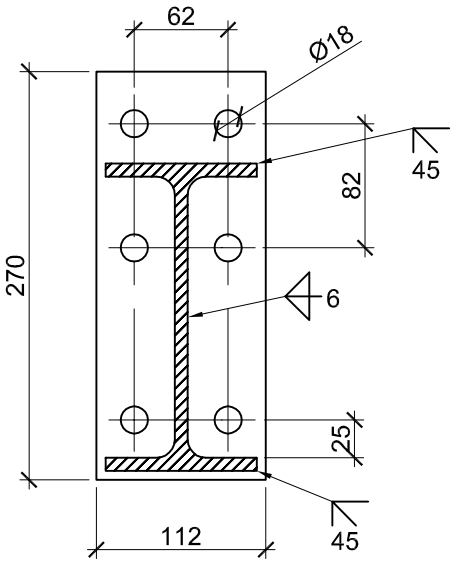

12mm
ENDPLATE

NOTE:
ALL WELDS E70XX
HOLES TO BE DRILLED
STEEL GRADE 355W

UNIVERSITY OF STELLENBOSCH			SCALE 1:5 MEASURED IN mm	TITLE APEX CONNECTION DETAIL	
STUDENT No. 14527774	DRAWN BY HL ALBERTYN		DATE 14/01/2011	SHEET 1 OF 1	No. 001-004

Appendix C

EXPERIMENTAL PORTAL FRAME DRAWINGS

The following drawings are included in this appendix:

- 002-001: Test Specimen Portal Frame Layout
- 002-002: Haunch Connection Detail
- 002-003: Apex Connection Detail
- 002-004: Column Base Detail

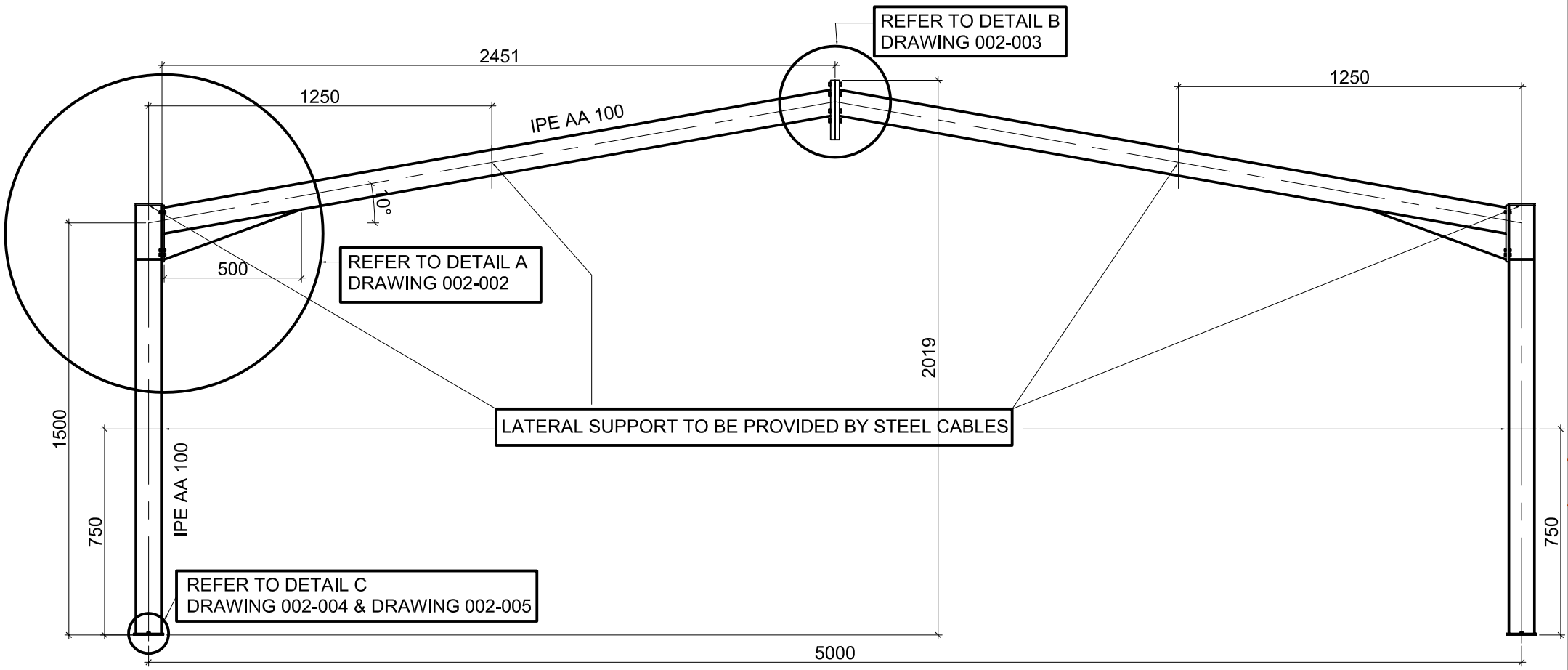

NOTES:
STEEL GRADE 355W
ALL WELDS E70xx
ALL HOLES TO BE DRILLED
DO NOT SCALE FROM DRAWING

UNIVERSITY OF STELLENBOSCH			SCALE 1:20 MEASURED IN mm	TITLE EXPERIMENTAL PORTAL FRAME	
STUDENT No. 14527774	DRAWN BY HL ALBERTYN		DATE 23/01/2011	SHEET 1 OF 1	No. 002-001

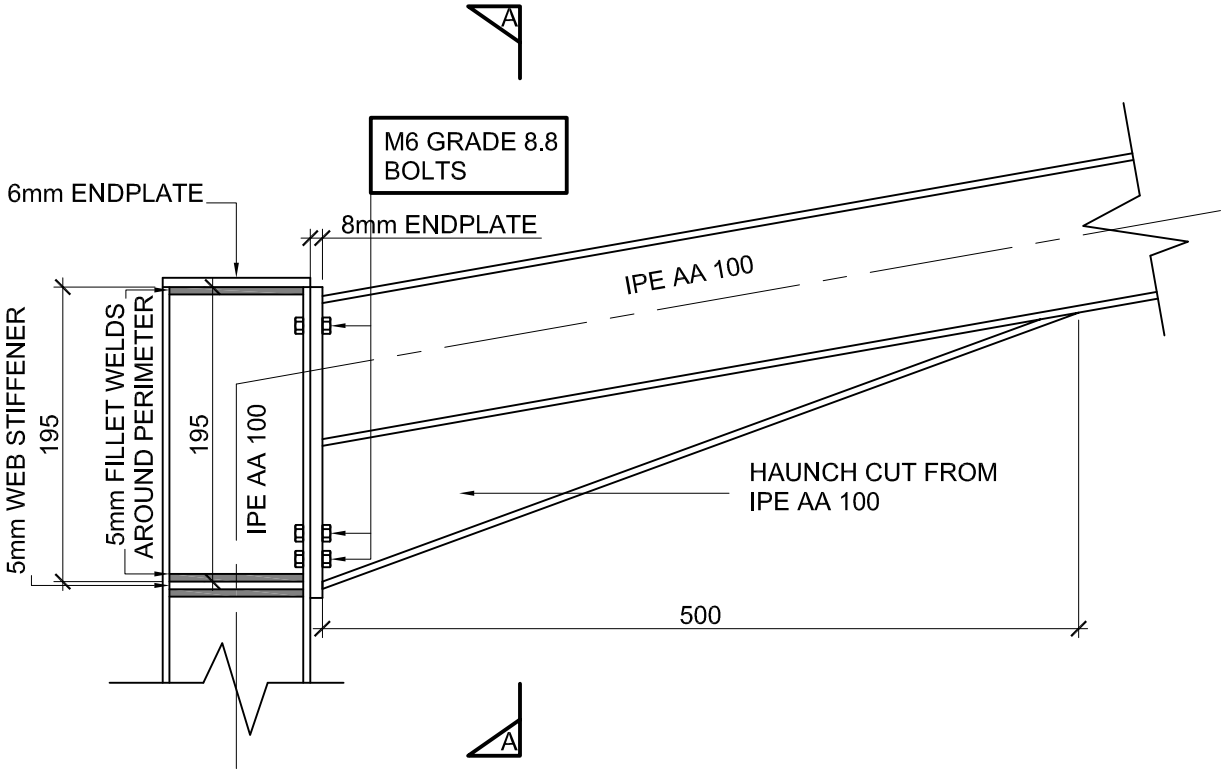

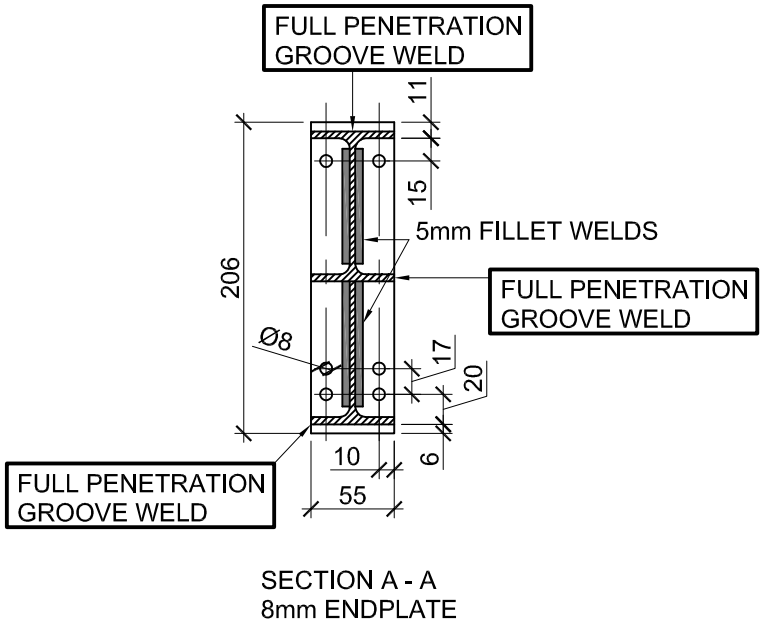

SECTION A - A
8mm ENDPLATE

THIS DRAWING IS TO BE READ IN CONJUNCTION WITH DWG 002-007

NOTES:
STEEL GRADE 355W
ALL WELDS E70xx
ALL HOLES TO BE DRILLED
DO NOT SCALE FROM DRAWING

UNIVERSITY OF STELLENBOSCH			SCALE 1:5 MEASURED IN mm	TITLE DETAIL A: HAUNCH CONNECTION	
STUDENT No. 14527774	DRAWN BY HL ALBERTYN		DATE 23/01/2011	SHEET 1 OF 1	No. 002-002

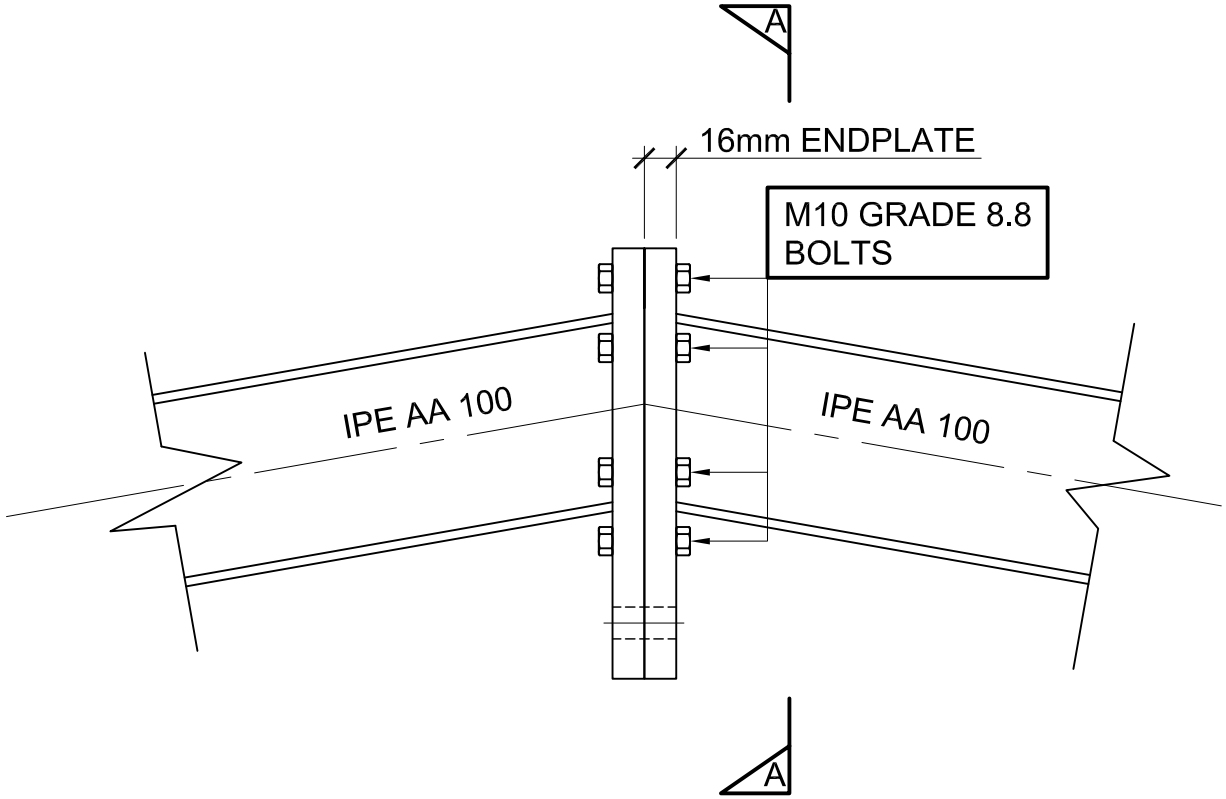

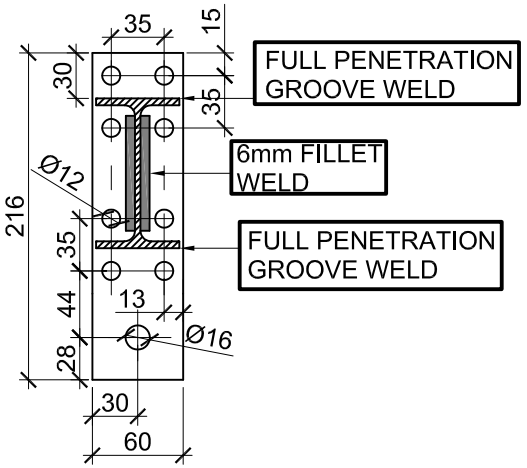

SECTION A - A
16mm ENDPLATE

NOTES:
STEEL GRADE 355W
ALL WELDS E70xx
ALL HOLES TO BE DRILLED
DO NOT SCALE FROM DRAWING

UNIVERSITY OF STELLENBOSCH			SCALE 1:5 MEASURED IN mm	TITLE DETAIL B: APEX CONNECTION	
STUDENT No. 14527774	DRAWN BY HL ALBERTYN		DATE 23/01/2011	SHEET 1 OF 1	No. 002-003

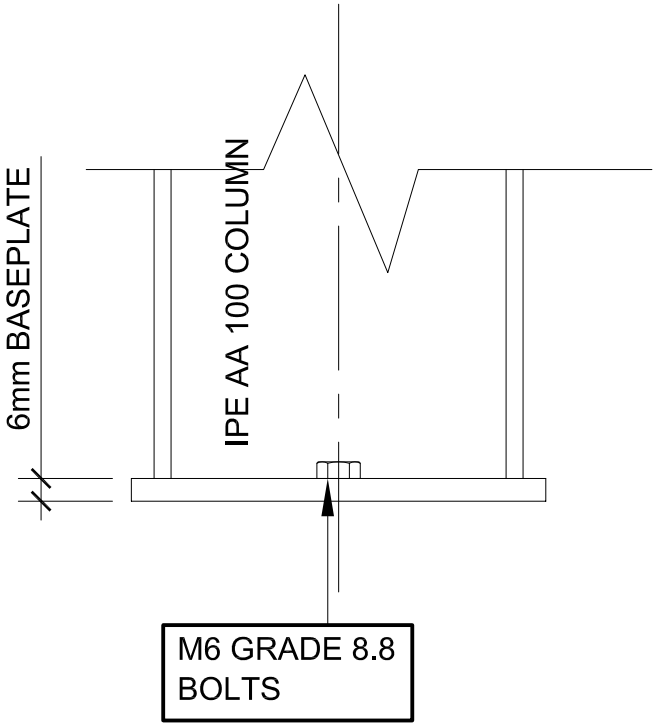

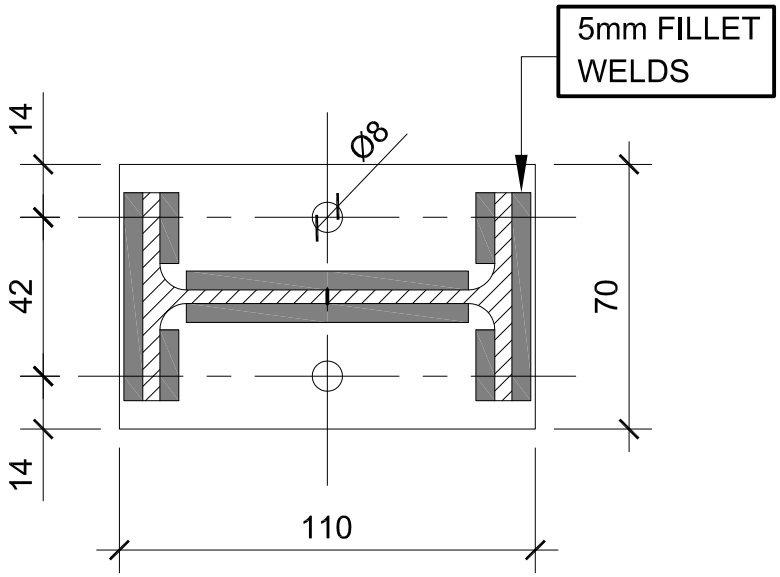

6mm BASEPLATE

NOTES:
STEEL GRADE 355W
ALL WELDS E70xx
ALL HOLES TO BE DRILLED
DO NOT SCALE FROM DRAWING

UNIVERSITY OF STELLENBOSCH			SCALE 1:2 MEASURED IN mm	TITLE DETAIL C: COLUMN BASE	
STUDENT No. 14527774	DRAWN BY HL ALBERTYN		DATE 23/01/2011	SHEET 1 OF 1	No. 002-004

Appendix D

EXPERIMENTAL SETUP DRAWINGS

The following drawings are included in this appendix:

- 002-005: Column Base Hinge Support Detail
- 002-006: Column Base Grout Support Detail
- 002-007: Haunch Horizontal Load Application Hinge Detail
- 002-008: Ridge Load Application Fork
- 002-009: Center Hydraulic Actuator Support Frame for Tension and Compression Load Application
- 002-010: Actuator Support Bracket for Support Frame
- 002-011: Center Hydraulic Actuator Support Frame Layouts for Tension and Compression Load Application

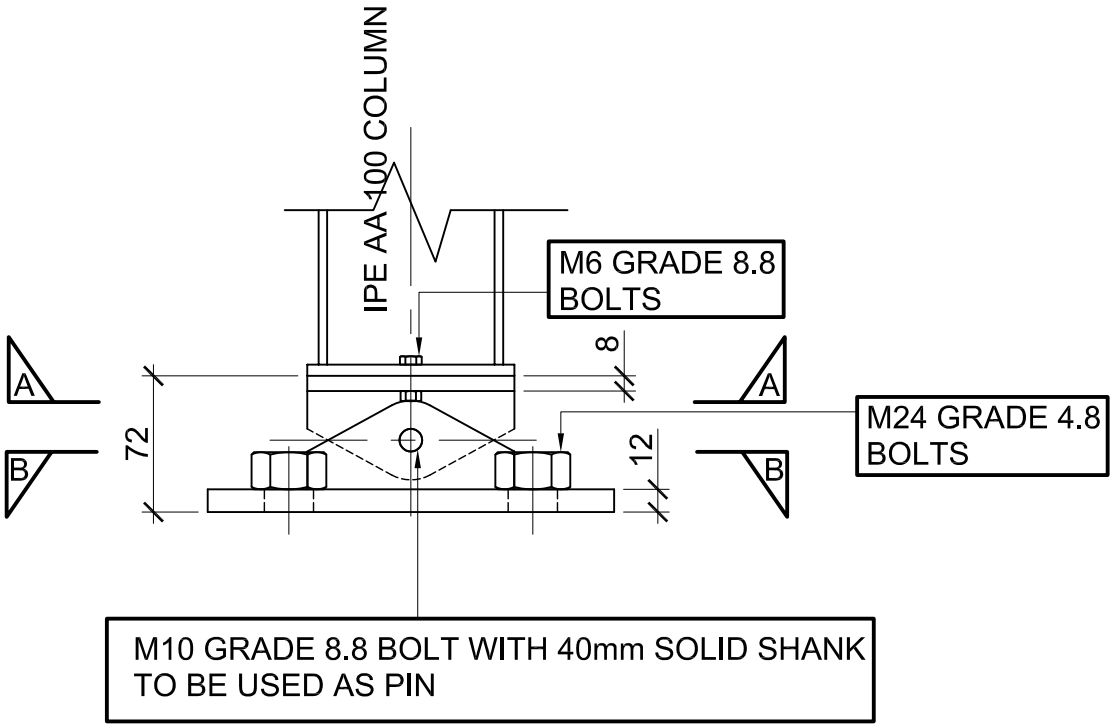

HINGE SUPPORT LAYOUT

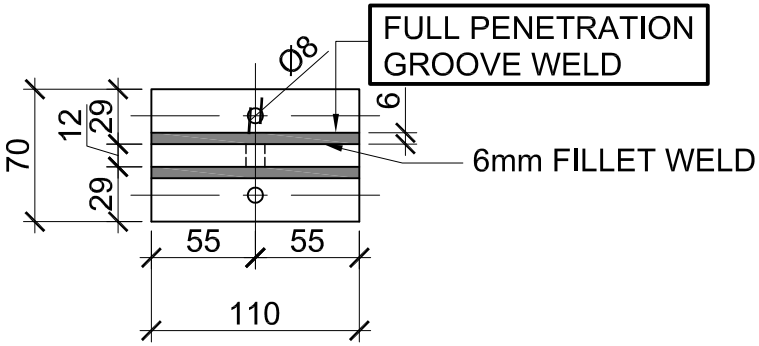

SECTION A - A
8mm TOP ENDPLATE

NOTES:
STEEL GRADE 355W
WELDS AFROX VITEMAX
ALL HOLES TO BE DRILLED
DO NOT SCALE FROM DRAWING

UNIVERSITY OF STELLENBOSCH			SCALE 1:4 MEASURED IN mm	TITLE COLUMN HINGE SUPPORT	
STUDENT No. 14527774	DRAWN BY HL ALBERTYN		DATE 23/01/2011	SHEET 1 OF 2	No. 002-005

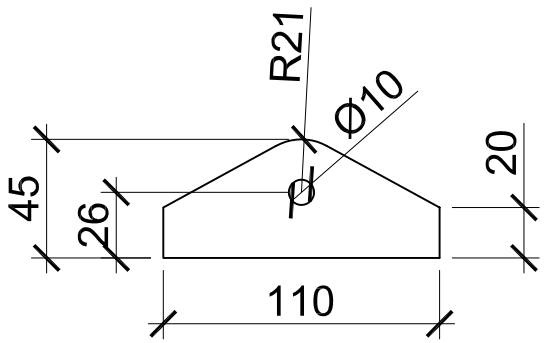

12mm UPSTAND LEG
DETAIL

6mm FILLET WELDS

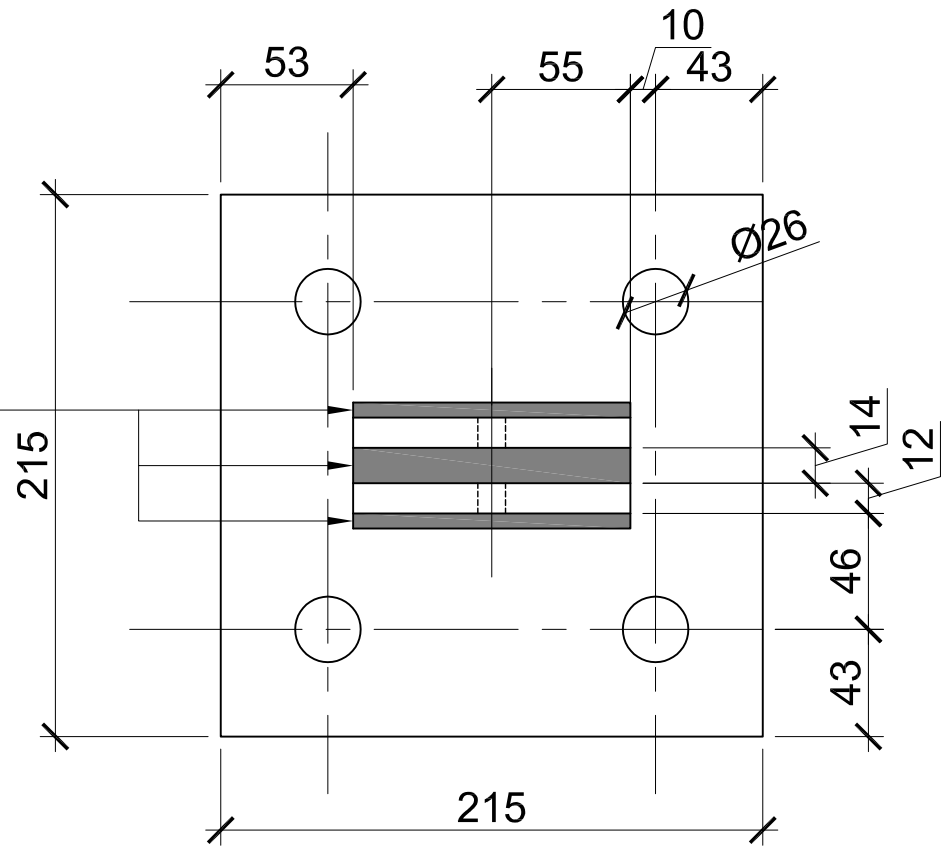

SECTION B - B
12mm BOTOTM ENDPLATE

NOTES:
STEEL GRADE 355W
WELDS AFROX VITEMAX
ALL HOLES TO BE DRILLED
DO NOT SCALE FROM DRAWING

UNIVERSITY OF STELLENBOSCH			SCALE 1:3 MEASURED IN mm	TITLE COLUMN HINGE SUPPORT	
STUDENT No. 14527774	DRAWN BY HL ALBERTYN		DATE 23/01/2011	SHEET 2 OF 2	No. 002-005

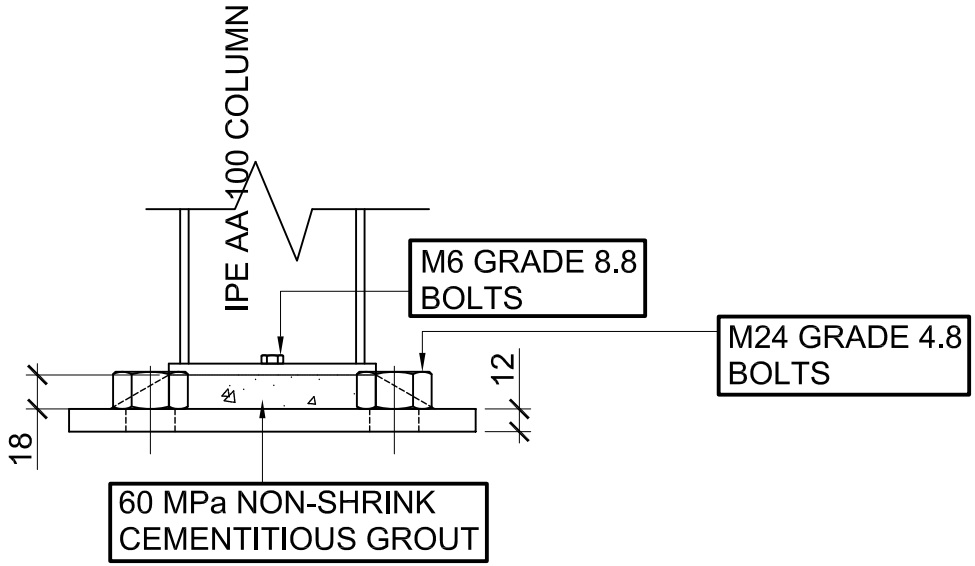

GROUT SUPPORT LAYOUT

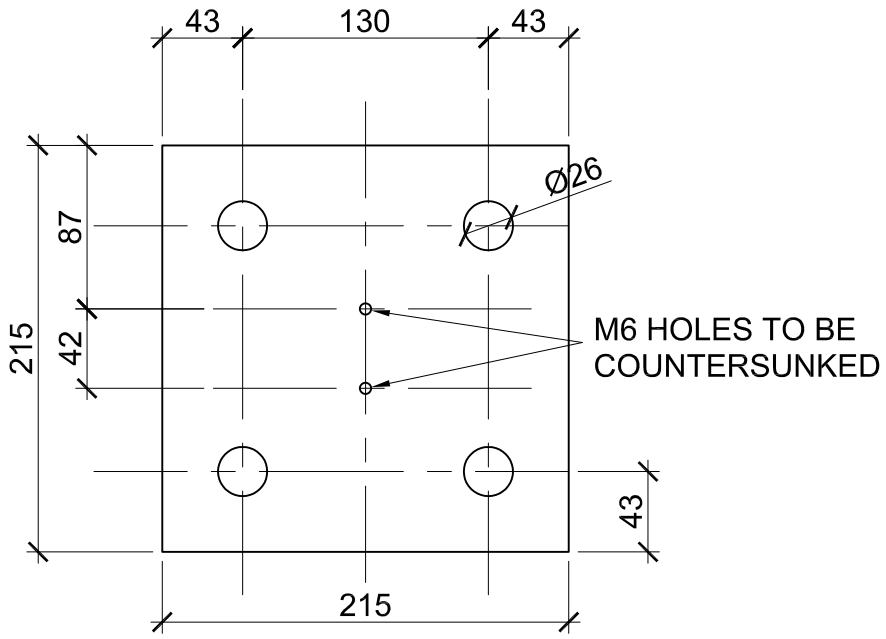

12mm ENDPLATE

NOTES:
STEEL GRADE 355W
WELDS AFROX VITEMAX
ALL HOLES TO BE DRILLED
DO NOT SCALE FROM DRAWING

UNIVERSITY OF STELLENBOSCH		SCALE 1:4 MEASURED IN mm	TITLE GROUT COLUMN SUPPORT	
STUDENT No. 14527774	DRAWN BY HL ALBERTYN	DATE 23/01/2011	SHEET 1 OF 1	No. 002-006

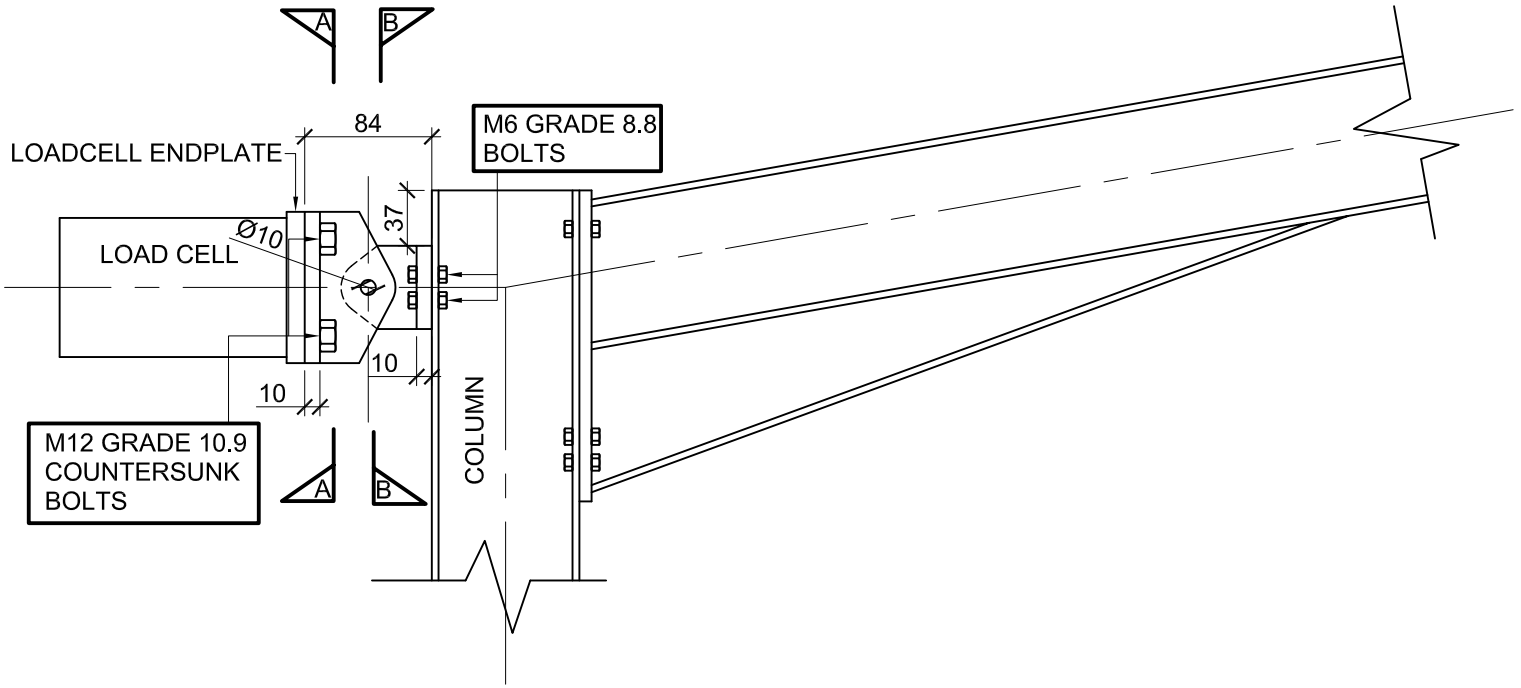

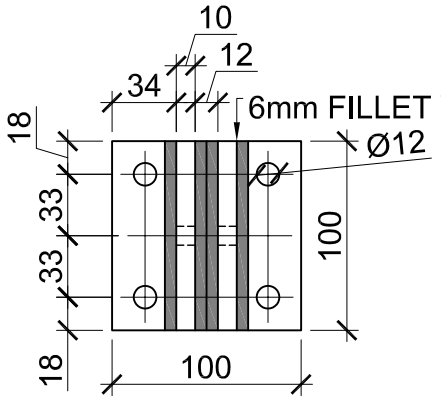

SECTION A - A
10mm ENDPLATE
SCALE 1:4

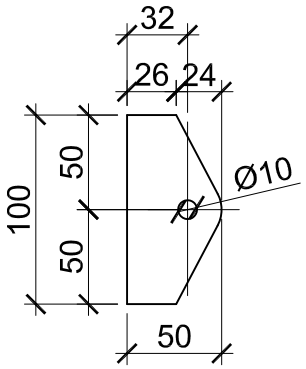

10mm THICK
OUTSTAND LEG

NOTES:
STEEL GRADE 355W
WELDS AFROX VITEMAX
ALL HOLES TO BE DRILLED
DO NOT SCALE FROM DRAWING

UNIVERSITY OF STELLENBOSCH		SCALE 1:5 MEASURED IN mm	TITLE HAUNCH APPLY HINGE	
STUDENT No. 14527774	DRAWN BY HL ALBERTYN	DATE 24/01/2011	SHEET 1 OF 2	No. 002-007

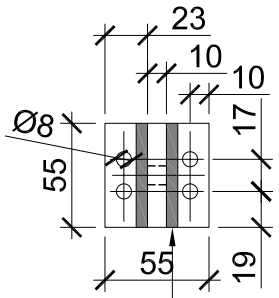

6mm FILLET
WELDS

SECTION B - B
10mm ENDPLATE
SCALE 1:4

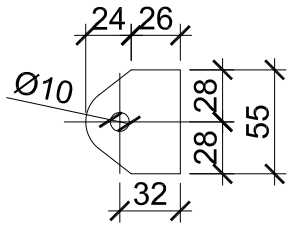

10mm THICK
OUTSTAND LEG

NOTES:
STEEL GRADE 355W
WELDS AFROX VITEMAX
ALL HOLES TO BE DRILLED
DO NOT SCALE FROM DRAWING

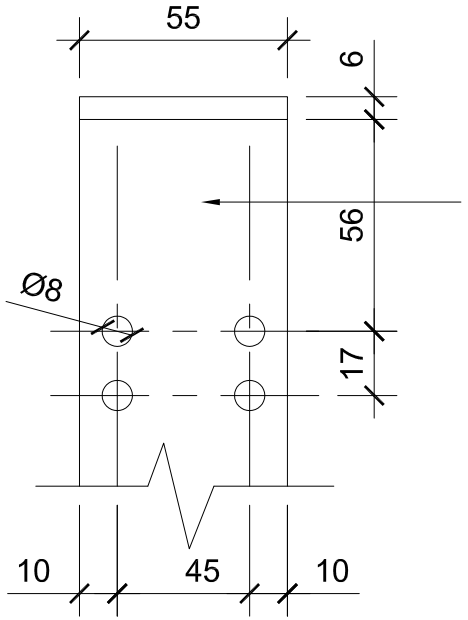

HINGE POSITION ON COLUMN
SCALE 1:2

UNIVERSITY OF STELLENBOSCH			SCALE 1:4 MEASURED IN mm	TITLE HAUNCH APPLY HINGE	
STUDENT No. 14527774	DRAWN BY HL ALBERTYN		DATE 24/01/2011	SHEET 2 OF 2	No. 002-007

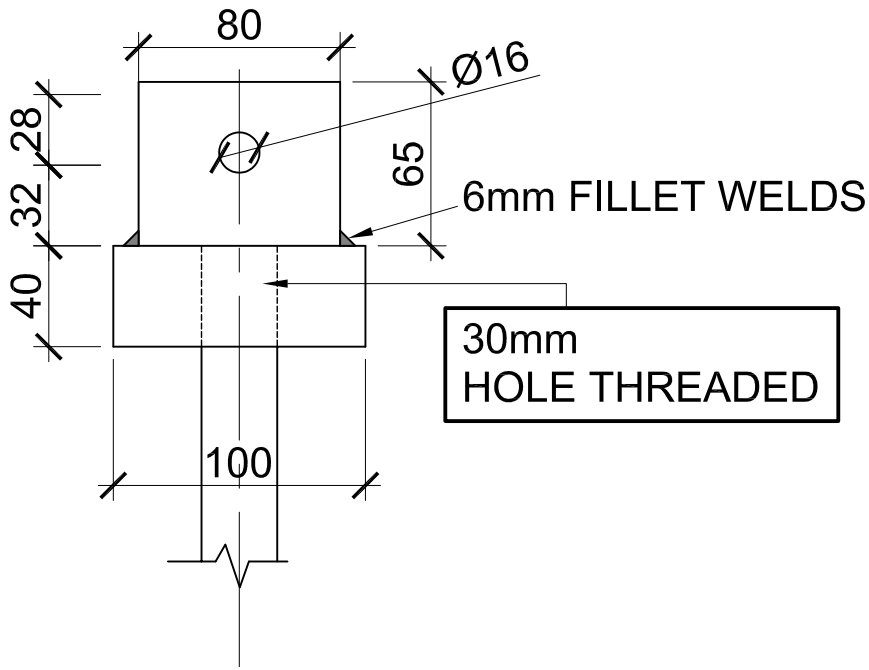

LOAD APPLICATION FORK

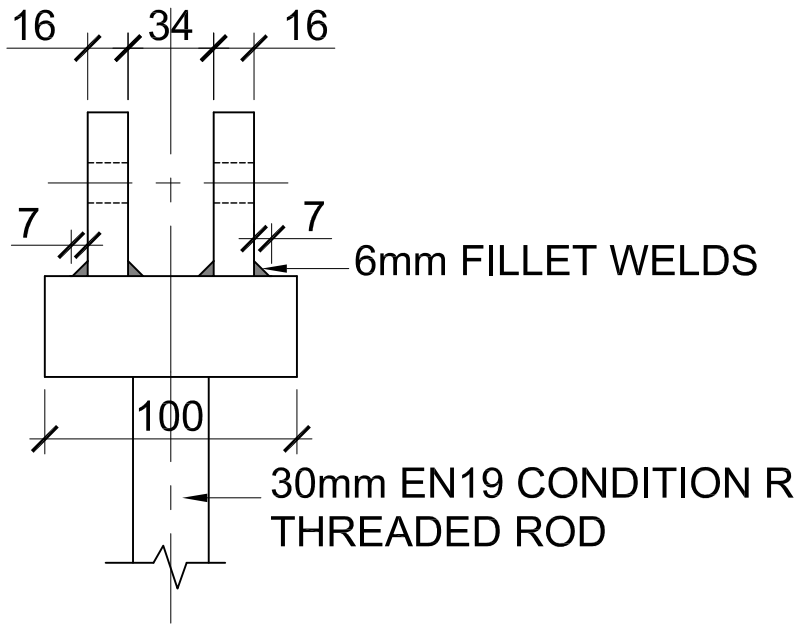

M16 GRADE 8.8 BOLT
WITH 70mm SOLID SHANK TO
BE USED AS PIN

NOTES:
STEEL GRADE 355W
WELDS AFROX VITEMAX
ALL HOLES TO BE DRILLED
DO NOT SCALE FROM DRAWING

UNIVERSITY OF STELLENBOSCH			SCALE 1:3 MEASURED IN mm	TITLE LOAD APPLICATION FORK	
STUDENT No. 14527774	DRAWN BY HL ALBERTYN		DATE 24/01/2011	SHEET 1 OF 2	No. 002-008

30mm DIAMETER EN19 ROD CONDITION R

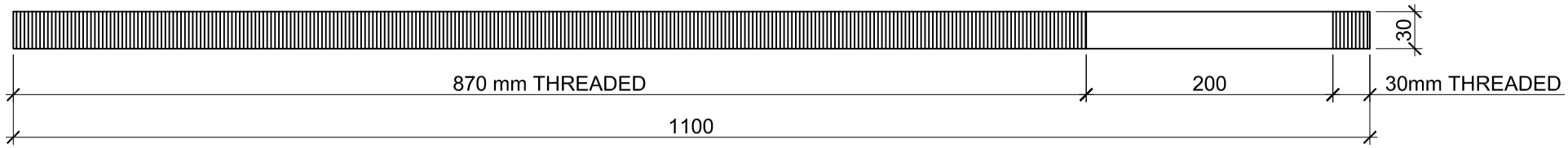

UNIVERSITY OF STELLENBOSCH			SCALE 1:5 MEASURED IN mm	TITLE LOAD APPLICATION FORK	
STUDENT No. 14527774	DRAWN BY HL ALBERTYN		DATE 24/01/2011	SHEET 2 OF 2	No. 002-008

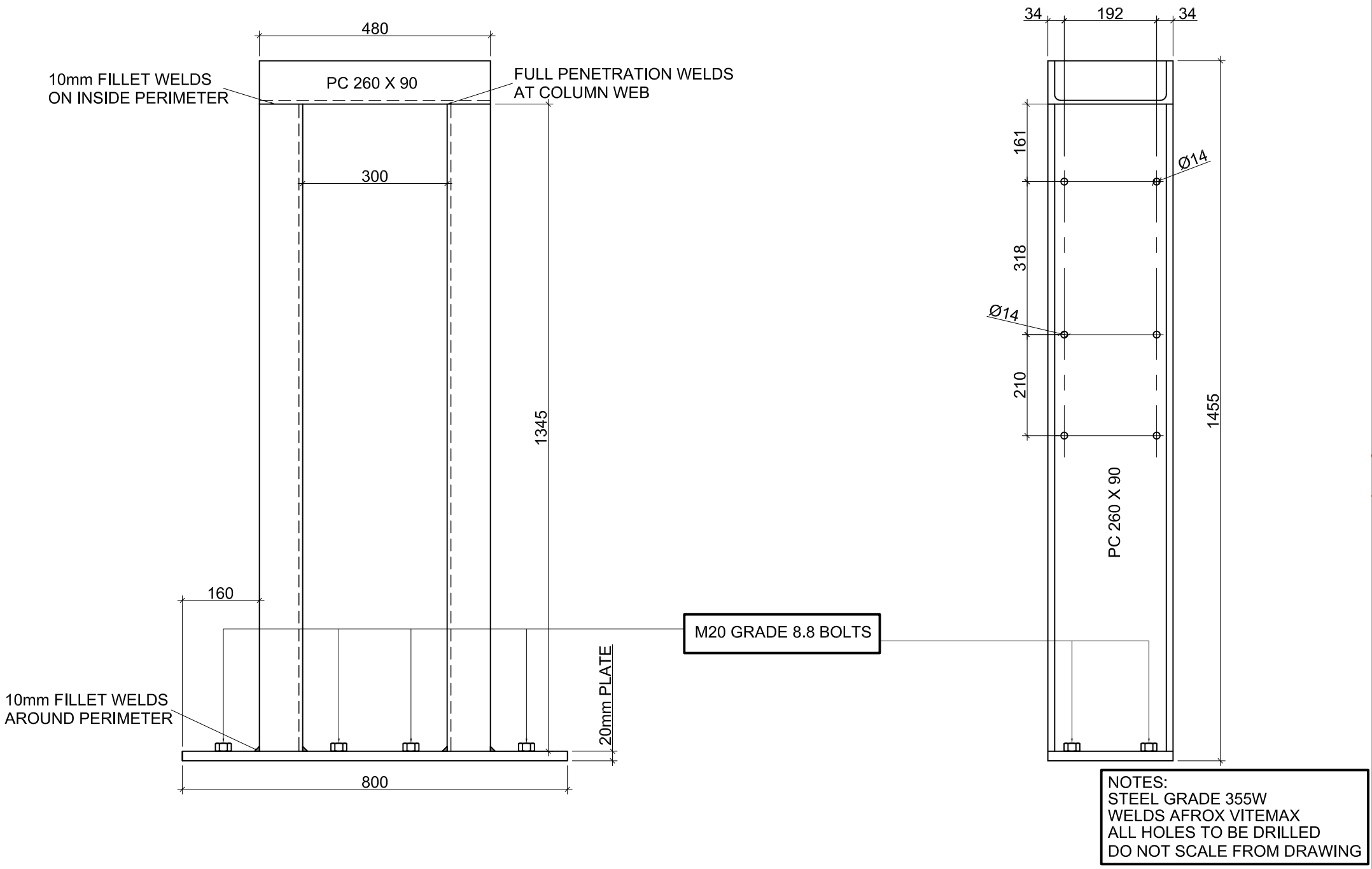

NOTES:
STEEL GRADE 355W
WELDS AFROX VITEMAX
ALL HOLES TO BE DRILLED
DO NOT SCALE FROM DRAWING

UNIVERSITY OF STELLENBOSCH		SCALE 1:10 MEASURED IN mm	TITLE FRAME	
STUDENT No. 14527774	DRAWN BY HL ALBERTYN	DATE 24/01/2011	SHEET 1 OF 2	No. 002-009

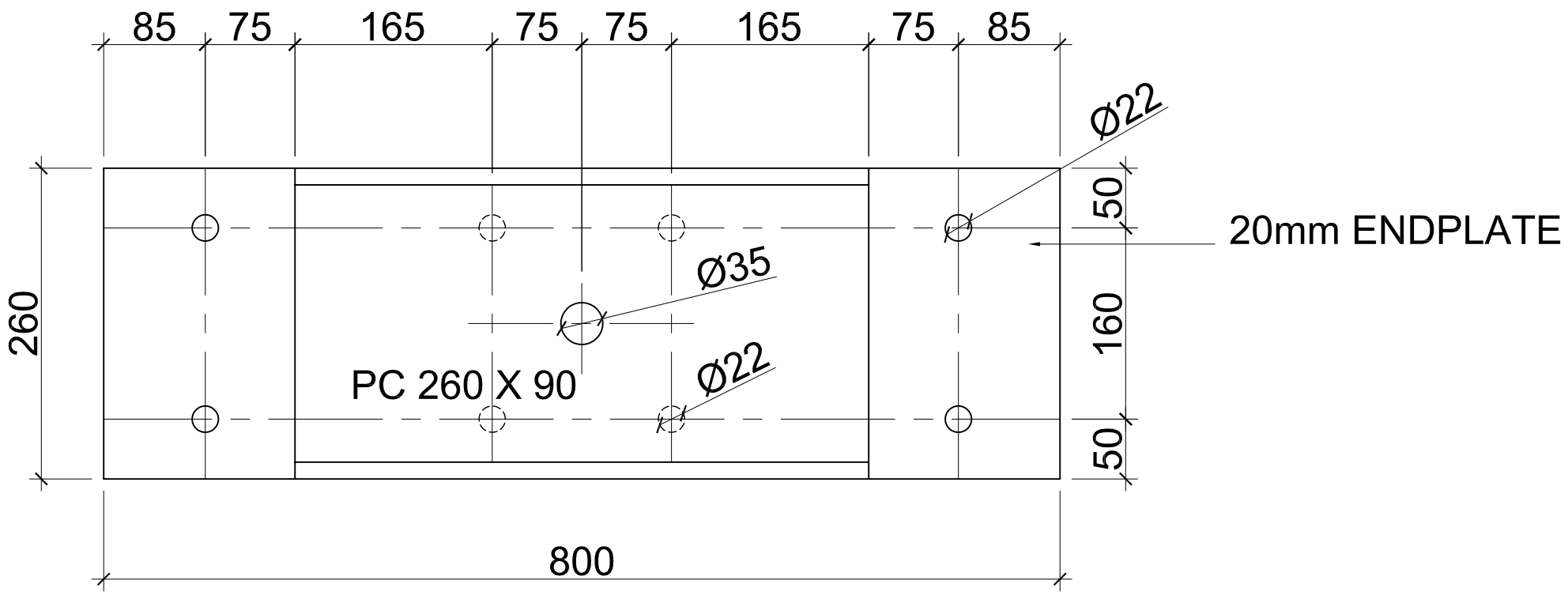

FRAME TOP LAYOUT

NOTES:
STEEL GRADE 355W
WELDS AFROX VITEMAX
ALL HOLES TO BE DRILLED
DO NOT SCALE FROM DRAWING

UNIVERSITY OF STELLENBOSCH		SCALE 1:5 MEASURED IN mm	TITLE FRAME	
STUDENT No. 14527774	DRAWN BY HL ALBERTYN	DATE 24/01/2011	SHEET 2 OF 2	No. 002-009

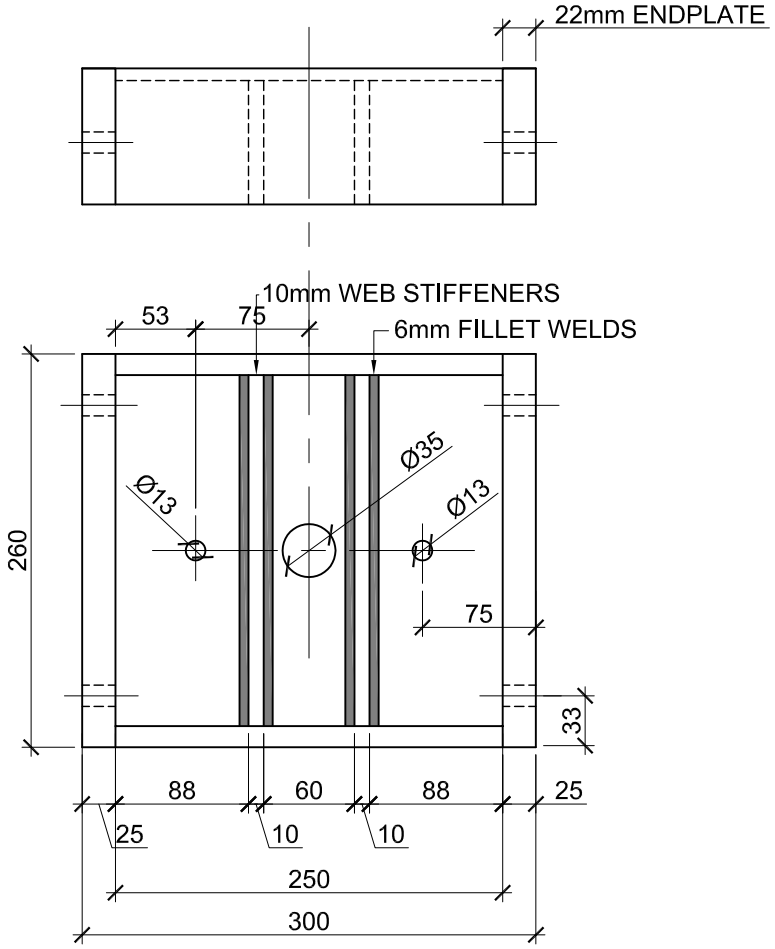

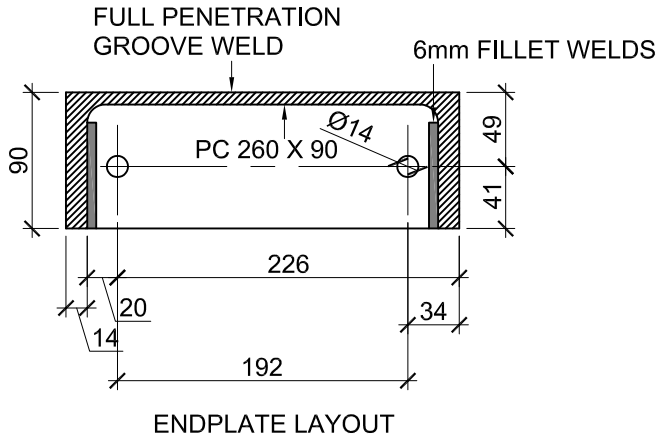

ENDPLATE LAYOUT

NOTES:
STEEL GRADE 355W
WELDS AFROX VITEMAX
ALL HOLES TO BE DRILLED
DO NOT SCALE FROM DRAWING

UNIVERSITY OF STELLENBOSCH			SCALE 1:5 MEASURED IN mm	TITLE FRAME JACK SUPPORT	
STUDENT No. 14527774	DRAWN BY HL ALBERTYN		DATE 24/01/2011	SHEET 1 OF 1	No. 002-010

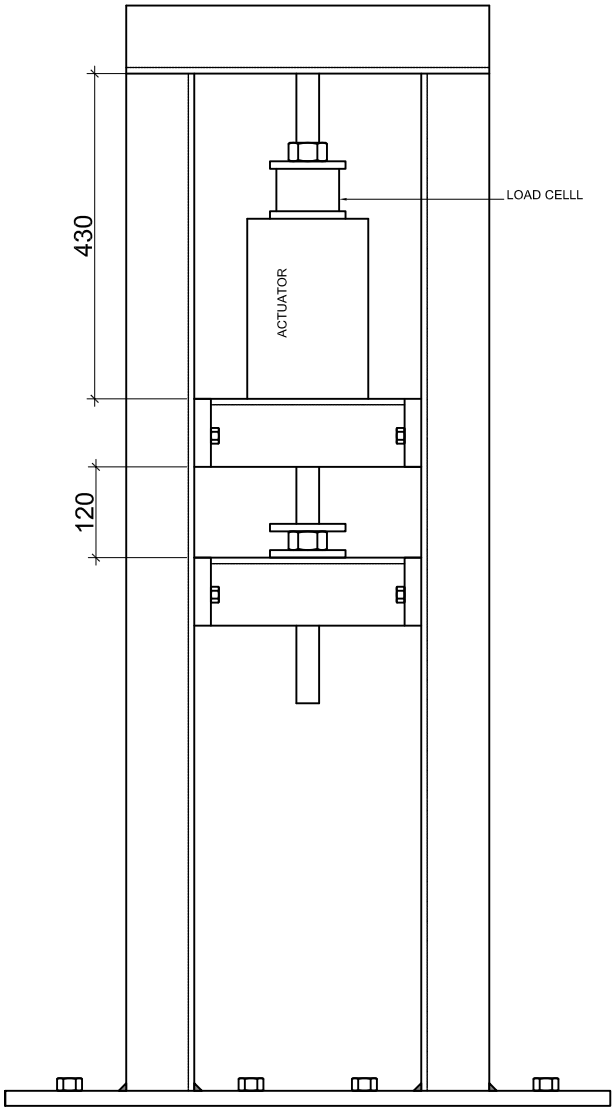

COMPRESSION

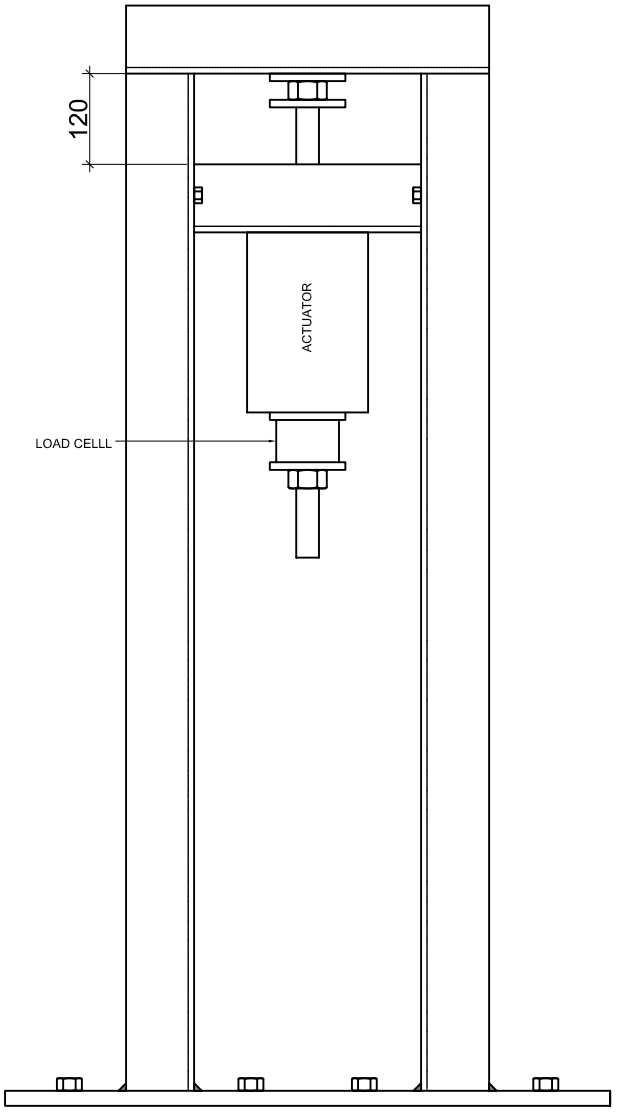

TENSION

UNIVERSITY OF STELLENBOSCH			SCALE 1:10 MEASURED IN mm	TITLE FRAME LAYOUTS	
STUDENT No. 14527774	DRAWN BY HL ALBERTYN		DATE 24/01/2011	SHEET 1 OF 1	No. 002-011

Appendix E

GROUT CUBE TEST RESULTS

Five cubes of cementitious grout was cast for the sensitivity analysis of the column base in chapter six and is illustrated in figure E.1. The investigation was motivated by the possible stiffening behaviour of the cementitious grout under loading. The supplier of the grout did not provide any technical information of the product with regards to Poisson's ratio and Young's modulus. Cube tests performed on the grout will this provide elastic properties of the grout, ultimate strength and the response of the grout in terms of stiffness under loading. The reader is referred to section 6.6.3 of chapter six for a detailed discussion on the investigation.

Figure E.1: Five 100 mm cementitious grout cubes.

The specification from the supplier is as follows:

SikaGrout® -212 by Sika South Africa (Pty) Ltd

Table E.1: Compressive-, flexural- and tensile-strengths of cementitious grout.

	1 day	**7 days**	**28 days**
Compressive Strength at 25°C	34 N/mm^2	57 N/mm^2	66 N/mm^2
Flexural Strength at 20°C	5.8 N/mm^2	8.3 N/mm^2	10.20 N/mm^2
Tensile Strength at 20°C	2.6 N/mm^2	4.7 N/mm^2	5.4 N/mm^2

EXPERIMENTAL TESTS

Compression tests were done on the five grout cubes. Load was measured with a load cell and displacement with two 10 mm LVDT's. The compression test setup is illustrated in figure E.2.

Figure E.2: Compression test on a grout cube.

The stress-strain curves for the five cubes are illustrated in figure E.3

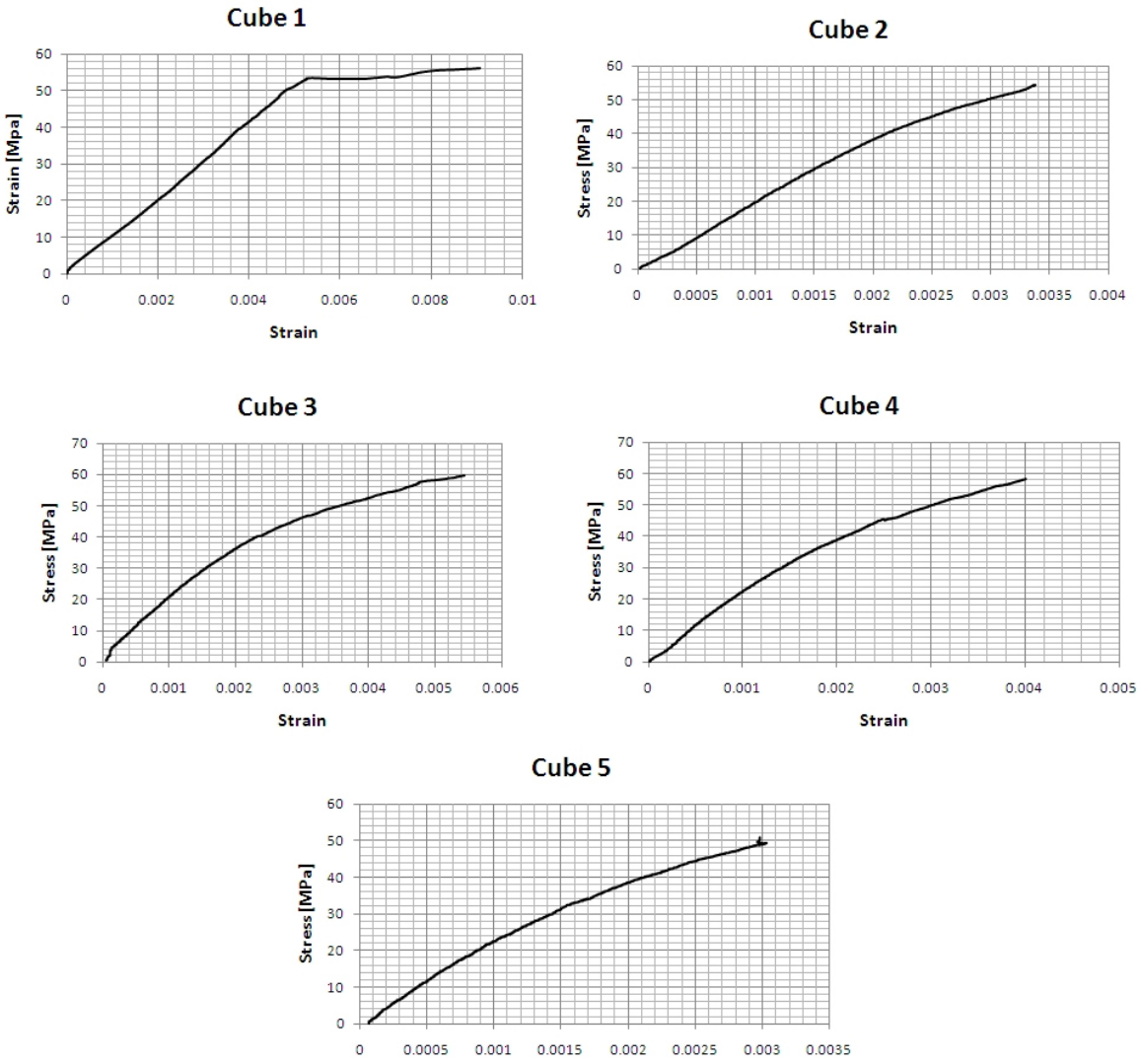

Figure E.3: Stress-strain curves for the five grout cubes.

The seven day compressive strength results of the five cube tests is given in table E.2 below.

Table E.2: Seven day compressive strength of the five cubes.

Cube	**Compressive Strength [MPa]**
1	62.80
2	60.00
3	61.87
4	61.63
5	60.04
Mean	**61.27**
Std. Deviation	1.22